

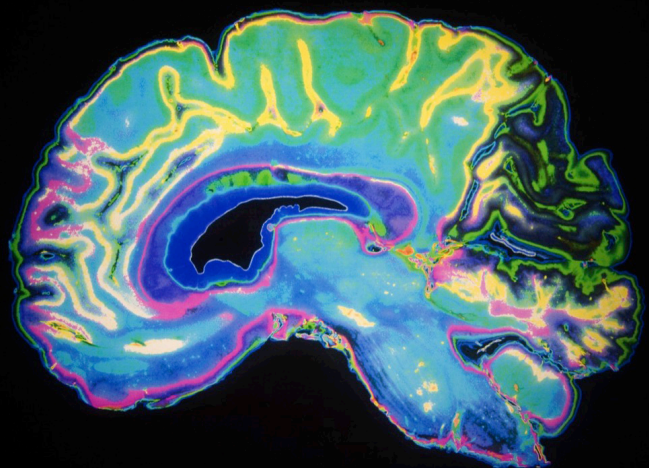
# Exploring brain connectivity to understand behavior

**Edited by**

João J. Cerqueira, India Morrison, Lars Michels, Carla Cannizzaro, Seth Davin Norrholm and Gennady Knyazev

**Published in**

Frontiers in Behavioral Neuroscience



## FRONTIERS EBOOK COPYRIGHT STATEMENT

The copyright in the text of individual articles in this ebook is the property of their respective authors or their respective institutions or funders. The copyright in graphics and images within each article may be subject to copyright of other parties. In both cases this is subject to a license granted to Frontiers.

The compilation of articles constituting this ebook is the property of Frontiers.

Each article within this ebook, and the ebook itself, are published under the most recent version of the Creative Commons CC-BY licence. The version current at the date of publication of this ebook is CC-BY 4.0. If the CC-BY licence is updated, the licence granted by Frontiers is automatically updated to the new version.

When exercising any right under the CC-BY licence, Frontiers must be attributed as the original publisher of the article or ebook, as applicable.

Authors have the responsibility of ensuring that any graphics or other materials which are the property of others may be included in the CC-BY licence, but this should be checked before relying on the CC-BY licence to reproduce those materials. Any copyright notices relating to those materials must be complied with.

Copyright and source acknowledgement notices may not be removed and must be displayed in any copy, derivative work or partial copy which includes the elements in question.

All copyright, and all rights therein, are protected by national and international copyright laws. The above represents a summary only. For further information please read Frontiers' Conditions for Website Use and Copyright Statement, and the applicable CC-BY licence.

ISSN 1664-8714  
ISBN 978-2-83252-034-5  
DOI 10.3389/978-2-83252-034-5

## About Frontiers

Frontiers is more than just an open access publisher of scholarly articles: it is a pioneering approach to the world of academia, radically improving the way scholarly research is managed. The grand vision of Frontiers is a world where all people have an equal opportunity to seek, share and generate knowledge. Frontiers provides immediate and permanent online open access to all its publications, but this alone is not enough to realize our grand goals.

## Frontiers journal series

The Frontiers journal series is a multi-tier and interdisciplinary set of open-access, online journals, promising a paradigm shift from the current review, selection and dissemination processes in academic publishing. All Frontiers journals are driven by researchers for researchers; therefore, they constitute a service to the scholarly community. At the same time, the *Frontiers journal series* operates on a revolutionary invention, the tiered publishing system, initially addressing specific communities of scholars, and gradually climbing up to broader public understanding, thus serving the interests of the lay society, too.

## Dedication to quality

Each Frontiers article is a landmark of the highest quality, thanks to genuinely collaborative interactions between authors and review editors, who include some of the world's best academicians. Research must be certified by peers before entering a stream of knowledge that may eventually reach the public - and shape society; therefore, Frontiers only applies the most rigorous and unbiased reviews. Frontiers revolutionizes research publishing by freely delivering the most outstanding research, evaluated with no bias from both the academic and social point of view. By applying the most advanced information technologies, Frontiers is catapulting scholarly publishing into a new generation.

## What are Frontiers Research Topics?

Frontiers Research Topics are very popular trademarks of the *Frontiers journals series*: they are collections of at least ten articles, all centered on a particular subject. With their unique mix of varied contributions from Original Research to Review Articles, Frontiers Research Topics unify the most influential researchers, the latest key findings and historical advances in a hot research area.

Find out more on how to host your own Frontiers Research Topic or contribute to one as an author by contacting the Frontiers editorial office: [frontiersin.org/about/contact](https://frontiersin.org/about/contact)

# Exploring brain connectivity to understand behavior

## Topic editors

João J. Cerqueira — University of Minho, Portugal

India Morrison — Linköping University, Sweden

Lars Michels — University of Zurich, Switzerland

Carla Cannizzaro — University of Palermo, Italy

Seth Davin Norrholm — Wayne State University, United States

Gennady Knyazev — State Scientific Research Institute of Physiology and Basic Medicine, Russia

## Citation

Cerqueira, J. J., Morrison, I., Michels, L., Cannizzaro, C., Norrholm, S. D., Knyazev, G., eds. (2023). *Exploring brain connectivity to understand behavior*. Lausanne: Frontiers Media SA. doi: 10.3389/978-2-83252-034-5

## Table of contents

- 04 Editorial: Exploring brain connectivity to understand behavior  
Gennady G. Knyazev
- 06 Trait Impulsivity Associated With Altered Resting-State Functional Connectivity Within the Somatomotor Network  
Aleksandra M. Herman, Hugo D. Critchley and Theodora Duka
- 15 Amygdala Structural Connectivity Is Associated With Impulsive Choice and Difficulty Quitting Smoking  
Ausaf A. Bari, Hiro Sparks, Simon Levinson, Bayard Wilson, Edythe D. London, Jean-Philippe Langevin and Nader Pouratian
- 26 Effects of Autonomous Sensory Meridian Response on the Functional Connectivity as Measured by Functional Magnetic Resonance Imaging  
Seonjin Lee, Jooyeon Kim and Sungho Tak
- 41 Evaluation of Effective Connectivity Between Brain Areas Activated During Simulated Driving Using Dynamic Causal Modeling  
Mi-Hyun Choi, Hyung-Sik Kim and Soon-Cheol Chung
- 51 Resting-State Functional Connectivity of the Punishment Network Associated With Conformity  
Yin Du, Yinan Wang, Mengxia Yu, Xue Tian and Jia Liu
- 64 Individualized Prediction of PTSD Symptom Severity in Trauma Survivors From Whole-Brain Resting-State Functional Connectivity  
Xueling Suo, Du Lei, Wenbin Li, Jing Yang, Lingjiang Li, John A. Sweeney and Qiyong Gong
- 74 Placebo Effects in the Context of Religious Beliefs and Practices: A Resting-State Functional Connectivity Study  
Anne Schienle, Andreas Gremsl and Albert Wabnegger
- 82 Brain-wide neuronal activation and functional connectivity are modulated by prior exposure to repetitive learning episodes  
Dylan J. Terstege, Isabella M. Durante and Jonathan R. Epp
- 97 The relationship between childhood emotional neglect experience and depressive symptoms and prefrontal resting functional connections in college students: The mediating role of reappraisal strategy  
Bin Xu, Shilin Wei, Xiaojuan Yin, Xiaokang Jin, Shizhen Yan and Lina Jia





## OPEN ACCESS

EDITED AND REVIEWED BY  
Richard G. Hunter,  
University of Massachusetts Boston,  
United States

\*CORRESPONDENCE  
Gennady G. Knyazev  
✉ knyazevgg@neuronm.ru

SPECIALTY SECTION  
This article was submitted to  
Emotion Regulation and Processing,  
a section of the journal  
Frontiers in Behavioral Neuroscience

RECEIVED 01 March 2023  
ACCEPTED 03 March 2023  
PUBLISHED 14 March 2023

CITATION  
Knyazev GG (2023) Editorial: Exploring brain  
connectivity to understand behavior.  
*Front. Behav. Neurosci.* 17:1176953.  
doi: 10.3389/fnbeh.2023.1176953

COPYRIGHT  
© 2023 Knyazev. This is an open-access article  
distributed under the terms of the [Creative  
Commons Attribution License \(CC BY\)](#). The use,  
distribution or reproduction in other forums is  
permitted, provided the original author(s) and  
the copyright owner(s) are credited and that  
the original publication in this journal is cited, in  
accordance with accepted academic practice.  
No use, distribution or reproduction is  
permitted which does not comply with these  
terms.

# Editorial: Exploring brain connectivity to understand behavior

Gennady G. Knyazev\*

Laboratory of Psychophysiology of Individual Differences, Institute of Neuroscience and Medicine,  
Novosibirsk, Russia

## KEYWORDS

fMRI, connectivity, neuroimaging, behavior, resting state—fMRI

## Editorial on the Research Topic

### Exploring brain connectivity to understand behavior

Since the seminal work of [Biswal et al. \(1995\)](#), the study of connectivity has occupied one of the most prominent places in neuroimaging, which is not surprising given the general understanding of its role in information transfer and implementation of brain functions. Beyond this general understanding, there are areas in which the study of connectivity has a distinct advantage over the study of activation. The realization of brain function at rest, when it is impossible to relate brain activity to the processing of specific stimuli, is one such area. However, there is reason to believe that the study of functional connectivity also has greater potential for identifying specific patterns associated with task performance than does the study of brain activation. One of the most difficult questions in neuroscience is how information is encoded in the brain. Numerous data accumulated by neuroimaging clearly show a lack of specificity in the task-related activation of most cortical areas. For example, [Anderson and Penner-Wilger \(2013\)](#) showed that the overall average diversity of different anatomical areas on a scale from 0 (active in only one cognitive area) to 1 (equally active in different cognitive areas) is 0.7. This diversity is much smaller for functional connections, which suggests that the specificity of information representation in the brain is provided by a task-specific pattern of connections rather than activations.

Most studies collected in this Research Topic use resting state fMRI (rs-fMRI) functional connectivity data. These data allow to investigate task-independent patterns of functional connections associated with pathological conditions or normal psychological processes. [Herman et al.](#), using independent component analysis to identify resting state networks, show that “decoupling” of the perceptual and somatosensory cortices, which can compromise effective integration of early perceptual information with behavioral control programs, may underlie impulsive behavior. [Du et al.](#) in their rs-fMRI study on a large sample of students show that task-independent spontaneous connectivity in the punishment network could explain the conformist tendency, which was measured using a conformity scale. [Schienle et al.](#) selected participants based on their responses in a survey about belief in miracles and showed that in people with high levels of belief, placebos can alter the experience of emotional salience and cognitive control, which is accompanied by connectivity changes in the associated brain networks. [Xu et al.](#) used rs-fMRI to reveal brain underpinning of the primary childhood emotional neglect (CEN) and found that college students with CEN history utilized the reappraisal strategy less frequently and displayed more depressive symptoms than a control group, which was accompanied by stronger

prefrontal functional connections with other brain regions. Suo et al. recorded rs-fMRI in 122 earthquake survivors 10–15 months after the event and used connectome-based predictive modeling (CPM) to identify brain function features that are related to symptom severity. CPM predicted symptom severity scores based on functional connectivity between visual cortex, subcortical-cerebellum, limbic, and motor systems. The study highlights the potential usefulness of this kind of data for clinical assessment of PTSD symptom severity at the individual level.

Two studies explore changes in connectivity during experimental manipulations. Lee et al. using seed-based functional connectivity analysis of fMRI data show that autonomous sensory meridian response (ASMR), a sensory phenomenon in which audio-visual stimuli evoke a tingling sensation accompanied by a feeling of calm and relaxation, is accompanied by ongoing interaction between regions that mainly include mentalizing and self-referential networks. Contrary to the previous studies that used functional connectivity measures, Choi et al. employ effective connectivity measures in the framework of dynamic causal modeling (Friston, 2011). They show that simulated driving requires multi-domain executive function in addition to vision, and pathway activation is influenced by the driving experience and familiarity of the driver. Bari et al. use probabilistic tractography to evaluate whether structural connectivity of the amygdala to the brain reward network is associated with impulsive choice and tobacco smoking. Using data from the Human Connectome database, they analyze how subject performance on a delayed discounting task and whether they met specified criteria for difficulty quitting smoking could be predicted from sMRI measures. Findings highlight the importance of the amygdala-hippocampal-anterior cingulate network in the valuation of future rewards and substance dependence. Authors suggest that these results may help to identify potential targets for neuromodulatory therapies for addiction and related disorders. Finally, a study by Terstege et al. using Morris water maze training in mice and quantification of c-Fos-labeled fluorescent cells examines the effect of prior chronic spatial training on task-specific functional connectivity associated with subsequent contextual fear recall. Results show an increase in global efficiency and in network resilience based on simulated targeted node deletion. Overall, this study suggests that chronic learning has transferable effects on the functional connectivity networks of other types of learning and memory. The generalized enhancements in network efficiency and

resilience suggest that learning itself may protect brain networks against deterioration.

To summarize, the collection of articles in this Research Topic demonstrates the variety of areas of neuroscience in which the study of connectivity can yield exciting discoveries. They range from elucidating the cerebral underpinnings of persistent individual differences, such as impulsivity, conformity, and suggestibility, to the short-term or long-term effects of experimental manipulations, such as ASMR, simulated driving, and water maze training, or environmental events and conditions, such as earthquakes or CEN. Even more exciting discoveries can be expected in the near future, when recently developed methods such as dynamic connectivity or multivariate pattern analysis breathe new life into the study of connectivity.

## Author contributions

The author confirms being the sole contributor of this work and has approved it for publication.

## Funding

The author was supported by the Russian Science Foundation under grant no. 22-15-00142.

## Conflict of interest

The author declares that the research was conducted in the absence of any commercial or financial relationships that could be construed as a potential conflict of interest.

## Publisher's note

All claims expressed in this article are solely those of the authors and do not necessarily represent those of their affiliated organizations, or those of the publisher, the editors and the reviewers. Any product that may be evaluated in this article, or claim that may be made by its manufacturer, is not guaranteed or endorsed by the publisher.

## References

- Anderson, M. L., Penner-Wilger, M. (2013). Neural reuse in the evolution and development of the brain: evidence for developmental homology? *Dev. Psychobiol.* 55, 42–51. doi: 10.1002/dev.21055
- Biswal, B., Yetkin, F. Z., Haughton, V. M., and Hyde, J. S. (1995). Functional connectivity in the motor cortex of resting human brain using echo-planar MRI. *Magn. Reson. Med.* 34, 537–541. doi: 10.1002/mrm.1910340409
- Friston, K. J. (2011). Functional and effective connectivity: a review. *Brain Connect.* 1, 13–36. doi: 10.1089/brain.2011.0008



# Trait Impulsivity Associated With Altered Resting-State Functional Connectivity Within the Somatomotor Network

Aleksandra M. Herman<sup>1,2\*</sup>, Hugo D. Critchley<sup>3,4</sup> and Theodora Duka<sup>2,5</sup>

<sup>1</sup> Department of Psychology, Royal Holloway, University of London, Egham, United Kingdom, <sup>2</sup> Behavioural and Clinical Neuroscience, University of Sussex, Brighton, United Kingdom, <sup>3</sup> Brighton and Sussex Medical School, Brighton, United Kingdom, <sup>4</sup> Sackler Centre for Consciousness Science, University of Sussex, Brighton, United Kingdom, <sup>5</sup> Sussex Addiction Research and Intervention Centre, Brighton, United Kingdom

## OPEN ACCESS

### Edited by:

Carla Cannizzaro,  
University of Palermo, Italy

### Reviewed by:

Olga M. Bazanova,  
State Scientific Research Institute  
of Physiology and Basic Medicine,  
Russia  
Walter Adriani,  
Istituto Superiore di Sanità (ISS), Italy

### \*Correspondence:

Aleksandra M. Herman  
aleksandra.herman@rhul.ac.uk;  
a.herman@sussex.ac.uk

### Specialty section:

This article was submitted to  
Individual and Social Behaviors,  
a section of the journal  
Frontiers in Behavioral Neuroscience

**Received:** 01 October 2019

**Accepted:** 05 June 2020

**Published:** 24 June 2020

### Citation:

Herman AM, Critchley HD and  
Duka T (2020) Trait Impulsivity  
Associated With Altered  
Resting-State Functional Connectivity  
Within the Somatomotor Network.  
Front. Behav. Neurosci. 14:111.  
doi: 10.3389/fnbeh.2020.00111

Knowledge of brain mechanisms underlying self-regulation can provide valuable insights into how people regulate their thoughts, behaviors, and emotional states, and what happens when such regulation fails. Self-regulation is supported by coordinated interactions of brain systems. Hence, behavioral dysregulation, and its expression as impulsivity, can be usefully characterized using functional connectivity methodologies applied to resting brain networks. The current study tested whether individual differences in trait impulsivity are reflected in the functional architecture within and between resting-state brain networks. Thirty healthy individuals completed a self-report measure of trait impulsivity and underwent resting-state functional magnetic resonance imaging. Using Probabilistic Independent Components Analysis in FSL MELODIC, we identified across participants 10 networks of regions (resting-state networks) with temporally correlated time courses. We then explored how individual expression of these spatial networks covaried with trait impulsivity. Across participants, we observed that greater self-reported impulsivity was associated with decreased connectivity of the right lateral occipital cortex (peak mm 46/-70/16, FWE 1- $p$  = 0.981) with the somatomotor network. No suprathreshold differences were observed in between-network connectivity. Our findings implicate the somatomotor network, and its interaction with sensory cortices, in the control of (self-reported) impulsivity. The observed “decoupling” may compromise effective integration of early perceptual information (from visual and somatosensory cortices) with behavioral control programs, potentially resulting in negative consequences.

**Keywords:** trait impulsivity, resting state, functional connectivity, Barratt Impulsiveness Scale, somatomotor network

## INTRODUCTION

Self-control allows people to make plans for the future, choose the best option from several alternatives, control impulses, inhibit unwanted thoughts, and regulate behaviors and emotions (Kelley et al., 2015). Past studies typically employed task-related functional magnetic resonance imaging (fMRI) to understand the neural substrates of transient fluctuations in self-control

in different circumstances or in distinct populations. Although this approach is well-suited to capture momentary changes in brain activity in response to specific (internal or external) stimuli, it is arguably insufficient to capture more tonic aspects of self-control (Kelley et al., 2015). A global whole-brain network approach can provide more comprehensive insight into neural substrates supporting individual differences in the capacity for self-control over longer timescales. Moreover, measurement of functional connectivity (FC) across “resting-state” (RS) networks has proven value as a tool for characterizing mechanisms underlying neurocognitive processes and psychiatric disorders, while overcoming technical and inferential limitations of task-related fMRI (De Luca et al., 2006; van den Heuvel and Hulshoff Pol, 2010; Cole et al., 2014; Dipasquale et al., 2015).

Specific studies using FC at rest have tested for differences in the interaction between brain regions that account for impulsivity and, more generally, the executive function and dysfunction, in children (Inuggi et al., 2014) and in young adults (Davis et al., 2013; Reineberg et al., 2015). In typically developing children (8–12 years old) parental ratings of trait impulsivity are related to lower RS brain connectivity within the default mode network (DMN), specifically between posterior cingulate cortex and right angular gyrus (Inuggi et al., 2014). The DMN is considered a “task-negative” network, where activity is strongest when an individual is not engaged in an external task (e.g., at rest). Correspondingly, DMN activity is typically anti-correlated to other “task-related” resting-state networks (RSN) (Uddin et al., 2009). In highly impulsive children, the canonical anti-phasic relation between the DMN and action-related networks is much reduced, indicating that trait impulsivity is linked to a reduced functional segregation of task-negative and task-positive networks (i.e., the natural degree of anti-correlation between these networks is reduced). By extension, impulsivity may putatively arise in the context of functional interference between brain systems directing internal and external attention (Inuggi et al., 2014).

In adults, self-report questionnaires are used to assess trait impulsivity, measuring one’s tendencies to show premature, unplanned and short-sighted actions and decisions in daily life (Herman et al., 2018). Applying graph-theory approaches to functional brain architecture at rest in adults revealed an association between trait impulsivity and increased segregation between cortical and sub-cortical regions (i.e., increased “modularity”) (Davis et al., 2013). This is coherent with findings in young adults for whom core aspects of executive function (quantified using three behavioral tasks) were positively associated with connectivity between the frontal pole and an “attentional” RSN, and also between the cerebellum and a right frontoparietal RSN. This suggests that individuals with better executive functioning manifest more expanded yet more integrated RSN relative to individuals with worse executive functioning (Reineberg et al., 2015). However, there are also contrasting findings: Individuals with increased motor impulsivity (i.e., poorer inhibitory capacity on the go/no-go task) and higher trait impulsivity (Barratt Impulsiveness Scale), reportedly show greater RS FC between the basal ganglia and thalamus, motor cortex, temporal lobe and prefrontal

cortex (Korponay et al., 2017). This suggests that increased connectivity between motor-brain regions may predispose to disinhibited actions.

The comparison between these earlier studies to disentangle the observed differences, however, is hindered by the different approaches to functional connectivity (e.g., focus on a single, pre-defined RSN, or the use of seed-based methods, instead of a whole-brain model-free approach) and diverse measures of disinhibited behaviors used (various behavioral tasks or trait measures). Their focus on general executive functioning instead of trait impulsivity or a specific behavioral impulsivity task is also a limitation. The present study set out to cover these gaps by testing for predicted associations between trait impulsivity and the strength of FC within as well as between resting-state networks.

An understanding of the brain mechanisms underlying self-regulation can provide valuable insights into how people regulate and control their thoughts, behaviors, and emotional states and can illuminate what happens on those occasions when this regulation fails (Kelley et al., 2015). The present study tested whether individual differences in trait impulsivity are reflected in within-and between-resting-state network architecture using a FC approach. Based on previous findings, we predicted that internal architecture of the default mode (Inuggi et al., 2014), frontoparietal, and attentional networks (Reineberg et al., 2015) would be linked to the expression impulsivity across individuals and that between-network connectivity pattern of task-negative (DMN) and task-positive networks (Inuggi et al., 2014) might also be modulated by the magnitude of trait impulsivity.

## MATERIALS AND METHODS

### Participants

Thirty volunteers (nine males) were recruited from staff and students of the University of Sussex. Participants were required to be between 18 and 40 years old and right-handed. Exclusion criteria included history of any psychological or neurological disorders, head injury, current treatment for any psychological or physical condition (including use of inhalers; excluding the contraceptive pill), pregnancy or breastfeeding, clinically significant impairment of vision, use of psychoactive substances 48 h before testing, and any MRI contradictions (claustrophobia, having any metal implants, teeth braces or bridges, or cardiac pacemakers).

All participants provided written informed consent. The study was conducted according to the Declaration of Helsinki. All procedures were approved by the Brighton and Sussex Medical School Research Governance and Ethics Committee.

### Questionnaires

Participants completed the *Barratt Impulsiveness Scale* (BIS; Patton et al., 1995), a 30-item questionnaire with three distinct impulsivity facets: attentional (eight items; a lack of focus on the ongoing task), motor (11 items; acting without thinking), and non-planning impulsivity (11 items; orientation to the present rather than to the future).



## MRI Experiment Design

In the MRI scanner, first, a structural scan was obtained followed by a 7-min resting-state scan (165 volumes) during which participants were instructed to rest with their eyes open focusing on a fixation cross in the center of the screen with the instruction to try not to think of anything and not to fall asleep. All participants were tested between 2 pm and 6 pm to control for possible time of day effects on an attentional level.

## MRI Acquisition

MRI was performed on a 1.5-Tesla MAGNETOM Avanto scanner (Siemens AG, Munich, Germany) with upgraded gradients and a 32-channel headcoil. Structural volumes were obtained using a high-resolution three-dimensional magnetization prepared rapid acquisition gradient echo sequence. Functional data sets used T2\*-weighted echo planar imaging sensitive to blood oxygenation-level-dependent signal (repetition time = 2.52 s, echo time = 43 ms, flip angle = 90°, 34 slices, 3-mm slice thickness, field of view = 192 mm, voxel size =  $3 \times 3 \times 3$  mm). Slices were angled  $-30^\circ$  in the anteroposterior axis to reduce the signal loss in orbitofrontal regions (Deichmann et al., 2003; Weiskopf et al., 2006).

## fMRI Data Pre-processing

Imaging analysis was performed using FEAT (FMRI Expert Analysis Tool) version 6.00, a part of FMRIB Software Library (FSLv6.0, Jenkinson et al., 2012). Pre-processing steps included (1) skull stripping of structural images with Brain Extraction Tool (BET), (2) removal of the first four functional volumes to allow for signal equilibration, (3) head movement correction by volume-realignment to the middle volume using MCFLIRT, (4) global 4D mean intensity normalization, (5) spatial smoothing (6mm full-width half-maximum), and (6) noise signals removal, (7) temporal high-pass filtering (100 s cut-off).

FMRI datasets were co-registered to the participant's structural image using affine boundary-based registration as implemented in FSL FLIRT (Jenkinson and Smith, 2001; Jenkinson et al., 2002) and subsequently transformed them to MNI152 standard space with 2 mm isotropic resolution using non-linear registration through FSL FNIRT (Andersson et al., 2010). Noise signals were identified individually and removed using ICA-AROMA toolbox (Pruim et al., 2015). ICA-AROMA incorporates probabilistic Independent Component Analysis (ICA) on the partly pre-processed single-subject fMRI data (following spatial smoothing and normalization but before high-pass filtering), identifies independent components (ICs) representing motion artifacts and removes them from the fMRI time-series using linear regression.

Since there was a broad age range within our population (18–37 years) and a larger number of females than males participated in the study, in all reported analyses, gender and mean-centered age were added as covariates of no interest.

## Independent Components Analysis

The RS data analysis pipeline is summarized in **Figure 1**. To decompose the RS data into various independent spatiotemporal components, Probabilistic Independent Components Analysis

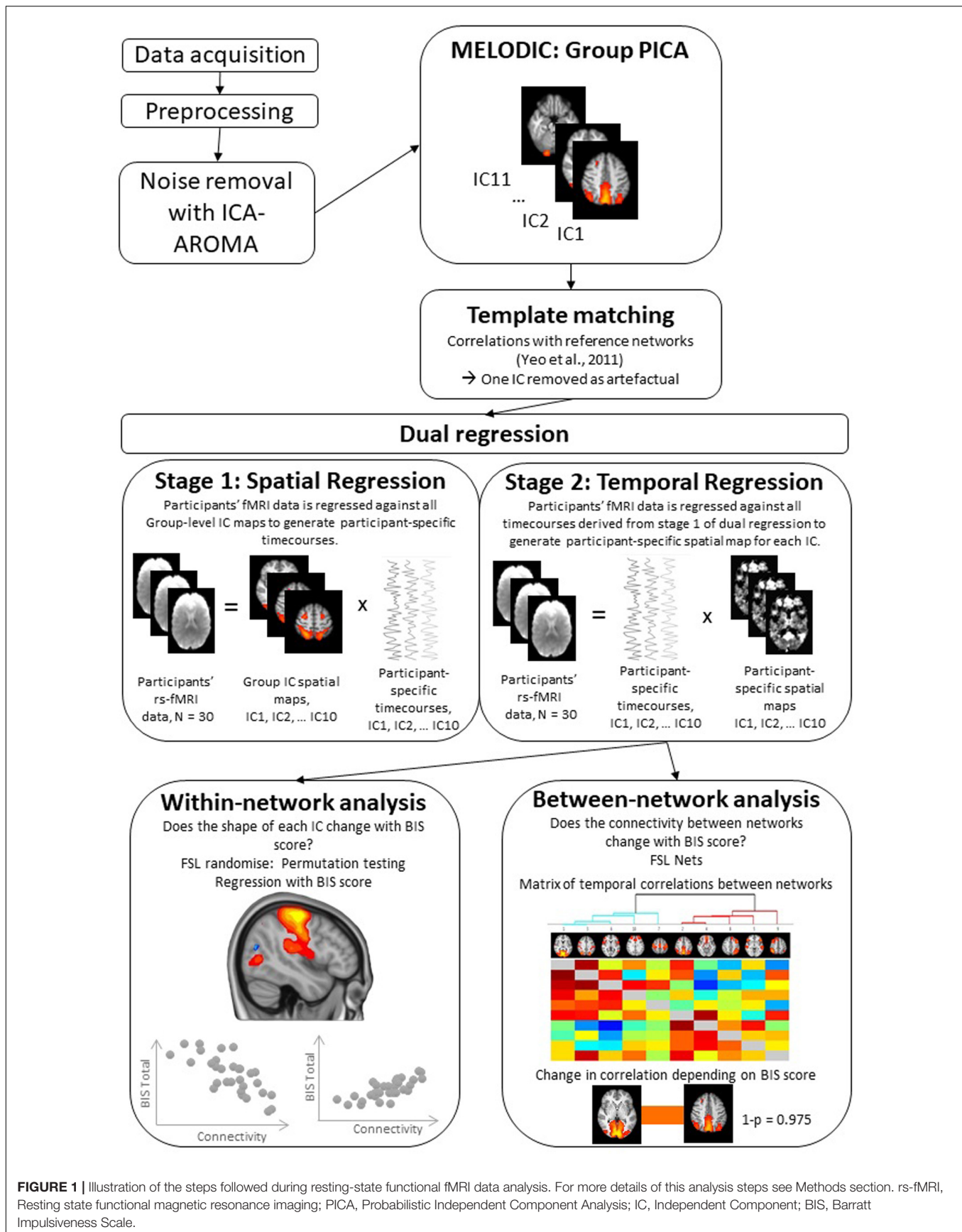
(PICA) was performed on the pre-processed functional scans using Melodic version 3.14 (Beckmann and Smith, 2004). A dimensionality estimation using the Laplace approximation to the Bayesian evidence of the model order (Beckmann and Smith, 2004) produced 11 spatiotemporal components. Following an approach described in Reineberg et al. (2015), we statistically compared the spatial map of each independent component (IC) to a set of seven reference RS networks from a previous large-scale RS analysis (Yeo et al., 2011). We used FSL's "fslcc" tool to calculate Pearson's  $r$  for each pairwise relationship and kept only those ICs that yielded a significant spatial correlation (Pearson's  $r > 0.3$ ) with one of the reference networks. This procedure identified and helped label 10 target ICs (see **Table 1** for details). Upon visual inspection, the remaining 1 IC was considered noise and was not subjected to further analysis.

## Dual regression

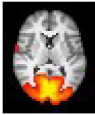


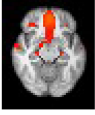
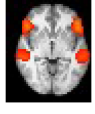
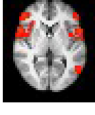
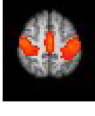

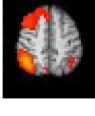

For the between-subject analysis, we carried out dual regression, a technique that back-reconstructs each un-thresholded group-level component map at the individual subject level, generating participant-specific spatial maps and time courses (Beckmann et al., 2009; Filippini et al., 2009). The dual regression consists of (1) a spatial regression of the group-average set of ICs that produces a set of participant-specific time series, one per group-level component, and (2) a temporal regression of those participant specific time series, resulting in a set of participant-specific spatial maps, one per group-level component (see **Figure 1**). Participant-specific components are whole brain images. For some individuals, the given IC might be very similar to the group level IC while others might show variations of the group level IC (i.e., have an expanded/constrained network or high/low connectivity of a particular region). Statistical analyses (discussed below) are performed on these whole brain participant-specific ICs to determine areas that covary with trait impulsivity measure, that is BIS total score.

## Within-network connectivity

To quantify the within-network variation in functional connectivity (FC), depending on BIS total score and participant-specific ICs, we carried out voxel-wise regression to assess statistically significant differences in FC in relation to trait impulsivity score. The analysis was conducted using Randomize, FSL's non-parametric permutation testing tool (Winkler et al., 2014), with 5000 permutations and threshold-free cluster enhancement (TFCE) with an alpha level of 0.05 to correct for multiple comparisons. The permutation testing procedure was run for each set of participant-specific ICs (one for each group-level ICs of interest); thus, the resulting statistical images reveal how variation in RS FC (functional connectivity estimates) predict differences in trait impulsivity (see **Figure 1**). For example, the permutation testing procedure could reveal that individuals with expanded one of the ICs (i.e., expanded to areas outside the areas included in the group-level IC) report greater impulsivity. Following studies using similar procedures (Uddin et al., 2013; Nomi and Uddin, 2015; Reineberg et al., 2015; de Bézenac et al., 2017; Herman et al., 2019), further correction for multiple component testing was not applied.



**TABLE 1** | Identified Independent Components (IC Number) and their characteristics.

IC number	Matching template network	Correlation with the template (Pearson's $r$ )	Regions	Lateralization	Number of voxels
1	Visual	0.745		Bilateral	1,138,587
2	Default mode network	0.746		Bilateral	761,539
3	Dorsal Attention/Visual	0.579/0.359		Bilateral	1,003,173
4	Default mode network	0.469		Bilateral	266,631
5	Default mode network	0.548		Bilateral	670,689
6	Ventral attention	0.454		Bilateral	181,331
7	Somatomotor	0.746		Bilateral	898,845
8	Frontoparietal	0.329		Left	944,938
9	Frontoparietal	0.513		Right	689,400
10	Ventral attention	0.301		Bilateral	211,073

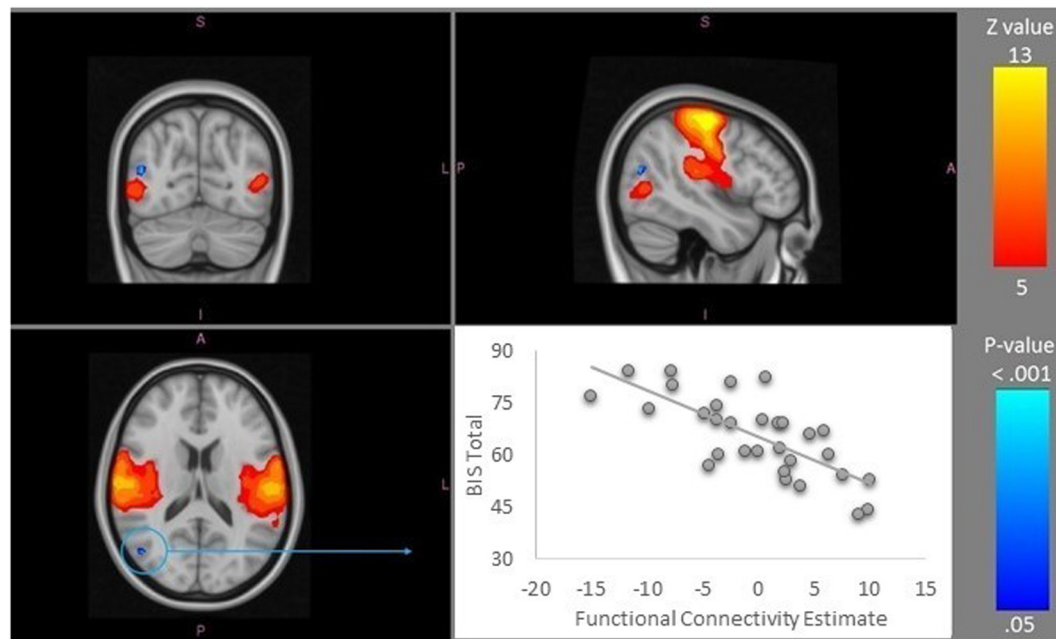
Images are presented in the radiological convention (left side of the brain is presented on the right side of the image). DMN, Default Mode Network.

### Between-network connectivity

*FSLNets*. To examine the relationship between trait impulsivity and between-network FC, we employed the *FSLNets* package<sup>1</sup> implemented in Matlab v2015b (The MathWorks, 2015). This analysis involved correlation of the participants' time courses

<sup>1</sup><http://fsl.fmrib.ox.ac.uk/fsl/fslwiki/FSLNets>

from the dual regression analysis and subjected them to between-network comparisons to determine how they are correlated with each other (Smith et al., 2013). We then calculated full and partial correlations between all pairs of ICs. Partial correlations are computed as correlations between two ICs while controlling for the effect of all other ICs and are thought to reflect more direct connections (Smith et al., 2011). Finally, BIS total score was



**FIGURE 2 |** Somatomotor resting-state network (IC 7), depicted in warm colors, was identified as the only network showing the significant differences across the BIS total score spectrum. The area that showed reduced resting state functional connectivity within this network was a region in the lateral occipital cortex (in blue;  $X = 46$ ,  $Y = -70$ ,  $Z = 16$ ). The visualization of the relationship is shown in the scatterplot in the bottom right corner. Images are presented in the radiological convention. A-anterior, I-inferior, L-left, P-posterior, R-right, S-superior. IC, Independent Component.

used as a regressor in the regression analysis in FSL randomize with 5000 permutations to assess differences in between-network connectivity across BIS spectrum. Results were FWE corrected for multiple comparisons.

## RESULTS

### Participants

No participant was removed because of extensive motion in the scanner. The final sample ( $N = 30$ , 9 males) was aged between 18 and 37 years old ( $M = 23.40$ ,  $SD = 5.01$ ). The average BIS Total score was  $65.30 \pm 11.39$ .

### Within-Network Connectivity

Greater self-reported impulsivity (BIS score) was associated with lower functional connectivity of the right lateral occipital cortex with IC7, a network that correlated significantly with Somatomotor template network (peak mm 46/-70/16, FWE 1- $p = 0.981$ ) (Figure 2).

### Between-Network Connectivity

Network analysis using FSLNets revealed a modular structure of functional networks, which could be segregated into clusters: Cluster 1 comprised of Visual, Somatomotor as well as Ventral and Dorsal Attention Networks (Figure 3, blue cluster), while Cluster 2 comprised of Frontoparietal and Default-Mode Networks (Figure 3, red cluster).

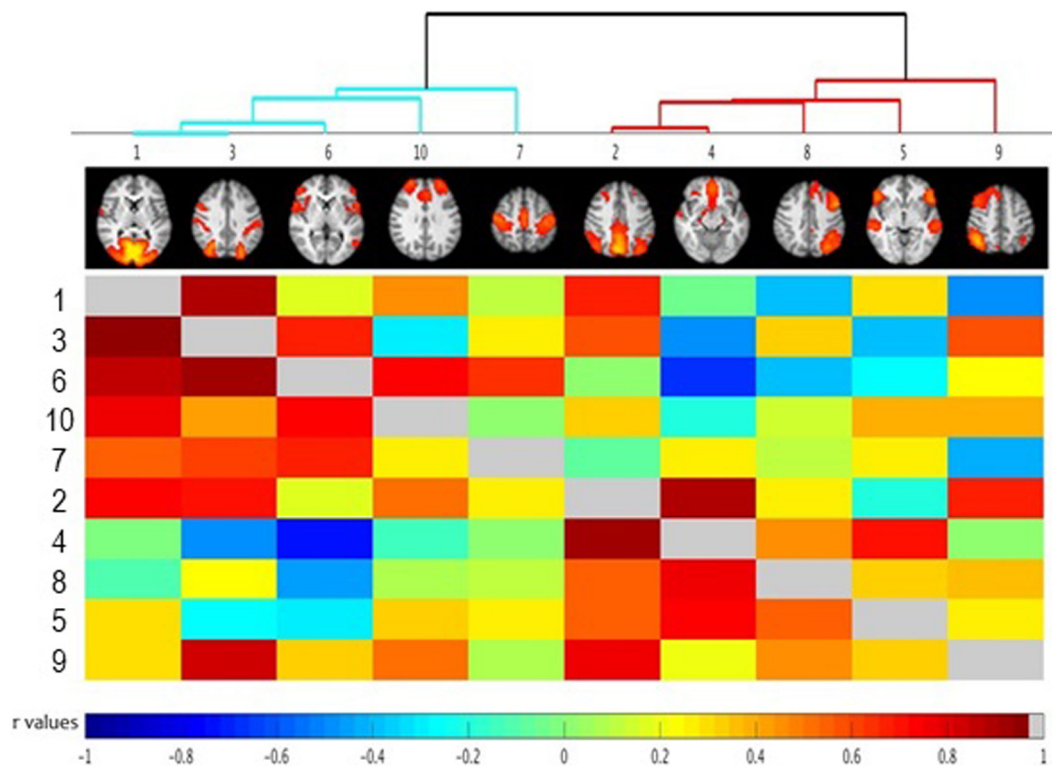
Using BIS as a predictor, no significant between-network differences in connectivity were found.

## DISCUSSION

This study investigated whether aspects of intrinsic functional architecture and between-network connectivity pattern is associated with individual differences in trait impulsivity in a normative (university) population. We showed that individual differences in trait impulsivity, assessed with BIS Total Score, are associated with altered aspects of the functional architecture of the Somatomotor RS network. Specifically, higher trait impulsivity was linked to decreased coupling between the lateral occipital cortex and the Somatomotor Network. Surprisingly, we did not find any significant differences in the network functional architecture of default mode or frontoparietal networks associated with impulsivity, as has been reported previously (Inuggi et al., 2014; Reineberg et al., 2015). However, it is important to note that such previous research used different measures of impulsivity. Therefore, those inconsistent findings might merely reflect a heterogeneous nature of impulsivity and its underlying neural mechanisms (Caswell et al., 2015; Herman et al., 2018).

The finding of disrupted FC within the Somatomotor RS network in relation to trait impulsivity level corroborates previous studies. The graph theory approach, has been used to test the relationship between impulsivity (as reflected in BIS score) and the functional segregation (i.e., modularity)





**FIGURE 3 |** FSLNets results of between network correlations ( $N = 30$ ). Each independent component (IC) is denoted by one column and a corresponding row. The colored matrix displays the correlations of the time series between networks pairs. Dark red squares indicate highly positive correlations, light green indicates a near-0 correlation, and dark blue represents highly negative correlation as denoted on the scale at the bottom of the figure. Full correlations between networks pairs are shown below the diagonal line (in gray) with partial correlations shown above the diagonal line (for detailed description of full and partial correlation please see main text). Groups of highly correlated ICs were clustered together according to a hierarchical clustering algorithm (visualized at the top of the matrix as a clustering tree). Please note that the color cut-off for hierarchical tree is arbitrary – just for visualization purposes. Numbers indicate specific independent components as described in **Table 1**. The ICs have been reordered, according to a hierarchical clustering algorithm. Small images at the top of each column summarize each IC's spatial map, with the right side of the images representing the left side of the brain. As described in the main text, the between-network connectivity was not modulated by trait impulsivity score.

of whole-brain resting state architecture (Davis et al., 2013). Overall, this reveals a shift in the functional connectivity between visual, sensorimotor, cortical, and subcortical structures across the impulsivity range; specifically pointing to increased functional modularity between cortical and sub-cortical regions as a function of impulsivity score.

The lateral occipital cortex supports both visual perception and multisensory integration (Grill-Spector et al., 2001; Beauchamp, 2005). Interestingly, it is recognized that visual cortices contribute to impulsivity (Davis et al., 2013) and disorders commonly associated with impulsivity, including as Attention Deficit-Hyperactivity Disorder (ADHD; Castellanos and Proal, 2013). The sensorimotor network consists of both motor cortices, known to play a critical role in response inhibition (Li et al., 2006; Duque et al., 2012; Rae et al., 2014), and somatosensory areas, which are vital for sensory integration. These regions show altered activity in inhibitory control in diseased states such as post-traumatic stress disorder (Falconer et al., 2008; van Rooij et al., 2014) or under pharmacological interventions with LSD (Schmidt et al., 2017). Here, the “decoupling” may itself reflect a deficit in effective integration of

perceptual information (visual and somatosensory cortices) with somatomotor outputs (motor cortex) associated with behavioral control, ultimately resulting in negative consequences, from poor planning for the future to excessive substance use (Dickman, 1990; Herman and Duka, 2019).

## Limitations

Some limitations merit comment. Our study was conducted on a moderately sized sample of students and employees of the university. The average BIS total score in our sample is  $65.30 \pm 11.39$ ; which is consistent with other reports in the literature of university sample [e.g.,  $65.67 \pm 9.92$  in males and  $64.58 \pm 10.36$  in females according to Caswell et al. (2015) and  $63.82 \pm 10.17$  according to Patton et al. (1995)] and normative community populations [ $59.18 \pm 9.54$  according to Reise et al. (2013) or  $62.3 \pm 10.3$  according to Stanford et al. (2009)]. However, our sample consists of relatively high-functioning young adults, who may have developed many mechanisms to cope with elevated impulsivity levels in daily life, which might have an effect on aspects of functional connectivity. It is also important to mention that the majority

of the sample consisted of females, some of which were using hormonal contraception, which can affect functional connectivity (Hausmann, 2005). Therefore, future research should replicate our findings in larger-scale studies with general population, including a range of individuals with various backgrounds and educational levels. Finally, we did not find any suprathreshold differences in between-network connectivity that could be related to elevated impulsivity levels. Possibly, this is because our sample consisted of highly functioning young adults, all from the university population, and differences in between-network connectivity may only reveal themselves in pathologically impulsive individuals.

## CONCLUSION

In the brain, aspects of the functional architecture of the Somatomotor Network were associated with individual differences in trait impulsivity (BIS Total score). Specifically, more impulsive individuals showed decreased connectivity between the lateral occipital cortex and the Somatomotor Network. Since perception informs action and vice versa (Creem-Regehr and Kunz, 2010), proper integration of sensory inputs is crucial for adaptive behavioral responses. Therefore, the observed decreased connectivity between the visual and somatosensory cortices and motor cortex, may reflect itself in less effective integration of perceptual information and behavioral control and, thus, in negative consequences. However, in this normative sample, the between-network architecture was not related to trait impulsivity level. This evidence supports the use of RS FC approaches to identify biomarkers for impulse-control problems.

## REFERENCES

- Andersson, J. L. R., Jenkinson, M., and Smith, S. (2010). *Non-Linear Registration, Aka Spatial Normalisation*. Oxford: Oxford Press.
- Beauchamp, M. S. (2005). See me, hear me, touch me: multisensory integration in lateral occipital-temporal cortex. *Curr. Opin. Neurobiol.* 15, 145–153. doi: 10.1016/j.conb.2005.03.011
- Beckmann, C. F., Mackay, C., Filippini, N., and Smith, S. (2009). Group comparison of resting-state fMRI data using multi-subject ICA and dual regression. *Neuroimage* 47:S148. doi: 10.1016/S1053-8119(09)71511-3
- Beckmann, C. F., and Smith, S. M. (2004). Probabilistic independent component analysis for functional magnetic resonance imaging. *IEEE Trans. Med. Imaging* 23, 137–152. doi: 10.1109/TMI.2003.822821
- Castellanos, X. F., and Proal, E. (2013). Large-scale brain systems in ADHD: beyond the prefrontal-striatal model. *Trends Cogn. Sci.* 16, 17–26. doi: 10.1016/j.tics.2011.11.007
- Caswell, A. J., Bond, R., Duka, T., and Morgan, M. J. (2015). Further evidence of the heterogeneous nature of impulsivity. *Pers. Individ. Diff.* 76, 68–74. doi: 10.1016/j.paid.2014.11.059
- Cole, M. W., Repovš, G., and Anticevic, A. (2014). The frontoparietal control system: a central role in mental health. *Neuroscientist* 20, 652–664. doi: 10.1177/1073858414525995
- Creem-Regehr, S. H., and Kunz, B. R. (2010). Perception and action. *Wiley Interdiscip. Rev. Cogn. Sci.* 1, 800–810. doi: 10.1002/wcs.82
- Davis, F. C., Knodt, A. R., Sporns, O., Lahey, B. B., Zald, D. H., Brigidi, B. D., et al. (2013). Impulsivity and the modular organization of resting-state neural networks. *Cereb. Cortex* 23, 1444–1452. doi: 10.1093/cercor/bhs126
- de Bézenac, C. E., Sluming, V., and Corcoran, R. (2017). Agency performance modulates resting-state variation in prefrontal brain regions. *Neuropsychologia* 111, 16–25. doi: 10.1016/j.neuropsychologia.2017.12.035
- De Luca, M., Beckmann, C. F., De Stefano, N., Matthews, P. M., and Smith, S. M. (2006). fMRI resting state networks define distinct modes of long-distance interactions in the human brain. *Neuroimage* 29, 1359–1367. doi: 10.1016/j.neuroimage.2005.08.035
- Deichmann, R., Gottfried, J. A., Hutton, C., and Turner, R. (2003). Optimized EPI for fMRI studies of the orbitofrontal cortex. *Neuroimage* 19, 430–441. doi: 10.1016/S1053-8119(03)00073-9
- Dickman, S. J. (1990). Functional and dysfunctional impulsivity: personality and cognitive correlates. *J. Pers. Soc. Psychol.* 58, 95–102. doi: 10.1037/0022-3514.58.1.95
- Dipasquale, O., Griffanti, L., Clerici, M., Nemni, R., Baselli, G., and Baglio, F. (2015). High-dimensional ICA analysis detects within-network functional connectivity damage of default-mode and sensory-motor networks in Alzheimer's disease. *Front. Hum. Neurosci.* 9:43. doi: 10.3389/fnhum.2015.00043
- Duque, J., Labruna, L., Verset, S., Olivier, E., and Ivry, R. B. (2012). Dissociating the role of prefrontal and premotor cortices in controlling inhibitory mechanisms during motor preparation. *J. Neurosci.* 32, 806–816. doi: 10.1523/JNEUROSCI.4299-12.2012
- Falconer, E., Bryant, R., Felmingham, K. L., Kemp, A. H., Gordon, E., Peduto, A., et al. (2008). The neural networks of inhibitory control in posttraumatic stress disorder. *J. Psychiatry Neurosci.* 33, 413–422.
- Filippini, N., MacIntosh, B. J., Hough, M. G., Goodwin, G. M., Frisoni, G. B., Smith, S. M., et al. (2009). Distinct patterns of brain activity in young carriers of the APOE-epsilon4 allele. *PNAS* 106, 7209–7214. doi: 10.1073/pnas.0811879106

## DATA AVAILABILITY STATEMENT

The datasets generated for this study are available on request to the corresponding author. All behavioral data is available within the manuscript.

## ETHICS STATEMENT

The studies involving human participants were reviewed and approved by the Brighton and Sussex Medical School Research Governance and Ethics Committee. The patients/participants provided their written informed consent to participate in this study.

## AUTHOR CONTRIBUTIONS

AH, HC, and TD were responsible for the study concept and design. AH carried out the study and the data analysis and drafted the manuscript. AH and TD interpreted the findings. HC and TD provided critical revisions of the manuscript for important intellectual content. All authors contributed to the article and approved the submitted version.

## FUNDING

The study was supported by the Sussex Neuroscience Ph.D. studentship awarded to AH as well as MRC Grant awarded to HC (Grant No. G2038).

- Grill-Spector, K., Kourtzi, Z., and Kanwisher, N. (2001). The lateral occipital complex and its role in object recognition. *Vis. Res.* 41, 1409–1422. doi: 10.1016/S0042-6989(01)00073-6
- Hausmann, M. (2005). Hemispheric asymmetry in spatial attention across the menstrual cycle. *Neuropsychologia* 43, 1559–1567. doi: 10.1016/j.neuropsychologia.2005.01.017
- Herman, A. M., Critchley, H. D., and Duka, T. (2018). The role of emotions and physiological arousal in modulating impulsive behaviour. *Biol. Psychol.* 133, 30–43. doi: 10.1016/j.biopsycho.2018.01.014
- Herman, A. M., Critchley, H. D., and Duka, T. (2019). Binge drinking is associated with attenuated frontal and parietal activation during successful response inhibition in fearful context. *Eur. J. Neurosci.* 50, 2297–2310. doi: 10.1111/ejn.14108
- Herman, A. M., and Duka, T. (2019). Facets of impulsivity and alcohol use: what role do emotions play? *Neurosci. Biobehav. Rev.* 106, 202–216. doi: 10.1016/j.neubiorev.2018.08.011
- Inuggi, A., Sanz-Arigita, E., González-Salinas, C., Valero-García, A. V., García-Santos, J. M., and Fuentes, L. J. (2014). Brain functional connectivity changes in children that differ in impulsivity temperamental trait. *Front. Behav. Neurosci.* 8:156. doi: 10.3389/fnbeh.2014.00156
- Jenkinson, M., Bannister, P., Brady, M., and Smith, S. (2002). Improved optimization for the robust and accurate linear registration and motion correction of brain images. *Neuroimage* 17, 825–841. doi: 10.1016/S1053-8119(02)91132-8
- Jenkinson, M., Beckmann, C. F., Behrens, T. E., Woolrich, M. W., and Smith, S. M. (2012). FSL. *Neuroimage* 62, 782–790. doi: 10.1016/j.neuroimage.2011.09.015
- Jenkinson, M., and Smith, S. (2001). A global optimisation method for robust affine registration of brain images. *Med. Image Anal.* 5, 143–156. doi: 10.1016/S1361-8415(01)00036-6
- Kelley, W. M., Wagner, D. D., and Heatherton, T. F. (2015). In search of a human self-regulation system. *Annu. Rev. Neurosci.* 38, 389–411. doi: 10.1146/annurev-neuro-071013-014243
- Korponay, C., Denticio, D., Kral, T., Ly, M., Kruis, A., Goldman, R., et al. (2017). Neurobiological correlates of impulsivity in healthy adults: lower prefrontal gray matter volume and spontaneous eye-blink rate but greater resting-state functional connectivity in basal ganglia-thalamo-cortical circuitry. *Neuroimage* 157, 288–296. doi: 10.1016/j.neuroimage.2017.06.015
- Li, C. R., Huang, C., Constable, R. T., and Sinha, R. (2006). Imaging response inhibition in a stop-signal task: neural correlates independent of signal monitoring and post-response processing. *J. Neurosci.* 26, 186–192. doi: 10.1523/JNEUROSCI.3741-05.2006
- Nomi, J. S., and Uddin, L. Q. (2015). Developmental changes in large-scale network connectivity in autism. *Neuroimage Clin.* 7, 732–741. doi: 10.1016/j.nicl.2015.02.024
- Patton, J. H., Stanford, M. S., and Barratt, E. S. (1995). Factor structure of the Barratt impulsiveness scale. *J. Clin. Psychol.* 51, 768–774. doi: 10.1002/1097-4679(199511)51:6<768
- Pruim, R. H. R., Mennes, M., van Rooij, D., Llera, A., Buitelaar, J. K., and Beckmann, C. F. (2015). ICA-AROMA: a robust ICA-based strategy for removing motion artifacts from fMRI data. *Neuroimage* 112, 267–277. doi: 10.1016/j.neuroimage.2015.02.064
- Rae, C. L., Hughes, L. E., Weaver, C., Anderson, M. C., and Rowe, J. B. (2014). Selection and stopping in voluntary action: a meta-analysis and combined fMRI study. *Neuroimage* 86, 381–391. doi: 10.1016/j.neuroimage.2013.10.012
- Reineberg, A. E., Andrews-Hanna, J. R., Depue, B. E., Friedman, N. P., and Banich, M. T. (2015). Resting-state networks predict individual differences in common and specific aspects of executive function. *Neuroimage* 104, 69–78. doi: 10.1016/j.neuroimage.2014.09.045
- Reise, S. P., Moore, T. M., Sabb, F. W., Brown, A. K., and London, E. D. (2013). The barratt impulsiveness scale-11: reassessment of its structure in a community sample. *Psychol. Assess.* 25, 631–642. doi: 10.1037/a0032161
- Schmidt, A., Muller, F., Lenz, C., Dolder, P. C., Schmid, Y., Zanchi, D., et al. (2017). Acute LSD effects on response inhibition neural networks. *Psychol. Med.* 48, 1464–1473. doi: 10.1017/S0033291717002914
- Smith, S. M., Miller, K. L., Salimi-Khorshidi, G., Webster, M., Beckmann, C. F., Nichols, T. E., et al. (2011). Network modelling methods for FMRI. *Neuroimage* 54, 875–891. doi: 10.1016/j.neuroimage.2010.08.063
- Smith, S. M., Vidaurre, D., Beckmann, C. F., Glasser, M. F., Jenkinson, M., Miller, K. L., et al. (2013). Functional connectomics from resting-state fMRI. *Trends Cogn. Sci.* 17, 666–682. doi: 10.1016/j.tics.2013.09.016
- Stanford, M. S., Mathias, C. W., Dougherty, D. M., Lake, S. L., Anderson, N. E., and Patton, J. H. (2009). Fifty years of the barratt impulsiveness scale: an update and review. *Pers. Individ. Dif.* 47, 385–395. doi: 10.1016/j.paid.2009.04.008
- The MathWorks (2015). *MATLAB Release 2015b*. Vienna: Springer.
- Uddin, L. Q., Kelly, A. M. C., Biswal, B. B., Castellanos, F. X., and Milham, M. P. (2009). Functional connectivity of default mode network components: correlation, anticorrelation, and causality. *Hum. Brain Mapp.* 30, 625–637. doi: 10.1002/hbm.20531
- Uddin, L. Q., Supekar, K., Lynch, C. J., Khourzam, A., Phillips, J., Feinstein, C., et al. (2013). Salience network-based classification and prediction of symptom severity in children with autism. *JAMA Psychiatry* 70, 869–879. doi: 10.1001/jamapsychiatry.2013.104
- van den Heuvel, M. P., and Hulshoff Pol, H. E. (2010). Exploring the brain network: a review on resting-state fMRI functional connectivity. *Eur. Neuropsychopharmacol.* 20, 519–534. doi: 10.1016/j.euroneuro.2010.03.008
- van Rooij, S. J. H., Rademaker, A. R., Kennis, M., Vink, M., Kahn, R. S., and Geuze, E. (2014). Impaired right inferior frontal gyrus response to contextual cues in male veterans with PTSD during response inhibition. *J. Psychiatry Neurosci.* 39, 330–338. doi: 10.1503/jpn.130223
- Weiskopf, N., Hutton, C., Josephs, O., and Deichmann, R. (2006). Optimal EPI parameters for reduction of susceptibility-induced BOLD sensitivity losses: a whole-brain analysis at 3 T and 1.5 T. *Neuroimage* 33, 493–504. doi: 10.1016/j.neuroimage.2006.07.029
- Winkler, A. M., Ridgway, G. R., Webster, M. A., Smith, S. M., and Nichols, T. E. (2014). Permutation inference for the general linear model. *Neuroimage* 92, 381–397. doi: 10.1016/j.neuroimage.2014.01.060
- Yeo, B. T. T., Krienen, F. M., Sepulcre, J., Sabuncu, M. R., Lashkari, D., Hollinshead, M., et al. (2011). The organization of the human cerebral cortex estimated by intrinsic functional connectivity. *J. Neurophysiol.* 106, 1125–1165. doi: 10.1152/jn.00338.2011

**Conflict of Interest:** The authors declare that the research was conducted in the absence of any commercial or financial relationships that could be construed as a potential conflict of interest.

Copyright © 2020 Herman, Critchley and Duka. This is an open-access article distributed under the terms of the Creative Commons Attribution License (CC BY). The use, distribution or reproduction in other forums is permitted, provided the original author(s) and the copyright owner(s) are credited and that the original publication in this journal is cited, in accordance with accepted academic practice. No use, distribution or reproduction is permitted which does not comply with these terms.



# Amygdala Structural Connectivity Is Associated With Impulsive Choice and Difficulty Quitting Smoking

Ausaf A. Bari<sup>1\*</sup>, Hiro Sparks<sup>1</sup>, Simon Levinson<sup>1</sup>, Bayard Wilson<sup>1</sup>, Edythe D. London<sup>2</sup>, Jean-Philippe Langevin<sup>1†</sup> and Nader Pouratian<sup>1†</sup>

<sup>1</sup>Department of Neurosurgery, University of California, Los Angeles, Los Angeles, CA, United States, <sup>2</sup>Department of Psychiatry and Biobehavioral Sciences, David Geffen School of Medicine and Semel Institute for Neuroscience and Human Behavior, University of California, Los Angeles, Los Angeles, CA, United States

## OPEN ACCESS

### Edited by:

Rutsuko Ito,  
University of Toronto, Canada

### Reviewed by:

Jibran Y. Khokhar,  
University of Guelph, Canada  
Maria Cristina Mostallino,  
National Research Council (CNR),  
Italy

### \*Correspondence:

Ausaf A. Bari  
abari@mednet.ucla.edu

<sup>†</sup>These authors have contributed  
equally to this work

### Specialty section:

This article was submitted to  
Motivation and Reward, a section of  
the journal *Frontiers in Behavioral  
Neuroscience*

**Received:** 16 March 2020

**Accepted:** 11 June 2020

**Published:** 03 July 2020

### Citation:

Bari AA, Sparks H, Levinson S,  
Wilson B, London ED, Langevin J-P  
and Pouratian N (2020) Amygdala  
Structural Connectivity Is Associated  
With Impulsive Choice and Difficulty  
Quitting Smoking.  
*Front. Behav. Neurosci.* 14:117.  
doi: 10.3389/fnbeh.2020.00117

**Introduction:** The amygdala is known to play a role in mediating emotion and possibly addiction. We used probabilistic tractography (PT) to evaluate whether structural connectivity of the amygdala to the brain reward network is associated with impulsive choice and tobacco smoking.

**Methods:** Diffusion and structural MRI scans were obtained from 197 healthy subjects (45 with a history of tobacco smoking) randomly sampled from the Human Connectome database. PT was performed to assess amygdala connectivity with several brain regions. Seed masks were generated, and statistical maps of amygdala connectivity were derived. Connectivity results were correlated with a subject performance both on a delayed discounting task and whether they met specified criteria for difficulty quitting smoking.

**Results:** Amygdala connectivity was spatially segregated, with the strongest connectivity to the hippocampus, orbitofrontal cortex (OFC), and brainstem. Connectivity with the hippocampus was associated with preference for larger delayed rewards, whereas connectivity with the OFC, rostral anterior cingulate cortex (rACC), and insula were associated with preference for smaller immediate rewards. Greater nicotine dependence with difficulty quitting was associated with less hippocampal and greater brainstem connectivity. Scores on the Fagerstrom Test for Nicotine Dependence (FTND) correlated with rACC connectivity.

**Discussion:** These findings highlight the importance of the amygdala-hippocampal-ACC network in the valuation of future rewards and substance dependence. These results will help to identify potential targets for neuromodulatory therapies for addiction and related disorders.

**Keywords:** amygdala, probabilistic tractography, smoking cessation, human connectome, impulsivity



## INTRODUCTION

The amygdala is a complex and heterogeneous structure with multiple sub-nuclei that exhibit differential connectivity with other brain regions (Swanson and Petrovich, 1998; Saygin et al., 2017) through which it mediates a wide range of behavioral responses to emotionally relevant information (Mormann et al., 2017). Although the amygdala was traditionally thought to mediate fear and aversive behavior, more recent evidence has demonstrated its role in appetitive behaviors, including reward learning, goal-directed behavior, and addiction (Wassum and Izquierdo, 2015). In rats, electrical stimulation of the basolateral nucleus of the amygdala (BLA) reinstates cocaine-seeking behavior, and inactivation of the central nucleus reduces the effect of punishment on cocaine self-administration (Xue et al., 2012). Amygdala volume also has been related to substance abuse as smaller right amygdala volumes have been associated with externalizing behaviors and cigarette smoking in adolescents (Cheetham et al., 2018).

The amygdala is a central node within a reward-related network, with connectivity to other key limbic cortical and subcortical structures that underlie reward-seeking behavior and addictive behavior. When exposed to smoking stimuli, tobacco smokers have repeatedly shown increased blood flow to a functional network involving the amygdala, nucleus accumbens (NAc), orbitofrontal cortex (OFC), hippocampus, and insula (Wilson et al., 2004; Franklin et al., 2007; Dagher et al., 2009). Imaging studies have also revealed an association between cocaine cravings and increased dopamine release in the amygdala, NAc, OFC, and anterior cingulate cortex (ACC; Koob and Volkow, 2016). Furthermore, amygdala connectivity modulates reward valuation where disconnection between the amygdala and ACC biases choices in favor of a low effort, small reward over a large reward at greater effort (Floresco and Ghods-Sharifi, 2007; Wassum and Izquierdo, 2015). Similarly, the functional disconnection between the amygdala and insula abolishes the ability to observe outcome devaluation during an instrumental conditioning task (Parkes and Balleine, 2013). Along these lines, relapse in drug addiction has been partially attributed to changes within the amygdala-hippocampus-NAc circuit. In animal models of cocaine dependence, electrical stimulation of the amygdala or the hippocampus elicits long-lasting dopamine release in the NAc which may underlie relapses in drug-seeking behavior (Blaha et al., 1997; Floresco et al., 1998; Hayes et al., 2003; Li et al., 2018). In addition to connectivity with midbrain dopaminergic neurons, amygdala connectivity to other monoaminergic nuclei within the brainstem contribute to pathological behavior. For example, the pharmacological blockade of the ventral noradrenergic bundle, which connects the amygdala to noradrenergic nuclei within the brainstem, leads to significant attenuation of heroin seeking behavior (Shaham et al., 2000; Leri et al., 2002). Connectivity of the amygdala with these structures likely influences addictive and reward-related behaviors through combined influences on reinforcement learning, reward valuation, and the subjective emotional experience associated with reward consumption.

A common feature in addiction is the preference for immediate reward even when the overall value of that reward is relatively low. This phenomenon has been formally modeled as temporal discounting in which subjects show a preference for receiving smaller immediate rewards over larger rewards in the future (McClure et al., 2004). Interpreted as a measure of impulsive choice, it has been linked with substance abuse, addiction, and relapse as well as a variety of neuropsychiatric disorders (Ahn et al., 2011; Elton et al., 2017; Owens et al., 2017). Tobacco smoking in particular has been associated with temporal discounting (Roewer et al., 2015; Ghahremani et al., 2018). Therefore, understanding the neural correlates of this behavior may yield a better understanding of the neural basis for maladaptive decision-making in individuals with various addictions, including nicotine dependence.

Previous work has shown associations between temporal discounting and several interconnected limbic structures, including the amygdala, NAc, hippocampus, OFC, parietal cortex, and ACC (Bertossi et al., 2016; Klein-Flugge et al., 2016; Frost and McNaughton, 2017; Chen et al., 2018). Here, we analyzed a large imaging and behavioral dataset to test for potential correlations between the structural connectivity of the amygdala to multiple reward-related brain regions and impulsive choice and nicotine dependence. Through this approach, we aim to evaluate the role of amygdala circuits in addictive behavior and to provide potential connectivity-based targets for future neuromodulatory therapies for nicotine dependence and other forms of addiction.

Specifically, we focus on the use of probabilistic tractography (PT) as a measure of the structural connectivity of the amygdala to other reward areas. While invasive tract tracing studies can be routinely used to study brain connectivity in animal models of addiction, their use is precluded in studies involving living human subjects. Therefore, MRI-based tractography has been used to study structural connectivity in human subjects. Increasingly, PT has been applied toward elucidating the structural organization and connectivity of the amygdala *in vivo* (Bach et al., 2011; Saygin et al., 2011), and to test for correlation of amygdala structural organization and connectivity with behavior (Greening and Mitchell, 2015; Li et al., 2018). As such, PT offers a noninvasive method of exploring how specific amygdala connections may influence addiction-related behavior and may be a promising clinical tool to evaluate potential imaging biomarkers of addiction.

## MATERIALS AND METHODS

### Subjects

Data were obtained from the publicly available WU-Minn HCP 1,200 Subjects data release repository<sup>1</sup> (Van Essen et al., 2013). The scanning protocol was approved by the Human Research Protection Office (HRPO), Washington University (IRB# 201 204 036). No human subject experimental procedures were undertaken at the authors' home institution. The participants

<sup>1</sup><https://www.humanconnectome.org/>

**TABLE 1 |** Demographics of study population.

<b>N</b>	<b>197</b>	<b>(%)</b>
<b>Age</b>		
22–25	41	(20.8)
26–30	91	(46.2)
31–35	64	(32.5)
36+	1	(0.5)
<b>Sex</b>		
F	103	(52.3)
M	94	(47.7)

included in the HCP 1,200 Subjects data release provided written informed consent as approved by the Washington University IRB. From this repository, 200 total non-twin subjects were randomly selected. The analysis was limited to 200 subjects based on available computational resources and the costs of performing the analysis. Of these, 45 reported a history of smoking tobacco. Of the 200 total subjects, three subjects were excluded due to incomplete diffusion MRI data and without *a priori* knowledge of their smoking history. The remaining 197 subjects were included in our analyses (Table 1).

## MRI Acquisition

The data were acquired in a modified Siemens 3T Skyra scanner with a customized protocol (Sotiropoulos et al., 2013). The T1-weighted MRI has an isotropic spatial resolution of 0.7 mm, and the dMRI data have an isotropic spatial resolution of 1.25 mm. The multi-shell dMRI data were collected over 270 gradient directions distributed over three b-values (1,000, 2,000, 3,000 s/mm<sup>2</sup>). For each subject, the multi-shell dMRI data were collected with both L/R and R/L phase encodings using the same gradient table, which were then merged into a single copy of multi-shell dMRI data after the correction of distortions with the HCP Preprocessing Pipeline (Glasser et al., 2013).

## Probabilistic Tractography

PT was performed using FSL's FMRIB Diffusion Toolbox (probtrackx) with modified Euler streaming (Woolrich et al., 2009; Jenkinson et al., 2012). Seed and target masks were generated using the Harvard-Oxford subcortical atlas (Desikan et al., 2006). Bilateral amygdala seed mask regions of interest (ROIs) were created. Target masks included the dorsolateral prefrontal cortex (DLPFC), hippocampus, insula, NAc, OFC, rostral anterior cingulate cortex (rACC), and brainstem. The brainstem was defined as the medulla, pons, and midbrain excluding the cerebellum as depicted by the mask in Figure 1G. All tractography was performed between each (right and left) amygdala and the ipsilateral target masks except that the entire brainstem (left and right side) was used as a target for each amygdala. Each target mask was also a termination mask such that tractography was terminated once a streamline entered the target. Ipsilateral white matter masks were used as waypoints. The ventricles and cerebellum were used as exclusion masks. We used the "one way condition," curvature 0.2, 2,000 samples, step length = 0.5, fibthresh = 0.01, distthresh = 1 and sampvox = 0.0. This resulted in 14 seed\_to\_target output files representing a voxelwise map of the number of seed samples from each

amygdala to target. To calculate the connection probability between each amygdala voxel to each of the seven targets, we ran the FSL proj\_thresh subroutine with a threshold of 1,250 on each probtrackx output. For each voxel in the seed mask with a value above the threshold, *proj\_thresh* calculates the number of samples reaching each of the target masks as a proportion of the total number of samples reaching any of the target masks. This yielded a separate map of each amygdala for each target with each voxel having a value between 0 and 1 representing the connection probability of that voxel to the given target. This method normalizes connectivity within each subject, controls for expected cohort-wide variation in amygdala volume, and enables comparisons across subjects. Thus, there were 14 maps for each subject (7 targets × 2 hemispheres). To produce an overall probability of connectivity from each amygdala to target, probabilities were averaged across all voxels in each map. Next, we created a population connectivity map across all 197 subjects. Each of the previously created proj\_thresh maps was registered to MNI 1 mm standard space, thresholded at a level of 0.1 and binarized. These maps were then added across all 197 subjects such that each voxel value now represented the number of subjects with connectivity to the target. FSL commands were performed using Amazon Web Services (AWS)<sup>2</sup> EC2 instances running in parallel. Each AWS EC2 instance was an r4.large clone of an Amazon Machine Image (AMI) running Ubuntu 14.04 with FSL software version 5.0.10. This allowed us to run tractography on all 197 subjects simultaneously in parallel. FSL bedpostx directories for each subject and the probtrackx output files were stored on an Amazon S3 bucket.

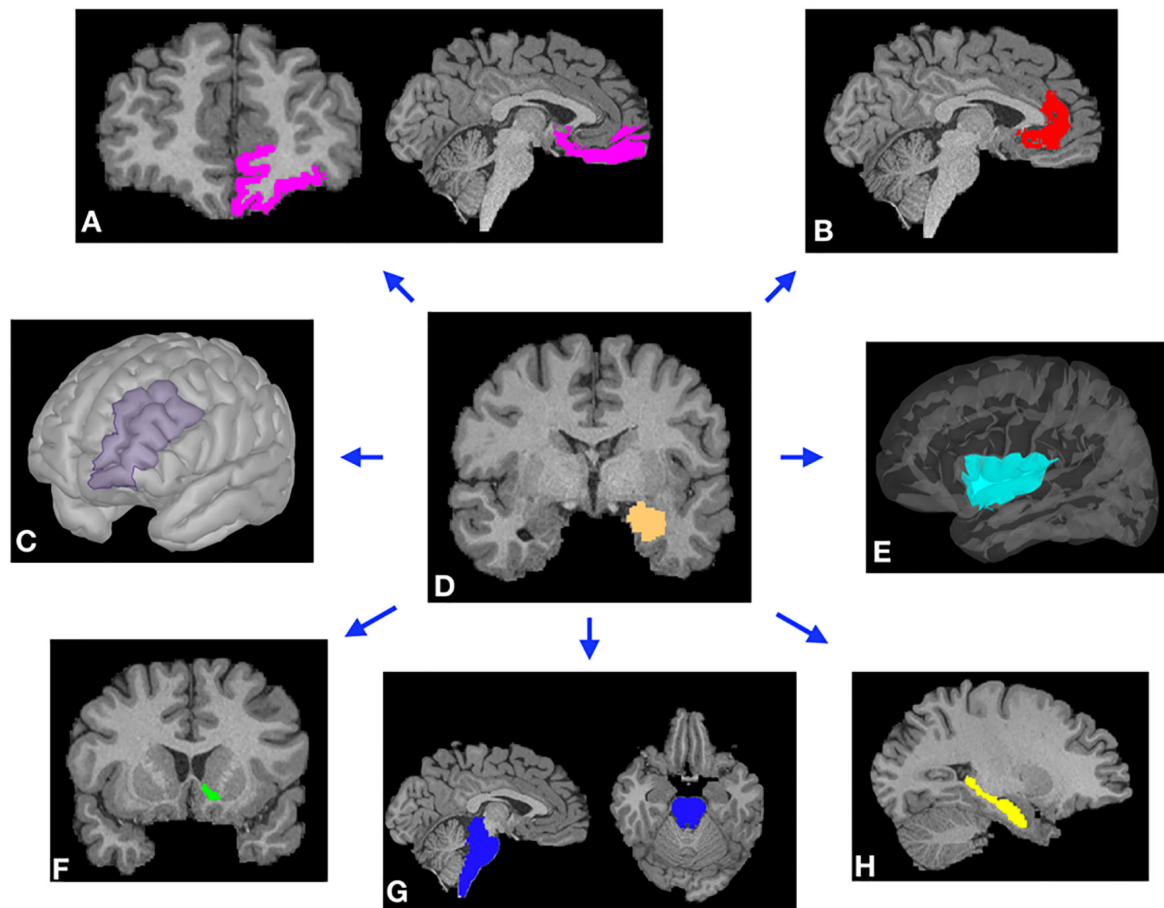
## Behavioral Assessments

As part of the screening process, all subjects were given a comprehensive assessment of psychiatric and substance use history over the phone including the Semi-Structured Assessment for the Genetics of Alcoholism (SSAGA), which is a well-validated diagnostic instrument used in numerous previous large-scale studies, assessing a range of diagnostic categories including tobacco dependence (Kozlowski et al., 1994; Barch et al., 2013). In particular, participants were scored as either low (1 point) or high (5 points) depending on whether they met DSM criteria for tobacco dependence with difficulty quitting ("DSM tobacco dependence—difficulty quitting"). Other measures of tobacco dependence included the Fagerstrom Test for Nicotine Dependence (FTND). All tests were performed by WU-MINN HCP researchers (Barch et al., 2013). None of the test data was collected by any of the authors.

## Temporal Discounting Task

The impulsive choice was measured using a paradigm originally developed by Kirby (2009). The task identifies "indifference points" at which a person is equally likely to choose a smaller reward (e.g., \$100 now) sooner rather than a larger reward (\$200 in 1 year). Based on the work of Green and Myerson,

<sup>2</sup><http://aws.amazon.com>



**FIGURE 1** | Representative examples of cortical (A–C,E) and subcortical (F–H) masks of the target brain areas and the amygdala (D, center) from a single subject. Masks were derived from Freesurfer automated segmentation included in the HCP dataset and were used to perform probabilistic tractography (PT) from the amygdala to each target. (A) Orbitofrontal cortex (OFC). (B) Rostral anterior cingulate cortex (rACC). (C) Dorsolateral prefrontal cortex (DLPFC). (D) Amygdala. (E) Insular cortex. (F) Nucleus accumbens (NAc). (G) Brainstem. (H) Hippocampus.

an adjusting-amount approach was used in which the delay is fixed but reward amounts are adjusted on a trial-by-trial basis based on the subject's choices (Estle et al., 2006). The area under the discounting curve (AUC<sub>200</sub>) was used as an index of discounting (Myerson et al., 2001). All data collection was performed by the WU-MINN consortium (Barch et al., 2013).

## Statistical Analysis

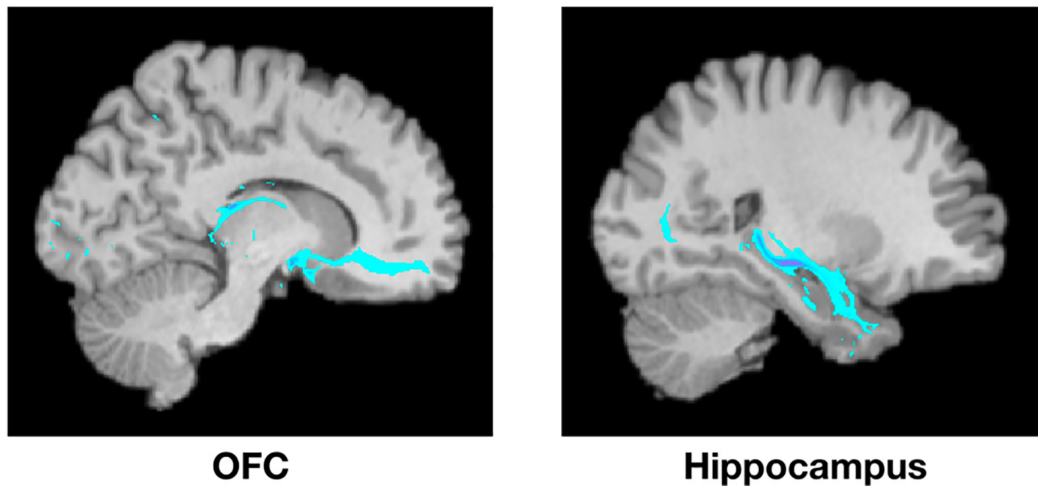
All statistical analysis was carried out using the R software package<sup>3</sup>. One factor analysis of variance (ANOVA) was used for amygdala connectivity to target regions with Tukey HSD used for multiple comparisons correction. For analysis of the association of connectivity with impulsivity, Pearson product-moment coefficients were calculated. For testing the association between connectivity to target and difficulty quitting tobacco smoking, a two factor ANOVA model was utilized with Tukey HSD used for multiple comparisons for the interaction effect.

<sup>3</sup><http://www.R-project.org/>

## RESULTS

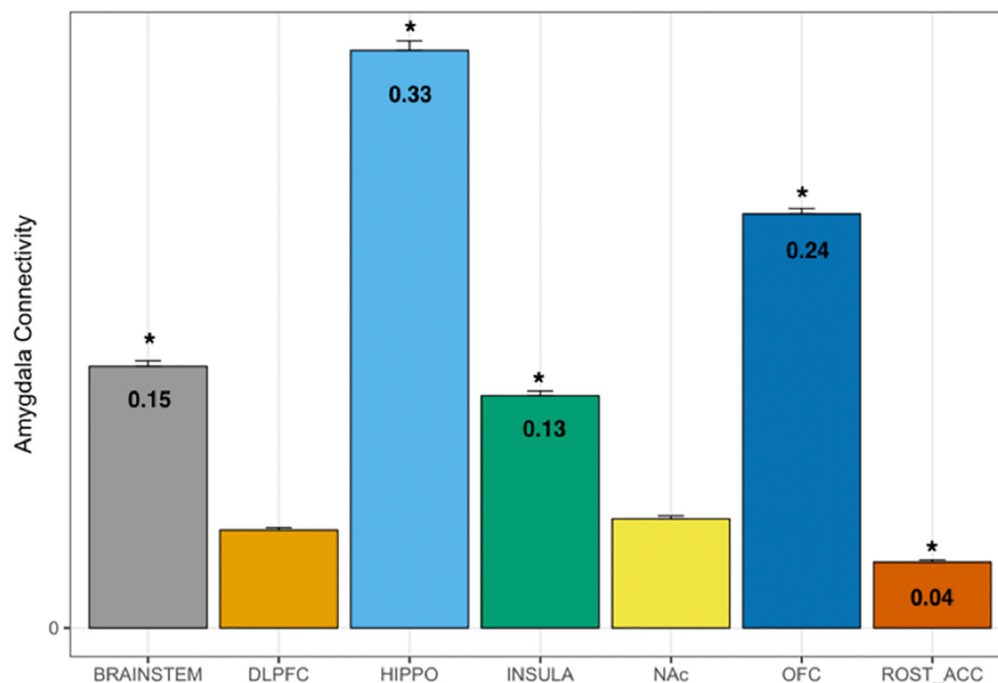
Using DTI data from 197 subjects, we performed PT from the amygdala to the following seven pre-determined target structures: whole brainstem, DLPFC, hippocampus, insula, NAc, OFC, and the rACC (Figures 1, 2). The relative probability of connectivity was averaged over all amygdala voxels and this value then averaged across all subjects (Figure 3). The amygdala displayed the highest probability of connectivity with the hippocampus relative to other targets (one-way ANOVA with Tukey HSD,  $n = 2,758$ ,  $p < 0.001$  for all significant comparisons, Tables 2, 3).

Next, we tested whether connectivity of the amygdala to these target structures was spatially segregated or diffuse across all amygdala voxels. Individual connectivity maps were normalized to MNI standard space, thresholded, binarized, and summed across all subjects to determine a population connectivity map for each amygdala voxel to each target (Figure 4). We found that connectivity with the insula, NAc, DLPFC, and rACC was



**FIGURE 2 |** Example of PT from the amygdala to the OFC (left) and the hippocampus (right) from a single representative subject. Highlighted areas represent the number of streamlines passing through each voxel. The number of streamlines reaching each target mask was added and divided by the total number of streamlines reaching any of the seven target masks to calculate the probability of connectivity between the amygdala and each target.

### Relative Connectivity Between Amygdala and Target Areas



**FIGURE 3 |** Probability of connectivity from the amygdala to each target region. Note that the highest probability of connectivity is to the hippocampus (33%). Thus, 33% of all tracks from the amygdala to the above targets terminated in the hippocampus. DLPFC, dorsolateral prefrontal cortex; HIPPO, hippocampus; NAc, nucleus accumbens; OFC, orbitofrontal cortex; ROST\_ACC, rostral anterior cingulate cortex; one-way ANOVA,  $p < 0.001$ .

relatively segregated with a preference toward the dorsolateral amygdala. Meanwhile, connectivity with the brainstem and

hippocampus was relatively diffuse with a localization trend toward the central, relatively medial amygdala.

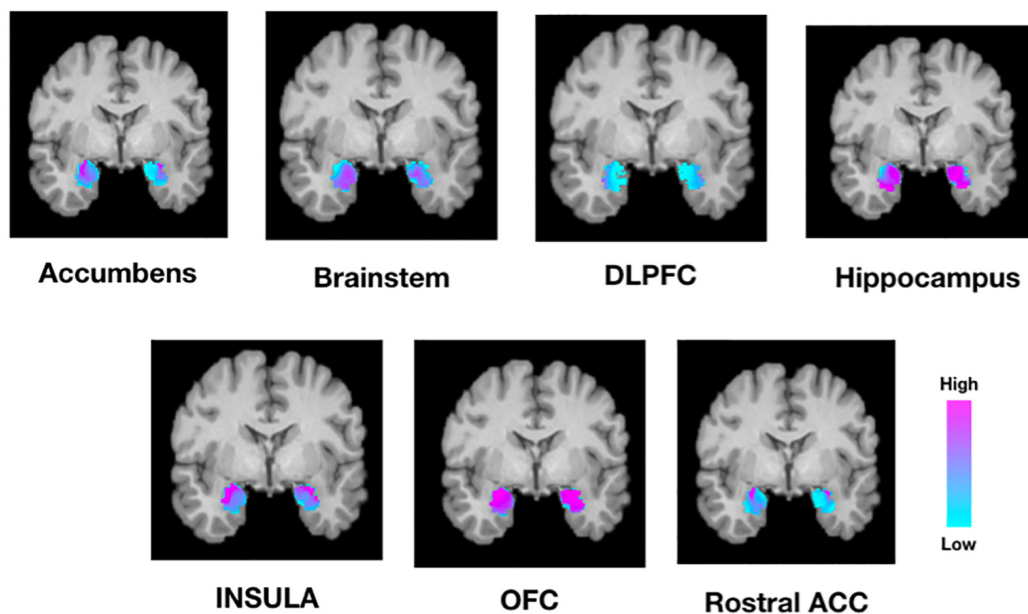


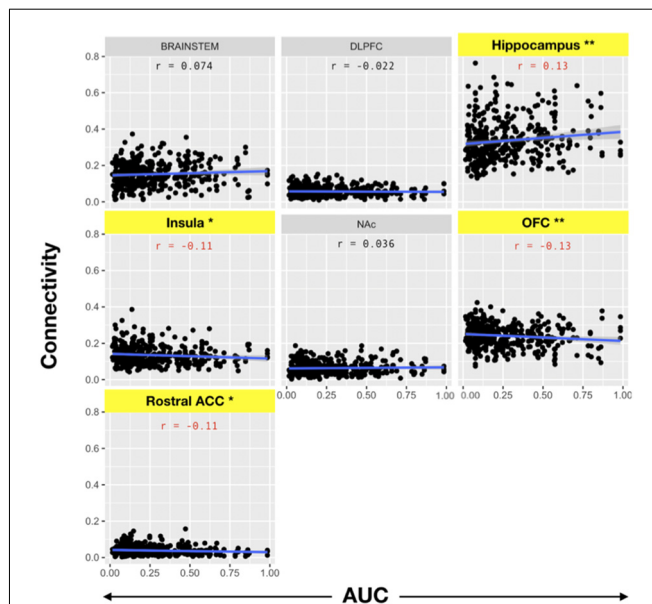
**TABLE 2** | ANOVA for connectivity by target.

	DF	Sum Sq.	Mean Sq.	F-value	Pr ( >F)
Target	6	28.21	4.702	1,267	<2e-16**
Residuals	2,751	10.21	0.004		

\*\* $p < 0.001$ **TABLE 3** | Tukey HSD Multiple Comparisons for mean connectivity between the amygdala and each target structure.

Target comparison	Estimate	Std. Error	t-value	Pr ( > t )	
DLPFC—BRAINSTEM	−0.095179	0.004341	−21.927	<0.001	**
HIPPO—BRAINSTEM	0.183838	0.004341	42.352	<0.001	**
INSULA—BRAINSTEM	−0.016964	0.004341	−3.908	= 0.00179	*
NAC—BRAINSTEM	−0.088717	0.004341	−20.439	<0.001	**
OFC—BRAINSTEM	0.088728	0.004341	20.441	<0.001	**
rACC—BRAINSTEM	−0.113867	0.004341	−26.233	<0.001	**
HIPPO—DLPFC	0.279018	0.004341	64.28	<0.001	**
INSULA—DLPFC	0.078215	0.004341	18.019	<0.001	**
NAC—DLPFC	0.006462	0.004341	1.489	= 0.75172	
OFC—DLPFC	0.183907	0.004341	42.368	<0.001	**
rACC—DLPFC	−0.018688	0.004341	−4.305	<0.001	**
INSULA—HIPPO	−0.200802	0.004341	−46.261	<0.001	**
NAC—HIPPO	−0.272556	0.004341	−62.791	<0.001	**
OFC—HIPPO	−0.095111	0.004341	−21.911	<0.001	**
rACC—HIPPO	−0.297705	0.004341	−68.585	<0.001	**
NAC—INSULA	−0.071753	0.004341	−16.53	<0.001	**
OFC—INSULA	0.105692	0.004341	24.349	<0.001	**
rACC—INSULA	−0.096903	0.004341	−22.324	<0.001	**
OFC—NAC	0.177445	0.004341	40.88	<0.001	**
rACC—NAC	−0.02515	0.004341	−5.794	<0.001	**
rACC—OFC	−0.202595	0.004341	−46.674	<0.001	**

\*\* $p < 0.001$ , \* $p < 0.05$ **FIGURE 4** | Population maps of amygdala connectivity to each target structure. The scale indicated the number of subjects that showed connectivity from each amygdala voxel to each target structure. For example, while the amygdala was homogeneously connected to the OFC and hippocampus, there was greater segregation of connectivity to the insula, rostral ACC, and nucleus accumbens. DLPFC, dorsolateral prefrontal cortex; OFC, orbitofrontal cortex; Rostral ACC, rostral anterior cingulate cortex.



**FIGURE 5 |** Pearson product-moment correlation of connectivity to the target structure and the area under the delay discounting curve [area under the curve (AUC)]. Connectivity between each target and the amygdala was calculated. Subsequently, the correlation coefficient between amygdala-target connectivity and the AUC of the temporal discounting behavior curve was determined. Note that AUC is inversely related to impulsive choice in that a high AUC indicates less discounting while lower AUC values indicate higher discounting or more impulsive choice. Yellow bars indicate structures with significant correlations with impulsive choice behavior. There was a significant correlation between the hippocampus ( $r = 0.13$ ) and the AUC (i.e., decreased discounting). On the other hand, there was a significant negative correlation between connectivity with the OFC ( $r = -0.13$ ), insula ( $r = -0.11$ ), and rACC ( $r = -0.11$ ) with the AUC (i.e., increased discounting;  $*p < 0.05$ ,  $**p < 0.001$ ).

We then evaluated the correlation between amygdala connectivity to each target structure and temporal discounting, using the area under the curve (AUC) for responses as an index of discounting reward value as a function of delay. Connectivity to the hippocampus was inversely correlated with temporal discounting whereas connectivity to the OFC, rACC, and insula were positively associated with greater preference for smaller, more immediate rewards (Pearson product-moment correlation,  $n = 197$ , hippocampus  $r = 0.13$ ,  $p < 0.01$ ; OFC  $r = -0.13$ ,  $p < 0.01$ ; insula  $r = -0.11$ ,  $p < 0.05$ ; rACC  $r = -0.11$ ,  $p < 0.05$ , **Figure 5, Table 4**). There was no significant correlation

**TABLE 4 |** Pearson product-moment correlation for amygdala connectivity and area under the curve (AUC) for the delay discounting task.

Target	Estimate ( $r$ )	$p$ -value
DLPFC	-0.022	0.657
rACC	-0.106	0.036*
NAc	0.036	0.482
OFC	-0.130	0.010**
INSULA	-0.107	0.034*
HIPPO	0.130	0.010**
BRAINSTEM	0.074	0.141

\*\* $p \leq 0.01$ , \* $p \leq 0.05$

between the AUC and connectivity with the brainstem, DLPFC, or NAc.

Addiction to nicotine, and substance abuse in general, has been previously associated with impulsivity (Moody et al., 2016; Hofmeyr et al., 2017). We sought to better characterize the role of the amygdala's structural connectivity to other brain reward areas in mediating nicotine addiction. To this end, we utilized behavioral measures of difficulty quitting and the FTND scores as measures of severity of nicotine dependence. We found a significant interaction effect between connectivity to reward targets and tobacco dependence with difficulty quitting and FTND scores. Comparisons revealed that connectivity of the amygdala to the hippocampus was associated with low difficulty quitting and connectivity with the brainstem was associated with high difficulty quitting. There was also a trend of high difficulty quitting associated with connectivity to the OFC and rACC but this was not statistically significant [Two-factor ANOVA (Target, Level of Difficulty Quitting),  $n = 45$ ,  $p < 0.001$ , **Table 5, Figure 6**]. Similarly, amygdala connectivity with the rACC was significantly correlated with higher FTND scores, indicative of dependence (**Table 6**).

## DISCUSSION

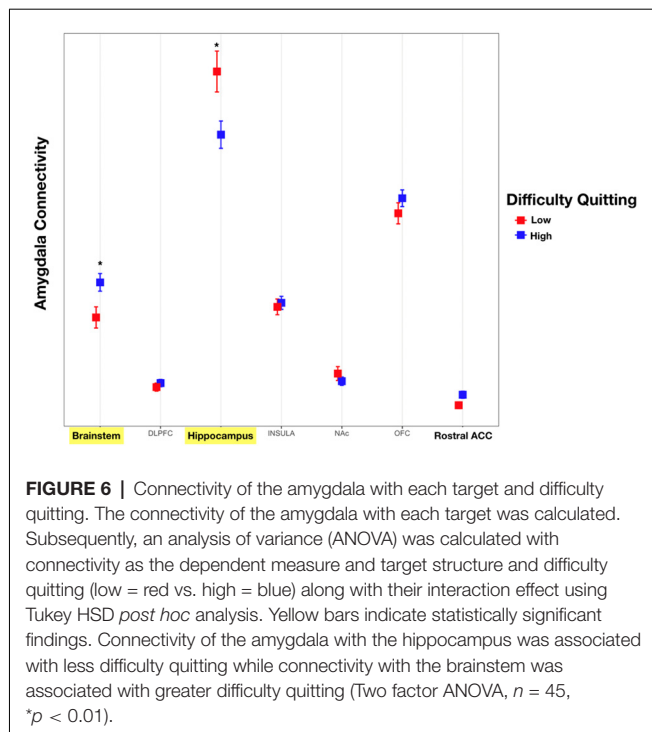
In this study, we utilize PT to compare the relative structural connectivity of the amygdala to other brain areas involved in reward processing to determine the correlation between this connectivity and behaviors associated with reward processing. The results show that an amygdala-hippocampal-OFC-ACC network plays a role in the valuation of future rewards and nicotine dependence. This is one of the highest-powered studies to utilize PT to correlate the structural connectivity of the

**TABLE 5 |** Tukey pairwise comparisons for an interaction effect between target and difficulty quitting smoking for both levels of the "Difficulty Quitting" factor (low vs. high).

Target	Df 1	Df 2	F-Ratio	$p$ -value
BRAINSTEM	1	630	7.355	0.0069*
DLPFC	1	630	0.098	0.7549
HIPPO	1	630	23.879	<0.0001**
INSULA	1	630	0.097	0.7554
NAc	1	630	0.347	0.5563
OFC	1	630	1.362	0.2436
rACC	1	630	0.658	0.4177

\*\* $p < 0.001$ , \* $p < 0.01$

Response Variable: Connectivity to Target.



amygdala with impulsive choice and substance abuse. This technique has been used before to segment the amygdala into subnuclear components corresponding to its *in vivo* organization (Bach et al., 2011; Abivardi and Bach, 2017; Saygin et al., 2017). Our results focused on the connectivity of the amygdala to brain areas implicated in reward and decision-making, including the DLPFC, hippocampus, insular cortex, NAc, OFC, and rACC. We also included the brainstem in our analysis because of evidence that the amygdala modulates the activity of midbrain dopaminergic neurons, and receives input from brainstem nuclei, such as the locus coeruleus and nucleus of the solitary tract in mediating behavioral and autonomic responses to emotional stimuli (Veening et al., 1984; Petrov et al., 1993; Rodríguez-Ortega et al., 2017). Of the pre-selected brain targets, the amygdala had the highest probability of connectivity with the hippocampus and OFC, followed by the brainstem and insula, and lowest connectivity to the DLPFC, NAc, and rACC (Figure 3). While functional connectivity between the amygdala and all of these regions has been confirmed in prior studies, the present study is the largest to date to delineate structural connectivity to these areas and correlate connectivity with impulsive choice and measures of nicotine addiction. Furthermore, it is the first to show an association of amygdala structural connectivity with both impulsive choice and nicotine dependence. The higher probability of connectivity with the hippocampus, OFC, and brainstem are particularly interesting given that these regions have been previously implicated in smoking behavior. For example, fMRI data shows that hippocampal activation is associated with subjects assigning a higher value to future rewards (Clewett et al., 2014). A separate study identified an association between functional

**TABLE 6 |** Pearson product-moment correlation for amygdala-rACC connectivity and the fagerstrom test for nicotine dependence.

Target	Score	Correlation coefficient	<i>p</i> -value
rACC	FTND	0.20	0.048*

\* $p < 0.05$

connectivity of the hippocampus and the ACC and a reduction in delay discounting when subjects invoked episodic future imagination (Hu et al., 2016). This association between the amygdala and memory for drug reward was corroborated by our findings of an inverse correlation between delay discounting and amygdala structural connectivity with the hippocampus (Figure 5). However, we found that connectivity with the ACC was related to preference for smaller sooner rewards. Our results support the involvement of an amygdala-hippocampal-ACC network in the valuation of future rewards. Others have proposed that the specific role of the amygdala in reward may not lie in Pavlovian or instrumental conditioned responding but rather in reward learning in the context of changing incentive values (Wassum and Izquierdo, 2015). Thus, connectivity with the ACC and hippocampus may support the structural mechanism underlying this phenomenon.

Performance on the delay discounting task has been interpreted as a measure of impulsivity and a possible model for substance abuse and relapse (Richards et al., 1999). For example, it has been shown that less temporal discounting is associated with a higher intention to quit smoking (Athamneh et al., 2017). In this article, we show that connectivity between the amygdala and hippocampus is associated with both decreased delay discounting as well as less difficulty quitting (Figures 5, 6). These findings support the concept that connectivity with the hippocampus enhances smoking cessation behavior by increasing the value of future rewards. On the other hand, connectivity with the brainstem was associated with more difficulty quitting. The brainstem is known to play a role in the neuropharmacology of nicotine and is a direct target of outputs from the central nucleus of the amygdala (Veening et al., 1984). For example, nicotine may modulate brainstem nuclei such as the ventral tegmental area, locus coeruleus, dorsal motor nucleus of the vagus, and the nucleus of the solitary tract through its activity at nicotinic receptors (Dehkordi et al., 2015). Noradrenergic signaling from the locus coeruleus to the extended amygdala is also associated with relapse to substance abuse, including smoking (Smith and Aston-Jones, 2008). Thus, structural connectivity between the amygdala and brainstem may mediate relapse to nicotine use.

In contrast to connectivity with the hippocampus, connectivity with the OFC, rACC, and insula was associated with preference for more immediate rewards (Figure 5). Based on non-human primate anatomical studies, the OFC is known to be directly connected to the amygdala (Cavada et al., 2000). The relative roles of these two structures in reward are dissociable. In rodent studies, lesions of the BLA increase preference for smaller immediate rewards, while OFC lesions paradoxically increase preference for more delayed rewards (Churchwell et al., 2009). It is known that the OFC updates the incentive value of

outcomes such as the effect of time on the devaluation of future rewards (Wallis and Miller, 2003). Thus, increasing time delays result in a devaluation of the corresponding reward, with the updated value represented by the OFC (Ainslie, 1975). Here, we show that greater OFC connectivity with the amygdala is linked to a preference for more immediate rather than larger delayed rewards. This was also reflected in our finding that increased OFC connectivity was associated with more difficulty quitting smoking, although this effect did not reach statistical significance (**Figure 6**). We found a similar trend with connectivity to the insula and rACC with higher connectivity associated with lower AUCs reflecting a preference for more immediate choices. Also, connectivity with the rACC was associated with higher FTND scores of nicotine dependence (**Table 6**). Resting state fMRI has shown that functional connectivity between the insula and ACC and a monetary reward network is associated with increased discounting (Li et al., 2013). However, their analysis did not include the amygdala which may limit comparability with our data. Taken together, our structural connectivity findings support a dissociable role of the hippocampus compared to the insula/OFC/rACC in the amygdala reward network.

To further validate connectivity results and potentially inform targeting strategies for future neuromodulatory therapies, we report topographical organization patterns of amygdala connectivity (**Figure 4**). The amygdala is comprised of several subnuclei which have been grouped according to cytoarchitecture, neuroanatomical connectivity, and putative function. The central nucleus (CeA) and the BLA are two subnuclei that have been particularly implicated in the control of emotional processes (Cardinal et al., 2002). The BLA is constituted by the lateral (LN), basal (BN), and accessory basal nuclei (ABN) with extensive projections to the neocortex and NAc (Cardinal et al., 2002). Meanwhile, the CeA is generally thought to regulate behavioral and autonomic responses *via* strong anatomical connectivity with the brainstem (Cardinal et al., 2002). Our tractography results are broadly consistent with this organizational framework, where the NAc, DLPFC, insula, and rACC most strongly connected to lateral portions of the amygdala, while brainstem connectivity appeared relatively medial (**Figure 4**).

Our findings may help to inform strategies and identify potential targets of neuromodulatory therapy. Our group previously reported an association between stimulation of the BN and hedonic emotions (e.g., happiness and euphoria) in PTSD patients (Avecillas-Chasin et al., 2020). This effect may be important to note with regards to future neuromodulatory therapies for addiction, especially given previous studies describing the increase in NAc dopamine release and relapse in drug-seeking behavior with non-specific BLA stimulation (Blaha et al., 1997; Floresco et al., 1998; Hayes et al., 2003; Li et al., 2018). Taken together with the topographical and behavioral results related to amygdala connectivity, it may be preferable to target stimulation toward the LN portion of the BLA, to inhibit pathological connectivity with the insula and rACC (which were found to be associated with more impulsive decision making). Alternatively, if stimulation protocols could be designed to enhance functional connectivity, there may be

benefits in targeting loci within the hippocampus to enhance beneficial communication between the hippocampus and the amygdala. Several other nodes within the tested network were found to correlate with pathological behavior and merit further investigation as potential targets of neuromodulation. For example, greater connectivity between the amygdala and the brainstem correlates with both impulsive decisions and greater difficulty quitting smoking. We previously discussed several possible brainstem nuclei which may underlie this behavioral effect. Future studies should be directed toward identifying these nuclei and testing feasibility of targeting for neuromodulation.

The current study has several limitations. Discounting behavior and addiction are complex phenomena with multiple neurophysiological, environmental, and genetic influences. Here, we attempt to correlate complex behaviors with discrete structural imaging findings. We were limited to the HCP database which only includes limited measures of smoking dependence with the majority of subjects did not respond to this questionnaire resulting in a highly powered temporal discounting analysis, but a relatively lower powered nicotine dependence analysis. Also, the temporal discounting monetary task may have limited generalizability to substance abuse and dependence (Lopez et al., 2015), and subjects did not undergo other independent explicit impulsivity assessments such as the Barrett Impulsivity Scale 11 (BIS-11). Other prior studies have shown associations between tobacco dependence and temporal discounting (Roewer et al., 2015; Ghahremani et al., 2018). Given that our analysis was correlational, we cannot definitively make conclusions regarding causality between these correlated behavioral measures and connectivity. Finally, we are skeptical of ascribing functional significance and directionality to structural connectivity as measured by PT. Thus, while, we describe an amygdala reward network with a tendency to view connectivity as efferent projections from a central amygdala hub to our target regions, it is equally valid to view the amygdala as the target of axonal projections from these areas. Future work must integrate functional neuroimaging and invasive neurophysiological recordings to corroborate these structural connectivity findings.

## DATA AVAILABILITY STATEMENT

The datasets generated for this study are available on request to the corresponding author.

## ETHICS STATEMENT

The studies involving human participants were reviewed and approved by Human Research Protection Office (HRPO), Washington University (IRB# 201 204 036). The patients/participants provided their written informed consent to participate in this study.

## AUTHOR CONTRIBUTIONS

AB and NP were responsible for the study concept and design. HS, BW, and SL assisted with data analysis. NP, J-PL, and



EL assisted with data analysis and interpretation of findings. AB drafted the manuscript. J-PL, EL, and NP provided critical revision of the manuscript for intellectual content. All authors critically reviewed content and approved the final version for publication.

## FUNDING

This study was supported by funds from the University of California, Los Angeles H.H. Lee Surgical Scholars Research Award. Data were provided (in part) by the

Human Connectome Project, WU-Minn Consortium (Principal Investigators: David Van Essen and Kamil Ugurbil; 1U54MH091657) funded by the 16 NIH Institutes and Centers that support the NIH Blueprint for Neuroscience Research; and by the McDonnell Center for Systems Neuroscience at Washington University.

## ACKNOWLEDGMENTS

We would like to acknowledge the Casa Colina Hospital and Centers for Healthcare for their generous support of this work.

## REFERENCES

- Abivardi, A., and Bach, D. R. (2017). Deconstructing white matter connectivity of human amygdala nuclei with thalamus and cortex subdivisions *in vivo*. *Hum. Brain Mapp.* 38, 3927–3940. doi: 10.1002/hbm.23639
- Ahn, W. Y., Rass, O., Fridberg, D. J., Bishara, A. J., Forsyth, J. K., Breier, A., et al. (2011). Temporal discounting of rewards in patients with bipolar disorder and schizophrenia. *J. Abnorm. Psychol.* 120, 911–921. doi: 10.1037/a0023333
- Ainslie, G. (1975). Specious reward: a behavioral theory of impulsiveness and impulse control. *Psychol. Bull.* 82, 463–496. doi: 10.1037/h0076860
- Athamneh, L. N., Stein, J. S., and Bickel, W. K. (2017). Will delay discounting predict intention to quit smoking? *Exp. Clin. Psychopharmacol.* 25, 273–280. doi: 10.1037/pha0000129
- Avecillas-Chasin, J. M., Justo, M., Levinson, S., Koek, R., Krah, S. E., Chen, J. W., et al. (2020). Structural correlates of emotional response to electrical stimulation of the amygdala in subjects with PTSD. *Brain Stimul.* 13, 424–426. doi: 10.1016/j.brs.2019.12.004
- Bach, D. R., Behrens, T. E., Garrido, L., Weiskopf, N., and Dolan, R. J. (2011). Deep and superficial amygdala nuclei projections revealed *in vivo* by probabilistic tractography. *J. Neurosci.* 31, 618–623. doi: 10.1523/JNEUROSCI.2744-10.2011
- Barch, D. M., Burgess, G. C., Harms, M. P., Petersen, S. E., Schlaggar, B. L., Corbetta, M., et al. (2013). Function in the human connectome: task-fMRI and individual differences in behavior. *NeuroImage* 80, 169–189. doi: 10.1016/j.neuroimage.2013.05.033
- Bertossi, E., Tesini, C., Cappelli, A., and Ciaramelli, E. (2016). Ventromedial prefrontal damage causes a pervasive impairment of episodic memory and future thinking. *Neuropsychologia* 90, 12–24. doi: 10.1016/j.neuropsychologia.2016.01.034
- Blaha, C. D., Yang, C. R., Floresco, S. B., Barr, A. M., and Phillips, A. G. (1997). Stimulation of the ventral subiculum of the hippocampus evokes glutamate receptor-mediated changes in dopamine efflux in the rat nucleus accumbens. *Eur. J. Neurosci.* 9, 902–911. doi: 10.1111/j.1460-9568.1997.tb01441.x
- Cardinal, R. N., Parkinson, J. A., Hall, J., and Everitt, B. J. (2002). Emotion and motivation: the role of the amygdala, ventral striatum and prefrontal cortex. *Neurosci. Biobehav. Rev.* 26, 321–352. doi: 10.1016/s0149-7634(02)00007-6
- Cavada, C., Compañy, T., Tejedor, J., Cruz-Rizzolo, R. J., and Reinoso-Suárez, F. (2000). The anatomical connections of the macaque monkey orbitofrontal cortex. A review. *Cereb. Cortex* 10, 220–242. doi: 10.1093/cercor/10.3.220
- Cheetham, A., Allen, N. B., Whittle, S., Simmons, J., Yücel, M., and Lubman, D. I. (2018). Amygdala volume mediates the relationship between externalizing symptoms and daily smoking in adolescence: a prospective study. *Psychiatry Res. Neuroimaging* 276, 46–52. doi: 10.1016/j.psychres.2018.03.007
- Chen, Z., Guo, Y., Suo, T., and Feng, T. (2018). Coupling and segregation of large-scale brain networks predict individual differences in delay discounting. *Biol. Psychol.* 133, 63–71. doi: 10.1016/j.biopsycho.2018.01.011
- Churchwell, J. C., Morris, A. M., Heurtelou, N. M., and Kesner, R. P. (2009). Interactions between the prefrontal cortex and amygdala during delay discounting and reversal. *Behav. Neurosci.* 123, 1185–1196. doi: 10.1037/a0017734
- Clewett, D., Luo, S., Hsu, E., Ainslie, G., Mather, M., and Monterosso, J. (2014). Increased functional coupling between the left fronto-parietal network and anterior insula predicts steeper delay discounting in smokers. *Hum. Brain Mapp.* 35, 3774–3787. doi: 10.1002/hbm.22436
- Dagher, A., Tannenbaum, B., Hayashi, T., Pruessner, J. C., and McBride, D. (2009). An acute psychosocial stress enhances the neural response to smoking cues. *Brain Res.* 1293, 40–48. doi: 10.1016/j.brainres.2009.07.048
- Dehkordi, O., Rose, J. E., Asadi, S., Manaye, K. F., Millis, R. M., and Jayam-Trouth, A. (2015). Neuroanatomical circuitry mediating the sensory impact of nicotine in the central nervous system. *J. Neurosci. Res.* 93, 230–243. doi: 10.1002/jnr.23477
- Desikan, R. S., Ségonne, F., Fischl, B., Quinn, B. T., Dickerson, B. C., Blacker, D., et al. (2006). An automated labeling system for subdividing the human cerebral cortex on MRI scans into gyral based regions of interest. *NeuroImage* 31, 968–980. doi: 10.1016/j.neuroimage.2006.01.021
- Elton, A., Smith, C. T., Parrish, M. H., and Boettiger, C. A. (2017). Neural systems underlying individual differences in intertemporal decision-making. *J. Cogn. Neurosci.* 29, 467–479. doi: 10.1162/jocn\_a\_01069
- Estle, S. J., Green, L., Myerson, J., and Holt, D. D. (2006). Differential effects of amount on temporal and probability discounting of gains and losses. *Mem. Cognit.* 34, 914–928. doi: 10.3758/bf03193437
- Floresco, S. B., and Ghods-Sharifi, S. (2007). Amygdala-prefrontal cortical circuitry regulates effort-based decision making. *Cereb. Cortex* 17, 251–260. doi: 10.1093/cercor/bhj143
- Floresco, S. B., Yang, C. R., Phillips, A. G., and Blaha, C. D. (1998). Basolateral amygdala stimulation evokes glutamate receptor-dependent dopamine efflux in the nucleus accumbens of the anesthetized rat. *Eur. J. Neurosci.* 10, 1241–1251. doi: 10.1046/j.1460-9568.1998.00133.x
- Franklin, T. R., Wang, Z., Wang, J., Sciortino, N., Harper, D., Li, Y., et al. (2007). Limbic activation to cigarette smoking cues independent of nicotine withdrawal: a perfusion fMRI study. *Neuropsychopharmacology* 32, 2301–2309. doi: 10.1038/sj.npp.1301371
- Frost, R., and McNaughton, N. (2017). The neural basis of delay discounting: a review and preliminary model. *Neurosci. Biobehav. Rev.* 79, 48–65. doi: 10.1016/j.neubiorev.2017.04.022
- Gahremani, D. G., Faulkner, P., Cox, C. M., and London, E. D. (2018). Behavioral and neural markers of cigarette-craving regulation in young-adult smokers during abstinence and after smoking. *Neuropsychopharmacology* 43, 1616–1622. doi: 10.1038/s41386-018-0019-7
- Glasser, M. F., Sotiropoulos, S. N., Wilson, J. A., Coalson, T. S., Fischl, B., Andersson, J. L., et al. (2013). The minimal preprocessing pipelines for the human connectome project. *NeuroImage* 80, 105–124. doi: 10.1016/j.neuroimage.2013.04.127
- Greening, S. G., and Mitchell, D. G. (2015). A network of amygdala connections predict individual differences in trait anxiety. *Hum. Brain Mapp.* 36, 4819–4830. doi: 10.1002/hbm.22952
- Hayes, R. J., Vorel, S. R., Spector, J., Liu, X., and Gardner, E. L. (2003). Electrical and chemical stimulation of the basolateral complex of the amygdala reinstates cocaine-seeking behavior in the rat. *Psychopharmacology* 168, 75–83. doi: 10.1007/s00213-002-1328-3
- Hofmeyr, A., Monterosso, J., Dean, A. C., Morales, A. M., Bilder, R. M., Sabb, F. W., et al. (2017). Mixture models of delay discounting and smoking behavior. *Am. J. Drug Alcohol. Abuse* 43, 271–280. doi: 10.1080/00952990.2016.1198797

- Hu, X., Kleinschmidt, H., Martin, J. A., Han, Y., Thelen, M., Meibeth, D., et al. (2016). A reduction in delay discounting by using episodic future imagination and the association with episodic memory capacity. *Front. Hum. Neurosci.* 10:663. doi: 10.3389/fnhum.2016.00663
- Jenkinson, M., Beckmann, C. F., Behrens, T. E., Woolrich, M. W., and Smith, S. M. (2012). FSL. *NeuroImage* 62, 782–790. doi: 10.1016/j.neuroimage.2011.09.015
- Kirby, K. N. (2009). One-year temporal stability of delay-discount rates. *Psychon. Bull. Rev.* 16, 457–462. doi: 10.3758/pbr.16.3.457
- Klein-Flügge, M. C., Kennerley, S. W., Friston, K., and Bestmann, S. (2016). Neural signatures of value comparison in human cingulate cortex during decisions requiring an effort-reward trade-off. *J. Neurosci.* 36, 10002–10015. doi: 10.1523/JNEUROSCI.0292-16.2016
- Koob, G. F., and Volkow, N. D. (2016). Neurobiology of addiction: a neurocircuitry analysis. *Lancet Psychiatry* 3, 760–773. doi: 10.1016/s2215-0366(16)00104-8
- Kozłowski, L. T., Porter, C. Q., Orleans, C. T., Pope, M. A., and Heatherston, T. (1994). Predicting smoking cessation with self-reported measures of nicotine dependence: FTQ, FTND, and HSI. *Drug Alcohol Depend.* 34, 211–216. doi: 10.1016/0376-8716(94)90158-9
- Leri, F., Flores, J., Rodaros, D., and Stewart, J. (2002). Blockade of stress-induced but not cocaine-induced reinstatement by infusion of noradrenergic antagonists into the bed nucleus of the stria terminalis or the central nucleus of the amygdala. *J. Neurosci.* 22, 5713–5718. doi: 10.1523/JNEUROSCI.22-13-05713.2002
- Li, N., Ma, N., Liu, Y., He, X. S., Sun, D. L., Fu, X. M., et al. (2013). Resting-state functional connectivity predicts impulsivity in economic decision-making. *J. Neurosci.* 33, 4886–4895. doi: 10.1523/JNEUROSCI.1342-12.2013
- Li, Y., Zhou, W., Dong, H., Shen, W., Zhang, J., Li, F., et al. (2018). Lower fractional anisotropy in the gray matter of amygdala-hippocampus-nucleus accumbens circuit in methamphetamine users: an *in vivo* diffusion tensor imaging study. *Neurotox. Res.* 33, 801–811. doi: 10.1007/s12640-017-9828-4
- Lopez, A. A., Skelly, J. M., White, T. J., and Higgins, S. T. (2015). Does impulsiveness moderate response to financial incentives for smoking cessation among pregnant and newly postpartum women? *Exp. Clin. Psychopharmacol.* 23, 97–108. doi: 10.1037/a0038810
- McClure, S. M., Laibson, D. I., Loewenstein, G., and Cohen, J. D. (2004). Separate neural systems value immediate and delayed monetary rewards. *Science* 306, 503–507. doi: 10.1126/science.1100907
- Moody, L., Franck, C., Hatz, L., and Bickel, W. K. (2016). Impulsivity and polysubstance use: a systematic comparison of delay discounting in mono-, dual- and trisubstance use. *Exp. Clin. Psychopharmacol.* 24, 30–37. doi: 10.1037/pha0000059
- Mormann, F., Kornblith, S., Cerf, M., Ison, M. J., Kraskov, A., Tran, M., et al. (2017). Scene-selective coding by single neurons in the human parahippocampal cortex. *Proc. Natl. Acad. Sci. U S A* 114, 1153–1158. doi: 10.1073/pnas.1608159113
- Myerson, J., Green, L., and Warusawitharana, M. (2001). Area under the curve as a measure of discounting. *J. Exp. Anal. Behav.* 76, 235–243. doi: 10.1901/jeab.2001.76-235
- Owens, M. M., Gray, J. C., Amlung, M. T., Oshri, A., Sweet, L. H., and MacKillop, J. (2017). Neuroanatomical foundations of delayed reward discounting decision making. *NeuroImage* 161, 261–270. doi: 10.1016/j.neuroimage.2017.08.045
- Parkes, S. L., and Balleine, B. W. (2013). Incentive memory: evidence the basolateral amygdala encodes and the insular cortex retrieves outcome values to guide choice between goal-directed actions. *J. Neurosci.* 33, 8753–8763. doi: 10.1523/JNEUROSCI.5071-12.2013
- Petrov, T., Krukoff, T. L., and Jhamandas, J. H. (1993). Branching projections of catecholaminergic brainstem neurons to the paraventricular hypothalamic nucleus and the central nucleus of the amygdala in the rat. *Brain Res.* 609, 81–92. doi: 10.1016/0006-8993(93)90858-k
- Richards, J. B., Zhang, L., Mitchell, S. H., and de Wit, H. (1999). Delay or probability discounting in a model of impulsive behavior: effect of alcohol. *J. Exp. Anal. Behav.* 71, 121–143. doi: 10.1901/jeab.1999.71-121
- Rodríguez-Ortega, E., Cañadas, F., Carvajal, F., and Cardona, D. (2017). *In vivo* stimulation of locus coeruleus: effects on amygdala subnuclei. *Acta Neurobiol. Exp.* 77, 261–268. doi: 10.21307/ane-2017-060
- Roewer, I., Wiehler, A., and Peters, J. (2015). Nicotine deprivation, temporal discounting and choice consistency in heavy smokers. *J. Exp. Anal. Behav.* 103, 62–76. doi: 10.1002/jeab.134
- Saygin, Z. M., Kliemann, D., Iglesias, J. E., van der Kouwe, A. J. W., Boyd, E., Reuter, M., et al. (2017). High-resolution magnetic resonance imaging reveals nuclei of the human amygdala: manual segmentation to automatic atlas. *NeuroImage* 155, 370–382. doi: 10.1016/j.neuroimage.2017.04.046
- Saygin, Z. M., Osher, D. E., Augustinack, J., Fischl, B., and Gabrieli, J. D. E. (2011). Connectivity-based segmentation of human amygdala nuclei using probabilistic tractography. *NeuroImage* 56, 1353–1361. doi: 10.1016/j.neuroimage.2011.03.006
- Shaham, Y., Highfield, D., Delfs, J., Leung, S., and Stewart, J. (2000). Clonidine blocks stress-induced reinstatement of heroin seeking in rats: an effect independent of locus coeruleus noradrenergic neurons. *Eur. J. Neurosci.* 12, 292–302. doi: 10.1046/j.1460-9568.2000.00899.x
- Smith, R. J., and Aston-Jones, G. (2008). Noradrenergic transmission in the extended amygdala: role in increased drug-seeking and relapse during protracted drug abstinence. *Brain Struct. Funct.* 213, 43–61. doi: 10.1007/s00429-008-0191-3
- Sotiropoulos, S. N., Jbabdi, S., Xu, J., Andersson, J. L., Moeller, S., Auerbach, E. J., et al. (2013). Advances in diffusion MRI acquisition and processing in the human connectome project. *NeuroImage* 80, 125–143. doi: 10.1016/j.neuroimage.2013.05.057
- Swanson, L. W., and Petrovich, G. D. (1998). What is the amygdala? *Trends Neurosci.* 21, 323–331. doi: 10.1016/s0166-2236(98)01265-x
- Van Essen, D. C., Smith, S. M., Barch, D. M., Behrens, T. E., Yacoub, E., Ugurbil, K., et al. (2013). The WU-minn human connectome project: an overview. *NeuroImage* 80, 62–79. doi: 10.1016/j.neuroimage.2013.05.041
- Veening, J. G., Swanson, L. W., and Sawchenko, P. E. (1984). The organization of projections from the central nucleus of the amygdala to brain-stem sites involved in central autonomic regulation—a combined retrograde transport immunohistochemical study. *Brain Res.* 303, 337–357. doi: 10.1016/0006-8993(84)91220-4
- Wallis, J. D., and Miller, E. K. (2003). Neuronal activity in primate dorsolateral and orbital prefrontal cortex during performance of a reward preference task. *Eur. J. Neurosci.* 18, 2069–2081. doi: 10.1046/j.1460-9568.2003.02922.x
- Wassum, K. M., and Izquierdo, A. (2015). The basolateral amygdala in reward learning and addiction. *Neurosci. Biobehav. Rev.* 57, 271–283. doi: 10.1016/j.neubiorev.2015.08.017
- Wilson, S. J., Sayette, M. A., and Fiez, J. A. (2004). Prefrontal responses to drug cues: a neurocognitive analysis. *Nat. Neurosci.* 7, 211–214. doi: 10.1038/nn1200
- Woolrich, M. W., Jbabdi, S., Patenaude, B., Chappell, M., Makni, S., Behrens, T., et al. (2009). Bayesian analysis of neuroimaging data in FSL. *NeuroImage* 45, S173–S186. doi: 10.1016/j.neuroimage.2008.10.055
- Xue, Y. Q., Steketee, J. D., and Sun, W. L. (2012). Inactivation of the central nucleus of the amygdala reduces the effect of punishment on cocaine self-administration in rats. *Eur. J. Neurosci.* 35, 775–783. doi: 10.1111/j.1460-9568.2012.08000.x

**Conflict of Interest:** AB: Medtronic: Consultant; BrainLab: Consultant. NP: Abbott: Consultant, Fellowship Support; Medtronic: Consultant, Fellowship Support; Boston Scientific: Consultant; Second Sight Medical Products: Consultant, Grant Support; BrainLab: Grant Support.

The remaining authors declare that the research was conducted in the absence of any commercial or financial relationships that could be construed as a potential conflict of interest.

Copyright © 2020 Bari, Sparks, Levinson, Wilson, London, Langevin and Pouratian. This is an open-access article distributed under the terms of the Creative Commons Attribution License (CC BY). The use, distribution or reproduction in other forums is permitted, provided the original author(s) and the copyright owner(s) are credited and that the original publication in this journal is cited, in accordance with accepted academic practice. No use, distribution or reproduction is permitted which does not comply with these terms.



# Effects of Autonomous Sensory Meridian Response on the Functional Connectivity as Measured by Functional Magnetic Resonance Imaging

Seonjin Lee<sup>1,2</sup>, Jooyeon Kim<sup>3</sup> and Sungho Tak<sup>1,2\*</sup>

<sup>1</sup> Research Center for Bioconvergence Analysis, Korea Basic Science Institute, Cheongju, South Korea, <sup>2</sup> Graduate School of Analytical Science and Technology, Chungnam National University, Daejeon, South Korea, <sup>3</sup> Center for Research Equipment, Korea Basic Science Institute, Cheongju, South Korea

## OPEN ACCESS

### Edited by:

India Morrison,  
Linköping University, Sweden

### Reviewed by:

Simone Di Plinio,  
University of Studies "G. d'Annunzio"  
Chieti-Pescara, Italy  
Andrea Scalabrini,  
University of Studies "G. d'Annunzio"  
Chieti-Pescara, Italy

### \*Correspondence:

Sungho Tak  
stak@kbsi.re.kr

### Specialty section:

This article was submitted to  
Emotion Regulation and Processing,  
a section of the journal  
Frontiers in Behavioral Neuroscience

**Received:** 24 March 2020

**Accepted:** 04 August 2020

**Published:** 27 August 2020

### Citation:

Lee S, Kim J and Tak S (2020)  
Effects of Autonomous Sensory  
Meridian Response on the Functional  
Connectivity as Measured by  
Functional Magnetic Resonance  
Imaging.  
Front. Behav. Neurosci. 14:154.  
doi: 10.3389/fnbeh.2020.00154

Autonomous sensory meridian response (ASMR) is a sensory phenomenon in which audio-visual stimuli evoke a tingling sensation and is accompanied by a feeling of calm and relaxation. Therefore, there has been an increasing interest in using stimuli that elicit ASMR in cognitive and clinical neuroscience studies. However, neurophysiological basis of sensory-emotional experiences evoked by ASMR remain largely unexplored. In this study, we investigated how functional connectivity is changed while watching ASMR video, compared to resting state, and assessed its potential association with affective state induced by ASMR. 28 subjects participated in fMRI experiment consisting of 2 sessions (resting-state and task of viewing ASMR-eliciting video). Using a seed-based correlation analysis, we found that functional connections between the posterior cingulate cortex, and superior/middle temporal gyri, cuneus, and lingual gyrus were significantly increased during ASMR compared to resting state. In addition, we found that with the pregenual anterior cingulate cortex seed region, functional connectivity of the medial prefrontal cortex was increased during ASMR condition, relative to resting state. These results imply that ASMR can be elicited and maintained by ongoing interaction between regional activity that are mainly involved in the mentalizing and self-referential processing. We also found that ASMR-induced affective state changes (high activation negative and high activation positive state) were negatively correlated with functional connectivity involved in visual information processing, suggesting that visual information processing in response to high arousal states can be weakened by ASMR-eliciting stimuli.

**Keywords:** autonomous sensory meridian response, functional connectivity, functional magnetic resonance imaging, default mode network, affective touch network, self-network

## INTRODUCTION

Stress is common in everyday life, and is believed to affect individual health and happiness (Segerstrom and Miller, 2004; Cohen et al., 2007). As a result, the development of stress management approaches has become an important endeavor of preventing stress-related health problems and accomplishing psychological well-being. In recent years, the autonomous sensory

meridian response (ASMR) videos have been widely used in the management of stress, by inducing relaxation and sleep (Barratt and Davis, 2015; Lee et al., 2019). Specifically, ASMR is a sensory phenomenon in which individuals experience a tingling in the head and neck, in response to specific triggering audio and visual stimuli (Barratt and Davis, 2015). The ASMR triggers lead to response of psychologically pleasant effects such as feeling of relaxation, reduction in anxiety, and sleep induction (Barratt et al., 2017; Cash et al., 2018; Poerio et al., 2018).

Several studies have explored the neurophysiological basis of ASMR using functional magnetic resonance imaging (fMRI) (Smith et al., 2017, 2019; Lochte et al., 2018). Specifically, Lochte et al. (2018) examined the brain activation during ASMR, and observed significant activation in regions of the medial prefrontal cortex (mPFC), dorsal anterior cingulate cortex, supplementary motor area, and insular cortex during ASMR condition, compared to the brain activity during resting state.

Smith et al. (2017, 2019) investigated the differences of resting-state network between ASMR experienced and non-ASMR experienced individuals. Using an independent component analysis (Beckmann et al., 2005), they found that participants with ASMR had less connections of the precuneus with other regions of the default mode network (DMN) than controls. These previous studies demonstrated the associations of ASMR with the changes in regional activity and networks of resting state. However, it is still unclear how connections among brain regions are explicitly modulated by ASMR.

To address this issue, this paper focuses on the investigation of ASMR condition-specific functional connectivity changes in a brain network, compared to the resting-state functional connectivity, using 3T functional magnetic resonance imaging (fMRI). Functional connectivity was assessed using a seed-based correlation approach (Biswal et al., 1995; Whitfield-Gabrieli and Nieto-Castanon, 2012). We hypothesized that ASMR condition would change the functional connectivity within the brain network involved in mentalization and self-referential processing as a meditation effect of ASMR. This is based on a previous study (Barratt and Davis, 2015) reporting that sitting quietly while watching relaxed scenes to arouse ASMR for a certain period of time could be regarded as a form of mindfulness. Mindfulness meditation can arouse relaxed and calm states by developing a level of mentalization that controls emotion using a capacity for resilience in the face of distressed conditions (Sharp et al., 2011; Bateman and Fonagy, 2013). Also, the meditation has been known to induce positive emotion using self- and other-referential processing (Logie and Frewen, 2015). The previous study (Logie and Frewen, 2015) has shown that participants who experienced mindfulness meditation had self-positive bias that led to positively affective responses during experimental self- and other-referential processing. Therefore, based on an association of ASMR and meditation conditions, we tested our hypothesis by investigating the ASMR condition-specific connectivity changes in the DMN that are involved in the mentalizing (Lombardo et al., 2010; Mars et al., 2012), and the self- and other-networks that are associated with self- and other-referential processing (Northoff et al., 2006; Murray et al., 2015). The self-network has a function of self-specific processing, indicating non-self-/self-distinction

to comprehend self in domain of perception, emotion, and cognition (Northoff et al., 2006). The other-network has a function of other-specific processing that represents other-/self-distinction in understanding others' mental and emotional states across the domains of perception, emotion, and cognition (Murray et al., 2015).

In addition, since the ASMR triggers have been known to induce a tingling sensation as a secondary phenomenon resulting from intensely positive emotion (Barratt and Davis, 2015), we explored the changes in the functional connectivity of the affective touch network while watching the ASMR stimuli (Morrison, 2016). We selected the seed regions for the default mode, affective touch, and self-/other-networks as follows. The posterior cingulate cortex (PCC), mPFC, and left/right lateral parietal cortex (ILPC, rLPC) were used as the seed regions for the DMN, because these regions are recognized as central hubs within the network (Greicius et al., 2003). For the affective touch network, we used the right posterior insular cortex (Ig2) as a seed region based on a previous meta-analysis study (Morrison, 2016). Morrison (2016) reported a higher activation of Ig2 in response to affective touch compared with discriminative touch. Using this seed region of Ig2, they observed an affective touch network composed of bilateral clusters, including posterior and anterior insular cortex, postcentral primary, and secondary somatosensory regions. For the self- and other-networks, we used the pregenual anterior cingulate cortex (pACC) and posterior cingulate cortex/precuneus (PCC/PC) regions as seed ROIs, because these two seed regions have been reliably shown to be involved in conceptual self- and conceptual other-processing, respectively (Murray et al., 2012). The self-network consisted of the pACC and anterior insular cortex, whereas the other-network consisted of the PCC/PC and angular gyrus/temporoparietal junction (Murray et al., 2015).

Finally, using the functional connectivity estimates, we further investigated the potential association of condition-specific connectivity changes with affective state changes while watching ASMR stimuli. Our hypothesis was that the changes in functional connectivity during ASMR would be closely associated with the changes in pleasant/unpleasant emotion and arousal states during ASMR. We assessed the affective outcomes of watching ASMR video clips using the Multi-Affect Indicator (Warr, 1990; Warr et al., 2014) and then performed a correlation analysis between the functional connectivity strengths and individual scores for affective state induced by ASMR.

## MATERIALS AND METHODS

### Participants and Experimental Protocol

Twenty-eight healthy subjects (13 females, 15 males; mean age:  $26.39 \pm 3.77$  years) participated in this study. No subjects had any history of neurological disorders. The study was approved by the Institutional Review Board (IRB) of Korea Basic Science Institute, and the experiment was performed with the understanding and written consent of each participant, according to IRB guidelines.

The experiment consisted of two sessions. In the first session, which served as a control experiment, participants underwent



a 5-min resting-state fMRI scan. During this scan, participants were instructed to stare at a fixation point in the center of the screen and remain awake. The scan duration of 5 min was based on previous studies showing that estimates of resting-state functional connectivity stabilized with this acquisition time (Van Dijk et al., 2010). We also determined the specific instructions for resting-state condition (eyes closed, eyes open, or eyes fixated on a cross), based on Patriat et al. (2013). It was found that reliability in the default mode, attention, and auditory networks was the highest when subjects kept their eyes fixated on a cross.

In the second session, participants underwent ASMR task in the MRI scanner. During the scan, participants were instructed to view ASMR-eliciting video for 5 min. This video was trimmed to a length of 5 min from the full-length version of the YouTube video, which comprised repetitive and slow movements with a scratching sound (i.e., scratching of a sand table). The web address is as follows: <https://youtu.be/bCFALoEfBGw>. While standards for ASMR videos have not yet been extensively examined, several studies (Barratt and Davis, 2015; Fredborg et al., 2017) have established the common stimuli that elicit an intense ASMR experience, including whispering, scratching sound, and slow/repetitive movements. Therefore, we selected the content of the video clips based on these criteria. The length of ASMR video clips was set to be consistent with that of the resting-state condition because the scan length has been known to affect the reliability of fMRI connectivity estimates (Birn et al., 2013).

After completing fMRI experiments, outside the scanner, participants responded to questionnaires for assessing the changes in affective states while watching ASMR video clips (see the Behavior Data Analysis section for more details). Overall, this study consisted of three phases: the first session for resting-state experiment in the MRI scanner (5 min), the second session for ASMR experiment in the MRI scanner (5 min), and behavioral data collection outside the scanner.

## MRI Acquisition

All images were acquired using a 3T Philips Achieva scanner (Philips Medical Systems, Best, The Netherlands). Structural images were acquired using a three-dimensional T1-weighted sequence [repetition time (TR) = 6.6 ms; echo time (TE) = 3.1 ms; flip angle = 9°; voxel size =  $1.0 \times 1.0 \times 1.2 \text{ mm}^3$ ; field of view (FOV) = 240 mm; 170 slices]. Blood oxygenation level dependent (BOLD) images were obtained using a T2\*-weighted gradient echo-planar imaging (EPI) sequence (TR = 2000 ms; TE = 35 ms; flip angle = 79°; voxel size =  $3.0 \times 3.0 \times 3.0 \text{ mm}^3$ , FOV = 195 mm, 34 interleaved slices without slice gap).

## Data Processing

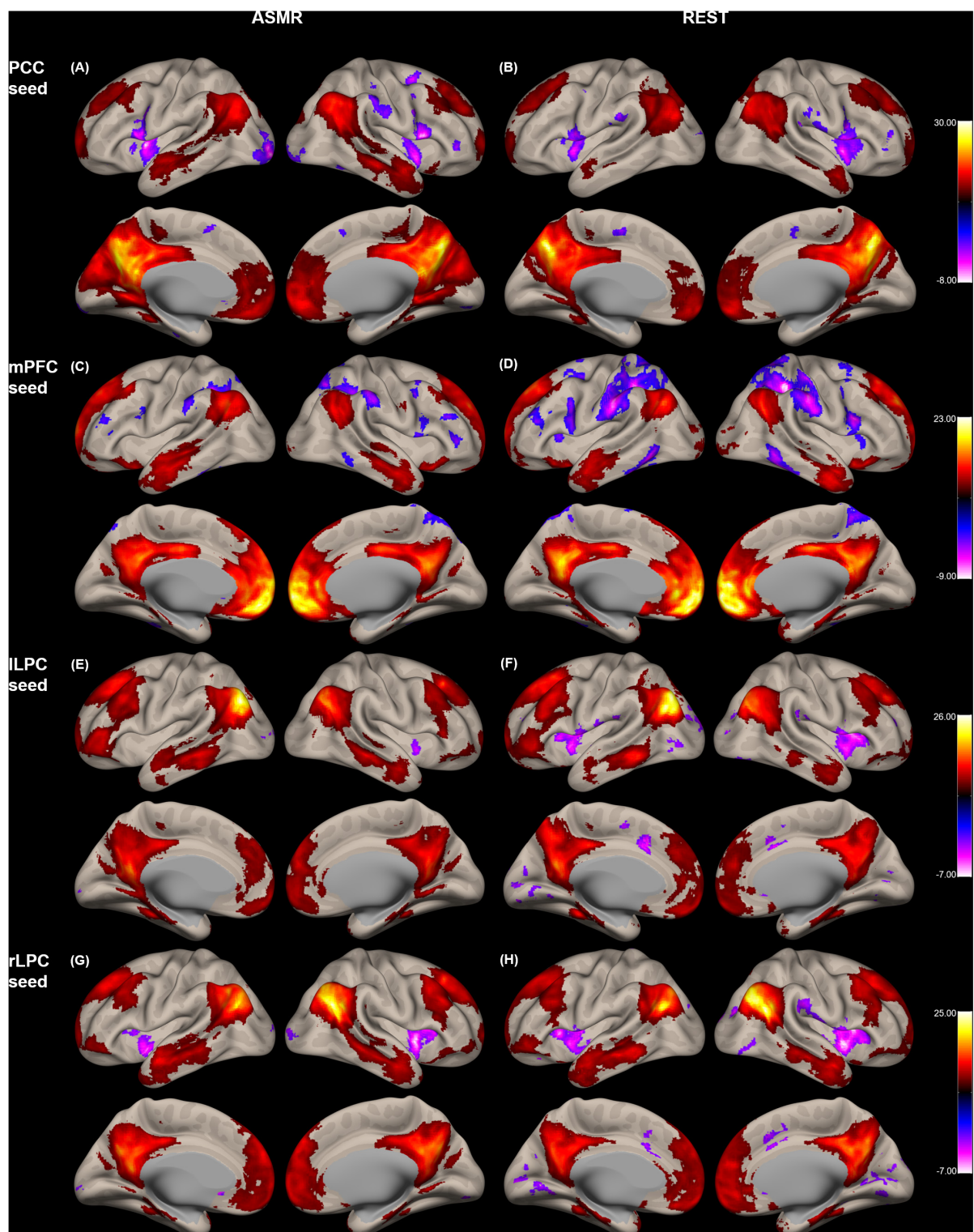
The functional connectivity toolbox (CONN toolbox, Whitfield-Gabrieli and Nieto-Castanon, 2012) with the statistical parametric mapping software package (SPM12, Friston et al., 2007) was used for pre-processing of the functional and structural images, and functional connectivity analysis.

The effects of head movement between scans were corrected by realigning all scans to the first image using a six-parameter affine spatial transformation; the geometric distortion was corrected by the unwarp function. The ensuing realignment

parameters were saved for modeling residual head motion effects in the BOLD time series. To further mitigate motion-related BOLD effects, including spikes, we used artifact detection tools (ART, [https://www.nitrc.org/projects/artifact\\_detect](https://www.nitrc.org/projects/artifact_detect)) interoperable with CONN toolbox. Specifically, outlying volumes in BOLD time series (scan “scrubbing”) were identified based on normalized global mean intensity values ( $> Z = 5$ ) and motion parameters ( $> 1 \text{ mm}$  translational movement in the x, y, or z planes or  $> 0.02$  rotation in yaw, pitch, or roll). The matrices of outliers and realignment parameters were then entered as first-level covariates (i.e., nuisance variables). To compensate for slice-acquisition delays, the signal in each slice was realigned temporally to a reference middle slice using sinc interpolation. The structural image was co-registered with functional images and segmented into gray matter (GM), white matter (WM), and cerebrospinal fluid (CSF). All images were spatially normalized to the Montreal Neurological Institute (MNI) space. Spatial smoothing with a 6 mm full-width at half-maximum (FWHM) Gaussian kernel was applied to the normalized images.

Systemic physiological confounds arising from cardiac and respiration have been known to cause spurious correlation structures throughout the brain (Birn et al., 2006; Chang and Glover, 2009; Murphy et al., 2013). We therefore reduced systemic physiological noise using the anatomical component-based noise correction method (aCompCor) (Behzadi et al., 2007). The method has also been shown to be effective in the suppression of motion-related artifacts (Muschelli et al., 2014). Assuming that the physiological noise contribution is globally distributed, and neuronal activity-related signals are low in the WM and CSF, the signals within the WM and CSF were used as sources that primarily reflect physiological noise. The top three components obtained from each of the WM and CSF using principal component analysis were included as the nuisance regressors in the first-level analysis. In addition, to remove spurious task-induced co-activation effects, we constructed a condition-specific regressor and included it as additional temporal confounding factors by convolving a canonical hemodynamic response function with a condition (either ASMR or resting-state) spanning the entire scanner acquisition length (Fair et al., 2007; Whitfield-Gabrieli and Nieto-Castanon, 2012). Prior to the first-level connectivity analysis, these temporal confounding factors (consisting of subject movement, cardiac/respiration, and spurious parameters related to task effects) were regressed out from BOLD time series at each voxel. The resulting residual time series were then band-pass filtered in the range of 0.01–0.1 Hz to constrain the low-frequency BOLD fluctuations presumed to be related to spontaneous neural activity (Biswal et al., 1995; Leopold et al., 2003).

First-level functional connectivity maps were generated by computing Pearson's correlation coefficients between average BOLD time series calculated across all the voxels of a given seed region and the time series of all other voxels in the brain (Biswal et al., 1995; Fox et al., 2005). The resulting correlation coefficients were converted to Z-scores using Fisher transformation (Fisher, 1915) to improve the normality assumptions of the subsequent second-level general linear model (GLM) analysis. Functional connectivity considered in our analysis was associated with (a)



**FIGURE 1 |** Group-level functional connectivity of the  $t$ -statistic in the default mode network during resting-state, and in response to ASMR effects. Functional connectivity strengths in terms of  $t$ -statistics were thresholded at a significance level of false discovery rate (FDR)-corrected  $p < 0.05$ , and overlaid on a cortical surface atlas. Functional connectivity of the posterior cingulate cortex (PCC) seed region in response to ASMR (A), and in resting-state (B). Functional connectivity of the medial prefrontal cortex (mPFC) seed region in response to ASMR (C), and in resting-state (D). Functional connectivity of the left lateral parietal cortex (ILPC) seed region in response to ASMR (E), and in resting-state (F). Functional connectivity of the right lateral parietal cortex (rLPC) seed region in response to ASMR (G), and in resting-state (H).

**TABLE 1 |** Statistical significance of the group-level functional connectivity generated during ASMR condition.

Connectivity (ASMR)	Brodman area	MNI (x, y, z)	Size	Peak-T	Peak-beta	Size p-FDR
<b>PCC seed</b>						
Precuneus	BA 7	(-2, -64, 40)	25801	30.715	0.977	0.00000
Medial frontal gyrus	BA 10	(4, 50, -6)	12173	11.445	0.342	0.00000
Angular gyrus	BA 39	(54, -62, 34)	6167	14.407	0.436	0.00000
Insular cortex	BA 48	(-36, 4, 2)	1195	-8.276	-0.170	0.00000
Cuneus	BA 18	(-26, -100, -8)	631	-7.666	-0.169	0.00000
Supramarginal gyrus	BA 1	(64, -24, 48)	355	-5.303	-0.204	0.00000
Cuneus	BA 17	(20, -102, -4)	221	-5.441	-0.144	0.00000
Superior frontal gyrus	BA 8	(22, 4, 54)	151	-5.831	-0.135	0.00004
<b>mPFC seed</b>						
Medial frontal gyrus	BA 10	(2, 60, -2)	22584	29.669	1.241	0.00000
Posterior cingulate cortex	BA 23	(6, -50, 22)	6927	14.525	0.562	0.00000
Angular gyrus	BA 39	(-50, -66, 32)	2558	11.710	0.487	0.00000
Postcentral gyrus	BA 40	(54, -32, 40)	1832	-6.744	-0.229	0.00000
Superior temporal gyrus	BA 21	(60, -58, 20)	1715	10.946	0.397	0.00000
Inferior temporal gyrus	BA 20	(54, -4, -36)	1659	8.214	0.256	0.00000
Inferior frontal gyrus	BA 45	(-44, 38, 16)	251	-5.211	-0.241	0.00000
Superior temporal gyrus	BA 38	(36, 20, -36)	146	6.139	0.163	0.00006
Parahippocampal gyrus	BA 30	(26, -32, -16)	144	5.305	0.132	0.00006
Inferior frontal gyrus	BA 45	(46, 38, 4)	109	-5.598	-0.212	0.00046
<b>ILPC seed</b>						
Superior frontal gyrus	BA 8	(24, 32, 48)	16420	14.658	0.390	0.00000
Angular gyrus	BA 39	(-44, -72, 32)	15617	25.964	1.003	0.00000
Angular gyrus	BA 39	(46, -70, 36)	5690	18.819	0.645	0.00000
Fusiform gyrus	BA 37	(36, -34, -20)	408	7.241	0.186	0.00000
<b>rLPC seed</b>						
Middle frontal gyrus	BA 8	(26, 30, 52)	17027	14.827	0.480	0.00000
Superior temporal gyrus	BA 39	(52, -60, 26)	7214	24.514	0.901	0.00000
Cuneus	BA 18	(2, -70, 30)	7204	17.547	0.501	0.00000
Middle temporal gyrus	BA 39	(-44, -68, 26)	4980	20.052	0.566	0.00000
Middle temporal gyrus	BA 20	(-54, -8, -22)	2654	9.443	0.267	0.00000
Insular cortex	BA 13	(42, 6, -4)	694	-7.820	-0.210	0.00000
Fusiform gyrus	BA 37	(-30, -36, -16)	358	7.388	0.271	0.00000
Parahippocampal gyrus	BA 36	(30, -20, -28)	316	5.600	0.147	0.00000
Insular cortex	BA 48	(-36, 14, 8)	197	-6.373	-0.135	0.00000
<b>pACC seed</b>						
Anterior cingulate cortex	BA 32	(-2, 38, 16)	25640	46.025	2.517	0.00000
Inferior temporal gyrus	BA 20	(-60, -56, -16)	2289	-8.354	0.160	0.00000
Inferior parietal lobule	BA 48	(-44, -34, 32)	2285	-2.731	-0.079	0.00000
Precuneus	BA 7	(8, -60, 70)	2062	-9.274	-0.176	0.00000
Middle occipital gyrus	BA 37	(50, -64, -10)	1555	-6.903	-0.132	0.00000
Inferior parietal cortex	BA 18	(58, -50, 50)	365	6.027	0.150	0.00000
<b>PCC/PC seed</b>						
Middle frontal gyrus	BA 8	(26, 40, 44)	12514	12.037	0.453	0.00000
Precuneus	BA 23	(2, -62, 26)	8240	51.265	2.433	0.00000
Angular gyrus	BA 39	(-44, -62, 26)	2753	12.495	0.521	0.00000
Middle temporal gyrus	BA 21	(-66, -28, -8)	2310	8.849	0.229	0.00000
Angular gyrus	BA 39	(54, -62, 34)	2107	13.294	0.493	0.00000
Inferior temporal gyrus	BA 20	(56, -4, -38)	1751	11.132	0.212	0.00000
Insular cortex	BA 48	(48, 12, 4)	1197	-7.101	-0.226	0.00000
Supramarginal gyrus	BA 2	(54, -34, 38)	1075	-7.354	-0.264	0.00000
Insular cortex	BA 48	(-36, 2, -4)	905	-7.141	-0.165	0.00000
Middle frontal gyrus	BA 46	(-40, 54, 8)	837	-8.354	-0.215	0.00000

(Continued)



TABLE 1 | Continued

Connectivity (ASMR)	Brodmann area	MNI (x, y, z)	Size	Peak-T	Peak-beta	Size p-FDR
Inferior frontal gyrus	BA 45	(44, 40, 2)	712	-6.300	-0.239	0.00000
Middle occipital gyrus	BA 18	(-30, -90, 8)	486	-7.160	-0.167	0.00000
Fusiform gyrus	BA 37	(-30, -36, -16)	342	7.493	0.204	0.00000
Parahippocampal gyrus	BA 35	(26, -22, -24)	229	9.158	0.199	0.00000
Superior temporal gyrus	BA 38	(40, 20, -34)	172	5.631	0.157	0.00006
Middle occipital gyrus	BA 37	(-50, -62, -10)	124	-6.009	-0.159	0.00010
<b>Ig2 seed</b>						
Insular cortex	BA 13	(42, -14, -8)	9980	63.964	0.669	0.00000
Postcentral gyrus	BA 40	(-58, -26, 16)	9729	16.404	0.298	0.00000
Anterior cingulate cortex	BA 24	(4, 22, 24)	6178	11.215	0.209	0.00000
Cuneus	BA 18	(-12, -72, 6)	5566	10.453	0.163	0.00000
Middle frontal gyrus	BA 46	(-32, 44, 22)	329	7.780	0.154	0.00000
Middle frontal gyrus	BA 9	(38, 26, 54)	184	-5.517	-0.085	0.00000

We report clusters having significant connections from the seed region, cluster size, and the peak-voxel location in each cluster.

the DMN (Greicius et al., 2003), (b) affective touch network (Morrison, 2016), and (c) the self-/other-networks (Northoff et al., 2006; Murray et al., 2015). As seeds of the DMN, we used the PCC centered at MNI coordinates [1, -61, 38], mPFC (MNI: [1 55 -3]), and l/rLPC (lLPC, MNI: [-55 -12 29], rLPC, MNI: [56 -10 29]). The seed regions of interest (ROIs) were defined using a standardized CONN toolbox atlas (networks.nii) that was originally derived from group-level independent component analysis (ICA) of the human connectome project dataset (Calhoun et al., 2001; Whitfield-Gabrieli and Nieto-Castanon, 2012; Van Essen et al., 2013). For an affective touch network, we used the Ig2 as a seed ROI that comprised all voxels within a sphere of 6 mm radius, centered on the MNI coordinates [42, -14, 8]. Finally, for the self- and other-networks, we used the pACC and PCC/PC regions as seed ROIs (spheres of 6 mm radius, centered on MNI coordinates: [-2, 38, 16] and [2, -61, 26]).

Following the computation for the first-level functional connectivity maps, the resulting voxel-specific Z-scores between a seed area and every other voxel for each subject were entered into a second-level GLM analysis. Specifically, we performed a one-sample *t*-test at the second level to test the statistical significance of each functional connectivity map in a group of subjects that was generated during resting-state or ASMR conditions (ASMR). We then tested our hypothesis that functional connectivity related to mentalizing and self-referential processing within the default mode, affective touch, and self-/other-networks would be greater during an ASMR condition than the resting-state, using a two-tailed paired sample *t*-test with a contrast “ASMR > resting-state” at the second-level. This analysis enabled us to compare the functional connectivity patterns between two conditions, including a resting-state and an ASMR condition, and assess their statistical significance in a sample. For false positive control in the whole-brain seed-to-voxel connectivity analysis, we applied a cluster-forming threshold using a height threshold of uncorrected *p*-value < 0.001 and a cluster-extent threshold of false discovery

rate (FDR)-corrected *p*-value < 0.05 (Friston et al., 1994; Whitfield-Gabrieli and Nieto-Castanon, 2012). We used a semi-automated search for finding local maxima (peaks) and their MNI coordinates within the cluster-corrected thresholded map, to identify regions within the significant functional connectivity maps. Their anatomical labels were determined using xjView toolbox (<https://www.alivelearn.net/xjview>), and the Brodmann area labels were identified using the Brodmann atlas, which is included in the MRICron software (<https://www.nitrc.org/projects/mricron>). Functional connectivity maps were overlaid on a cortical surface atlas using the CONN toolbox (Whitfield-Gabrieli and Nieto-Castanon, 2012).

## Behavioral Data Analysis

To investigate the potential association of functional connectivity estimates with the psychological changes of ASMR, we measured the affective outcomes of watching ASMR video clips using the Multi-Affect Indicator (Warr, 1990; Warr et al., 2014). This multi-affect indicator has been designed to specify different kinds of feelings in terms of two dimensions, including the conventional negative-to-positive continuum (from unpleasant to pleasant state) and low-to-high mental activation (arousal) that defines one's state of readiness for action or energy expenditure (Russell, 2003). Particular feelings were then categorized into four affective states: low-activation positive (LAP, which corresponds to comfort and calmness), high-activation positive (HAP, related to enthusiasm and excitement), low-activation negative (LAN, related to depression and sadness), and high-activation negative states (HAN, related to anxiety and stress). In this study, we used 12 items to measure these affective states (Warr, 1990; Poerio et al., 2018): “calm,” “relaxed,” and “at ease” for LAP; “enthusiastic,” “joyful,” and “excited” for HAP; “depressed,” “dejected,” and “hopeless” for LAN; and “anxious,” “nervous,” and “tense” for HAN. After completing the fMRI experiments, the participants were asked to rate each item in the range of 1 (much less) to 7 (much more) by responding to the question: How did

**TABLE 2 |** Statistical significance of the group-level functional connectivity generated during resting-state condition.

Connectivity (Resting state)	Brodmann area	MNI (x, y, z)	Size	Peak-T	Peak-beta	Size p-FDR
<b>PCC seed</b>						
Precuneus	BA 7	(-2, -64, 40)	22585	33.057	0.930	0.00000
Medial frontal gyrus	BA 11	(8, 54, -12)	8607	11.036	0.303	0.00000
Middle frontal gyrus	BA 9	(-28, 42, 42)	2296	9.627	0.263	0.00000
Insular cortex	BA 22	(50, 2, -2)	1748	-7.633	-0.161	0.00000
Middle temporal gyrus	BA 21	(52, 0, -26)	613	7.965	0.195	0.00000
Middle temporal gyrus	BA 21	(-62 0 -26)	311	6.144	0.133	0.00000
<b>mPFC seed</b>						
Medial orbital gyrus	BA 11	(0, 50, -10)	23406	27.766	1.122	0.00000
Posterior cingulate cortex	BA 23	(-10, -54, 22)	6945	16.959	0.422	0.00000
Supramarginal gyrus	BA 40	(44, -34, 38)	4216	-9.262	-0.150	0.00000
Inferior parietal lobe	BA 40	(-38, -42, 44)	4023	-8.222	-0.270	0.00000
Angular gyrus	BA 39	(-46, -64, 30)	2171	13.206	0.383	0.00000
Angular gyrus	BA 39	(52, -68, 34)	1983	12.751	0.433	0.00000
Inferior temporal gyrus	BA 37	(-58, -60, -8)	877	-7.902	-0.191	0.00000
Fusiform gyrus	BA 37	(54, -50, -24)	812	-9.106	-0.167	0.00000
Parahippocampal gyrus	BA 30	(24, -20, -24)	571	7.417	0.230	0.00000
Inferior frontal gyrus	BA 44	(-48, 8, 20)	422	-5.921	-0.175	0.00000
Middle occipital gyrus	BA 18	(34, -92, 10)	384	9.068	0.194	0.00000
<b>ILPC seed</b>						
Superior frontal gyrus	BA 8	(-30, 24, 58)	27546	14.534	0.440	0.00000
Angular gyrus	BA 19	(-40, -74, 38)	12347	28.357	0.992	0.00000
Middle temporal gyrus	BA 39	(40, -66, 28)	4118	18.926	0.446	0.00000
Middle temporal gyrus	BA 20	(-60, -44, -14)	1331	12.042	0.366	0.00000
Superior temporal gyrus	BA 38	(-52, 2, -4)	788	-6.582	-0.190	0.00000
Parahippocampal gyrus	BA 36	(26, -28, -20)	615	8.237	0.154	0.00000
Fusiform gyrus	BA 37	(-28, -38, -18)	551	11.315	0.353	0.00000
Middle cingulate cortex	BA 32	(-8, 16, 36)	355	-5.982	-0.151	0.00000
Supramarginal gyrus	BA 40	(-52, -26, 14)	180	-5.442	-0.158	0.00000
Cuneus	BA 18	(22, -88, 8)	161	-5.987	-0.166	0.00001
<b>rLPC seed</b>						
Middle frontal gyrus	BA 8	(28, 32, 52)	17537	17.430	0.542	0.00000
Superior temporal gyrus	BA 39	(48, -58, 22)	10591	25.784	0.839	0.00000
Middle temporal gyrus	BA 39	(-42, -64, 24)	4687	21.402	0.546	0.00000
Middle temporal gyrus	BA 20	(-60, -44, -14)	2905	10.013	0.275	0.00000
Middle temporal gyrus	BA 21	(52, -4, -26)	2185	9.641	0.289	0.00000
Insular cortex	BA 13	(40, 4, -2)	1521	-6.337	-0.207	0.00000
Parahippocampal gyrus	BA 30	(26, -20, -24)	653	7.891	0.215	0.00000
Fusiform gyrus	BA 37	(-28, -38, -16)	652	8.397	0.235	0.00000
Middle cingulate cortex	BA 24	(2, 16, 40)	342	-6.416	-0.188	0.00000
Cuneus	BA 19	(22, -82, 18)	193	-5.855	-0.159	0.00000
Lingual gyrus	BA 18	(-10, -64, -6)	160	-5.583	-0.132	0.00002
<b>pACC seed</b>						
Anterior cingulate cortex	BA 32	(-2, 38, 16)	24791	53.786	2.502	0.00000
Inferior parietal cortex	BA 7	(34, -50, 58)	1299	-7.197	-0.170	0.00000
Fusiform gyrus	BA 20	(54, -36, -26)	368	-9.512	-0.128	0.00000
Paracentral lobule	BA 4	(-14, -38, 64)	143	-4.862	-0.105	0.00005
<b>PCC/PC seed</b>						
Superior frontal gyrus	BA 10	(-4, 64, -6)	11827	14.727	0.388	0.00000
Precuneus	BA 23	(2, -62, 26)	7292	49.964	2.393	0.00000
Insular cortex	BA 48	(34, 16, 6)	3232	-13.322	-0.252	0.00000
Middle temporal gyrus	BA 38	(-42, 14, -32)	2957	8.952	0.193	0.00000
Middle temporal gyrus	BA 39	(-48, -66, 28)	2802	13.988	0.515	0.00000

(Continued)

TABLE 2 | Continued

Connectivity (Resting state)	Brodmann area	MNI (x, y, z)	Size	Peak-T	Peak-beta	Size p-FDR
Supramarginal gyrus	BA 2	(66, -24, 28)	2555	-11.081	-0.281	0.00000
Superior temporal gyrus	BA 39	(56, -60, 28)	2461	15.897	0.506	0.00000
Middle temporal gyrus	BA 21	(54, -2, -26)	2302	9.784	0.345	0.00000
Middle cingulate cortex	BA 32	(6, 14, 42)	996	-8.940	-0.169	0.00000
Middle frontal gyrus	BA 46	(-32, 46, 28)	790	-7.645	-0.208	0.00000
Parahippocampal gyrus	BA 36	(28, -16, -30)	743	8.167	0.155	0.00000
Precuneus	BA 7	(-12, -58, 60)	388	-5.490	-0.142	0.00000
<b>Ig2 seed</b>						
Insular cortex	BA 13	(42, -12, -8)	13955	59.166	1.709	0.00000
Middle cingulate cortex	BA 31	(6, -52, 32)	6103	-6.661	-0.146	0.00000
Parahippocampal gyrus	BA 30	(-20, -42, -8)	464	5.728	0.108	0.00000
Cuneus	BA 18	(16, -72, 8)	157	6.563	0.129	0.00003
Middle frontal gyrus	BA 10	(4, 68, 18)	121	-6.164	-0.081	0.00005

We report clusters having significant connections from the seed region, cluster size, and the peak-voxel location in each cluster.

you feel while watching ASMR video clip during the MRI scan, compared to before you watched the video?

We then performed two-tailed paired samples *t*-tests to compare the means of two affective states that were selected from LAP, HAP, LAN, and HAN, and determined whether there was a significant difference between the two states that can be observed from ASMR stimuli. In addition, we performed a correlation analysis to investigate the associations of these affective state changes with ASMR condition-specific functional connectivity changes. Specifically, for each brain network, we identified clusters that had a significantly higher functional connectivity from a seed region for ASMR condition than the resting-state condition (a height threshold of uncorrected *p*-value < 0.001 and a cluster-extent threshold of FDR-corrected *p*-value < 0.05). Then, we extracted the functional connectivity values (z-score) of peak coordinates (i.e., the local maxima of the cluster) for all subjects, and calculated Pearson's correlation coefficients between these functional connectivity strengths and individual scores for each affective state. We decided that the computed correlation value is significantly different from zero if the *p*-value is less than 0.05.

## RESULTS

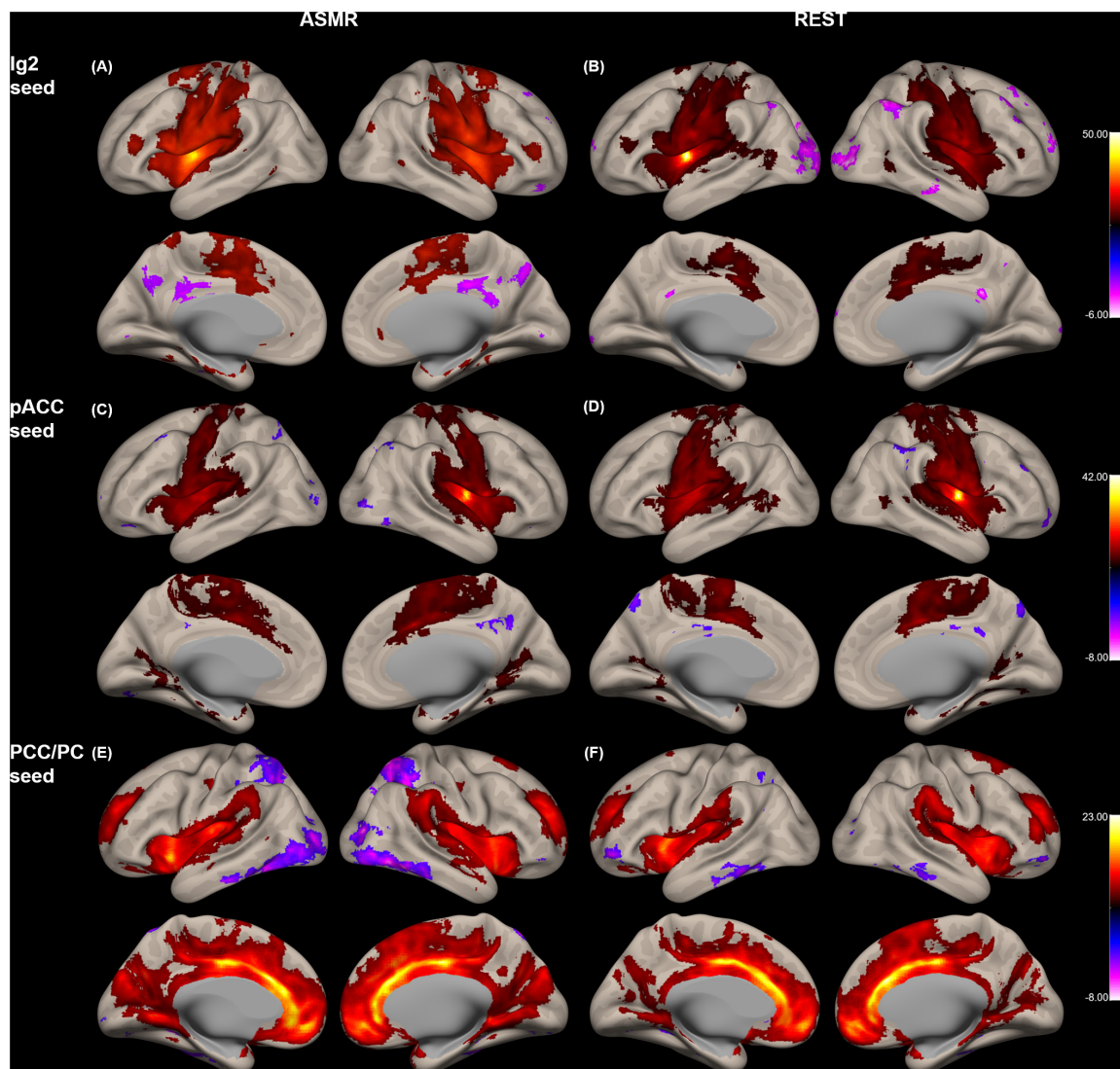
### Functional Connectivity

**Figure 1** shows the group-level functional connectivity of the *t*-statistic in the default mode network generated during either ASMR or resting-state conditions. Statistical significance of clusters and their peak coordinates for ASMR and resting-state conditions are summarized in **Tables 1, 2**, respectively. While the global maxima of the functional connectivity was located in the seed cluster, in both conditions of resting-state and ASMR, the significant hubs (local maxima of the functional connectivity within the cluster) were reliably positioned in the PCC, mPFC, ILPC, rLPC, and superior/middle/inferior temporal gyri, and superior/inferior frontal gyri. For seed regions of the PCC and rLPC, the negative functional connectivity was observed in the insular cortex.

**Figure 2** shows the group-level functional connectivity of the *t*-statistic in the affective touch, self-, and other-networks generated during either ASMR or resting-state conditions. For the affective touch network with Ig2 seed region, the significant clusters were estimated in the insular cortex and postcentral gyrus in both conditions of resting-state and ASMR. In the self-network with the pACC seed region, we found the positive functional connectivity of the anterior cingulate cortex. In other-network with the PCC/PC seed region, the positive functional connectivity was observed in the angular gyrus, precuneus, and frontal regions extending orbitofrontal and medial prefrontal cortices.

**Figure 3** shows the group-level functional connectivity of the *t*-statistic obtained by the "ASMR > resting-state" contrast. **Table 3** summarizes statistical significance of clusters functionally connected to the seed regions of the PCC, l/rLPC, pACC, and Ig2, and their peak coordinates. There were no significant clusters in the DMN with the mPFC seed region and the other-network with the PCC/PC seed region. In the DMN with the PCC seed region, 5 clusters having positive functional connectivity were significantly detected in peaks in the cuneus, superior/middle temporal gyri, and lingual gyrus. In addition, 6 clusters having negative functional connectivity were significantly detected in peaks in the superior/middle frontal gyri, middle occipital lobe, precuneus, and visual area. In the DMN with the ILPC seed region, 2 positive and 1 negative clusters were observed in peaks in the superior temporal gyrus and visual area (calcarine sulcus), and precuneus, respectively. In the DMN with the rLPC seed region, 2 positive clusters were generated in peaks in the cuneus and lingual gyrus. In the self-network with the pACC seed region, a positive cluster was detected in peaks in the middle frontal lobe. In the affective touch network with the the Ig2 seed region, one cluster having positive functional connectivity was observed in peaks in the cuneus.

The beta-values of the group-level functional connectivity for ASMR, resting-state, and ASMR > resting-state contrast are provided in **Supplementary Figures**.



**FIGURE 2 |** Group-level functional connectivity of the  $t$ -statistic in the other networks during resting-state, and in response to ASMR effects. Functional connectivity strengths in terms of  $t$ -statistics were thresholded at a significance level of false discovery rate (FDR)-corrected  $p < 0.05$ , and overlaid on a cortical surface atlas. Functional connectivity of the right posterior insular cortex seed (lg2) region in response to ASMR (A), and in resting-state (B). Functional connectivity of the pregenual anterior cingulate cortex (pACC) seed region in response to ASMR (C), and in resting-state (D). Functional connectivity of the posterior cingulate cortex/precuneus (PCC/PC) seed regions in response to ASMR (E), and in resting state (F).

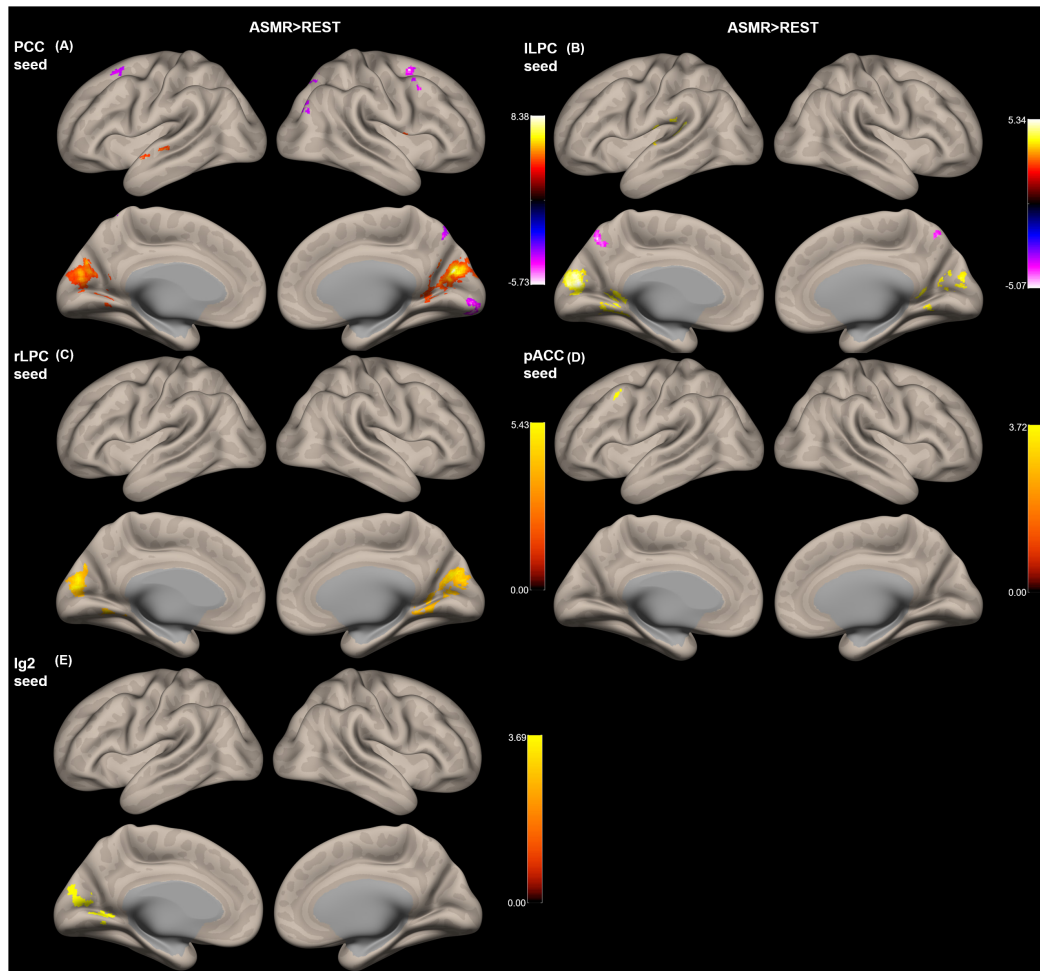
## Behavioral Data

There was a significant overall main effect on the affective response while watching ASMR video clips. As shown in **Figure 4**, participants had the most increase in low-activation positive state during the ASMR condition among four affective states that we have considered: LAP (group mean  $\pm$  standard deviation:  $3.94 \pm 1.46$ ), HAP ( $1.51 \pm 0.63$ ), LAN ( $1.45 \pm 0.64$ ), and HAN ( $1.38 \pm 0.78$ ). Statistical significance of the comparison between two selected states are as follows: LAP > HAP [ $\beta = 2.429$ ,  $t = 8.349$ ,  $p = 5.86 \times 10^{-9}$ ,  $df = 27$ , 95% confidence interval of the mean = (1.832–3.025); LAP > LAN ( $\beta = 2.488$ ,  $t = 8.471$ ,  $p = 4.39 \times 10^{-9}$ ,  $df = 27$ , 95% confidence interval of the mean = (1.885–3.091); LAP > HAN ( $\beta = 2.560$ ,

$t = 7.638$ ,  $p = 3.25 \times 10^{-8}$ ,  $df = 27$ , 95% confidence interval of the mean = (1.872–3.247)]. **Table 4** summarizes the statistical significance of affective states in response to ASMR.

Correlation coefficients between each of the four affective states and ASMR condition-specific connectivity changes are summarized in **Table 5**. In the DMN with the PCC seed region, significantly negative correlation was estimated between HAN and clusters with peaks in the lingual gyrus. Associations of HAP with clusters of the cuneus and lingual gyrus were also negatively correlated. In the affective touch and self-/other-networks, there were no significant correlation between the affective state scores and the ASMR-condition specific connectivity changes.





**FIGURE 3 |** Group-level functional connectivity of the  $t$ -statistic obtained by the “ASMR > resting-state” contrast. The default mode networks with seed regions of (A) the posterior cingulate cortex (PCC), (B) left lateral parietal cortex (LLPC), and (C) right lateral parietal cortex (rLPC). (D) The self-network with the pregenual anterior cingulate cortex (pACC) seed region. (E) Affective touch network with the posterior insular cortex (Ig2) seed region. There were no significant clusters in the default mode network with the mPFC seed region and the other-network with the PCC/PC seed region.

## DISCUSSION

In this study, we sought to test whether changes in functional connectivity within specific networks, including the DMN, affective touch network, and self-/other-networks occurred during ASMR. As a result, relative to connectivity in the resting-state, significantly altered connectivity of seed regions during viewing of ASMR-eliciting stimulus was found in the main hub composing each network. Furthermore, we confirmed that the strength of connectivity in involved in visual information processing was negatively correlated with the behavior score, including the HAN, and HAP states. We now discuss the implications of these results in more detail.

### Default Mode Network (ASMR > REST)

Our results showed that in the DMN, functional connectivity between the PCC seed region and the superior/middle temporal gyri, cuneus, and lingual gyrus were significantly increased

during ASMR condition, compared to the resting-state. Previous functional imaging studies (Carrington and Bailey, 2009; Spreng et al., 2009) have found that the PCC and superior temporal gyrus (STG) are involved in the “mentalizing,” also known as “theory of mind” that is an ability to make inferences about other people’s mental states [i.e., an understanding that the behaviors of others is determined by their desires, attitude, and beliefs (Frith and Frith, 2003)]. Specifically, Castelli et al. (2000) revealed that the superior temporal region was activated while watching silent or computer-presented animations, and this process was related to the attribution of mental states. Fletcher et al. (1995) reported significantly increased cerebral blood flow in the PCC during the condition necessitating the attribution of mental task. Therefore, the increased functional connectivity between the STG and PCC during ASMR condition can be associated with the increased covariance of the STG and the PCC activities compared to the resting-state, which may be interpreted as activation of mentalizing process to infer others’ mental and emotional

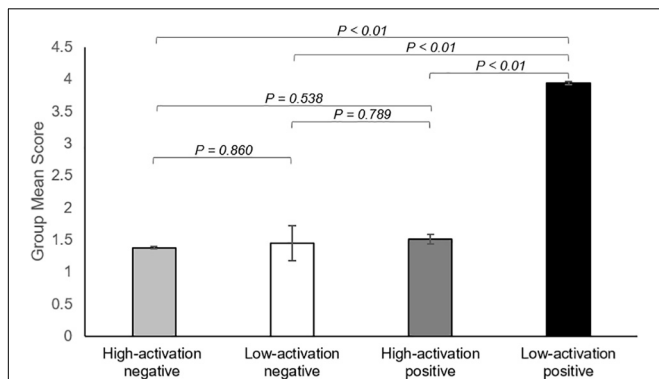


**TABLE 3 |** Statistical significance of the group-level functional connectivity obtained by the “ASMR > resting-state” contrast.

Connectivity (ASMR > REST)	Brodmann area	MNI (x, y, z)	Size	Peak-t	Peak-beta	Peak p-unc	Size p-FDR
<b>PCC seed</b>							
Cuneus	BA 18	(8, -74, 22)	1451	8.799	0.283	0.00000	0.00000
Superior frontal gyrus	BA 6	(24, 4, 56)	176	-5.498	-0.159	0.00000	0.00001
Visual area	BA 18	(10, -90, -6)	173	-6.020	-0.207	0.00000	0.00001
Lingual gyrus	BA 18	(-18, -70, 2)	59	4.290	0.176	0.00021	0.01692
Precuneus	BA 7	(6, -66, 48)	49	-4.552	-0.171	0.00010	0.02626
Superior temporal gyrus	BA 48	(54, 0, 0)	49	4.840	0.178	0.00004	0.02626
Superior temporal gyrus	BA 22	(-54, -2, -8)	42	5.822	0.158	0.00000	0.04210
Precuneus	BA 7	(-6, -64, 66)	37	-4.331	-0.219	0.00018	0.04281
Middle frontal gyrus	BA 8	(-24, 16, 58)	37	-4.434	-0.177	0.00014	0.04281
Middle occipital lobe	BA 39	(40, -78, 24)	37	-4.187	-0.200	0.00027	0.04281
Middle temporal gyrus	BA 21	(-62, -20, -6)	37	5.742	0.140	0.00000	0.04281
<b>ILPC seed</b>							
Visual area	BA 17	(-6, -78, 16)	526	5.702	0.186	0.00000	0.00000
Superior temporal gyrus	BA 22	(-56, -32, 10)	266	5.599	0.168	0.00000	0.00000
Precuneus	BA 7	(-6, -66, 50)	118	-5.131	-0.176	0.00002	0.00296
<b>rLPC seed</b>							
Cuneus	BA 18	(8, -76, 22)	1014	5.812	0.211	0.00000	0.00000
Lingual gyrus	BA 18	(-14, -64, -6)	113	5.501	0.187	0.00000	0.00002
<b>pACC seed</b>							
Middle frontal lobe	BA 9	(-50, 18, 44)	53	4.426	0.183	0.00014	0.03391
<b>Ig2 seed</b>							
Cuneus	BA 17	(-10, -68, 6)	301	5.565	0.143	0.00000	0.00000

We report clusters having significant connections from the seed region, the peak-voxel location in each cluster, and the corresponding *t*-, *beta*-, and *p*-values.

states by observing objects and perceiving intended actions and using ourselves to simulate their experience to understand them (Blakemore and Decety, 2001; Allen et al., 2003; Frith and Frith, 2006; Liew et al., 2011; Rieki et al., 2018).



**FIGURE 4 |** Summary of the results showing changes in affect state after viewing ASMR, relative to before watching ASMR. Bar graphs represent group mean scores for affective state assessed using the Multi-Affect Indicator (Warr, 1990). All variables range from 1 to 7. For self-reported changes in affect, 1 = much less; 7 = much more. The participants had the most increase in low-activation positive state during the ASMR condition among four affective states: low-activation positive state (group mean  $\pm$  standard deviation:  $3.94 \pm 1.46$ ), high-activation positive state ( $1.51 \pm 0.63$ ), low-activation negative state ( $1.45 \pm 0.64$ ), and high-activation negative state ( $1.38 \pm 0.78$ ). Statistical significance was determined by a *p*-value of less than 0.05.

We also found the reduced connectivity between the dorsolateral prefrontal cortex (dlPFC) and the PCC during ASMR condition, compared with the resting-state. Lévesque et al. (2003) reported that the dlPFC was involved in inhibition processing such as voluntary suppression of a negative emotion (sadness) while the participants suppressed their emotional reaction to the sad stimuli. For the PCC, this region has been known to be a part of network for emotion evaluation (Lee and Siegle, 2012), including an automatic perception for the emotion salience of stimulus (Maddock, 1999). Thus, compared to the resting state, the decreased functional connectivity between the dlPFC and PCC during ASMR condition can be interpreted as the decrease in voluntary suppression of negative emotion. This process may occur due to the nature of ASMR triggers that often lead to response of psychologically pleasant effects (Poerio et al., 2018).

With the DMN of the bilateral LPC seed regions, we found that the functional connectivity between the l/rLPC seeds and the visual areas of the cuneus and calcarine sulcus was significantly higher during the ASMR condition than during the resting-state. The cuneus is involved in visual information processing that interacts with the primary visual cortex (Vanni et al., 2001) and is known to integrate somatosensory information with other sensory stimuli (Price, 2000). In addition, the LPC is involved in receiving a visual input from the occipital regions, which belong to the dorsal stream of visual processing (Rizzolatti and Matelli, 2003). In terms of the visual stimuli, in our experiment, ASMR-eliciting video clips were much richer in visual information than

the instruction for resting-state condition (with eyes fixated on a cross). Therefore, greater functional connectivity of the cuneus and calcarine sulcus within the DMN may reflect the increased visual input and processing from ASMR-eliciting stimuli through functional connectivity, compared to the resting-state condition.

## Affective Touch and Self-Networks (ASMR > REST)

This study showed significant connectivity differences not only in the DMN but also in other network areas, including affective touch network, and self-network. In terms of the affective touch network, we found a greater connectivity between the Ig2 and

the cuneus of the occipital region during the ASMR condition than the resting-state. The cuneus is a part of the visual areas and engages in processing of visual input (Waberski et al., 2008) and the insular cortex integrates information from multiple modalities, including visual and auditory sensory modalities (Bamiou et al., 2003). Thus, the increased connection between Ig2 and cuneus indicates the higher visuoauditory influence of ASMR stimulus.

In terms of the self-network involved in the reflection of one's own experiences against other stimuli (Northoff et al., 2006), we found an increased connectivity between the pACC and the mPFC during ASMR condition, compared to resting-state. Murray et al. (2012) revealed that the mPFC and dorsal anterior cingulate cortex were activated in the self-referencing processing state rather than the other-relevant processing, and Gusnard et al. (2001) showed that these regions were particularly involved in self-referential processing in emotion domain. In addition, Northoff et al. (2006) reported that cortical midline structures including the mPFC and pACC mediate self-referential processing in psychological or physical domain such as autobiographical, emotional, and motor stimuli. Therefore, the increased connectivity between the pACC and the mPFC during ASMR may reflect the self-referential processing triggered by ASMR stimulus.

## Correlation Between Connectivity and Affective State

Although the major focus of this study is the connectivity on which the effects of ASMR are neural underpinnings, a correlation analysis was performed to investigate how these changed connections relate to the feelings felt during ASMR. As a result, in the PCC region, significantly negative correlation was estimated between clusters with peaks in the lingual gyrus and HAN. For rLPC seed region, connectivities in clusters of the lingual gyrus and cuneus were also negatively correlated in HAP. The PCC receives visual information from visual systems (Vogt et al., 2006) and the LPC also accepts visual input through dorsal stream (Rizzolatti and Matelli, 2003). The ASMR stimulus contains audio-visual stimuli that lead to a positive emotional response to calmness and a tingling sensation that emerges from a positive emotion (Barratt and Davis, 2015). Thus, these results imply that visual information processing in response to high arousal states can be weakened by ASMR-eliciting stimuli.

As a limitation of this finding, we did not explicitly measure the affective outcomes of resting state using the behavioral questionnaire [e.g., the Multi-Affect Indicator (Warr, 1990; Warr et al., 2014)]. As described in the Behavioral Data Analysis section, the participants were instructed to indicate how they felt while watching the ASMR video clip during the MRI scan, compared to before they watched the video. Therefore, individual behavioral scores that we measured may reflect relative affective states of ASMR condition to resting state. However, a control acquisition of the behavioral questionnaire after the resting state session would be required to compare the affective state changes between

**TABLE 4 |** Mean and standard deviation of behavioral score among emotional states.

Item	Average score	Standard deviation
Nervous	1.464	0.865
Anxious	1.321	0.847
Tense	1.357	0.934
<b>HAN</b>	<b>1.381</b>	<b>0.775</b>
Depressed	1.214	0.619
Dejected	2.107	1.496
Hopeless	1.036	0.186
<b>LAN</b>	<b>1.452</b>	<b>0.644</b>
Enthusiastic	1.536	0.906
Joyful	1.786	1.013
Excited	1.214	0.674
<b>HAP</b>	<b>1.512</b>	<b>0.627</b>
Calm	3.964	1.742
Relaxed	4.071	1.731
At ease	3.786	1.820
<b>LAP</b>	<b>3.940</b>	<b>1.456</b>

Paired <i>t</i> -test	<i>p</i>	<i>t</i>	beta	(95% CI)	df
LAP-HAP	0.00000	8.349	2.429	(1.832–3.025)	27
LAP-LAN	0.00000	8.471	2.488	(1.885–3.091)	27
LAP-HAN	0.00000	7.638	2.560	(1.872–3.247)	27
HAP-LAN	0.6858	0.409	0.060	(-0.239–0.358)	27
HAP-HAN	0.4957	0.691	0.131	(-0.258–0.520)	27
LAN-HAN	0.6078	0.519	0.071	(-0.211–0.354)	27

We report *t*-test results for comparing affective states during ASMR. HAN, High-activation negative state; LAN, Low-activation negative state; HAP, High-activation positive state; LAP, Low-activation positive state; df, Degrees of freedom.

**TABLE 5 |** Statistical results of correlation coefficients between each of the four affective states and ASMR condition-specific connectivity changes.

Connectivity-behavioral correlation	MNI (x, y, z)	<i>r</i>	<i>p</i>
<b>PCC seed</b>			
HAN-Lingual gyrus *	(-18, -70, 2)	-0.411	0.030
<b>rLPC seed</b>			
HAP-Cuneus **	(8, -76, 22)	-0.5085	0.006
HAP-Lingual gyrus**	(-14, -64, -6)	-0.497	0.007

\*\**p*-value < 0.01, \**p*-value < 0.05. PCC, Posterior cingulate cortex; rLPC, Right lateral parietal cortex. HAN, High-activation negative state; HAP, High-activation positive state.

resting-state and ASMR conditions more explicitly. Thus, caution should be exercised when interpreting the correlation coefficient between functional connectivity estimates and behavioral scores used in this study.

In conclusion, using fMRI functional connectivity estimates, we explored the ASMR-condition specific connectivity changes in the DMN, self-/other-networks, and the affective touch network. Compared with the resting-state functional connectivity, we found that several connections within the selected networks were significantly altered while watching ASMR video. In particular, the connections between the PCC and the superior temporal gyrus, between the pACC and the mPFC, and between the Ig2 and the cuneus were significantly greater during ASMR condition than resting state. These results suggest that ASMR process can be associated with ongoing interaction between regional activity that are involved in the integration of visual and auditory information followed by the mentalizing and self-referential processing. In terms of the relationship between connectivity and affective state changes, we found that ASMR-induced affective states (i.e., high activation negative and high activation positive state) were significantly negatively correlated with functional connectivity involved in visual information processing. These results imply that high arousal states can be attenuated in the process of perception of ASMR-eliciting stimuli. Our findings have implications for neurophysiological mechanisms of an ASMR effects in relation to functional connectivity changes.

## DATA AVAILABILITY STATEMENT

The fMRI data that support the findings of this study are available from the corresponding author on request.

## ETHICS STATEMENT

The studies involving human participants were reviewed and approved by the Institutional Review Board of Korea Basic Science Institute. The patients/participants provided their written informed consent to participate in this study.

## REFERENCES

- Allen, J. G., Bleiberg, E., and Haslam-Hopwood, T. (2003). Mentalizing as a compass for treatment. *Bull. Menninger Clin.* 67, 1–11.
- Bamiou, D., Musiek, F. E., and Luxon, L. M. (2003). The insula (Island of Reil) and its role in auditory processing: literature review. *Brain Res. Rev.* 42, 143–154. doi: 10.1016/s0165-0173(03)00172-3
- Barratt, E. L., and Davis, N. J. (2015). Autonomous Sensory Meridian Response (ASMR): a flow-like mental state. *PeerJ* 3:e851. doi: 10.7717/peerj.851
- Barratt, E. L., Spence, C., and Davis, N. J. (2017). Sensory determinants of the autonomous sensory meridian response (ASMR): understanding the triggers. *PeerJ* 5:e3846. doi: 10.7717/peerj.3846
- Bateman, A., and Fonagy, P. (2013). Mentalization-based treatment. *Psychoanal. Inq.* 33, 595–613.
- Beckmann, C. F., DeLuca, M., Devlin, J. T., and Smith, S. M. (2005). Investigations into resting-state connectivity using independent component analysis. *Philos. Trans. R. Soc. B* 360, 1001–1013. doi: 10.1098/rstb.2005.1634

## AUTHOR CONTRIBUTIONS

SL designed the study. SL and JK conducted the experiment and performed the fMRI data acquisition. SL and ST performed the data analysis, discussed the study idea, analysis, and results, and wrote the manuscript. All authors reviewed the manuscript.

## FUNDING

This work was supported in part by the grants from the Korea Basic Science Institute (T38609 and C030130) and the National Research Foundation of Korea (NRF) grant funded by the Korea Government (MIST) (2019R1C1C1011281).

## SUPPLEMENTARY MATERIAL

The Supplementary Material for this article can be found online at: <https://www.frontiersin.org/articles/10.3389/fnbeh.2020.00154/full#supplementary-material>

**FIGURE S1** | Group-level functional connectivity of the beta-value in the default mode network during resting-state, and in response to ASMR effects. Functional connectivity of the posterior cingulate cortex seed region in response to (A) ASMR, and (B) resting-state. Functional connectivity of the medial prefrontal cortex seed region in response to (C) ASMR, and (D) resting-state. Functional connectivity of the left lateral parietal cortex seed region in response to (E) ASMR, and (F) resting-state. Functional connectivity of the right lateral parietal cortex seed region in response to (G) ASMR, and (H) resting-state.

**FIGURE S2** | Group-level functional connectivity of the beta-value in the affective touch, self-, and other-networks during resting-state, and in response to ASMR effects. Functional connectivity of the right posterior insular cortex seed region in response to (A) ASMR, and (B) resting-state. Functional connectivity of the pregenual anterior cingulate cortex seed region (C) in response to ASMR, and (D) resting-state. Functional connectivity of the posterior cingulate cortex/precuneus seed region in response to (E) ASMR, and (F) resting-state.

**FIGURE S3** | Group-level functional connectivity of the beta-value for ASMR > resting-state contrast. Default mode networks with seed regions of (A) the posterior cingulate cortex, (B) medial prefrontal cortex, (C) left lateral parietal cortex, and (D) right lateral parietal cortex. (E) Self-network with the pregenual anterior cingulate cortex seed region. (F) Other-network with the posterior cingulate cortex/precuneus seed region. (G) Affective touch network with the posterior insular cortex seed region.

- Behzadi, Y., Restom, K., Liau, J., and Liu, T. T. (2007). A component based noise correction method (CompCor) for BOLD and perfusion based fMRI. *Neuroimage* 37, 90–101. doi: 10.1016/j.neuroimage.2007.04.042
- Birn, R. M., Diamond, J. B., Smith, M. A., and Bandettini, P. A. (2006). Separating respiratory-variation-related fluctuations from neuronal-activity-related fluctuations in fMRI. *Neuroimage* 31, 1536–1548. doi: 10.1016/j.neuroimage.2006.02.048
- Birn, R. M., Molloy, E. K., Patriat, R., Parker, T., Meier, T. B., Kirk, G. R., et al. (2013). The effect of scan length on the reliability of resting-state fMRI connectivity estimates. *Neuroimage* 83, 550–558. doi: 10.1016/j.neuroimage.2013.05.099
- Biswal, B., Zerrin Yetkin, F., Haughton, V. M., and Hyde, J. S. (1995). Functional connectivity in the motor cortex of resting human brain using echo-planar MRI. *Magn. Reson. Med.* 34, 537–541.
- Blakemore, S. J., and Decety, J. (2001). From the perception of action to the understanding of intention. *Nat. Rev. Neurosci.* 2, 561–567. doi: 10.1038/35086023

- Calhoun, V. D., Adali, T., Pearlson, G. D., and Pekar, J. J. (2001). A method for making group inferences from functional MRI data using independent component analysis. *Hum. Brain Mapp.* 14, 140–151. doi: 10.1002/hbm.1048
- Carrington, S. J., and Bailey, A. J. (2009). Are there theory of mind regions in the brain? A review of the neuroimaging literature. *Hum. Brain Mapp.* 30, 2313–2335.
- Cash, D. K., Heisick, L. L., and Papesh, M. H. (2018). Expectancy effects in the autonomous sensory meridian response. *PeerJ* 6:e5229. doi: 10.7717/peerj.5229
- Castelli, F., Happé, F., Frith, U., and Frith, C. (2000). Movement and mind: a functional imaging study of perception and interpretation of complex intentional movement patterns. *Neuroimage* 12, 314–325. doi: 10.1006/nimg.2000.0612
- Chang, C., and Glover, G. H. (2009). Relationship between respiration, end-tidal CO<sub>2</sub>, and BOLD signals in resting-state fMRI. *Neuroimage* 47, 1381–1393. doi: 10.1016/j.neuroimage.2009.04.048
- Cohen, S., Janicki-Deverts, D., and Miller, G. E. (2007). Psychological stress and disease. *JAMA* 298, 1685–1687.
- Fair, D. A., Schlaggar, B. L., Cohen, A. L., Miezin, F. M., Dosenbach, N. U., Wenger, K. K., et al. (2007). A method for using blocked and event-related fMRI data to study “resting state” functional connectivity. *Neuroimage* 35, 396–405. doi: 10.1016/j.neuroimage.2006.11.051
- Fisher, R. A. (1915). Frequency distribution of the values of the correlation coefficient in samples from an indefinitely large population. *Biometrika* 10, 507–521. doi: 10.1093/biomet/10.4.507
- Fletcher, P. C., Happe, F., Frith, U., Baker, S. C., Dolan, R. J., Frackowiak, R. S., et al. (1995). Other minds in the brain: a functional imaging study of “theory of mind” in story comprehension. *Cognition* 57, 109–128. doi: 10.1016/0010-0277(95)00692-r
- Fox, M. D., Snyder, A. Z., Vincent, J. L., Corbetta, M., Van Essen, D. C., and Raichle, M. E. (2005). The human brain is intrinsically organized into dynamic, anticorrelated functional networks. *Proc. Natl. Acad. Sci. U.S.A.* 102, 9673–9678. doi: 10.1073/pnas.0504136102
- Fredborg, B., Clark, J., and Smith, S. D. (2017). An examination of personality traits associated with autonomous sensory meridian response (ASMR). *Front. Psychol.* 8:247.
- Friston, K., Ashburner, J., Kiebel, S., Nichols, T., and Penny, W. (2007). *Statistical Parametric Mapping: The Analysis of Functional Brain Images*. Boston: Academic Press.
- Friston, K. J., Worsley, K. J., Frackowiak, R. S., Mazziotta, J. C., and Evans, A. C. (1994). Assessing the significance of focal activations using their spatial extent. *Hum. Brain Mapp.* 1, 210–220. doi: 10.1002/hbm.460010306
- Frith, C. D., and Frith, U. (2006). The neural basis of mentalizing. *Neuron* 50, 531–534. doi: 10.1016/j.neuron.2006.05.001
- Frith, U., and Frith, C. D. (2003). Development and neurophysiology of mentalizing. *Philos. Trans. R. Soc. Lond. Ser. B Biol. Sci.* 358, 459–473.
- Greicius, M. D., Krasnow, B., Reiss, A. L., and Menon, V. (2003). Functional connectivity in the resting brain: a network analysis of the default mode hypothesis. *Proc. Natl. Acad. Sci. U.S.A.* 100, 253–258. doi: 10.1073/pnas.0135058100
- Gusnard, D. A., Akbudak, E., Shulman, G. L., and Raichle, M. E. (2001). Medial prefrontal cortex and self-referential mental activity: relation to a default mode of brain function. *Proc. Natl. Acad. Sci. U.S.A.* 98, 4259–4264. doi: 10.1073/pnas.071043098
- Lee, K. H., and Siegle, G. J. (2012). Common and distinct brain networks underlying explicit emotional evaluation: a meta-analytic study. *Soc. Cogn. Affect. Neurosci.* 7, 521–534. doi: 10.1093/scan/nsp001
- Lee, M., Song, C. -B., Shin, G. -H., and Lee, S. -W. (2019). Possible effect of binaural beat combined with autonomous sensory meridian response for inducing sleep. *Front. Hum. Neurosci.* 13:425.
- Leopold, D. A., Murayama, Y., and Logothetis, N. K. (2003). Very slow activity fluctuations in monkey visual cortex: implications for functional brain imaging. *Cereb. Cortex* 13, 422–433. doi: 10.1093/cercor/13.4.422
- Lévesque, J., Eugène, F., Joannette, Y., Paquette, V., Mensour, B., Beaudoin, G., et al. (2003). Neural circuitry underlying voluntary suppression of sadness. *Biol. Psychiatry* 53, 502–510. doi: 10.1016/s0006-3223(02)01817-6
- Liew, S. L., Han, S., and Aziz-Zadeh, L. (2011). Familiarity modulates mirror neuron and mentalizing regions during intention understanding. *Hum. Brain Mapp.* 32, 1986–1997. doi: 10.1002/hbm.21164
- Lochte, B. C., Guillory, S. A., Richard, C. A., and Kelley, W. M. (2018). An fMRI investigation of the neural correlates underlying the autonomous sensory meridian response (ASMR). *Bioimpacts* 8:295. doi: 10.15171/bi.2018.32
- Logie, K., and Frewen, P. (2015). Self/other referential processing following mindfulness and loving-kindness meditation. *Mindfulness* 6, 778–787. doi: 10.1007/s12671-014-0317-z
- Lombardo, M. V., Chakrabarti, B., Bullmore, E. T., and Wheelwright, S. J. (2010). Shared neural circuits for mentalizing about the self and others. *J. Cogn. Neurosci.* 22, 1623–1635. doi: 10.1162/jocn.2009.21287
- Maddock, R. J. (1999). The retrosplenial cortex and emotion: new insights from functional neuroimaging of the human brain. *Trends Neurosci.* 22, 310–316. doi: 10.1016/s0166-2236(98)01374-5
- Mars, R. B., Neubert, F. X., Noonan, M. P., Sallet, J., Toni, I., and Rushworth, M. F. (2012). On the relationship between the “default mode network” and the “social brain”. *Front. Hum. Neurosci.* 6:189.
- Morrison, I. (2016). ALE meta-analysis reveals dissociable networks for affective and discriminative aspects of touch. *Hum. Brain Mapp.* 37, 1308–1320. doi: 10.1002/hbm.23103
- Murphy, K., Birn, R. M., and Bandettini, P. A. (2013). Resting-state fMRI confounds and cleanup. *Neuroimage* 80, 349–359. doi: 10.1016/j.neuroimage.2013.04.001
- Murray, R. J., Debbané, M., Fox, P. T., Bzdok, D., and Eickhoff, S. B. (2015). Functional connectivity mapping of regions associated with self-and other-processing. *Hum. Brain Mapp.* 36, 1304–1324. doi: 10.1002/hbm.22703
- Murray, R. J., Schaer, M., and Debbané, M. (2012). Degrees of separation: a quantitative neuroimaging meta-analysis investigating self-specificity and shared neural activation between self-and other-reflection. *Neurosci. Biobehav. Rev.* 36, 1043–1059. doi: 10.1016/j.neubiorev.2011.12.013
- Muschelli, J., Nebel, M. B., Caffo, B. S., Barber, A. D., Pekar, J. J., and Mostofsky, S. H. (2014). Reduction of motion-related artifacts in resting state fMRI using aCompCor. *Neuroimage* 96, 22–35. doi: 10.1016/j.neuroimage.2014.03.028
- Northoff, G., Heinzel, A., de Greck, M., Bermpohl, F., Dobrowolny, H., and Panksepp, J. (2006). Self-referential processing in our brain: a meta-analysis of imaging studies on the self. *Neuroimage* 31, 440–457. doi: 10.1016/j.neuroimage.2005.12.002
- Patriat, R., Molloy, E.K., Meier, T.B., Kirk, G.R., Nair, V.A., Meyerand, M.E., Prabhakaran, V., Birn, R.M. (2013). The effect of resting condition on resting-state fMRI reliability and consistency: a comparison between resting state with eyes open, closed, and fixated. *Neuroimage* 78, 463–473.
- Poerio, G. L., Blakey, E., Hostler, T. J., and Veltri, T. (2018). More than a feeling: autonomous sensory meridian response (ASMR) is characterized by reliable changes in affect and physiology. *PLoS One* 13:e0196645. doi: 10.1371/journal.pone.0196645
- Price, D. D. (2000). Psychological and neural mechanisms of the affective dimension of pain. *Science* 288, 1769–1772. doi: 10.1126/science.288.5472.1769
- Riekk, T., Svedholm-Häkkinen, A. M., and Lindeman, M. (2018). Empathizers and systemizers process social information differently. *Soc. Neurosci.* 13, 616–627. doi: 10.1080/17470919.2017.1368700
- Rizzolatti, G., and Matelli, M. (2003). Two different streams form the dorsal visual system: anatomy and functions. *Exp. Brain Res.* 153, 146–157. doi: 10.1007/s00221-003-1588-0
- Russell, J. A. (2003). Core affect and the psychological construction of emotion. *Psychol. Rev.* 110, 145–172.
- Segerstrom, S. C., and Miller, G. E. (2004). Psychological stress and the human immune system: a meta-analytic study of 30 years of inquiry. *Psychol. Bull.* 130, 601–630. doi: 10.1037/0033-2909.130.4.601
- Sharp, C., Pane, H., Ha, C., Venta, A., Patel, A. B., Sturek, J., et al. (2011). Theory of mind and emotion regulation difficulties in adolescents with borderline traits. *J. Am. Acad. Child. Adolesc. Psychiatry* 50, 563–573.
- Smith, S. D., Fredborg, B. K., and Kornelsen, J. (2019). Atypical functional connectivity associated with autonomous sensory meridian response: an examination of five resting-state networks. *Brain* 9, 508–518
- Smith, S. D., Katherine Fredborg, B., and Kornelsen, J. (2017). An examination of the default mode network in individuals with autonomous sensory meridian

- response (ASMR). *Soc. Neurosci.* 1, 361–365. doi: 10.1080/17470919.2016.1188851
- Spreng, R. N., Mar, R. A., and Kim, A. S. (2009). The common neural basis of autobiographical memory, prospection, navigation, theory of mind, and the default mode: a quantitative meta-analysis. *J. Cogn. Neurosci.* 21, 489–510. doi: 10.1162/jocn.2008.21029
- Van Dijk, K. R., Hedden, T., Venkataraman, A., Evans, K. C., Lazar, S. W., and Buckner, R. L. (2010). Intrinsic functional connectivity as a tool for human connectomics: theory, properties, and optimization. *J. Neurophysiol.* 103, 297–321.
- Van Essen, D. C., Smith, S. M., Barch, D. M., Behrens, T. E., Yacoub, E., Ugurbil, K., et al. (2013). The WU-Minn human connectome project: an overview. *Neuroimage* 80, 62–79.
- Vanni, S., Tanskanen, T., Seppä, M., Uutela, K., and Hari, R. (2001). Coinciding early activation of the human primary visual cortex and anteromedial cuneus. *Proc. Natl. Acad. Sci. U.S.A.* 98, 2776–2780.
- Vogt, B. A., Vogt, L., and Laureys, S. (2006). Cytology and functionally correlated circuits of human posterior cingulate areas. *Neuroimage* 29, 452–466.
- Waberski, T. D., Gobbelé, R., Lamberty, K., Buchner, H., Marshall, J. C., and Fink, G. R. (2008). Timing of visuo-spatial information processing: electrical source imaging related to line bisection judgements. *Neuropsychologia* 46, 1201–1210.
- Warr, P. (1990). The measurement of well-being and other aspects of mental health. *J. Occup. Psychol.* 63, 193–210.
- Warr, P., Bindl, U. K., Parker, S. K., and Inceoglu, I. (2014). Four-quadrant investigation of job-related affects and behaviours. *Eur. J. Work Org. Psychol.* 23, 342–363.
- Whitfield-Gabrieli, S., and Nieto-Castanon, A. (2012). Conn: a functional connectivity toolbox for correlated and anticorrelated brain networks. *Brain Connect.* 2, 125–141.
- Conflict of Interest:** The authors declare that the research was conducted in the absence of any commercial or financial relationships that could be construed as a potential conflict of interest.

Copyright © 2020 Lee, Kim and Tak. This is an open-access article distributed under the terms of the Creative Commons Attribution License (CC BY). The use, distribution or reproduction in other forums is permitted, provided the original author(s) and the copyright owner(s) are credited and that the original publication in this journal is cited, in accordance with accepted academic practice. No use, distribution or reproduction is permitted which does not comply with these terms.





# Evaluation of Effective Connectivity Between Brain Areas Activated During Simulated Driving Using Dynamic Causal Modeling

Mi-Hyun Choi, Hyung-Sik Kim and Soon-Cheol Chung\*

Biomedical Engineering, Research Institute of Biomedical Engineering, School of ICT Convergence Engineering, College of Science and Technology, Konkuk University, Chungju, South Korea

## OPEN ACCESS

### Edited by:

Lars Michels,  
University of Zurich, Switzerland

### Reviewed by:

Alexander Nikolaevich  
Savostyanov,  
State Scientific Research Institute  
of Physiology and Basic Medicine,  
Russia

Kostas Hadjilimitrakis,  
University of Bologna, Italy

### \*Correspondence:

Soon-Cheol Chung  
sccchung@kku.ac.kr

### Specialty section:

This article was submitted to  
Individual and Social Behaviors,  
a section of the journal  
Frontiers in Behavioral Neuroscience

**Received:** 11 March 2020

**Accepted:** 10 August 2020

**Published:** 23 September 2020

### Citation:

Choi M-H, Kim H-S and  
Chung S-C (2020) Evaluation  
of Effective Connectivity Between  
Brain Areas Activated During  
Simulated Driving Using Dynamic  
Causal Modeling.  
Front. Behav. Neurosci. 14:158.  
doi: 10.3389/fnbeh.2020.00158

This study was examined the effective connectivity between brain areas activated during driving. Using a driving simulator, the subjects controlled a wheel with both of their hands as well as an accelerator and brake pedal with their right foot. Of the areas activated during driving, three areas from each hemisphere were analyzed for effective connectivity using dynamic causal modeling. In the right hemisphere, bidirectional connectivity was prominent between the inferior temporal gyrus, precuneus, and lingual gyrus, which provided driving input (driving input refers to the area of input among areas connected with effective connectivity). In the left hemisphere, the superior temporal gyrus provided driving input, and bidirectional connectivity was prominent between the superior temporal gyrus, inferior parietal lobule, and inferior frontal gyrus. The visual attention pathway was activated in the right hemisphere, whereas the inhibitory control movement and task-switching pathways, which are responsible for synesthesia, were activated in the left hemisphere. In both of the hemispheres, the visual attention, inhibitory control movement, and episodic memory retrieval pathways were prominent. The activation of these pathways indicates that driving requires multi-domain executive function in addition to vision. Moreover, pathway activation is influenced by the driving experience and familiarity of the driver. This study elucidated the overall effective connectivity between brain areas related to driving.

**Keywords:** effective connectivity, driving, visual attention pathway, inhibitory control movement pathway, episodic memory retrieval pathway

## INTRODUCTION

The development of functional magnetic resonance imaging (fMRI) has enabled research on the function and connectivity of brain areas. Previous fMRI studies on driving, which requires complex cognitive processing, such as attention, learning, memory, and decision making, were conducted using driving simulators. Michon (1984) reported that driving requires complex cognitive processing of three interacting hierarchical levels, including the strategic (i.e., trip planning and route finding), tactical (i.e., planning of relevant actions based on the current driving context), and operational (i.e., action execution and perception) levels. Drivers should drive appropriately, paying attention to not making mistakes, which requires complex cognitive processing. Most driving

accidents are caused by drivers' mistakes in cognition and judgment, demonstrating that cognition and judgment are crucial for driving. More than 90% of the information required for such cognition and judgment during driving is acquired through vision.

In particular, many studies on changes in brain activation related to visual cognition and spatial attention during driving have been conducted (Arrington et al., 2000; Friston and Buchel, 2000; Tomasi et al., 2004). The main areas related to visual cognition are the primary visual (V1) and motion-sensitive visual regions [V5/area middle temporal (MT)] and the parietal cortex (Brodmann area 7; Friston and Buchel, 2000). Further, the brain areas related to high-order visual processing are the posterior cingulate, cerebellum, and occipital and parietal cortices (Calhoun et al., 2002). Areas related to visual attention are the occipital, inferotemporal, and parahippocampal cortices, thalamus, cerebellum, and frontal cortex (Arrington et al., 2000; Tomasi et al., 2004) and those related to spatial attention (vigilance) are the frontal and parietal cortical regions (Graydon et al., 2004). When a video game of cars was used for subjects to recognize whether the speed was slow or fast, areas related to the high-order visual, such as the occipital fusiform, cerebellum, middle and superior occipital lobes, inferior temporal lobe, and superior parietal lobe, were activated, and those related to vigilance, such as the medial, inferior, middle, superior frontal lobes, and precuneus (parietal), were activated (Calhoun et al., 2002).

Recently, there have been many studies on extraction of interaction between activated brain regions using "effective connectivity" for various cognitive performances and on direction and connection strength between regions. Studies on effective connectivity for cognitive processing are also being conducted, but there are not many studies on effective connectivity between areas that are activated during driving. In particular, Wang et al. (2015) conducted a driving experiment with drivers and non-drivers and reported greater functional connectivity in the left fronto-parietal and primary visual resting-state networks (RSNs) in people with more driving experience. The left fronto-parietal network is a connectivity related to higher-order cognitive functions, and the primary visual resting-state networks is a network related to functions of visual cognition. The driving behavior altered the functional connectivity between the cognitive and sensory intrinsic connectivity networks (ICNs), and the strength of specific connections between the left fronto-parietal and primary visual network significantly correlated with the number of years as a taxi driver (Wang et al., 2015). Shen et al. (2016) reported that the strength of connectivity between areas in the vigilance network decreased with increasing driving experience. The vigilance network is a network containing areas of anterior cingulate cortex and anterior insula. The vigilance is the ability to sustain attention over prolonged periods of time. Among the cognitive types that may appear when driving, only the results of studies on the above-mentioned networks have been reported using functional connectivity analysis.

The aforementioned studies investigated differences in functional connectivity between brain areas during driving in

certain subject groups and for certain cognitive aspects, and research on overall brain connectivity during driving has so far been lacking. Particularly, connectivity among the left, right, and bilateral hemispheres during driving, their meaning and input areas, and directivity and correlation between input and other areas are yet to be investigated; however, such information can be obtained through an effective connectivity analysis.

Based on other studies and previous studies from our research team, we expect the following results on brain effective connectivity when driving. As mentioned above, since driving requires complex cognitive processing, such as attention, learning, memory, and decision making, we expect that certain cognitive areas would appear dominant in the left and right hemispheres when driving. In the right hemisphere, connectivity between areas related to the high-order visual and concentration would be dominant, and in the left hemisphere, connectivity between areas related to synesthesia and motion control is expected to be large. In addition, because the steering wheel is controlled with both hands, the motor cortex areas of the left and right hemispheres would be activated simultaneously, and since the right foot is used to operate the pedal, the motor cortex of the parietal lobe in the left hemisphere would be predominantly activated.

To investigate the correlation between brain areas activated during driving, this fMRI study analyzed effective connectivity between areas in the left, right, and bilateral hemispheres using dynamic causal modeling (DCM).

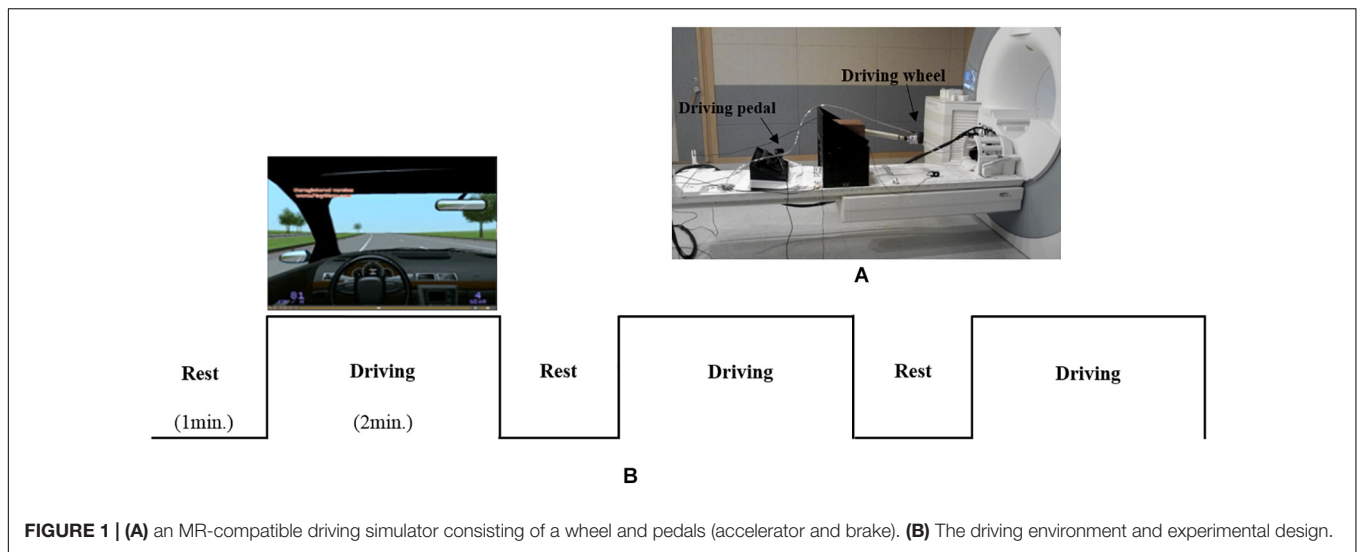
## MATERIALS AND METHODS

### Subjects

Fifteen adult men (mean age:  $26.0 \pm 1.4$  years old), without any history of mental or neurological disease and with a mean driving experience of  $2.5 \pm 1.6$  years, were selected as subjects. All subjects were right-handed as a result of the revised Edinburgh Reading Test (Oldfield, 1971). Individuals with metal inside their bodies (e.g., cardiac pacemaker or medical wiring), which could interfere with magnetic resonance (MR) imaging, as well as those with claustrophobia were excluded. External factors, such as smoking, alcohol consumption, and coffee intake, which can influence driving and brain activation, were restricted in the subjects prior to the experiment. The purpose and details of the experiment were explained to the subjects. Practice driving was conducted until the subjects became familiar with the driving simulator environment and could drive without any accidents.

### MR-Compatible Driving Simulator

As shown in **Figure 1A**, an MR-compatible driving simulator consisting of a wheel and pedals (i.e., accelerator and brake) was used for this study (Kim et al., 2020). The driving environment (**Figure 1B**), which mostly consisted of straight streets without many visual distractors, was presented using Lightrock Entertainment software. The subjects controlled the wheel with both of their hands as well as the accelerator and brake with their right foot. The subjects were asked to drive at a constant speed of 80 km/h without changing lanes. Visual



**FIGURE 1 |** (A) an MR-compatible driving simulator consisting of a wheel and pedals (accelerator and brake). (B) The driving environment and experimental design.

information for driving was presented to the subjects through the visual system attached to the head coil. Visual system is  $800 \times 600$  pixels, aspect ratio is 4:3, and FOV is  $30^\circ$  horizontal/ $23^\circ$  vertical.

## Experimental Design

As shown in **Figure 1B**, the experiment consisted of three blocks, with each block consisting of rest (1 min) and driving (2 min) phases. During the rest phase, the subjects were asked to look at a fixed screen without driving. During rest phase, subjects placed both hands on the steering wheel and a right foot on the pedal without any movement. During the driving phase, the subjects were asked to drive at a constant speed of 80 km/h. To help the subjects maintain a speed of 80 km/h, speed information was presented on the lower left corner of the simulator screen. During the driving phase, alerts signaling the start (i.e., “please start driving”) and completion (i.e., “please stop driving”) of the driving task were orally provided by a researcher through the headset worn by each subject. Oral driving cues were given to subjects at each driving phase.

## Image Acquisition

Images were acquired with a 3T MRI scanner (Magnetom TrioTim, Siemens Medical Systems, Erlangen, Germany) using a standard 32-channel head coil. Single-shot echo planar fMRI scans were acquired in 29 continuous slices, parallel to the anterior commissure-posterior commissure line. The fMRI parameters were as follows: TR/TE = 3000/30 ms, FOV = 200 mm, flip angle =  $90^\circ$ , matrix =  $128 \times 128$ , slice thickness = 5 mm, and voxel size =  $1.6 \times 1.6 \times 5.0$  mm. Anatomical images were obtained using a T1-weighted 3D-MPRAGE sequence with TR/TE = 1900/2.48 ms, FOV = 200 mm, flip angle =  $9^\circ$ , matrix =  $256 \times 256$ , slice thickness = 1 mm, and voxel size =  $0.8 \times 0.8 \times 1.0$  mm.

## Image Analysis

The fMRI data were analyzed with Statistical Parametric Mapping (SPM) 8 software (Wellcome Department of Cognitive

Neurology, London, United Kingdom). All functional images were aligned with anatomic images using affine transformation routines built into SPM 8. The realigned scans were co-registered to anatomic images obtained within each session and normalized to a template image in Montreal Neurologic Institute (MNI) space. Motion correction was done using a Sinc interpolation. Time-series data were filtered with a 240 s high-pass filter to remove artifacts due to cardiorespiratory and other cyclical influences. The functional map was smoothed with an 8 mm isotropic Gaussian kernel prior to statistical analysis. Statistical analysis was performed at the group level using the general linear model and theory of Gaussian random fields implemented in SPM8. A group analysis was performed to extend the inference of individual activation to the general population from which the subjects were drawn. This will list all clusters above the chosen level of significance as well as separate ( $>8$  mm apart) maxima within a cluster, with details of significance thresholds (height threshold  $T = 4.69$  ( $p < 0.05$ ), extent threshold  $k = 0$  voxels) and search volume underneath.

Subtraction method was used to obtain the activated area in the driving phase compared to the rest phase (Driving phase – Rest phase). This result is a functional map obtained through group analysis. It may be that, due to this extraction method, driving-like response from the previous driving phase was minimized in the rest phase.

## Connectivity Analysis

To extract the effective connectivity between brain areas activated during driving, DCM was used to investigate the correlation between areas of interest. DCM, which is a model-based analysis method, can be applied not only to the analysis of brain activation through general linear modeling (GLM), but also to the analysis of brain area connectivity. In this analysis, the relationship between each variable is estimated through covariate or linear regression analysis, and a model of the correlation between brain areas is constructed based on this

information. For DCM analysis, models are defined in SPM8 based on MATLAB, which is followed by variable estimation and Bayesian model selection (BMS). Operating under the hypothesis that all activated areas form a network, DCM analyzes the correlation between areas with blood oxygen level-dependent (BOLD) signals and establishes optimal dynamic causality models (Friston et al., 2003).

Of the areas activated during driving, three areas from each hemisphere with the highest *z*-scores had their effective connectivity analyzed. As discussed in the results section, the three areas from the right hemisphere with the highest *z*-scores were the inferior temporal gyrus (ITG), precuneus (PCu), and lingual gyrus (LiG), whereas those from the left hemisphere with the highest *z*-scores were the inferior parietal lobule (IPL), superior temporal gyrus (STG), and inferior frontal gyrus (IFG; **Figure 2**). The effective connectivity was analyzed for the three areas in the left and right hemispheres as well as for all six areas in both hemispheres. Effective connectivity analysis involved the selection of driving input areas as areas of interest and modeling connectivity based on the correlation between the BOLD signals of the areas of interest. For connectivity analysis, the time-series of the BOLD signal of each area of interest was extracted from 5 mm diameter spherical regions centered around the voxel with the greatest *z*-score.

Specifically, effective connectivity analysis began by selecting driving inputs to the left and right hemispheres (i.e., three areas from each) as well as both hemispheres (i.e., six areas). After selecting areas of interest as fully connected (i.e., full bidirectional connection between all areas of interest), models hypothesizing each area as the input were established. For example, the inferior temporal gyrus, precuneus, and lingual gyrus of the right hemisphere were selected as fully connected, and three models, in which each area was set as the driving input, were established. Subsequently, using BMS, the most significant driving input model was selected using fixed effect calculations.

After selecting the driving input areas of the right, left, and both hemispheres, the connectivity between areas of interest was analyzed. Sixty-four models for each hemisphere were established to investigate the connectivity between the three areas of the left and right hemispheres (**Figure 3**). In **Figure 3**, the first and second columns are models of the three areas of the right and left hemispheres, respectively, and the third column shows models of the six areas of both hemispheres. As shown in the first and second columns of **Figure 3**, Model 1 is a full connection model indicating intrinsic connection with bidirectional connections between all areas. Moreover, Models 2–63 differ in the direction of connections while considering external connections. Model 64 has no connections between areas.

A total of 299 models of the connectivity between the six areas in both hemispheres were established (see **Figure 3**, third column). Similar to the models within the first and second columns, in the third column, Model 1 is a full connection model, Models 2–298 differ in the connectivity between areas of interest, and Model 299 has no connectivity.

This analysis was performed for each subject. The posterior model probability for each model was extracted for each

subject using BMS fixed effects (FFX) to compare models in each hemisphere. Based on the data from each subject, group comparison of models was performed using BMS random fixed effects (RFX). RFX analysis obtains the optimal probability for presumed models, and was used to estimate the probability of each model. Model probability was tested at the group level, and the model with the highest probability was used to derive the mean correlation between areas and determine the effective connectivity.

## RESULTS

Of the brain areas activated during driving, the three areas in the right hemisphere with the highest *z*-scores were the ITG, PCu, and LiG (**Figures 2A–C**), which had *z*-scores of 9.33, 8.28, and 8.05, respectively. The most significant of the three models, in which each area was set as the driving input, was that with the LiG as the driving input (probabilities: 1.00, C-direct effects: 0.1 Hz). The connectivity between these three areas was bidirectional and had significant effects (**Table 1** and **Figure 4A**).

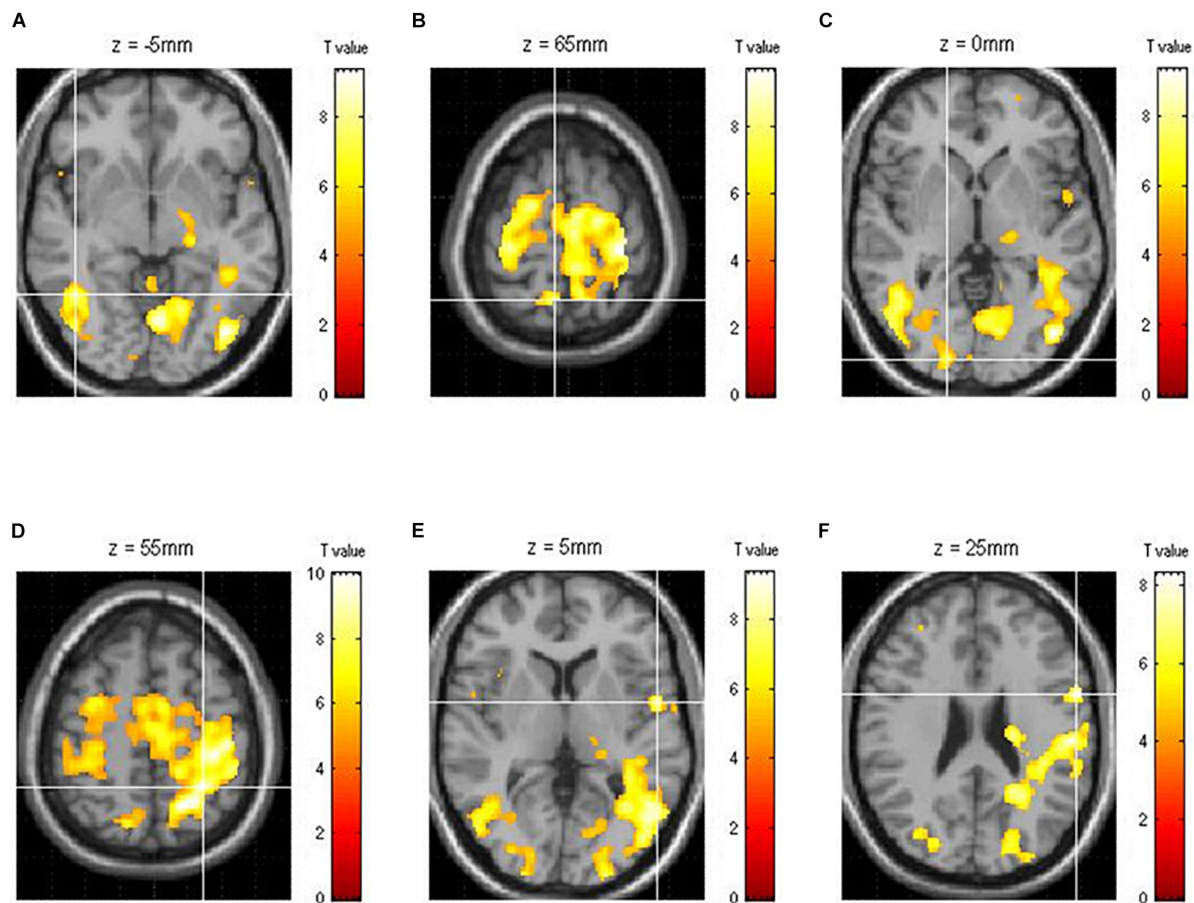
The three areas in the left hemisphere with the highest *z*-scores were the IPL, STG, and IFG (**Figures 2D–F**), which had *z*-scores of 9.91, 7.14, and 7.66, respectively. The most significant of the three models analyzed was that with the STG as the driving input (probabilities: 1.00, C-direct effects: 0.13 Hz). Similar to the right hemisphere, the connectivity between these three areas was bidirectional and had high correlations (**Table 1** and **Figure 4B**).

For both of the hemispheres, the effective connectivity was analyzed between the right ITG (rITG), right PCu (rPCu), right LiG (rLiG), left IPL (lIPL), left STG (lSTG), and left IFG (lIFG; **Table 2** and **Figure 4**<sup>®</sup>). Of the six models with each of the six areas set as the driving input, the most significant model was that with the lSTG as the driving input (probabilities: 1.00, C-direct effects: 0.15 Hz). There was prominent connectivity from the lSTG to the rITG (A-intrinsic connections: 0.15, correlation parameters: 100%), rLiG (0.16, 100%), lIPL (0.1, 99%), and lIFG (0.13, 100%).

## DISCUSSION

For driving, various cognitive processes, such as vision, synesthesia, motion control, judgment, concentration, attention, and memory, are required. In previous studies, visual network (Wang et al., 2015), vigilance network (Shen et al., 2016), and left fronto-parietal network (Wang et al., 2015) among the brain networks for various cognitive types that may appear when driving is reported using functional connectivity. The main difference between this study's results and previous studies is to be mentioned in three ways. First, by using effective connectivity, the meaning of connectivity and the input area in each connectivity are presented. Second, the results for directionality and connection strength from the input region to other regions are presented. Third, these results are reported as brain networks that predominate in each of the left and right hemispheres. This study sought to analyze the connectivity





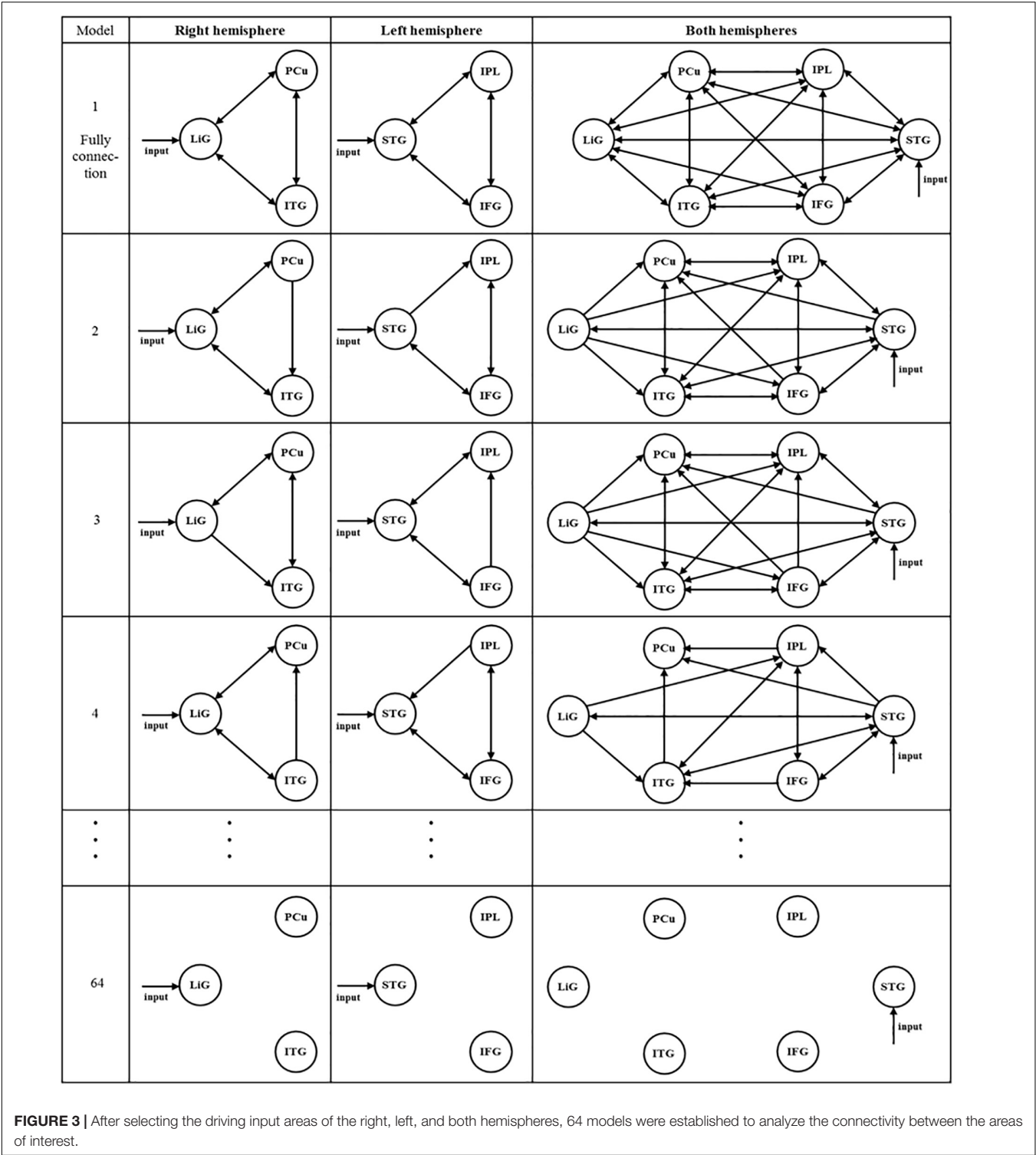
**FIGURE 2 |** Functional brain map showing the average of all subjects obtained through group analysis. The three right [(A) ITG, inferior temporal gyrus; (B) PCu, precuneus; (C) LiG, lingual gyrus] and left [(D) IPL, inferior parietal lobule; (E) STG, superior temporal gyrus; (F) IFG, inferior frontal gyrus] hemispheric areas with the highest z-scores during driving.

between brain areas responsible for cognitive processing during driving in the right, left, and both hemispheres.

## Effective Connectivity Between Areas Activated in the Right Hemisphere

In the right hemisphere, the LiG, which processes visual linguistic information and plays a crucial role in the analysis of encoded visual memories (Mechelli et al., 2000), PCu, which is related to recollection and memory as well as the integration of information relating to environment perception (Lundstrom et al., 2005; Cavanna and Trimble, 2006), and ITG, which is related to higher-level visual processing (Kolb and Whishaw, 2014) had significant bidirectional connectivity. Since the right hemisphere visually perceives the driving environment and processes information for this purpose, the LiG would have been selected as the input area. Previous fMRI studies have reported that the aforementioned three areas form the visual attention pathway (Milner and Goodale, 1998; Macaluso et al., 2000; Purves et al., 2008). Visual attention can best be defined as a family of processing resources or cognitive mechanisms that

can modulate signals at almost every level of the visual system. Research shows that visual attention can perform this function by actively suppressing irrelevant stimuli or by selecting potentially relevant stimuli. The connectivity from the LiG to the PCu is the dorsal stream pathway, which processes the location of objects (Milner and Goodale, 1998). Moreover, this pathway has been reported to analyze motion as well as the spatial relationship (i.e., “where”) between objects, thus being responsible for visual synesthesia (Purves et al., 2008). The connectivity from the LiG to the ITG is the ventral stream pathway, which processes information on “what” an object is (Milner and Goodale, 1998). This pathway has been reported to be responsible for high-resolution vision (Purves et al., 2008). This study, which analyzed brain connectivity related to driving, also clearly observed visual attention pathways related to the “where” and “what” of an object as in previous studies. This study also found significant bidirectional connectivity between the PCu and the ITG. Although a pathway between these two areas has not been previously reported, this finding is reasonable given the functions of each area. Information processing for driving is mostly performed through vision, and visual information is processed



through simple and higher-order processing. High-resolution visual processing is necessary for driving, and recollection and memory as well as the integration of information relating to the perception of the environment play important roles in driving tasks. Therefore, the PCu and ITG would have had a significant correlation. In addition to the aforementioned functions, the PCu is also associated with episodic memory retrieval (Lundstrom et al., 2005) and vigilance performance (Shen et al., 2016). Vigilance, which is a fundamental component of attention, refers to the ability to maintain attention over a long period of time. Vigilance is crucial in driving, in which an individual must continuously monitor and react to rare signals while ignoring

**TABLE 1 |** Correlation between three left (IPL, inferior parietal lobule; STG, superior temporal gyrus; IFG, inferior frontal gyrus; and right (ITG, inferior temporal gyrus; PCu, precuneus; LiG, lingual gyrus) hemispheric areas activated during driving.

		From		
		ITG	PCu	LiG
<b>Right hemisphere</b>				
<i>To</i>				
ITG			0.46 (97%)	0.63 (100%)
PCu	0.3 (93%)			0.25 (90%)
LiG	0.54 (100%)	0.33 (91%)		
		From		
		IPL	STG	IFG
<b>Left Hemisphere</b>				
<i>To</i>				
IPL			0.4 (99%)	0.43 (97%)
STG	0.46 (98%)			0.44 (98%)
IFG	0.38 (96%)	0.41 (98%)		

ITG, Inferior Temporal Gyrus; PCu, Precuneus; LiG, Lingual Gyrus; IPL, Inferior Parietal Lobule; STG, Superior Temporal Gyrus; IFG, Inferior Frontal Gyrus.

irrelevant stimuli. Therefore, it is possible that the PCu and ITG had a significant correlation not only because drivers perceive the driving environment based on higher-order visual processing, but also because their episodic memories and vigilance influence driving. Thus, the connectivity between the LiG, PCu, and ITG during driving, with the LiG as the input area, may serve as the visual attention-(episodic) memory retrieval pathway.

## Effective Connectivity Between Areas Activated in the Left Hemisphere

In the left hemisphere, the STG, which is primarily involved in auditory recognition and understanding language meaning (Howard et al., 2000), IFG, which is associated with information selection and monitoring as well as cognitive control (Lundstrom et al., 2005; Grindrod et al., 2008), and IPL, which is associated with perspective difference cognition,<sup>2</sup> spatial cognition, and visually guided movement (Andersen, 2011; Hadjidimitrakakis et al., 2012, 2019; Yttri et al., 2014; Kaas and Stepniewska, 2016), had significant bidirectional connectivity. In particular, a study reported that inferior frontal junction area (IFJ) (located at the junction of the inferior frontal sulcus and the inferior precentral sulcus), which includes the IFG region, has three main component processes (task switching, inhibitory control and working memory) (Brass et al., 2005; Derrfuss et al., 2005, 2009; Levy and Wagner, 2011; Kim et al., 2012).

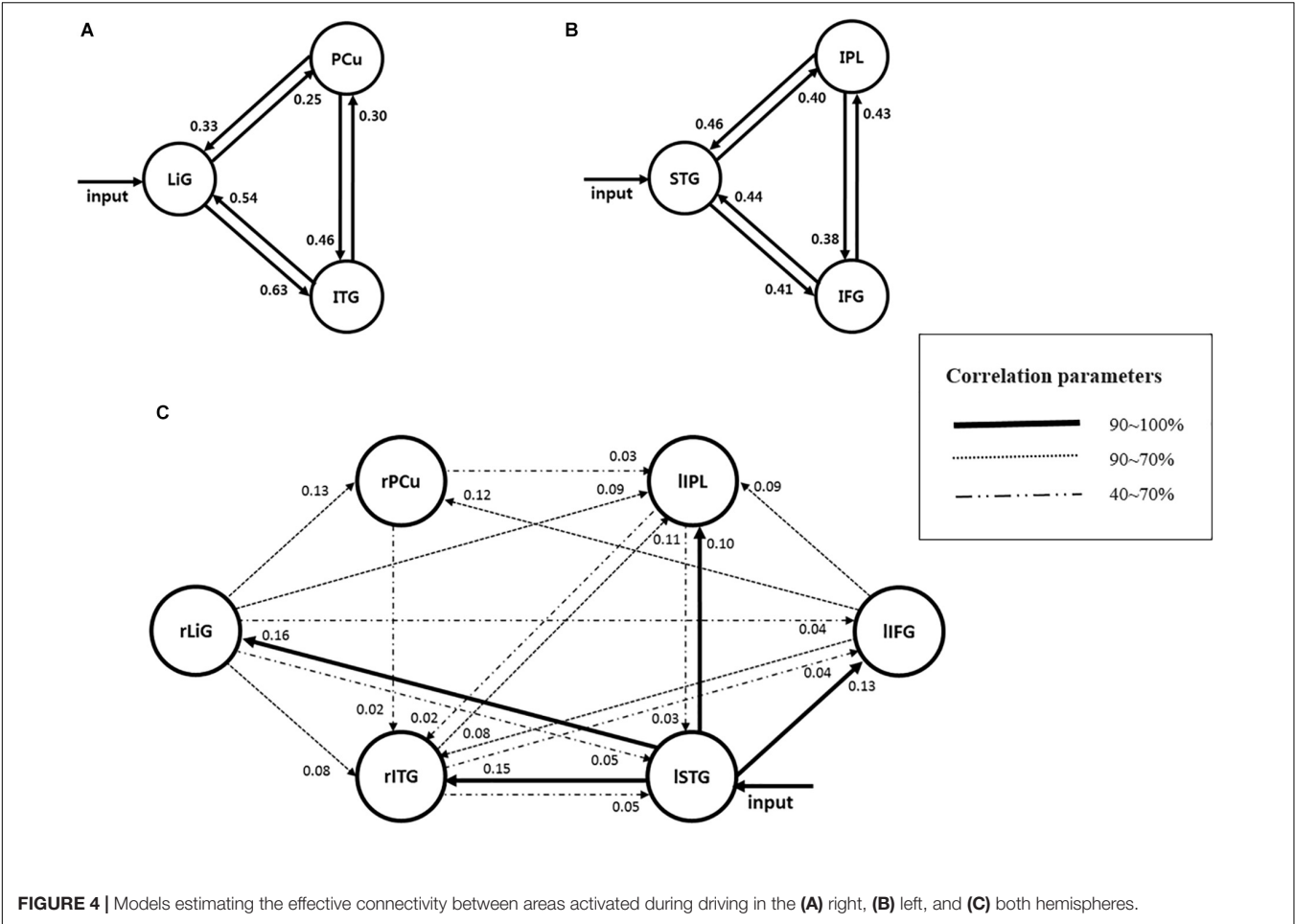
<sup>2</sup>With “perspective difference cognition” or, for short, “perspective tracking” we want to merely grasp the existence of this concept required for registering an actual or potential conflict between perspectives. The more common term “perspective taking” suggests the ability to put oneself into another perspective than the perspective one currently has. This would require the tracking of a particular perspective not just the tracking of a potential perspective difference. There is growing evidence that the dorsal part of the left temporo-parietal junction (TPJ), which overlaps with the left inferior parietal lobe (IPL), is reliably activated by perspective tasks (Goel et al., 1995; Ruby and Decety, 2003).

Since oral driving alerts (i.e., “Please start driving” and “Please stop driving”) were provided by a researcher to the subjects during each phase, the STG, which is associated with language processing, would have been selected as the input area. The connectivity between the STG and IFG has previously been reported as a wide language network (Jeong et al., 2009); however, these areas may have driving functions as well. The STG and IFG have been associated with convergent semantic processing, which controls, suppresses, and modulates various options to successfully perform multiple related tasks (Friederici et al., 2003). Since this study required the subjects to maintain their driving lane and speed, they had to simultaneously control the wheel and pedals, which required convergent semantic processing. This task led to significant bidirectional connectivity between the STG and IFG, in which these areas formed a network associated with inhibitory control in addition to language processing. Inhibitory control, also known as response inhibition, is a cognitive process and more specifically, an executive function – that permits an individual to inhibit their impulses and natural, habitual, or dominant behavioral responses to stimuli (a.k.a. prepotent responses) in order to select a more appropriate behavior that is consistent with completing their goals (Diamond, 2013; Ilieva et al., 2015). Inhibitory control revealed that frontal, subcortical, insula (INS), and parietal regions are active.

The connectivity between the STG and IPL can be predicted according to the following observations. First, the dorsal part of the left temporo-parietal junction (TPJ) is activated during perspective tasks (Goel et al., 1995; Ruby and Decety, 2003), which require tracking of potential, or actual, perspective differences (Arora et al., 2015). The driving images presented in this study were similar to actual driving environments, requiring spatial perception of near and far perspectives. Since oral driving cues (ISTG) and driving images with perspective differences (IPL) were used for this driving task, bidirectional connectivity between these two areas would have been significant. Second, the driving cues (STG) as well as the spatial cognition and hand and leg movements needed to control the wheel and pedals for visually guided driving (IPL) are predictive of these areas having significant bidirectional connectivity.

The bidirectional connection between the Inferior Frontal Gyrus and the Inferior Parietal Lobule may be related to movement control for controlling the steering wheel and pedals when driving. By initiating and modulating cognitive control abilities, the fronto-parietal network (Sundermann and Pfeleiderer, 2012) is involved in a wide variety of tasks. Thus, cognitive control of driving by the IFG as well as control of the wheel and pedals to maintain speed by the IPL led to significant connectivity between these two areas.

Due to the use of oral driving cues, the STG was selected as the input area. The overall connectivity of the STG with the IFG and IPL can be interpreted in terms of movement during driving. First, the connectivity from the STG to the IFG, and then to the IPL, selects and monitors driving information, and permits driving (IPL) through inhibitory control (IFG). Therefore, this pathway could serve as an inhibitory control movement pathway. With the STG as the input, the IPL performs driving through spatial recognition and vision. Moreover, the



cognitive control of the IFG switches between different tasks, such as controlling the wheel and pedals. Consequently, this pathway could serve as a task-switching pathway. Although these pathways may be considered identical since they both regulate movements associated with driving, they still differ in terms of whether a driving motion is performed.

**TABLE 2 |** Correlation between six left and right hemispheric areas (rITG, right inferior temporal gyrus; rPCu, right precuneus; rLiG, right lingual gyrus; lIPL, left inferior parietal lobule; lSTG, left superior temporal gyrus; lIFG, left inferior frontal gyrus) activated during driving.

	From					
	rITG	rPCu	rLiG	lIPL	lSTG	lIFG
To						
rITG		0.02 (56%)	0.08 (73%)	0.02 (71%)	0.15 (100%)	0.08 (71%)
rPCu	0		0.13 (87%)	0	0	0.12 (85%)
rLiG	0	0		0	0.16 (100%)	0
lIPL	0.11 (80%)	0.03 (58%)	0.09 (75%)		0.1 (100%)	0.09 (74%)
lSTG	0.05 (64%)	0	0.05 (64%)	0.03 (60%)		0
lIFG	0.04 (63%)	0	0.04 (62%)	0	0.13 (100%)	

r, right hemisphere; l, Left hemisphere.

### Effective Connectivity Between Areas Activated in Both Hemispheres

Of the six areas activated in both hemispheres, the ISTG was selected as the input area since oral driving cues were provided to the subjects during each phase. The following pathways, with the input area as the start and correlations above 70%, are explained below (Figure 4):

- ① As described previously, the connectivity between the ISTG → lIFG → lIPL is the inhibitory control movement pathway. In the left hemisphere, inhibitory control movement and task-switching pathways were observed, whereas, in both hemispheres, the inhibitory control movement pathway was dominant.
- ② There was a prominent connectivity between the ISTG → lIFG → rPCu. Previous studies have reported that the lIFG and rPCu were activated during episodic memory retrieval (Lundstrom et al., 2005). This pathway would likely act to select and monitor information on certain driving aspects (i.e., maintenance of speed and lane) acquired prior to driving and apply the subject's episodic memory. Therefore, this pathway could act as an episodic memory retrieval pathway.



- ③ The pathway between the ISTG → rITG → IPL could have resulted from the subjects using higher-order visual functions to perceive the driving environment (Kolb and Whishaw, 2014), spatial cognition (Andersen, 2011), and perspective differences cognition for driving.
- ④ The pathways between the ISTG → rLiG → rPCu and ⑤ ISTG → rLiG → rITG are visual attention pathways (see section “Effective Connectivity Between Areas Activated in the Right Hemisphere”) that were dominant in the left and right hemispheres.
- ⑥ The pathway between the ISTG → rLiG → IPL → rITG appeared since the perception of perspective differences and spatial cognition (IPL) were added to the visual attention pathway (i.e., ⑤).

## CONCLUSION

This study investigated the effective connectivity between brain areas activated during driving for the left, right, and both hemispheres.

Since visual cognition and processing are crucial for driving, the visual attention pathway was prominent in the right and both hemispheres. Moreover, the inhibitory control movement and task-switching pathways, which are related to synesthesia required for driving, were prominent in the left hemisphere. An interesting finding of this study was the observation of the inhibitory control movement pathway, which was prominent in the left and both hemispheres. Although research on inhibitory control has been largely conducted using go/no-go tasks (Chikazoe, 2010; Ma et al., 2015), no reports associated with driving have been made. Inhibitory control is a multi-domain executive function critical for flexible responsivity to changing task demands, and, thus, is an essential component of adaptive behavioral regulation. As expected, pathways regulating movement through inhibitory control were prominent during driving.

The episodic memory retrieval pathway observed in the right and both hemispheres is associated with drivers recalling their own experiences, indicating that driving is influenced by driving experience and familiarity.

In accordance with the hypothesis proposed in this study, connectivity between areas related to specific cognition in the right and the left hemispheres was predominant, but we could also observe interesting results that were not consistent with the hypothesis. Because both hands and right foot were used, we expected that activation would be dominant in the area

including the premotor cortex and supplementary motor area. However, IPL parietal cortex, the area responsible for controlling the movement by perceiving the situation through spatial and visual perception (controlling steering wheel with both hands and pedal with right foot in this study), was predominantly activated. As such, we suggest that IPL cortex, which is involved in complex cognitive processing that controls behavior according to the surrounding environment, is more activated than motor cortex such as premotor cortex and supplementary motor area.

Although the driving simulator was similar to actual driving conditions, it still differed from actual conditions. Moreover, events that were not directly associated with driving, such as the oral driving cues, were included in the experiment. However, this study is still significant by being the first to investigate the overall effective connectivity between brain areas associated with driving.

## DATA AVAILABILITY STATEMENT

The datasets generated for this study are available on request to the corresponding author.

## ETHICS STATEMENT

The studies involving human participants were reviewed and approved by the Institutional Review Committee of Konkuk University. The patients/participants provided their written informed consent to participate in this study.

## AUTHOR CONTRIBUTIONS

M-HC conceived the project and performed the experiments. H-SK made the experimental system. M-HC and S-CC designed the experiments and wrote the manuscript. All authors read and edited the manuscript prior to publication.

## FUNDING

This work was supported by the Mid-Career Researcher Program Grant through the National Research Foundation of Korea (NRF), funded by the Ministry of Education (MOE) (Grant No. 2017R1A2B2004629) and this research was supported by Basic Science Research Program through the National Research Foundation of Korea (NRF) funded by the Ministry of Education (Grant No. 2017R1D1A1B03029585).

## REFERENCES

- Andersen, R. A. (2011). Inferior parietal lobule function in spatial perception and visuomotor integration. *Comprehens. Physiol.* 11, 483–518.
- Arora, A., Weiss, B., Schurz, M., Aichhorn, M., Wieshofer, R. C., and Perner, J. (2015). Left inferior-parietal lobe activity in perspective tasks: identity statements. *Front. Hum. Neurosci.* 9:360. doi: 10.3389/fnhum.2015.0360
- Arrington, C. M., Carr, T. H., Mayer, A. R., and Rao, S. M. (2000). Neural mechanisms of visual attention: object-based selection of a region in space. *J. Cogn. Neurosci.* 2, 106–117. doi: 10.1162/089982900563975
- Brass, M., Derrfuss, J., Forstmann, B., and von Cramon, D. Y. (2005). The role of the inferior frontal junction area in cognitive control. *Trends Cogn. Sci.* 9, 314–316. doi: 10.1016/j.tics.2005.05.001
- Calhoun, V. D., Pekar, J. J., McGinty, V. B., Adali, T., Watson, T. D., and Pearlson, G. D. (2002). Different activation dynamics in multiple neural systems during simulated driving. *Hum. Brain. Mapp.* 16, 158–167. doi: 10.1002/hbm.10032

- Cavanna, A. E., and Trimble, M. R. (2006). The precuneus: a review of its functional anatomy and behavioural correlates. *Brain* 129, 564–583. doi: 10.1093/brain/awl004
- Chikazoe, J. (2010). Localizing performance of go/no-go tasks to prefrontal cortical subregions. *Curr. Opin. Psychiatry* 23, 267–272. doi: 10.1097/ycp.0b013e3283387a9f
- Derrfuss, J., Brass, M., Neumann, J., and von Cramon, D. Y. (2005). Involvement of the inferior frontal junction in cognitive control: meta-analyses of switching and Stroop studies. *Hum. Brain Mapp.* 25, 22–34. doi: 10.1002/hbm.20127
- Derrfuss, J., Brass, M., von Cramon, D. Y., Lohmann, G., and Amunts, K. (2009). Neural activations at the junction of the inferior frontal sulcus and the inferior precentral sulcus: interindividual variability, reliability, and association with sulcal morphology. *Hum. Brain Mapp.* 30, 299–311. doi: 10.1002/hbm.20501
- Diamond, A. (2013). Executive functions. *Annu. Rev. Psychol.* 64, 135–168.
- Friederici, A. D., Rüschemeyer, S. A., Hahne, A., and Fiebach, C. J. (2003). The role of left inferior frontal and superior temporal cortex in sentence comprehension: localizing syntactic and semantic processes. *Cereb. Cortex* 13, 170–177. doi: 10.1093/cercor/13.2.170
- Friston, K. J., and Buchel, C. (2000). “Attentional modulation of effective connectivity from V2 to V5/MT in humans,” in *Proceedings of the National Academy of Sciences*, 97, 7591–7596.
- Friston, K. J., Harrison, L., and Penny, W. (2003). Dynamic causal modelling. *NeuroImage* 19, 1273–1302. doi: 10.1016/s1053-8119(03)00202-7
- Goel, V., Grafman, J., Sadato, N., and Hallett, M. (1995). Modeling other minds. *Neuroreport* 6, 1741–1746.
- Graydon, F. X., Young, R. A., Tdss, M. D., Genik, R. J., Posse, S., Hsieh, L., et al. (2004). Visual event detection during simulated driving: identifying the neural correlates with functional neuroimaging. *J. Neurosci.* 24, 271–286. doi: 10.1016/j.trf.2004.09.006
- Grindrod, C. M., Bilenko, N. Y., Myers, E. B., and Blumstein, S. E. (2008). The role of the left inferior frontal gyrus in implicit semantic competition and selection: an event-related fMRI study. *Brain Res.* 1229, 167–178. doi: 10.1016/j.brainres.2008.07.017
- Hadjidimitrakis, K., Bakola, S., Wong, Y. T., and Hagan, M. A. (2019). Mixed spatial and movement representations in the primate posterior parietal cortex. *Front. Neural Circ.* 13:15. doi: 10.3389/fncir.2019.00015
- Hadjidimitrakis, K., Breveglieri, R., Bosco, A., and Fattori, P. (2012). Three-dimensional eye position signals shape both peripersonal space and arm movement activity in the medial posterior parietal cortex. *Front. Integr. Neurosci.* 6:37. doi: 10.3389/fnint.2012.00037
- Howard, M. A., Volkov, I. O., Mirsky, R., Garell, P. C., Noh, M. D., Granner, M., et al. (2000). Auditory cortex on the human posterior superior temporal gyrus. *J. Comp. Neurol.* 416, 79–92. doi: 10.1002/(sici)1096-9861(20000103)416:1<79::aid-cne6>3.0.co;2-2
- Ilieva, I. P., Hook, C. J., and Farah, M. J. (2015). Prescription stimulants' effects on healthy inhibitory control, working memory, and episodic memory: a meta-analysis. *J. Cogn. Neurosci.* 27, 1–21.
- Jeong, B., Wible, C. G., Hashimoto, R., and Kubicki, M. (2009). Functional and anatomical connectivity abnormalities in left inferior frontal gyrus in schizophrenia. *Hum. Brain Mapp.* 30, 4138–4151. doi: 10.1002/hbm.20835
- Kaas, J. H., and Stepniewska, I. (2016). Evolution of posterior parietal cortex and parietal-frontal networks for specific actions in primates. *J. Comp. Neurol.* 524, 595–608. doi: 10.1002/cne.23838
- Kim, C., Cilles, S. E., Johnson, N. F., and Gold, B. T. (2012). Domain general and domain preferential brain regions associated with different types of task switching: a meta-analysis. *Hum. Brain Mapp.* 33, 130–142. doi: 10.1002/hbm.21199
- Kim, H. S., Mun, K. R., Choi, M. H., and Chung, S. C. (2020). Development of an fMRI-compatible driving simulator with simultaneous measurement of physiological and kinematic signals: the multi-biosignal measurement system for driving (MMSD). *Technol. Health Care* 28, S335–S345.
- Kolb, B., and Whishaw, I. Q. (2014). *An Introduction to Brain and Behavior Fourth edition*. New York, NY: Worth, 282–312.
- Levy, B. J., and Wagner, A. D. (2011). Cognitive control and right ventrolateral prefrontal cortex: reflexive reorienting, motor inhibition, and action updating. *Ann. N. Y. Acad. Sci.* 1224, 40–62. doi: 10.1111/j.1749-6632.2011.05958.x
- Lundstrom, B. N., Ingvar, M., and Petersson, K. M. (2005). The role of precuneus and left inferior frontal cortex during source memory episodic retrieval. *NeuroImage* 27, 824–834. doi: 10.1016/j.neuroimage.2005.05.008
- Ma, L., Steinberg, J. L., Cunningham, K. A., Lane, S. D., Bjork, J. M., Neelakantan, H., et al. (2015). Inhibitory behavioral control: a stochastic dynamic causal modeling study comparing cocaine dependent subjects and controls. *NeuroImage Clin.* 7, 837–847. doi: 10.1016/j.nicl.2015.03.015
- Macaluso, E., Frith, C. D., and Driver, J. (2000). Modulation of human visual cortex by crossmodal spatial attention. *Science* 289, 1206–1208. doi: 10.1126/science.289.5482.1206
- Mechelli, A., Humphreys, G. W., Mayall, K., Olson, A., and Price, C. J. (2000). Differential effects of word length and visual contrast in the fusiform and lingual gyri during reading. *Proc. R. Soc. B* 267, 1909–1913. doi: 10.1098/rspb.2000.1229
- Michon, J. A. (1984). “Traffic and mobility,” in *Handbook of Work and Organizational Psychology*, Vol. 2, eds P. J. D. Drenth, H. Thierry, P. J. Willems, and J. de Wolff (New York: Wiley), 1165–1196.
- Milner, A. D., and Goodale, M. A. (1998). *The Visual Brain in Action*. Oxford: Oxford University Press.
- Oldfield, R. C. (1971). The assessment and analysis of handedness: the Edinburgh inventory. *Neuropsychologia* 9, 97–113. doi: 10.1016/0028-3932(71)90067-4
- Purves, D., Cabeza, R., Huettel, S. A., Labar, K. S., Platt, M. L., and Woldorff, M. G. (2008). *Principles of Cognitive Neuroscience*. Sunderland, MA: Sinauer Associates.
- Ruby, P., and Decety, J. (2003). What you believe versus what you think they believe: a neuroimaging study of conceptual perspective-taking. *Eur. J. Neurosci.* 17, 2475–2480. doi: 10.1046/j.1460-9568.2003.02673.x
- Shen, H., Li, Z., Qin, J., Liu, Q., Wang, L., Zeng, L. L., et al. (2016). Changes in functional connectivity dynamics associated with vigilance network in taxi drivers. *NeuroImage* 124, 367–378. doi: 10.1016/j.neuroimage.2015.09.010
- Sundermann, B., and Pfeleiderer, B. (2012). Functional connectivity profile of the human inferior frontal junction: involvement in a cognitive control network. *BMC Neurosci.* 13:119. doi: 10.1186/1471-2202-13-119
- Tomasí, D., Ernst, T., Caparelli, E. C., and Chang, L. (2004). Practice-induced changes of brain function during visual attention: a parametric fMRI study at 4 Tesla. *Neuroimage* 23, 1414–1421. doi: 10.1016/j.neuroimage.2004.07.065
- Wang, L., Liu, Q., Shen, H., Li, H., and Hu, D. (2015). Large-scale functional brain network changes in taxi drivers: evidence from resting-state fMRI. *Hum. Brain Mapp.* 36, 862–871. doi: 10.1002/hbm.22670
- Yttri, E. A., Wang, C., Liu, Y., and Snyder, L. H. (2014). The parietal reach region is limb specific and not involved in eye-hand coordination. *J. Neurophysiol.* 111, 520–532. doi: 10.1152/jn.00058.2013

**Conflict of Interest:** The authors declare that the research was conducted in the absence of any commercial or financial relationships that could be construed as a potential conflict of interest.

Copyright © 2020 Choi, Kim and Chung. This is an open-access article distributed under the terms of the Creative Commons Attribution License (CC BY). The use, distribution or reproduction in other forums is permitted, provided the original author(s) and the copyright owner(s) are credited and that the original publication in this journal is cited, in accordance with accepted academic practice. No use, distribution or reproduction is permitted which does not comply with these terms.



# Resting-State Functional Connectivity of the Punishment Network Associated With Conformity

Yin Du<sup>1</sup>, Yanan Wang<sup>1\*</sup>, Mengxia Yu<sup>1</sup>, Xue Tian<sup>1</sup> and Jia Liu<sup>2\*</sup>

<sup>1</sup>Faculty of Psychology, Beijing Normal University, Beijing, China, <sup>2</sup>Department of Psychology, Tsinghua Laboratory of Brain and Intelligence, Tsinghua University, Beijing, China

## OPEN ACCESS

### Edited by:

Gennady Knyazev,  
State Scientific Research Institute of  
Physiology and Basic Medicine,  
Russia

### Reviewed by:

Tingyong Feng,  
Southwest University, China  
Wenbin Guo,  
Central South University, China

### \*Correspondence:

Yinan Wang  
yynnwang@gmail.com  
Jia Liu  
liujiaTHU@tsinghua.edu.cn

### Specialty section:

This article was submitted to  
Individual and Social Behaviors,  
a section of the journal  
Frontiers in Behavioral Neuroscience

**Received:** 14 October 2020

**Accepted:** 26 November 2020

**Published:** 16 December 2020

### Citation:

Du Y, Wang Y, Yu M, Tian X and Liu J  
(2020) Resting-State Functional  
Connectivity of the Punishment  
Network Associated With Conformity.  
Front. Behav. Neurosci. 14:617402.  
doi: 10.3389/fnbeh.2020.617402

Fear of punishment prompts individuals to conform. However, why some people are more inclined than others to conform despite being unaware of any obvious punishment remains unclear, which means the dispositional determinants of individual differences in conformity propensity are poorly understood. Here, we explored whether such individual differences might be explained by individuals' stable neural markers to potential punishment. To do this, we first defined the punishment network (PN) by combining all potential brain regions involved in punishment processing. We subsequently used a voxel-based global brain connectivity (GBC) method based on resting-state functional connectivity (FC) to characterize the hubs in the PN, which reflected an ongoing readiness state (i.e., sensitivity) for potential punishment. Then, we used the within-network connectivity (WNC) of each voxel in the PN of 264 participants to explain their tendency to conform by using a conformity scale. We found that a stronger WNC in the right thalamus, left insula, postcentral gyrus, and dACC was associated with a stronger tendency to conform. Furthermore, the FC among the four hubs seemed to form a three-phase ascending pathway, contributing to conformity propensity at every phase. Thus, our results suggest that task-independent spontaneous connectivity in the PN could predispose individuals to conform.

**Keywords:** punishment network, functional connectivity, conformity propensity, thalamus, insula, postcentral gyrus, dACC

## INTRODUCTION

*"The idea that men are created free and equal is both true and misleading: men are created different; they lose their freedom and their autonomy in seeking to become like each other."*

David Riesman, *The Lonely Crowd: A Study of the Changing American Character*

Conformity is a prevailing social phenomenon, which means behaving in accordance with the common norms, social standards, attitudes, beliefs, and values of a given culture (Riesman, 1950; Riesman et al., 2001). At an individual level, conformity refers to the act of changing one's behavior to match the responses of others (Cialdini and Goldstein, 2004). Marcuse (1964) defined this social character as one-dimensionality in his book, *One-Dimensional Man*, describing a state of affairs that conforms to existing thought and behavior, in which there is a lack of critical dimension.

Individuals are prompted to conform due to a fear of punishment (Cialdini and Goldstein, 2004; Spitzer et al., 2007; Haun and Tomasello, 2011; Gelfand, 2012). First, from a social psychological perspective, a minority position is aversive (Asch, 1956; Hornsey et al., 2003); it can lead to hostility, disapproval, rejection from others, or social isolation (Heerdink et al., 2015). To avoid such social punishment, people might be motivated to conform to the majority position (Falk et al., 2012). Second, from an evolutionary perspective, evolutionary game-theoretic models (Smith, 1982) show that groups that face greater societal threats require harsher punishment for norm deviators to avoid a breakdown of cooperation and to survive (Gelfand, 2012). Regarding the prominent role of such peer punishment in human evolution (Boyd et al., 2003), humans could have developed corresponding neural mechanisms that made them constantly vigilant to the threat of potential punishment (Fehr and Gächter, 2002; De Quervain et al., 2004; Spitzer et al., 2007), which implies that the dispositional determinants of individual differences in conformity propensity (Egerton et al., 2010; Jolles et al., 2011) might be a stable neural trait (i.e., sensitivity to punishment at a neural level). Also, as the tendency to imitate is usually swift and automatic (Griskevicius et al., 2006), the individual differences in conformity propensity might be driven by differences in early automatic perception of potential punishment (Franzen and Brinkmann, 2015).

Therefore, in the present study, we explored whether and what neural traits—dispositional brain-based characteristics—might explain individual differences in conformity propensity. To measure individuals' neural markers of punishment sensitivity, one of the best options is to use spontaneous resting-state functional magnetic resonance imaging (rs-fMRI) to measure the level of coactivation of functional time series [i.e., functional connectivity (FC)] in a specific functional network [i.e., the brain punishment network (PN; Salvador et al., 2005; Damoiseaux et al., 2006; Van den Heuvel and Hulshoff Pol, 2010)]. Because brain regions often have to work together to form a functional network during rest (Damoiseaux et al., 2006; Fox and Raichle, 2007; Smith et al., 2013), this makes spontaneous rs-fMRI oscillations a robust measure to examine ongoing functional communication between brain regions absent of actual stimulus (Peelen et al., 2013; Hutchison et al., 2014; Stevens et al., 2015; Wang et al., 2016). Unlike task-based imaging, which typically highlights brain responses associated with any given task, rs-fMRI allows researchers to observe how a brain's resting-state connectivity is ready for prime time in the absence of any explicit task (Shen, 2015). Therefore, we can measure rs-fMRI in PN to characterize individuals' preparation and anticipation states for potential punishment. Hence, the resting-state FC in the PN is an ideal neural marker of punishment sensitivity.

Here, we defined the PN by including all brain regions potentially involved in punishment processing. According to neuroscience studies, punishment processing may be underpinned by several distinct brain systems (Palminteri and Pessiglione, 2017). The first system has suggested that punishment-avoidance processing is driven by dopamine (DA) activity (Brooks and Berns, 2013). Specifically, some fMRI studies have shown that the dorsal parts of the frontostriatal

circuits (dorsal striatum) could reinforce punishment avoidance (Seymour et al., 2007; Delgado et al., 2008; Shenhav and Buckner, 2014; Pauli et al., 2015). Additionally, some studies have emphasized that punishment processing is mediated by aversive signals encoded in other brain areas, such as the insula, dorsal anterior cingulate cortex (dACC), and amygdala (Gonzalez et al., 2014; Namburi et al., 2016; Bernardi and Salzman, 2017). The involvement of these regions in experiencing punishment has been supported by some fMRI studies as well as meta-analyses (Palminteri et al., 2012, 2015; Bartra et al., 2013; Garrison et al., 2013; Hayes et al., 2014). These results demonstrate the critical and specific role that various brain structures could play in punishment sensitivity: first, some were implicated in the DA system (striatum), and second, other subcortical and cortical structures were implicated in aversive processing, such as the insula, dACC, and amygdala. Therefore, the aforementioned brain regions all possibly contributed to punishment sensitivity and worked in an integrative manner, despite the absence of any punishment stimulus, to predispose individuals to conform.

To test this hypothesis, we first combined all potential brain regions associated with punishment processing to form the PN using an automated meta-analysis (i.e., Neurosynth; Palminteri and Pessiglione, 2017). Then, we characterized the voxel-wise FC within the PN in a large sample of participants ( $N = 272$ ) with voxel-based global brain connectivity (GBC) method using rs-fMRI (Cole et al., 2012; Wang et al., 2016). For the brain-wide GBC analyses, a voxel's GBC was computed as the average connectivity of that voxel with the rest of the brain; For the ROI GBC analyses, voxel-wise connectivity was based on average correlations of a voxel with the rest of all within-region voxels (Cole et al., 2010). Thus, in this study, to focus on investigating punishment sensitivity the voxel-wise GBC maps were computed within the PN. Specifically, the functional integration of the PN was determined by calculating the within-network connectivity (WNC) of each voxel in the PN as the average FC of a voxel with the rest of the punishment-selective voxels in the PN. Next, we examined whether the WNC in the PN was related to conformity propensity (tendency), measured with a conformity scale (Mehrabian and Steffl, 1995) to explore attributes of conforming. Hence, by correlating the WNC of each voxel in the PN with the tendency of conformity across participants, we characterized the conformity propensity relevance of integration (i.e., a stronger WNC) of the PN, which could elucidate the dispositional determinant (i.e., punishment sensitivity) of conformity behaviors. We hypothesized that the integration (i.e., a stronger WNC) of the PN is positively associated with conformity propensity.

## MATERIALS AND METHODS

### Participants

A total of 272 participants [146 female participants; 272 self-reported right-handed; mean age = 20.4 years, standard deviation (SD) = 0.9 years] from Beijing Normal University participated in the rs-fMRI scan and behavioral session. All participants had a normal or corrected-to-normal vision and reported no history of neurological or psychiatric disorders



**TABLE 1** | Demographic information for participants.

	<i>n</i> = 272
Age	20.4 (0.9)
Gender	146 F (54%), 126 M (46%)
Left-handed	0%
History of neurological disorders	N/A
History of psychiatric disorders	N/A

(Table 1). All investigation protocols were approved by the Institutional Review Board of Beijing Normal University. Written informed consent was obtained from all the participants before the study.

## PN Map From Neurosynth Meta-analysis

To obtain an activation map relevant for punishment processing, we used an automated meta-analysis tool called Neurosynth<sup>1</sup> (Yarkoni et al., 2011) to generate the association test map displaying brain regions preferentially related to the key terms “punishment,” “aversive,” and “pain” (Palminteri and Pessiglione, 2017). The meta-analysis was performed by automatically identifying all studies in the Neurosynth database that loaded highly on the term. Meta-analyses were then performed to identify brain regions consistently or preferentially reported in the tables of those studies, including the key terms. Despite the automaticity and potentially high noise resulting from the association between the term frequency and coordinate tables, this approach has been demonstrated to be robust and reliable (Yarkoni et al., 2011; Helfinstein et al., 2014; Kong et al., 2017). The database was accessed in February 2019. “Punishment” was searched for in 92 studies with 2,881 activations, “aversive” was searched for in 238 studies with 8,529 activations, and “pain” was searched for in 516 studies with 23,295 activations. The generated maps were corrected using a false discovery rate (FDR) approach with an expected FDR of 0.01. We combined all three maps to create the final map of the PN. As expected, the resulting statistical map included the dACC, postcentral gyrus (PG), bilateral insula, striatum, thalamus, and amygdala, which is similar to the results obtained in previous punishment-processing studies (Delgado et al., 2008; Palminteri et al., 2012; Bartra et al., 2013; Garrison et al., 2013; Eisenberger, 2015; Pauli et al., 2015; Bernardi and Salzman, 2017; Palminteri and Pessiglione, 2017).

## Image Acquisition

The images were acquired using a 3T scanner (MAGNETOM Trio, A Tim System; Siemens) with a 12-channel phased-array head coil at the Beijing Normal University Imaging Center for Brain Research in Beijing, China. The rs-fMRI scanning was conducted using a gradient-echo echo-planar imaging (GRE-EPI) sequence [repetition time (TR) = 2,000 ms, echo time (TE) = 30 ms, flip angle = 90°, number of slices = 33, voxel size = 3.125 × 3.125 × 3.6 mm<sup>3</sup>]. Scanning lasted for 8 min and consisted of 240 contiguous EPI volumes. During the scan, the participants were

instructed to relax without engaging in any specific task and remain still with their eyes closed. In addition, high-resolution T1-weighted images were acquired with a magnetization-prepared gradient-echo sequence (MPRAGE: TR/TE/TI = 2,530/3.39/1,100 ms, flip angle = 7°, matrix = 256 × 256, number of slices = 128, and voxel size = 1 × 1 × 1.33 mm<sup>3</sup>) for spatial registration. Earplugs were used to attenuate scanner noise, and a foam pillow and extendable padded head clamps were used to restrain the participants' head motion.

## Image Preprocessing

The rs-fMRI data were preprocessed using the FMRIB Software Library (FSL)<sup>2</sup>. Preprocessing included removal of the first four images, correction for head motion (by aligning each volume to the middle volume of the image with the MCFLIRT), spatial Gaussian smoothing [with a Gaussian kernel of 6 mm full-width at half-maximum (FWHM)], intensity normalization, and linear trend removal. A temporal bandpass filter (0.01–0.1 Hz) was then applied to reduce low-frequency drifts and high-frequency noise.

To further eliminate physiological noise, such as the fluctuations caused by motion, cardiac and respiratory cycles, nuisance signals from cerebrospinal fluid, white matter, whole-brain average, motion correction parameters, and the first derivatives of these signals were regressed out using the methods described in previous studies (Fox et al., 2005; Biswal et al., 2010). The four-dimensional residual time series obtained after removing the nuisance covariates were used for the rs-FC analyses. The strength of the intrinsic FC between two voxels was estimated using Pearson's correlation of the residual resting-state time series for those voxels.

The rs-fMRI images of each participant to the structural images were registered using FLIRT to produce a six-degrees-of-freedom affine transformation matrix. The registration of each participant's structural images to a common stereotaxic space [the Montreal Neurological Institute (MNI) 152-brain template with a resolution of 2 × 2 × 2 mm<sup>3</sup>, MNI152] was accomplished using FLIRT to produce a 12-degrees-of-freedom linear affine matrix (Jenkinson and Smith, 2001; Jenkinson et al., 2002).

## Behavioral Tests

The participants' conformity propensity was measured using an 11-items conformity scale based on Mehrabian and Steffl (1995). Conformity was defined as involving the characteristic willingness to identify with others and emulate them, giving in to others to avoid conflict, and being a follower rather than a leader in terms of ideas, values, and behaviors (Mehrabian and Steffl, 1995). Seven items were positively scored (+), showing a stronger tendency toward conformity, while the remaining four items were negatively scored (−). The items are statements such as “I often rely and act upon the advice of others” (+), “Generally, I'd rather give in and go along with the majority of others for consistency” (+), and “I am

<sup>1</sup><https://github.com/neurosynth/>

<sup>2</sup><http://fsl.fmrib.ox.ac.uk/fsl/fslwiki/>

more independent than conforming in my ways" (–). The participants were asked to evaluate themselves on a 6-point Likert scale ranging from 1 (never or almost never true) to 6 (always or almost always true), with higher scores indicating a higher tendency to conform. In the current study, the internal consistency for all items was provided by a Cronbach's coefficient of 0.78.

## WNC Analyses in the PN

The GBC method, which is a recently developed analytical approach for fMRI data, was used to characterize the intrinsic WNC of each voxel within the PN (Cole et al., 2012). The GBC of a voxel was generally defined as the averaged FC of that voxel to the remaining voxels in the entire brain or a predefined mask (Cole et al., 2012; Wang et al., 2016; Pan et al., 2019; Li et al., 2020). This method enabled the characterization of a specific region's full-range FC with the voxel-wise resolution, allowing us to comprehensively examine the role of each region's FC in punishment sensitivity. Specifically, the FC of a PN voxel to the remaining PN voxels was computed one by one and then averaged as the WNC of the PN voxel. Then, participant-level WNC maps were transformed to *z*-score maps by using Fisher's *z*-transformation to yield normally distributed values (Cole et al., 2012; Gotts et al., 2013). A one-sample *t*-test was performed for each voxel WNC to identify the distribution of hub regions within the PN (Song et al., 2020). The significance was determined using the FDR correction approach with  $p < 0.01$ . Moreover, we conducted two-sample *t*-tests to compare the WNC in the PN between male and female participants to determine whether gender differences existed in punishment sensitivity. The significance was determined using the FDR correction approach with  $p < 0.01$ .

## WNC–Conformity Propensity Correlation Analyses

A correlation analysis was conducted to examine the relationship between the WNC of each voxel in the PN and the individual differences in conformity propensity. Specifically, a Pearson's correlation between the WNC and conformity scores was conducted for each voxel with a GLM tool implemented in FSL, where the conformity scores were set as an independent variable and the WNC in the PN was set as the dependent variable. Multiple comparison correction was performed on the statistical map using the 3dClustSim program implemented in AFNI<sup>3</sup> (version 16.1.13, 2016). The voxel- and cluster-level thresholds of  $p < 0.002$  and  $p < 0.05$ , respectively, were set based on Monte Carlo simulations in the PN mask.

Furthermore, control analyses were performed to rule out other possible confounding factors such as head motion and gender, because recent studies have shown that rs-FC is largely affected by head motion (Satterthwaite et al., 2012; Van Dijk et al., 2012) and gender was identified as a possible modulator of conformity (Rosander and Eriksson, 2012). Thus, we calculated the partial correlation between WNC and conformity propensity while controlling for head motion and gender. The extent of head

motion was measured by the mean framewise displacement (FD) for each participant (Van Dijk et al., 2012).

## Seed-Based FC–Conformity Correlation Analysis

We further investigated with which specific regions the FCs of the identified clusters in the aforementioned WNC–conformity correlation analyses were correlated with conformity propensity. In this regard, seed-based FC analyses were performed with each identified cluster as the seed. For a seed identified in the WNC–conformity correlation analysis, we calculated the FC between the mean time series in the seed (Fisher's *z*-transformed) and each PN voxel and correlated the FC with conformity scores. Again, multiple comparison correction was performed using the 3dClusSim program implemented in AFNI (version 16.1.13, 2016)<sup>3</sup>. A threshold of voxel-level  $p < 0.002$  and cluster-level  $p < 0.05$  was set based on Monte Carlo simulations in the PN. Furthermore, similar control analyses were performed to rule out the confounding effects of head motion and gender.

## Participant Exclusion

The exclusion criterion for fMRI data was head motion  $> 2.0^\circ$  in rotation or 2.0 mm in translation throughout the fMRI scan. Four participants (three male and one female) were excluded based on this criterion. For the behavioral tests, Tukey's outlier filter (Hoaglin et al., 1983) was used to identify outlier participants with exceptionally low ( $3 \times$  the interquartile range below the first quartile) or high ( $3 \times$  the interquartile range above the third quartile) scores. Four additional participants (two male and two female) were excluded using this method.

## RESULTS

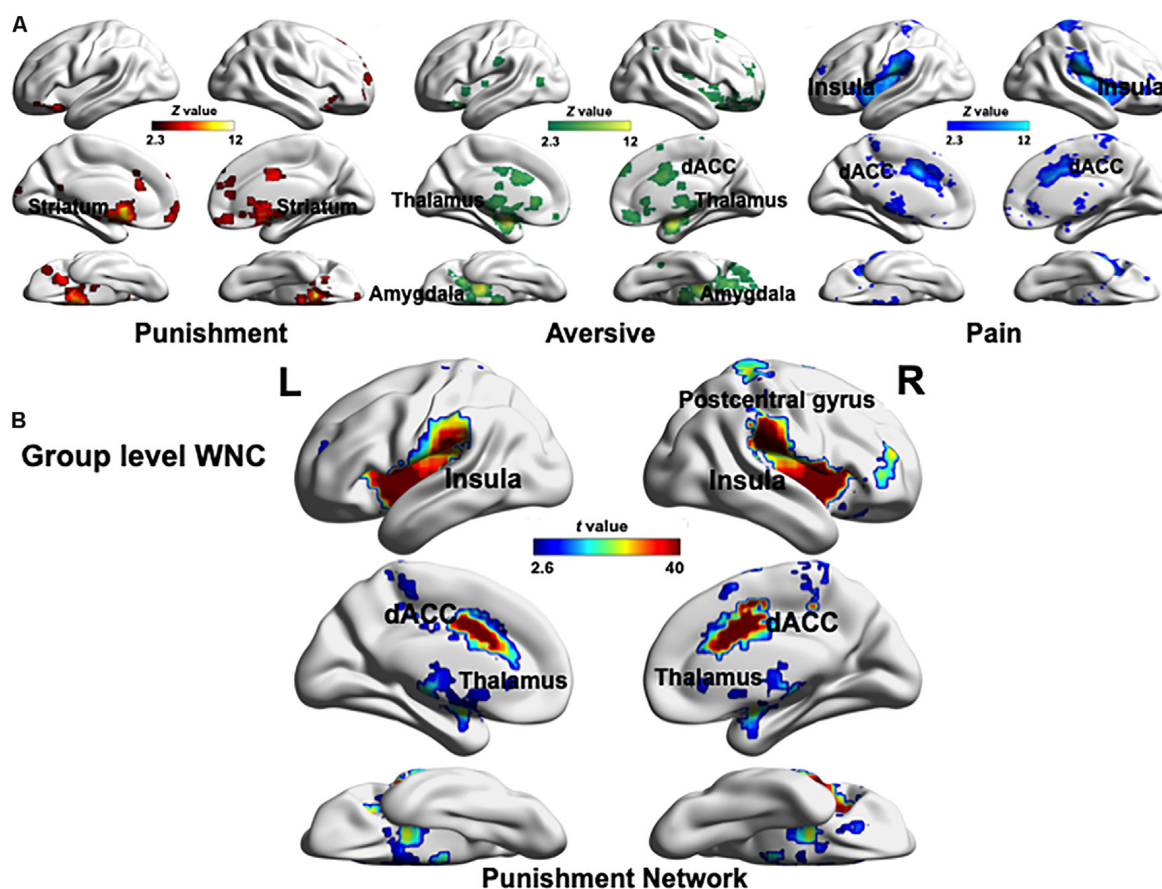
### Behavior Results

Participants' conformity propensity was measured using the conformity scale (Mehrabian and Steffl, 1995), and the mean score obtained by the sample ( $N = 264$ ) was 3.47 ( $SD = 0.58$ ). Also, an independent sample *t*-test was used to examine the difference in the conformity propensity between male and female participants. The results revealed significant differences between male (mean = 3.29,  $SD = 0.56$ ) and female (mean = 3.63,  $SD = 0.55$ ),  $t_{(262)} = 5.06$ ,  $p < 0.001$ , Cohen's  $d = 0.61$ ) participants, which is consistent with previous studies that a gender difference in conformity propensity might exist at the behavioral level (Rosander and Eriksson, 2012). Therefore, we used gender as a control variable for further analysis.

### Definition of PN

To define the PN, we used the results of the Neurosynth meta-analysis with the terms "punishment," "aversive," and "pain" ( $Z > 2.3$ , uncorrected, **Figure 1A**) and recreated a PN mask combining the three association test maps (Palminteri and Pessiglione, 2017). As a result, the PN included the dACC, PG, bilateral insula, thalamus, amygdala, and striatum (**Figure 1B**). The regions in the PN were in agreement with the punishment-selective regions identified in studies on punishment processing (Delgado et al., 2008; Palminteri et al., 2012; Bartra et al.,

<sup>3</sup><http://afni.nimh.nih.gov>



**FIGURE 1 | (A)** Maps resulting from automatized large-scale meta-analyses as implemented in Neurosynth. Three association test maps displaying brain regions preferentially related to the key terms “punishment,” “aversive,” and “pain” created in the Neurosynth meta-analysis ( $Z > 2.3$ , uncorrected). These three maps involve both similar (the dACC) and specific (notably the striatum, thalamus, amygdala, and insula) brain regions. **(B)** Global pattern of within-network connectivity (WNC) in the punishment network (PN; combining aforementioned “punishment,” “aversive,” and “pain” maps). The group-level (one-sample  $t$ -test) WNC map is overlaid on the cortical surface (FDR corrected  $p < 0.01$ ). L, left; R, right. The visualization was provided by BrainNet Viewer (<http://www.nitrc.org/projects/bnv/>).

2013; Garrison et al., 2013; Eisenberger, 2015; Pauli et al., 2015; Bernardi and Salzman, 2017; Palminteri and Pessiglione, 2017).

## WNC in the PN

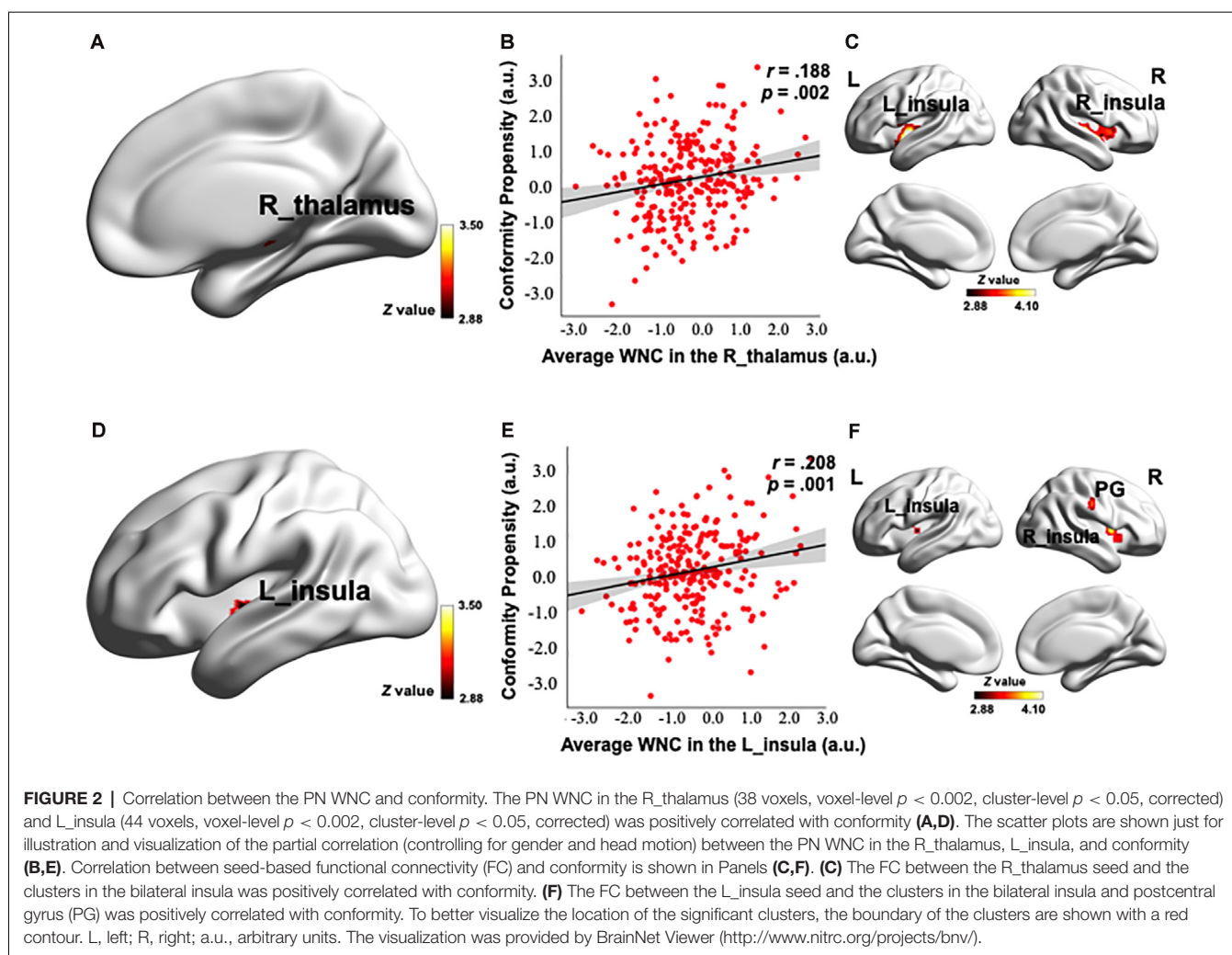
After identifying the PN, we computed each voxel's WNC in the PN by using the rs-fMRI data, where the WNC measured the voxel-wise FC within the PN. First, a one-sample  $t$ -test was used to identify the hubs distribution in the PN. Specifically, we used a one-sample  $t$ -test to calculate the WNC across voxels in the entire sample ( $N = 264$ ). The results showed that almost all voxels in the PN exhibited positive WNC (FDR-corrected  $p < 0.01$ ), suggesting that the PN is a relatively encapsulated network, and among all the PN regions (FDR-corrected  $p < 0.01$ ), the insula, thalamus, dACC, and PG had the largest WNC values (Figure 1B), among which the WNC values of the right thalamus, bilateral insula, dACC, and PG was 1 SD higher than the mean WNC value of the PN, suggesting that these regions serve as hubs of the PN (Dai et al., 2015; Wang et al., 2016). Also, a two-sample  $t$ -test between male and female participants across voxels in the WNC value within the PN revealed no significant

difference between genders, which indicated that male and female participants have similar sensitivity to punishment at the neural level.

## Correlation Between WNC and Conformity Propensity

To investigate how the resting-state FC patterns in the PN were related to conformity propensity, we performed a voxel-wise correlation analysis to search for any PN voxels exhibiting a correlation between WNC and conformity propensity across the participants. As shown in Figures 2A,D, 3A,D and Table 2, four clusters (voxel-level  $p < 0.002$ , cluster-level  $p < 0.05$ , corrected) in the right thalamus (38 voxels,  $r = 0.217$ ,  $p < 0.001$ , MNI coordinates of peak: 14, -22, -2, Figures 2A,B), left insula (44 voxels,  $r = 0.215$ ,  $p < 0.001$ , MNI coordinates of peak: -38, -10, -4, Figures 2D,E), PG (121 voxels,  $r = 0.252$ ,  $p < 0.001$ , MNI coordinates of peak: 26, -28, 58, Figures 3A,B), and dACC (47 voxels,  $r = 0.217$ ,  $p < 0.001$ , MNI coordinates of peak: -42, 24, 34, Figures 3D,E) showed significant positive correlation between the WNC and conformity propensity, suggesting that





individuals with stronger within-network integration in these four regions during resting state were more inclined to conform. No clusters showed a negative correlation between the WNC and conformity propensity. In brief, these results suggested that individuals' conformity propensity was positively correlated with the integration of the right thalamus, left insula, PG, and dACC in the PN.

Control analyses were then performed to ensure that the WNC-conformity correlation in the right thalamus, left insula, PG, and dACC was not caused by confounding factors, such as head motion or gender. We reanalyzed the WNC-conformity correlation while controlling for head motion (Van Dijk et al., 2012) and gender. We found that the correlation remained significant (right thalamus: partial  $r = 0.188$ ,  $p = 0.002$ ; left insula: partial  $r = 0.208$ ,  $p = 0.001$ ; PG: partial  $r = 0.219$ ,  $p < 0.001$ ; dACC: partial  $r = 0.179$ ,  $p = 0.004$ ). These results indicated that the WNC-conformity correlations in the four clusters were not an artifact resulted from head motion or gender.

To examine the reliability of the correlation, the top and bottom 25% of the participants, according to the WNC (in

the significantly positive WNC-conformity correlation clusters: right thalamus, left insula, PG and dACC), were labeled as the high- and low-punishment sensitivity groups ( $N = 66$  for both groups), respectively. Consistent with the correlation results, the high punishment sensitivity group (a group divided according to the WNC in the cluster in the right thalamus: conformity = 3.60; in the left insula: conformity = 3.58; in the PG: conformity = 3.56; and in the dACC: conformity = 3.64) exhibited higher conformity scores than did the low-punishment sensitivity group (group divided according to WNC in the cluster in the right thalamus: conformity = 3.28; in the left insula: conformity = 3.27; in the PG: conformity = 3.24; and in the dACC: conformity = 3.31) according to the WNC in four clusters, respectively (the difference of conformity scores between the top and low WNC groups in the right thalamus:  $t_{(130)} = -3.099$ ,  $p = 0.002$ , Cohen's  $d = 0.55$ ; in the left insula:  $t_{(130)} = -2.946$ ,  $p = 0.004$ , Cohen's  $d = 0.51$ ; in the PG:  $t_{(130)} = -3.595$ ,  $p < 0.001$ , Cohen's  $d = 0.64$ ; and in the dACC:  $t_{(130)} = -3.351$ ,  $p = 0.001$ , Cohen's  $d = 0.58$ ). These results indicated that individuals with superior punishment sensitivity (specifically reflected in the right



thalamus, left insula, PG, and dACC integration) are more likely to conform.

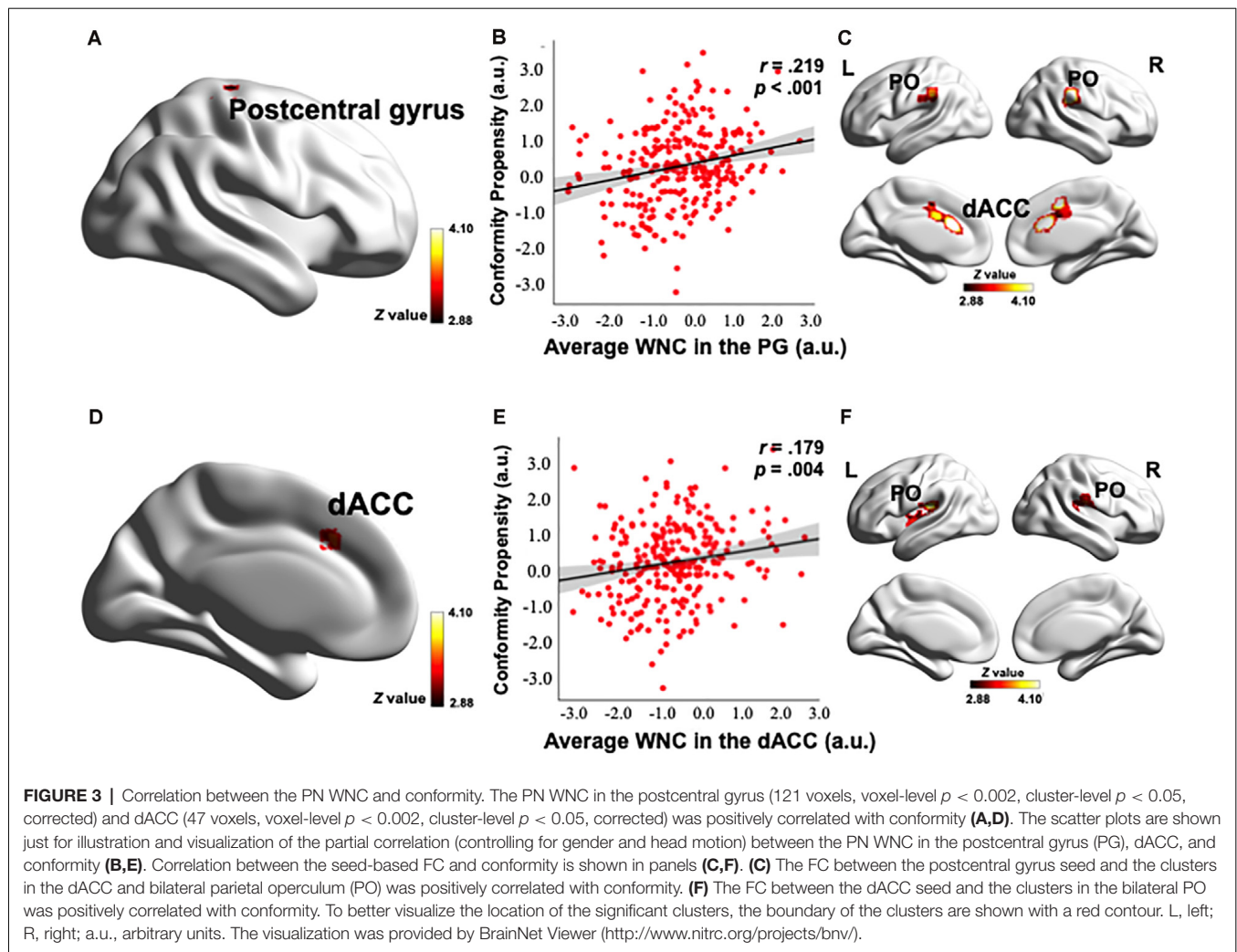
## Conformity Relevance of Seed-Based FC in the PN

After identifying the right thalamus, left insula, PG, and dACC as the connection hubs within the PN associated with conformity propensity, we examined with which specific regions in the PN the FC of the identified clusters in the aforementioned WNC–conformity correlation analysis were correlated with conformity. For this purpose, we performed seed-based FC analyses with the identified four clusters as seeds. We then calculated the FC between the mean time series in the seed (Fisher's  $z$ -transformed) and each PN voxel and correlated the FC with conformity scores (the results of correlation analyses were summarized in **Table 2**). First, we found that the FC between the right thalamus and two clusters were positively correlated with conformity propensity (voxel-level  $p < 0.002$ , cluster-level  $p < 0.05$ , corrected, **Figure 2C**), including the bilateral insula (right, 655 voxels, MNI coordinates: 40, −11, −4; left, 407 voxels, MNI coordinates: −40, −5, −4). In addition, the correlations remained unchanged while controlling for the participants' head motion (Van Dijk et al., 2012) and gender (right thalamus-right insula: partial  $r = 0.270$ ,  $p < 0.001$ ; right thalamus-left insula: partial  $r = 0.264$ ,  $p < 0.001$ ). Second, the FC between the left insula and three clusters were positively correlated with conformity propensity (voxel-level  $p < 0.002$ , cluster-level  $p < 0.05$ , corrected, **Figure 2F**), including the PG (59 voxels, MNI coordinates: 60, −15, 34) and the bilateral insula (right, 119 voxels, MNI coordinates: 34, 4, 6; left, 70 voxels, MNI coordinates: −30, −17, 4). Additionally, the correlations remained unchanged while controlling for the participants' head motion and gender (left insula-PG: partial  $r = 0.178$ ,  $p = 0.004$ ; left insula-right insula: partial  $r = 0.254$ ,  $p < 0.001$ ; left insula-left insula: partial  $r = 0.239$ ,  $p < 0.001$ ). Third, the FC between the PG and three clusters were positively correlated with conformity propensity (voxel-level  $p < 0.002$ , cluster-level  $p < 0.05$ , corrected, **Figure 3C**), including the dACC (759 voxels, MNI coordinates: 8, 24, 20) and the bilateral parietal operculum (PO; right, 334 voxels, MNI coordinates: 56, −29, 32; left, 161 voxels, MNI coordinates: −52, −35, 36). The correlations remained unchanged while controlling for the participants' head motion and gender (PG-dACC: partial  $r = 0.251$ ,  $p < 0.001$ ; PG-rPO: partial  $r = 0.216$ ,  $p < 0.001$ ; PG-lPO: partial  $r = 0.215$ ,  $p < 0.001$ ). Finally, the FC between the dACC and two clusters were positively correlated with conformity propensity (voxel-level  $p < 0.002$ , cluster-level  $p < 0.05$ , corrected, **Figure 3F**), including the bilateral PO (right, 241 voxels, MNI coordinates: 58, −21, 20; left, 463 voxels, MNI coordinates: −55, −21, 10). In addition, the correlations remained unchanged while controlling for the participants' head motion and gender (dACC-rPO: partial  $r = 0.210$ ,  $p = 0.001$ ; dACC-lPO: partial  $r = 0.262$ ,  $p < 0.001$ ). Taken together, these results suggest that from the right thalamus to the bilateral insula to the PG to the dACC, these regions might not only play parallel hub-like roles in punishment sensitivity but also seem to have integrated as an ascending pathway to facilitate conformity behaviors (**Figure 4**).

**TABLE 2** | Correlation coefficients between conformity propensity and two kinds of functional connectivity (FC) measurements in the punishment network (i.e., voxel-wise WNC and seed-based FC).

Region as seeds	WNC		Seed-based FC					
	Significant conformity-WNC correlated brain regions		Conformity seed-based FC correlated brain regions					
	$r$		R_insula	L_insula	PG	R_PO	L_PO	dACC
R_thalamus	0.217*** (0.188**)		0.279*** (0.270***)	0.275*** (0.264***)	-	-	-	-
L_insula	0.215*** (0.208**)		0.255*** (0.254***)	0.248*** (0.239**)	0.207** (0.178**)	-	-	-
PG	0.252*** (0.219***)		-	-	-	0.252*** (0.216***)	0.240*** (0.215***)	0.283*** (0.251***)
dACC	0.217*** (0.179**)		-	-	-	0.231*** (0.210**)	0.290*** (0.262***)	-

Notes: \*\*\*correlation is significant at the 0.001 level (two-tailed); \*\*correlation is significant at the 0.01 level (two-tailed). The coefficients of partial correlation controlling for gender and head motion presenting in parentheses. WNC, within-network connectivity; PG, postcentral gyrus; PO, parietal operculum; L, left; R, right.

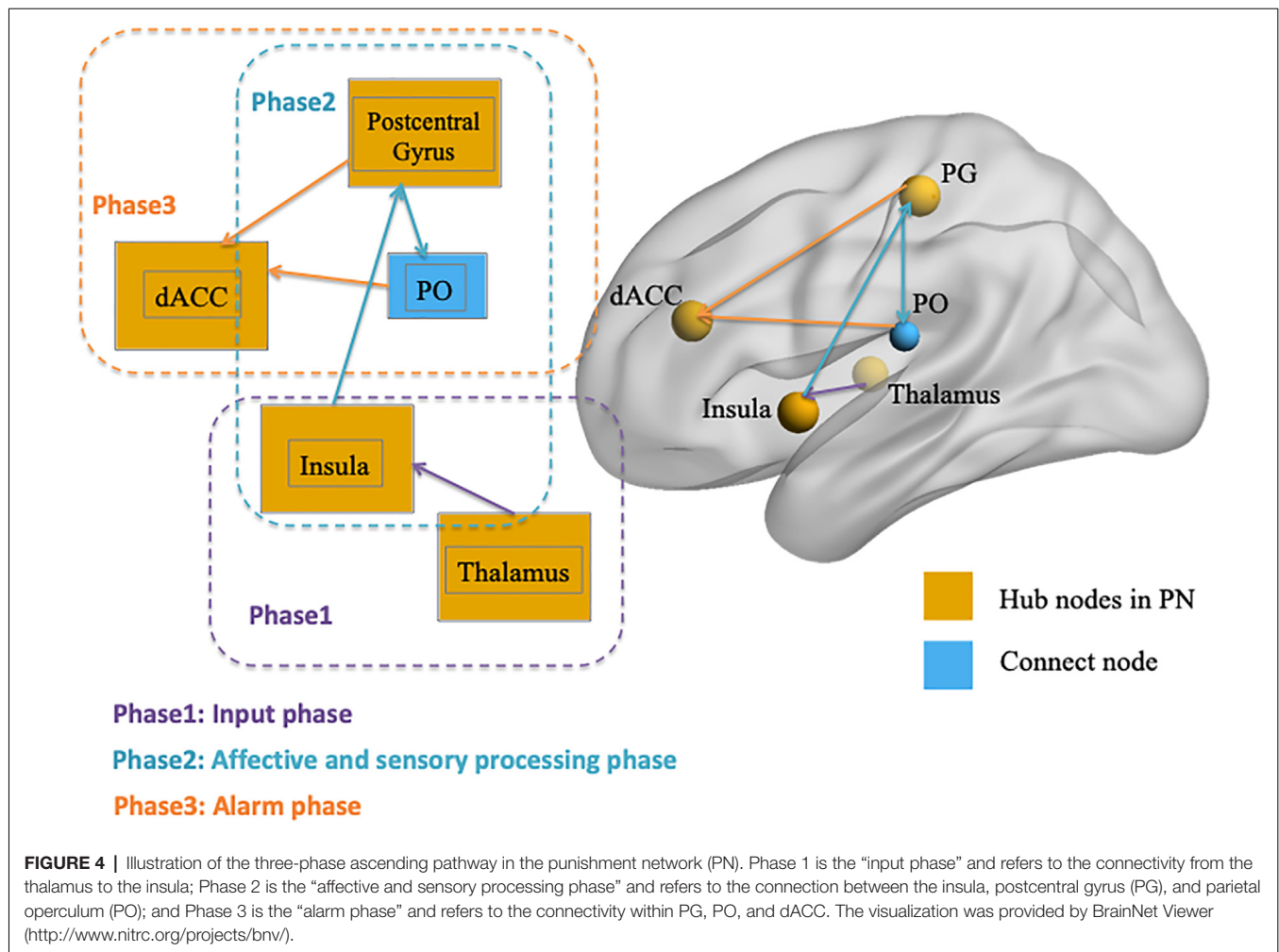


## DISCUSSION

Using rs-fMRI, we demonstrated that task-independent FC in the PN related to individual differences in conformity propensity: higher WNC in the PN was associated with a stronger tendency to conform. Specifically, first, we identified the right thalamus, bilateral insula, PG, and dACC as hubs for integrating all other regions in the PN. Then, the correlation analysis between WNC and the conformity scores demonstrated that individuals with stronger WNC in the right thalamus, left insula, PG, and dACC (i.e., high PN integration) exhibited considerably higher conformity propensity. Furthermore, through seed-based analysis, the results suggested that the specific connections from all four brain regions seemed to form an ascending pathway and that the connection of each phase in this pathway all contribute to conformity propensity. Therefore, stronger WNC in the PN might predispose conformity behaviors by fostering punishment sensitivity. Every phase in this ascending pathway for punishment sensitivity was positively correlated with conformity propensity.

By using the GBC approach, our finding that the right thalamus, left insula, PG, and dACC are hub areas integrating the whole PN is consistent with previous findings that these brain regions play a central role in punishment processing, such as the processing of aversive, and painful stimuli (Frot et al., 2007; Chai et al., 2010; Straube and Miltner, 2011; Kobayashi, 2012; Wiech et al., 2014). Thus, the fact that these four hubs integrating the PN at resting state indicate that they were in an ongoing readiness state for priming of multiple potential punishments (Simmons and Martin, 2011; Shen, 2015). This readiness state positively correlated with individuals' conformity propensity, suggesting that this task-independent neural functioning might predispose individuals toward conformity.

Also, seed-based FC-conformity correlation analyses were conducted with four clusters as seeds in the right thalamus, left insula, PG, and dACC, respectively, and the results showed that the FCs in the four hub regions seemed to form an ascending pathway that was positively correlated with conformity propensity in each phase. It is also worth mentioning that the PO was not the hubs in the PN but connected with two hubs (i.e., the PG and dACC) in the ascending pathway



to contribute to the behavior tendency of conformity. This result is consistent with previous studies that have indicated that the function of the PO might not be the hub region to integrate the whole PN, but that it plays an essential role in transmitting signals within the hubs (Eickhoff et al., 2010; Garcia-Larrea, 2012; Mano et al., 2017). More importantly, unilateral severe physical punishment (e.g., painful stimulation) evoked bilateral activation of PO but also activated the insula, PG, and cingulate cortices in the contralateral hemisphere in completely callosotomized patients (Fabri et al., 2002), which indicated that PO could play a powerful function in transferring information bilaterally, even in subjects with resection of the corpus callosum and distributing signals to both hemispheric brain regions. Thus, the major role of the PO could be facilitating connectivity within the PG and dACC in the ascending pathway. Our results suggested that the mechanism of punishment sensitivity comprises multiple phases of processing (Ernst et al., 2006), and this sensitivity could result from stronger connectivity of one or multiple phases.

Specifically, this punishment sensitivity pathway in the PN could be divided into three phases (Figure 4): Phase 1 is the “input phase” and refers to the connectivity from the

thalamus to the insula, which is responsible for processing early sensory input (Dum et al., 2009; Liang et al., 2012; Cho et al., 2013). Phase 2 is the “affective and sensory processing phase” and contributes to the connection between the insula, PO, and PG (where the somatosensory cortex is located). According to research, the insula is responsible for processing the “affective” components of punishment stimulus (Touroutoglou et al., 2012; Duerden et al., 2013; Rogers-Carter et al., 2018), activation during aversive anticipation (Simmons et al., 2006; Carlson and Mujica-Parodi, 2010; Haase et al., 2014), and arousal during negative affection processing (Caria et al., 2010; Duerden et al., 2013), whereas the somatosensory cortex is responsible for processing “sensory-discrimination” and is implicated in self-awareness of a person’s own body (Frot et al., 2007; Khalsa et al., 2009) as the perception of bodily states playing a crucial role for affective and emotional experiences (Straube and Miltner, 2011). Phase 3 occurs in the ascending pathway and is the combined affective and sensory signal projected to the dACC (i.e., accomplished by the connectivity within the somatosensory cortex, PO, and dACC), which acts as a neural “alarm system” or conflict monitor, detecting “something is wrong” and preparing for a

response (Eisenberger and Lieberman, 2004; Ullsperger et al., 2004; Gonzalez et al., 2014; Chester and DeWall, 2015; Coste and Kleinschmidt, 2016). The connectivity in every phase is positively associated with conformity propensity, which means that every phase is preparing for punishment stimulus and the sensitivity in each phase plays a role in explaining individual differences in conforming tendency.

Also, two regions included in our predefined PN did not seem to play essential roles in punishment sensitivity and did not contribute to conformity propensity. First, the dorsal striatum is mentioned in a few previous studies to be associated with punishment avoidance (Seymour et al., 2007; Delgado et al., 2008; Pauli et al., 2015). While reward processing being associated with striatum activation has been almost consistently reported, results regarding punishment processing have been less consistent (Rutledge et al., 2009; Jocham et al., 2011; Eisenegger et al., 2014). The fact is that the meaning of positive or negative outcomes always been reframed in studies about reward- or punishment-processing tasks, which means the absence of punishment could be perceived as a reward (Vlaev et al., 2011; Rangel and Clithero, 2012; Palminteri et al., 2015). Thus, the dorsal striatum might play a major role in value-coding in these tasks, rather than being a response specific to punishment. Second, the amygdala has not presented as a hub area in punishment sensitivity. The possible reason is that the amygdala is an area associated with emotional processing, such as emotional salience, valence, and discrimination (Pessoa and Adolphs, 2010). So in punishment relevance tasks, the function of the amygdala is more likely to process the emotional response to individuals' own errors before punishment is inflicted (Jackson et al., 2015) or to the succeeding emotional processing after suffering punishment (Sladky et al., 2013). Thus, it is not responsible for processing the direct experience associated with the punishment itself; therefore, it has not played a role in punishment sensitivity or contributed to conformity propensity in this study.

## LIMITATIONS AND FUTURE DIRECTIONS

The limitations and several unaddressed issues of the present study need to be explored in future research. First, given that the processing ascending pathway in the PN presented in this study was based on seed-based analysis, future studies are invited to investigate directed FC within PN (e.g., using Granger causality analysis, GCA; Khazaei et al., 2017; Price et al., 2017; Xue et al., 2019), and how the directed FC in the PN are associated with conformity propensity. Second, the present study used resting-state FC when participants were not performing punishment processing tasks since the present study aims to investigate the intrinsic FC in the PN as an indicator for task-free, stable trait-like neural activity in potential punishment (Tavor et al., 2016), yet future fMRI studies measuring task-state FC during the performance of the punishment processing relevant tasks (Palminteri et al., 2012; Palminteri and Pessiglione, 2017) may help further elucidate the distinct function of each region related to punishment processing and the specific role they play in

promoting conformity behaviors. Third, the generalization of the present finding is limited by the purely college-aged sample. It will be interesting for future studies to investigate the punishment sensitivity at the neural level in other age groups and the corresponding associations with group varieties of conformity propensity.

## CONCLUSION

In summary, the present study evidences that a neural trait marker—task-independent FC in the PN—explains individual differences in conformity propensity. That might be the reason why the conformity phenomenon is so prevalent in our society today because the neural connectivity in the PN is a consistent and automatic motivational factor in our brain. Hence, our study revealed a paradox: we conform because of sensitivity to punishment, but avoiding potential punishment leads us to be a “one-dimensional man,” which itself is the most severe punishment. The significance of this study is probably cautionary at best. As American historian Wilfred M. McClay evaluated Riesman's *The Lonely Crowd*, “It warns us against the peculiar forms of bondage to which our era is especially prone. And in doing so, it draws us into a deeper consideration of what freedom might be, both now and in the future,” (McClay, 1998). Thus, constructing a new sensibility of being nonconforming is the antidote to regaining one's drive for personal liberation.

## DATA AVAILABILITY STATEMENT

The raw data supporting the conclusions of this article will be made available by the authors, without undue reservation.

## ETHICS STATEMENT

The studies involving human participants and all investigation protocols were reviewed and approved by the Institutional Review Board of Beijing Normal University. The patients/participants provided their written informed consent to participate in this study.

## AUTHOR CONTRIBUTIONS

YD contributed to the study conception and design, performed data analysis and interpretation, and wrote the manuscript. YW contributed to the study conception and design, and critically revised the article. MY and XT performed material preparation and data collection. JL designed the work and critically revised the article. All authors contributed to the article and approved the submitted version.

## FUNDING

This study was funded by the National Natural Science Foundation of China (31700978, 31861143039, and 31872786), the National Basic Research Program of China (2018YFC0810602), and Changjiang Scholars Programme of China.



## REFERENCES

- Asch, S. E. (1956). Studies of independence and conformity: I. A minority of one against a unanimous majority. *Psychol. Monogr.* 70, 1–70. doi: 10.1037/h0093718
- Bartra, O., McGuire, J. T., and Kable, J. W. (2013). The valuation system: a coordinate-based meta-analysis of BOLD fMRI experiments examining neural correlates of subjective value. *NeuroImage* 76, 412–427. doi: 10.1016/j.neuroimage.2013.02.063
- Bernardi, S., and Salzman, D. (2017). “Appetitive and aversive systems in the amygdala,” in *Decision Neuroscience*, eds J.-C. Dreher and L. Tremblay (Salt Lake City: Academic Press), 33–45. doi: 10.1016/B978-0-12-805308-9.00003-8
- Biswal, B. B., Mennes, M., Zuo, X.-N., Gohel, S., Kelly, C., Smith, S. M., et al. (2010). Toward discovery science of human brain function. *Proc. Natl. Acad. Sci. U S A* 107, 4734–4739. doi: 10.1073/pnas.0911855107
- Boyd, R., Gintis, H., Bowles, S., and Richerson, P. J. (2003). The evolution of altruistic punishment. *Proc. Natl. Acad. Sci. U S A* 100, 3531–3535. doi: 10.1073/pnas.0630443100
- Brooks, A. M., and Berns, G. S. (2013). Aversive stimuli and loss in the mesocorticolimbic dopamine system. *Trends Cogn. Sci.* 17, 281–286. doi: 10.1016/j.tics.2013.04.001
- Caria, A., Sitaram, R., Veit, R., Begliomini, C., and Birbaumer, N. (2010). Volitional control of anterior insula activity modulates the response to aversive stimuli. A real-time functional magnetic resonance imaging study. *Biol. Psychiatry* 68, 425–432. doi: 10.1016/j.biopsych.2010.04.020
- Carlson, J. M., and Mujica-Parodi, L. R. (2010). A disposition to reappraise decreases anterior insula reactivity during anxious anticipation. *Biol. Psychol.* 85, 383–385. doi: 10.1016/j.biopsycho.2010.08.010
- Chai, S.-C., Kung, J.-C., and Shyu, B.-C. (2010). Roles of the anterior cingulate cortex and medial thalamus in short-term and long-term aversive information processing. *Mol. Pain* 6:42. doi: 10.1186/1744-8069-6-42
- Chester, D. S., and DeWall, C. N. (2015). Sound the alarm: the effect of narcissism on retaliatory aggression is moderated by dACC reactivity to rejection. *J. Pers.* 84, 361–368. doi: 10.1111/jopy.12164
- Cho, Y. T., Fromm, S., Guyer, A. E., Detloff, A., Pine, D. S., Fudge, J. L., et al. (2013). Nucleus accumbens, thalamus and insula connectivity during incentive anticipation in typical adults and adolescents. *NeuroImage* 66, 508–521. doi: 10.1016/j.neuroimage.2012.10.013
- Cialdini, R. B., and Goldstein, N. J. (2004). Social influence: compliance and conformity. *Annu. Rev. Psychol.* 55, 591–621. doi: 10.1146/annurev.psych.55.090902.142015
- Cole, M. W., Pathak, S., and Schneider, W. (2010). Identifying the brain’s most globally connected regions. *NeuroImage* 49, 3132–3148. doi: 10.1016/j.neuroimage.2009.11.001
- Cole, M. W., Yarkoni, T., Repovs, G., Anticevic, A., and Braver, T. S. (2012). Global connectivity of prefrontal cortex predicts cognitive control and intelligence. *J. Neurosci.* 32, 8988–8999. doi: 10.1523/JNEUROSCI.0536-12.2012
- Coste, C. P., and Kleinschmidt, A. (2016). Cingulo-opercular network activity maintains alertness. *NeuroImage* 128, 264–272. doi: 10.1016/j.neuroimage.2016.01.026
- Dai, Z., Yan, C., Li, K., Wang, Z., Wang, J., Cao, M., et al. (2015). Identifying and mapping connectivity patterns of brain network hubs in Alzheimer’s disease. *Cereb. Cortex* 25, 3723–3742. doi: 10.1093/cercor/bhu246
- Damoiseaux, J. S., Rombouts, S. A. R. B., Barkhof, F., Scheltens, P., Stam, C. J., Smith, S. M., et al. (2006). Consistent resting-state networks across healthy subjects. *Proc. Natl. Acad. Sci. U S A* 103, 13848–13853. doi: 10.1073/pnas.0601417103
- De Quervain, D. J.-F., Fischbacher, U., Treyer, V., Schellhammer, M., Schnyder, U., Buck, A., et al. (2004). The neural basis of altruistic punishment. *Science* 305, 1254–1258. doi: 10.1126/science.1100735
- Delgado, M. R., Li, J., Schiller, D., and Phelps, E. A. (2008). The role of the striatum in aversive learning and aversive prediction errors. *Philos. Trans. R Soc. Lond. B Biol. Sci.* 363, 3787–3800. doi: 10.1098/rstb.2008.0161
- Duerden, E. G., Arsalidou, M., Lee, M., and Taylor, M. J. (2013). Lateralization of affective processing in the insula. *NeuroImage* 78, 159–175. doi: 10.1016/j.neuroimage.2013.04.014
- Dum, R. P., Levinthal, D. J., and Strick, P. L. (2009). The spinothalamic system targets motor and sensory areas in the cerebral cortex of monkeys. *J. Neurosci.* 29, 14223–14235. doi: 10.1523/JNEUROSCI.3398-09.2009
- Egerton, A., Rees, E., Bose, S. K., Lappin, J. M., Stokes, P. R. A., Turkheimer, F. E., et al. (2010). Truth, lies or self-deception? Striatal D2/3 receptor availability predicts individual differences in social conformity. *NeuroImage* 53, 777–781. doi: 10.1016/j.neuroimage.2010.06.031
- Eickhoff, S. B., Jbabdi, S., Caspers, S., Laird, A. R., Fox, P. T., Zilles, K., et al. (2010). Anatomical and functional connectivity of cytoarchitectonic areas within the human parietal operculum. *J. Neurosci.* 30, 6409–6421. doi: 10.1523/JNEUROSCI.5664-09.2010
- Eisenberger, N. I. (2015). Social pain and the brain: controversies, questions and where to go from here. *Annu. Rev. Psychol.* 66, 601–629. doi: 10.1146/annurev-psych-010213-115146
- Eisenberger, N. I., and Lieberman, M. D. (2004). Why rejection hurts: a common neural alarm system for physical and social pain. *Trends Cogn. Sci.* 8, 294–300. doi: 10.1016/j.tics.2004.05.010
- Eisenegger, C., Naef, M., Linssen, A., Clark, L., Gandamaneni, P. K., Müller, U., et al. (2014). Role of dopamine D2 receptors in human reinforcement learning. *Neuropsychopharmacology* 39, 2366–2375. doi: 10.1038/npp.2014.84
- Ernst, M., Pine, D. S., and Hardin, M. (2006). Triadic model of the neurobiology of motivated behavior in adolescence. *Psychol. Med.* 36, 299–312. doi: 10.1017/S0033291705005891
- Fabri, M., Polonara, G., Quattrini, A., and Salvolini, U. (2002). Mechanical noxious stimuli cause bilateral activation of parietal operculum in callosotomized subjects. *Cereb. Cortex* 12, 446–451. doi: 10.1093/cercor/12.4.446
- Falk, E. B., Way, B. M., and Jasinska, A. J. (2012). An imaging genetics approach to understanding social influence. *Front. Hum. Neurosci.* 6:168. doi: 10.3389/fnhum.2012.00168
- Fehr, E., and Gächter, S. (2002). Altruistic punishment in humans. *Nature* 415, 137–140. doi: 10.1038/415137a
- Fox, M. D., and Raichle, M. E. (2007). Spontaneous fluctuations in brain activity observed with functional magnetic resonance imaging. *Nat. Rev. Neurosci.* 8, 700–711. doi: 10.1038/nrn2201
- Fox, M. D., Snyder, A. Z., Vincent, J. L., Corbetta, M., Van Essen, D. C., and Raichle, M. E. (2005). The human brain is intrinsically organized into dynamic, anticorrelated functional networks. *Proc. Natl. Acad. Sci. U S A* 102, 9673–9678. doi: 10.1073/pnas.0504136102
- Franzen, J., and Brinkmann, K. (2015). Blunted cardiovascular reactivity in dysphoria during reward and punishment anticipation. *Int. J. Psychophysiol.* 95, 270–277. doi: 10.1016/j.ijpsycho.2014.11.007
- Frot, M., Magnin, M., Mauguire, F., and Garcia-Larrea, L. (2007). Human SII and posterior insula differently encode thermal laser stimuli. *Cereb. Cortex* 17, 610–620. doi: 10.1093/cercor/bhk007
- Garcia-Larrea, L. (2012). The posterior insular-opercular region and the search of a primary cortex for pain. *Neurophysiol. Clin.* 42, 299–313. doi: 10.1016/j.neucli.2012.06.001
- Garrison, J., Erdeniz, B., and Done, J. (2013). Prediction error in reinforcement learning: a meta-analysis of neuroimaging studies. *Neurosci. Biobehav. Rev.* 37, 1297–1310. doi: 10.1016/j.neubiorev.2013.03.023
- Gelfand, M. J. (2012). Culture’s constraints: international differences in the strength of social norms. *Curr. Direct. Psychol. Sci.* 21, 420–424. doi: 10.1177/0963721412460048
- Gonzalez, M. Z., Beckes, L., Chango, J., Allen, J. P., and Coan, J. A. (2014). Adolescent neighborhood quality predicts adult dACC response to social exclusion. *Soc. Cogn. Affect. Neurosci.* 10, 921–928. doi: 10.1093/scan/nsu137
- Gotts, S. J., Jo, H. J., Wallace, G. L., Saad, Z. S., Cox, R. W., and Martin, A. (2013). Two distinct forms of functional lateralization in the human brain. *Proc. Natl. Acad. Sci. U S A* 110, E3435–E3444. doi: 10.1073/pnas.1302581110
- Griskevicius, V., Goldstein, N. J., Mortensen, C. R., Cialdini, R. B., and Kenrick, D. T. (2006). Going along versus going alone: when fundamental motives facilitate strategic (non)conformity. *J. Pers. Soc. Psychol.* 91, 281–294. doi: 10.1037/0022-3514.91.2.281
- Haase, L., Thom, N. J., Shukla, A., Davenport, P. W., Simmons, A. N., Stanley, E. A., et al. (2014). Mindfulness-based training attenuates insula response to an aversive interoceptive challenge. *Soc. Cogn. Affect. Neurosci.* 11, 182–190. doi: 10.1093/scan/nsu042

- Haun, D. B. M., and Tomasello, M. (2011). Conformity to peer pressure in preschool children. *Child Dev.* 82, 1759–1767. doi: 10.1111/j.1467-8624.2011.01666.x
- Hayes, D. J., Duncan, N. W., Xu, J., and Northoff, G. (2014). A comparison of neural responses to appetitive and aversive stimuli in humans and other mammals. *Neurosci. Biobehav. Rev.* 45, 350–368. doi: 10.1016/j.neubiorev.2014.06.018
- Heerdink, M. W., van Kleef, G. A., Homan, A. C., and Fischer, A. H. (2015). Emotional reactions to deviance in groups: the relation between number of angry reactions, felt rejection and conformity. *Front. Psychol.* 6:830. doi: 10.3389/fpsyg.2015.00830
- Helfinstein, S. M., Schonberg, T., Congdon, E., Karlsgodt, K. H., Mumford, J. A., Sabb, F. W., et al. (2014). Predicting risky choices from brain activity patterns. *Proc. Natl. Acad. Sci. U S A* 111, 2470–2475. doi: 10.1073/pnas.1321728111
- Hoaglin, D. C., Mosteller, F., and Tukey, J. W. (1983). *Understanding Robust and Exploratory Data Analysis*. New York, NY: Wiley.
- Hornsey, M. J., Majkut, L., Terry, D. J., and McKimmie, B. M. (2003). On being loud and proud: non-conformity and counter-conformity to group norms. *Br. J. Soc. Psychol.* 42, 319–335. doi: 10.1348/01446660322438189
- Hutchison, R. M., Culham, J. C., Everling, S., Flanagan, J. R., and Gallivan, J. P. (2014). Distinct and distributed functional connectivity patterns across cortex reflect the domain-specific constraints of object, face, scene, body and tool category-selective modules in the ventral visual pathway. *NeuroImage* 96, 216–236. doi: 10.1016/j.neuroimage.2014.03.068
- Jackson, F., Nelson, B. D., and Proudfit, G. H. (2015). In an uncertain world, errors are more aversive: evidence from the error-related negativity. *Emotion* 15, 12–16. doi: 10.1037/emo0000020
- Jenkinson, M., Bannister, P., Brady, M., and Smith, S. (2002). Improved optimization for the robust and accurate linear registration and motion correction of brain images. *NeuroImage* 17, 825–841. doi: 10.1016/s1053-8119(02)91132-8
- Jenkinson, M., and Smith, S. (2001). A global optimisation method for robust affine registration of brain images. *Med. Image Anal.* 5, 143–156. doi: 10.1016/s1361-8415(01)00036-6
- Jocham, G., Klein, T. A., and Ullsperger, M. (2011). Dopamine-mediated reinforcement learning signals in the striatum and ventromedial prefrontal cortex underlie value-based choices. *J. Neurosci.* 31, 1606–1613. doi: 10.1523/JNEUROSCI.3904-10.2011
- Jolles, J. W., de Visser, L., and van den Bos, R. (2011). Male wistar rats show individual differences in an animal model of conformity. *Anim. Cogn.* 14, 769–773. doi: 10.1007/s10071-011-0395-4
- Khalsa, S. S., Rudrauf, D., Feinstein, J. S., and Tranel, D. (2009). The pathways of interoceptive awareness. *Nat. Neurosci.* 12, 1494–1496. doi: 10.1038/nn.2411
- Khazaei, A., Ebrahimzadeh, A., and Babajani-Feremi, A. (2017). Classification of patients with MCI and AD from healthy controls using directed graph measures of resting-state fMRI. *Behav. Brain Res.* 322, 339–350. doi: 10.1016/j.bbr.2016.06.043
- Kobayashi, S. (2012). Organization of neural systems for aversive information processing: pain, error and punishment. *Front. Neurosci.* 6:136. doi: 10.3389/fnins.2012.00136
- Kong, X.-Z., Song, Y., Zhen, Z., and Liu, J. (2017). Genetic variation in S100B modulates neural processing of visual scenes in han chinese. *Cereb. Cortex* 27, 1326–1336. doi: 10.1093/cercor/bhv322
- Li, H., Ou, Y., Liu, F., Chen, J., Zhao, J., Guo, W., et al. (2020). Reduced connectivity in anterior cingulate cortex as an early predictor for treatment response in drug-naïve, first-episode schizophrenia: a global-brain functional connectivity analysis. *Schizophr. Res.* 215, 337–343. doi: 10.1016/j.schres.2019.09.003
- Liang, M., Mouraux, A., and Iannetti, G. D. (2012). Bypassing primary sensory cortices—a direct thalamocortical pathway for transmitting salient sensory information. *Cereb. Cortex* 23, 1–11. doi: 10.1093/cercor/bhr363
- Mano, H., Yoshida, W., Shibata, K., Zhang, S., Koltzenburg, M., Kawato, M., et al. (2017). Thermosensory perceptual learning is associated with structural brain changes in parietal-opercular (SII) cortex. *J. Neurosci.* 37, 9380–9388. doi: 10.1523/JNEUROSCI.1316-17.2017
- Marcuse, H. (1964). *One-Dimensional Man: Studies in the Ideology of Advanced Industrial Society*. London: Routledge/Kegan Paul.
- McClay, W. M. (1998). Fifty years of the lonely crowd. *Wilson Q.* 22, 34–42.
- Mehrabian, A., and Steffl, C. A. (1995). Basic temperament components of loneliness, shyness and conformity. *Soc. Behav. Pers.* 23, 253–263. doi: 10.2224/sbp.1995.23.3.253
- Namburi, P., Al-Hasani, R., Calhoun, G. G., Bruchas, M. R., and Tye, K. M. (2016). Architectural representation of valence in the limbic system. *Neuropsychopharmacology* 41, 1697–1715. doi: 10.1038/npp.2015.358
- Palmiter, S., Justo, D., Jauffret, C., Pavlicek, B., Dauta, A., Delmaire, C., et al. (2012). Critical roles for anterior insula and dorsal striatum in punishment-based avoidance learning. *Neuron* 76, 998–1009. doi: 10.1016/j.neuron.2012.10.017
- Palmiter, S., Khamassi, M., Joffily, M., and Coricelli, G. (2015). Contextual modulation of value signals in reward and punishment learning. *Nat. Commun.* 6:8096. doi: 10.1038/ncomms9096
- Palmiter, S., and Pessiglione, M. (2017). “Opponent brain systems for reward and punishment learning: causal evidence from drug and lesion studies in humans,” in *Decision Neuroscience*, eds J.-C. Dreher and L. Tremblay (Salt Lake City: Academic Press), 291–303. doi: 10.1016/B978-0-12-805308-9.00023-3
- Pan, P., Ou, Y., Su, Q., Liu, F., Chen, J., Zhao, J., et al. (2019). Voxel-based global-brain functional connectivity alterations in first-episode drug-naïve patients with somatization disorder. *J. Affect. Disord.* 254, 82–89. doi: 10.1016/j.jad.2019.04.099
- Pauli, W. M., Larsen, T., Collette, S., Tyszka, J. M., Seymour, B., and O’Doherty, J. P. (2015). Distinct contributions of ventromedial and dorsolateral subregions of the human substantia nigra to appetitive and aversive learning. *J. Neurosci.* 35, 14220–14233. doi: 10.1523/JNEUROSCI.2277-15.2015
- Peelen, M. V., Bracci, S., Lu, X., He, C., Caramazza, A., and Bi, Y. (2013). Tool selectivity in left occipitotemporal cortex develops without vision. *J. Cogn. Neurosci.* 25, 1225–1234. doi: 10.1162/jocn\_a\_00411
- Pessoa, L., and Adolphs, R. (2010). Emotion processing and the amygdala: from a “low road” to “many roads” of evaluating biological significance. *Nat. Rev. Neurosci.* 11, 773–782. doi: 10.1038/nrn2920
- Price, R. B., Gates, K., Kravynak, T. E., Thase, M. E., and Siegle, G. J. (2017). Data-driven subgroups in depression derived from directed functional connectivity paths at rest. *Neuropsychopharmacology* 42, 2623–2632. doi: 10.1038/npp.2017.97
- Rangel, A., and Clithero, J. A. (2012). Value normalization in decision making: theory and evidence. *Curr. Opin. Neurobiol.* 22, 970–981. doi: 10.1016/j.conb.2012.07.011
- Riesman, D. (1950). *The Lonely Crowd: A Study of the Changing American Character*. New Haven: Yale University Press.
- Riesman, D., Glazer, N., and Denney, R. (2001). *The Lonely Crowd: A Study of the Changing American Character*. New Haven: Yale University Press.
- Rogers-Carter, M. M., Varela, J. A., Gribbons, K. B., Pierce, A. F., McGoe, M. T., Ritchey, M., et al. (2018). Insular cortex mediates approach and avoidance responses to social affective stimuli. *Nat. Neurosci.* 21, 404–414. doi: 10.1038/s41593-018-0071-y
- Rosander, M., and Eriksson, O. (2012). Conformity on the Internet—the role of task difficulty and gender differences. *Comput. Hum. Behav.* 28, 1587–1595. doi: 10.1016/j.chb.2012.03.023
- Rutledge, R. B., Lazzaro, S. C., Lau, B., Myers, C. E., Gluck, M. A., and Glimcher, P. W. (2009). Dopaminergic drugs modulate learning rates and perseveration in Parkinson’s patients in a dynamic foraging task. *J. Neurosci.* 29, 15104–15114. doi: 10.1523/JNEUROSCI.3524-09.2009
- Salvador, R., Suckling, J., Coleman, M. R., Pickard, J. D., Menon, D., and Bullmore, E. (2005). Neurophysiological architecture of functional magnetic resonance images of human brain. *Cereb. Cortex* 15, 1332–1342. doi: 10.1093/cercor/bhi016
- Satterthwaite, T. D., Wolf, D. H., Loughhead, J., Ruparel, K., Elliott, M. A., Hakonarson, H., et al. (2012). Impact of in-scanner head motion on multiple measures of functional connectivity: relevance for studies of neurodevelopment in youth. *NeuroImage* 60, 623–632. doi: 10.1016/j.neuroimage.2011.12.063
- Seymour, B., Daw, N., Dayan, P., Singer, T., and Dolan, R. (2007). Differential encoding of losses and gains in the human striatum. *J. Neurosci.* 27, 4826–4831. doi: 10.1523/JNEUROSCI.0400-07.2007
- Shen, H. H. (2015). Core concept: resting-state connectivity. *Proc. Natl. Acad. Sci. U S A* 112, 14115–14116. doi: 10.1073/pnas.1518785112

- Shenhav, A., and Buckner, R. L. (2014). Neural correlates of dueling affective reactions to win-win choices. *Proc. Natl. Acad. Sci. U S A* 111, 10978–10983. doi: 10.1073/pnas.1405725111
- Simmons, A., Strigo, I., Matthews, S. C., Paulus, M. P., and Stein, M. B. (2006). Anticipation of aversive visual stimuli is associated with increased insula activation in anxiety-prone subjects. *Biol. Psychiatry* 60, 402–409. doi: 10.1016/j.biopsych.2006.04.038
- Simmons, W. K., and Martin, A. (2011). Spontaneous resting-state BOLD fluctuations reveal persistent domain-specific neural networks. *Soc. Cogn. Affect. Neurosci.* 7, 467–475. doi: 10.1093/scan/nsr018
- Sladky, R., Höflich, A., Küblböck, M., Kraus, C., Baldinger, P., Moser, E., et al. (2013). Disrupted effective connectivity between the amygdala and orbitofrontal cortex in social anxiety disorder during emotion discrimination revealed by dynamic causal modeling for fMRI. *Cereb. Cortex* 25, 895–903. doi: 10.1093/cercor/bht279
- Smith, M. J. (1982). *Evolution and the Theory of Games*. Cambridge: Cambridge University Press.
- Smith, S. M., Vidaurre, D., Beckmann, C. F., Glasser, M. F., Jenkinson, M., Miller, K. L., et al. (2013). Functional connectomics from resting-state fMRI. *Trends Cogn. Sci.* 17, 666–682. doi: 10.1016/j.tics.2013.09.016
- Song, L., Peng, Q., Liu, S., and Wang, J. (2020). Changed hub and functional connectivity patterns of the posterior fusiform gyrus in chess experts. *Brain Imaging Behav.* 14, 797–805. doi: 10.1007/s11682-018-0020-0
- Spitzer, M., Fischbacher, U., Herrnberger, B., Grön, G., and Fehr, E. (2007). The neural signature of social norm compliance. *Neuron* 56, 185–196. doi: 10.1016/j.neuron.2007.09.011
- Stevens, W. D., Tessler, M. H., Peng, C. S., and Martin, A. (2015). Functional connectivity constrains the category-related organization of human ventral occipitotemporal cortex. *Hum. Brain Mapp.* 36, 2187–2206. doi: 10.1002/hbm.22764
- Straube, T., and Miltner, W. H. R. (2011). Attention to aversive emotion and specific activation of the right insula and right somatosensory cortex. *NeuroImage* 54, 2534–2538. doi: 10.1016/j.neuroimage.2010.10.010
- Tavor, I., Jones, O. P., Mars, R. B., Smith, S. M., Behrens, T. E., and Jbabdi, S. (2016). Task-free MRI predicts individual differences in brain activity during task performance. *Science* 352, 216–220. doi: 10.1126/science.aad8127
- Touroutoglou, A., Hollenbeck, M., Dickerson, B. C., and Barrett, L. F. (2012). Dissociable large-scale networks anchored in the right anterior insula subserve affective experience and attention. *NeuroImage* 60, 1947–1958. doi: 10.1016/j.neuroimage.2012.02.012
- Ullsperger, M., Volz, K. G., and von Cramon, D. Y. (2004). A common neural system signaling the need for behavioral changes. *Trends Cogn. Sci.* 8, 445–446. doi: 10.1016/j.tics.2004.08.013
- Van den Heuvel, M. P., and Hulshoff Pol, H. E. (2010). Exploring the brain network: a review on resting-state fMRI functional connectivity. *Eur. Neuropsychopharmacol.* 20, 519–534. doi: 10.1016/j.euroneuro.2010.03.008
- Van Dijk, K. R. A., Sabuncu, M. R., and Buckner, R. L. (2012). The influence of head motion on intrinsic functional connectivity MRI. *NeuroImage* 59, 431–438. doi: 10.1016/j.neuroimage.2011.07.044
- Vlaev, I., Chater, N., Stewart, N., and Brown, G. D. A. (2011). Does the brain calculate value? *Trends Cogn. Sci.* 15, 546–554. doi: 10.1016/j.tics.2011.09.008
- Wang, X., Zhen, Z., Song, Y., Huang, L., Kong, X., and Liu, J. (2016). The hierarchical structure of the face network revealed by its functional connectivity pattern. *J. Neurosci.* 36, 890–900. doi: 10.1523/JNEUROSCI.2789-15.2016
- Wiech, K., Jbabdi, S., Lin, C. S., Andersson, J., and Tracey, I. (2014). Differential structural and resting state connectivity between insular subdivisions and other pain-related brain regions. *Pain* 155, 2047–2055. doi: 10.1016/j.pain.2014.07.009
- Xue, J., Guo, H., Gao, Y., Wang, X., Cui, H., Chen, Z., et al. (2019). Altered directed functional connectivity of the hippocampus in mild cognitive impairment and Alzheimer's disease: a resting-state fMRI study. *Front. Aging Neurosci.* 11:326. doi: 10.3389/fnagi.2019.00326
- Yarkoni, T., Poldrack, R. A., Nichols, T. E., Van Essen, D. C., and Wager, T. D. (2011). Large-scale automated synthesis of human functional neuroimaging data. *Nat. Methods* 8, 665–670. doi: 10.1038/nmeth.1635

**Conflict of Interest:** The authors declare that the research was conducted in the absence of any commercial or financial relationships that could be construed as a potential conflict of interest.

Copyright © 2020 Du, Wang, Yu, Tian and Liu. This is an open-access article distributed under the terms of the Creative Commons Attribution License (CC BY). The use, distribution or reproduction in other forums is permitted, provided the original author(s) and the copyright owner(s) are credited and that the original publication in this journal is cited, in accordance with accepted academic practice. No use, distribution or reproduction is permitted which does not comply with these terms.



# Individualized Prediction of PTSD Symptom Severity in Trauma Survivors From Whole-Brain Resting-State Functional Connectivity

Xueling Suo<sup>1,2,3</sup>, Du Lei<sup>1,2,3,4</sup>, Wenbin Li<sup>1,2,3</sup>, Jing Yang<sup>1,2,3</sup>, Lingjiang Li<sup>5</sup>, John A. Sweeney<sup>1,4</sup> and Qiyong Gong<sup>1,2,3,4\*</sup>

<sup>1</sup>Huaxi MR Research Center (HMRRC), Department of Radiology, West China Hospital of Sichuan University, Chengdu, China, <sup>2</sup>Research Unit of Psychoradiology, Chinese Academy of Medical Sciences, Chengdu, China, <sup>3</sup>Functional and Molecular Imaging Key Laboratory of Sichuan Province, West China Hospital of Sichuan University, Chengdu, China, <sup>4</sup>Department of Psychiatry and Behavioral Neuroscience, University of Cincinnati, Cincinnati, OH, United States, <sup>5</sup>Mental Health Institute, The Second Xiangya Hospital of Central South University, Changsha, China

## OPEN ACCESS

### Edited by:

Seth Davin Norrholm,  
Wayne State University,  
United States

### Reviewed by:

Bruno Jacson Martynhak,  
Federal University of Paraná, Brazil  
Daniela Rabellino,  
Western University, Canada  
Margit Jehna,  
Medical University of Graz, Austria

### \*Correspondence:

Qiyong Gong  
qiyonggong@hmrcc.org.cn

### Specialty section:

This article was submitted to  
Pathological Conditions,  
a section of the journal  
Frontiers in Behavioral Neuroscience

**Received:** 18 May 2020

**Accepted:** 23 November 2020

**Published:** 21 December 2020

### Citation:

Suo X, Lei D, Li W, Yang J, Li L,  
Sweeney JA and Gong Q  
(2020) Individualized Prediction of  
PTSD Symptom Severity in Trauma  
Survivors From Whole-Brain  
Resting-State Functional  
Connectivity.  
Front. Behav. Neurosci. 14:563152.  
doi: 10.3389/fnbeh.2020.563152

Previous studies have demonstrated relations between spontaneous neural activity evaluated by resting-state functional magnetic resonance imaging (fMRI) and symptom severity in post-traumatic stress disorder. However, few studies have used brain-based measures to identify imaging associations with illness severity at the level of individual patients. This study applied connectome-based predictive modeling (CPM), a recently developed data-driven and subject-level method, to identify brain function features that are related to symptom severity of trauma survivors. Resting-state fMRI scans and clinical ratings were obtained 10–15 months after the earthquake from 122 earthquake survivors. Symptom severity of post-traumatic stress disorder features for each survivor was evaluated using the Clinician Administered Post-traumatic Stress Disorder Scale (CAPS-IV). A functionally pre-defined atlas was applied to divide the human brain into 268 regions. Each individual's functional connectivity 268 × 268 matrix was created to reflect correlations of functional time series data across each pair of nodes. The relationship between CAPS-IV scores and brain functional connectivity was explored in a CPM linear model. Using a leave-one-out cross-validation (LOOCV) procedure, findings showed that the positive network model predicted the left-out individual's CAPS-IV scores from resting-state functional connectivity. CPM predicted CAPS-IV scores, as indicated by a significant correspondence between predicted and actual values ( $r = 0.30$ ,  $P = 0.001$ ) utilizing primarily functional connectivity between visual cortex, subcortical-cerebellum, limbic, and motor systems. The current study provides data-driven evidence regarding the functional brain features that predict symptom severity based on the organization of intrinsic brain networks and highlights its potential application in making clinical evaluation of symptom severity at the individual level.

**Keywords:** psychoradiology, post-traumatic stress disorder, functional magnetic resonance imaging, resting-state, functional connectivity, connectome-based predictive modeling



## INTRODUCTION

There is a high risk for trauma survivors to develop post-traumatic stress disorder (PTSD; Yehuda and Flory, 2007), a highly debilitating psychiatric disorder characterized by symptoms including avoidance of trauma-related stimuli, re-experiencing of the trauma, hyperarousal, and altered cognition and mood (American Psychiatric Association, 2013). Psychoradiology, a new field of radiology, aims to use brain imaging to not only advance understanding of psychiatric disorders but also play a clinical role in diagnostic and treatment planning decisions (Sun et al., 2018; Huang et al., 2019; Gong, 2020). Previous studies have identified brain connectivity network alterations in trauma survivors who develop PTSD compared with those who do not (Patel et al., 2012; Lei et al., 2015; Kennis et al., 2016; Akiki et al., 2018; Niu et al., 2018). However, these alterations were based on group-level comparisons. Thus, it remains unclear whether image data can be helpful for the clinical evaluation of symptom severity in individual trauma survivors.

Functional magnetic resonance imaging (fMRI) is a noninvasive technique assessing neural activity. Functional connectivity analyses, examining associations of activity across different brain regions, have demonstrated robust and unique patterns of brain activity that predict neuropsychological traits and clinical symptoms across individuals (Dubois and Adolphs, 2016; Rosenberg et al., 2018). Modeling the associations between phenotypic measures (e.g., ratings of illness severity) and functional brain organization can provide a basis for establishing the clinical utility of imaging data (Gao et al., 2019).

The comprehensive map of functional connectivity in the human brain is defined as the “functional connectome” (Biswal et al., 2010). Recent research has applied functional connectome analysis to predict a broad range of phenotypic measures, including intelligence (Finn et al., 2015), creativity (Beaty et al., 2018), attention (Rosenberg et al., 2016), cocaine abstinence (Yip et al., 2019), cognitive impairment (Lin et al., 2018), and symptom severity of autism spectrum disorder and attention deficit hyperactivity disorder (Lake et al., 2019). Few studies have attempted to investigate the relationship between functional connectivity and PTSD symptom severity (Lanius et al., 2010; Zhou et al., 2012; Tursich et al., 2015; Zandvakili et al., 2020). Further, most included participants were receiving treatment with psychotropic medications and had psychiatric comorbidities, which may have influenced study findings. Also, some studies used a seed-based method in which findings may have been biased by the particular seed region chosen. While resting-state functional connectivity analyses of symptom severity in PTSD have been informative, the prediction of PTSD symptom severity using the whole brain functional connectome before drug treatment remains to be established in noncomorbid trauma survivors.

In the current study, we applied a recently developed connectome-based predictive modeling (CPM) method (Shen et al., 2017) to identify the neural networks that allow for accurate prediction of individual PTSD symptom severity reflected in CAPS-IV scores in a cohort of trauma survivors using

resting-state brain functional connectome features. Clinician-Administered PTSD Scale (CAPS), a widely used structured interview, is considered the gold standard in PTSD research for measuring its severity, and is a rating scale with excellent psychometric properties including strong discriminant and convergent validity, good clinical utility, and sensitivity to clinical alteration (Weathers et al., 2001). There are two neural models when investigating the neuropathophysiology underlying PTSD. One is the traditional neural circuit of PTSD based on studies of fear processing, with critical structures including medial prefrontal cortex, amygdala, and hippocampus (Rauch et al., 2006). The other is the triple network model including central executive, default mode, and salience networks (Patel et al., 2012). Based on prior research, we hypothesized that individual symptom severity would be related to intrinsic functional connectivity across distributed networks, e.g., traditional fear neural circuit or the triple network model.

## MATERIALS AND METHODS

### Participants

This retrospective study was approved by the Medical Research Ethics Committee of West China Hospital, Sichuan University, and informed written consent was obtained from all participants before the study. One-hundred and twenty-two survivors were recruited between 10 and 15 months after the 2008 Sichuan earthquake event (see **Table 1**). Inclusion criteria were as follows: (i) physical experience of the earthquake; (ii) without any physical injury; and (iii) personally witness serious injury, death, and/or the collapse of buildings. Exclusion criteria included history of any neurological or psychiatric disorder other than PTSD, psychiatric comorbidities evaluated by the structured clinical interview for DSM IV diagnosis (SCID), pregnancy, history of drug or alcohol abuse, and recent medication that might have an effect on brain function. Each participant was evaluated by using the CAPS-IV as a continuous measure of symptom severity (Blake et al., 1995). Of the 122 traumatized earthquake survivors included, 64 fulfilled diagnostic criteria for current PTSD at the time of fMRI examination. All participants had received no prior treatment with psychiatric medications. fMRI data from these participants have been reported previously elsewhere. In 2014, Gong et al. (2014a) investigated the relationship between resting-state fMRI data and PTSD Checklist scores using a multivariate analytical method, whereas our current work constructed a prediction model at the level of individual patients using the CAPS-IV and a CPM method.

### Data Acquisition

Resting-state fMRI is a technique for measuring spontaneous blood oxygen level-dependent (BOLD) fluctuations that reflect resting neurophysiological activity of the brain. The acquisition of fMRI from survivors took place between 10 and 15 months after the earthquake at the same day of clinical assessment. A total of 200 image volumes sensitized to BOLD signal changes were collected for each participant using a 3-T MRI system (GE EXCITE, Milwaukee, WI, USA) equipped with an eight-channel

**TABLE 1 |** Demographics and clinical characteristics of the subjects.

Characteristic	Earthquake survivors ( <i>n</i> = 122)
Age (years) <sup>b</sup>	43.0 ± 10.3 (20–67) <sup>a</sup>
Gender (male/female)	36/86
Years of education <sup>b</sup>	7.3 ± 3.4 (0–16) <sup>a</sup>
Time since trauma (months) <sup>b</sup>	12.2 ± 2.2 (8–15) <sup>a</sup>
Clinician-administered PTSD scale	40.1 ± 22.3 (3–95) <sup>a</sup>

<sup>a</sup>Data are presented as the mean ± SD (range of minimum–maximum). <sup>b</sup>Age, years of education, and time since trauma were reported by participants at the time of magnetic resonance scanning.

phased array head coil. The fMRI data were obtained with the following scanning parameters: repetition time = 2,000 ms; echo time = 30 ms; field of view = 240 × 240 mm<sup>2</sup>; voxel size = 3.75 × 3.75 × 5 mm<sup>3</sup>; matrix size = 64 × 64; flip angle = 90°; slice thickness = 5 mm, no slice gap; and 30 axial slice per volume. For each participant, each functional run resulted in a total scanning time of 400 s. Each subject was instructed to lie quietly with their eyes closed during the scanning.

## Data Pre-processing

SPM8 software<sup>1</sup> was used to perform the pre-processing of fMRI image data. First, the original 10 time points were deleted to establish magnetic tissue stabilization. Then, slice timing correction was conducted to correct for intra-volume acquisition delay. The images were further realigned for the correction of head movement. To reduce the influences of head motion, a scrubbing method was performed, which deleted volumes with frame-wise displacement (FD) >0.5 mm. Images were normalized using echo-planar imaging templates (voxel size: 3 × 3 × 3). Subsequently, linear trends in time series were removed. Nuisance signal (including the Friston 24-parameter head motion model, the white matter signal, the cerebrospinal fluid signal, and the global signal) were regressed out. Finally, functional data were linearly detrended and temporally bandpass (0.01–0.1 Hz) filtered to eliminate effects of high-frequency noise and low-frequency drift, and smoothed (Gaussian kernel with a full-width at half-maximum of 4 mm). None of the participants showed excessive head motion (defined as rotation >2°, translation >2 mm, or mean FD >0.15 mm) throughout the course of scans.

## Functional Connectivity

Using the GRETNA<sup>2</sup> toolbox (Wang et al., 2015), the functional brain network was constructed. The Shen brain atlas was applied to parcellate the brain into 268 region of interest including the cortex, subcortex, and cerebellum (**Supplementary Table 1** and **Supplementary Figure 1**) to define the network nodes (Shen et al., 2013), as in previous CPM work (Rosenberg et al., 2016; Beaty et al., 2018; Lake et al., 2019; Yip et al., 2019). This involved computation of mean time courses for each of the 268 nodes (i.e., average time course of voxels within the node) for use in node-by-node pairwise Pearson's correlations. The resultant *r* coefficients were transformed using Fisher's *z*-transformation to

create symmetric 268 × 268 connectivity matrices in which each value of the matrix represents the connection strength between all pairs of nodes.

## Connectome-Based Predictive Modeling

CPM was conducted using previously validated and freely available custom MATLAB scripts (Shen et al., 2017). Briefly, CPM took brain connectivity data and behavioral measures (in this case, functional brain connectivity matrices and CAPS-IV scores, respectively) as input to create a linear predictive model of the PTSD symptom severity using the connectivity matrices. Spearman's correlations with a statistical significance *P*-value threshold of 0.05 were calculated between edge weights and disease symptom measures across the training participants to identify negative and positive predictive networks. According to the suggestion of Shen et al. (2017), the Spearman's correlation rather than the Pearson's correlation were calculated as the CAPS-IV scores do not follow a normal distribution. For the positive prediction network, edges were positively associated with the disease symptom measures, and for the negative prediction network, edges were negatively associated with the disease symptom measures. Therefore, elements in the negative and positive prediction network were defined by associations with CAPS-IV scores instead of negative or positive functional connectivity themselves. While both networks were used for predicting the same variable, they were by definition independent, because a single edge was either a negative or a positive predictor. Individual summary values were then calculated by summing the significant functional connectivity strength in each network and were applied to construct linear predictive models to estimate the relationships between network strength with CAPS-IV scores. The resultant polynomial coefficients (including slope and intercept) were then used to predict symptom severity. In the current study, leave-one-out cross-validation (LOOCV) analysis was employed. Briefly, the "left-out" participant's predicted CAPS-IV score was obtained by the predictive model trained on all other participants' data iteratively until all participants had a predicted score.

Spearman's correlations between the predicted and actual CAPS-IV scores were used to assess the model performance. To address the problem of non-independence of analyses in the leave-one-out folds, nonparametric permutation testing rather than parametric testing was performed to evaluate statistical significance. To obtain empirical null distributions for Spearman correlation coefficients, the correspondence between CAPS-IV scores and connectivity matrices were randomly shuffled 1,000 times and the CPM analysis was re-conducted using the shuffled data. The *p*-values for leave-one-out predictions were computed based on the null distributions as previous suggested (Shen et al., 2017).

## Contributing Nodes and Edges in the Prediction of CAPS-IV Scores

To investigate the functional anatomy of the contributing elements, the distribution of nodes and edges were summarized in two methods. First, the 268 nodes were classified into 10 macroscale brain regions that were anatomically defined,

<sup>1</sup><http://www.fil.ion.ucl.ac.uk/spm>

<sup>2</sup><http://www.nitrc.org/projects/gretna/>

including the prefrontal cortex (46 nodes), cerebellum (41 nodes), temporal lobe (39 nodes), limbic cortex (36 nodes), parietal lobe (27 nodes), occipital lobe (25 nodes), motor cortex (21 nodes), subcortical structures (17 nodes), brainstem (9 nodes), and insular cortex (7 nodes; Finn et al., 2015; Rosenberg et al., 2016). Second, the 268 nodes were parcellated into eight canonical networks previously defined using a clustering algorithm (Finn et al., 2015), including medial frontal, motor, subcortical-cerebellum, visual (I, II, and association), frontoparietal, and default mode networks. The number of connections between all pairs of macroscale brain regions or canonical networks was then computed. Last, the number of each node's connections was used to evaluate their importance (Rosenberg et al., 2016; Beaty et al., 2018). The functional connectivity patterns of the top 10 nodes with the most connections were determined.

## Validation Analyses

The following procedures were performed to further evaluate reproducibility of our results. First, a 1,000-iteration permutation test was used to generate an empirical null distribution of the test statistic. To determine whether our main results depended on the choice of different iterations, we reran the CPM analysis using a 5,000-iteration permutation test. Second, we constructed functional connectomes using another parcellation scheme, the automated anatomical labeling (AAL) atlas (Tzourio-Mazoyer et al., 2002) and repeated the entire analyses. Third, we also performed CAPS-IV score prediction using LIBSVM (Chang and Lin, 2011) to implement support vector machine regression (SVR) with a linear kernel. Positive and negative edges were selected the same way as in CPM, and both positive and negative edges were input into SVR as features. The performance of the SVR algorithm was evaluated using correlation between the observed and predicted values.

## Support Vector Machine (SVM) Analysis

Exploratory SVM analyses were applied to the functional connectivity matrices to determine whether functional networks can detect PTSD patients and trauma-exposed non-PTSD (TENP) controls at the individual level. For full details of SVM evaluation, please refer to our recent study (Lei et al., 2020).

## RESULTS

### Preliminary Analyses

Subjects differed widely in respect to their degree of psychological distress reflected in CAPS-IV scores (Figure 1A). There were no statistically significant correlations between CAPS-IV scores and age ( $r = 0.072$ ,  $P = 0.430$ ) as well as the mean FD head motion ( $r = -0.076$ ,  $P = 0.407$ ). CAPS-IV scores did not differ between genders ( $P = 0.881$ ).

### Predicting CAPS-IV

The relations between connection strength of the positive/negative network and CAPS-IV scores in individual trauma survivors were examined by implementing a LOOCV approach. Model performance was evaluated using Spearman's

rank correlation on predicted and actual scores, and statistical significance was determined using a 1,000-iteration permutation test, repeating the prediction analysis, and determining the fraction of correlations between predicted and actual scores that were as extreme as the original data. Results indicated that resting-state brain functional connectivity in the positive network was related to individuals' CAPS-IV scores (correlation between actual and predicted scores:  $r = 0.30$ ,  $P = 0.001$ , permutation test, Figures 1B,C). However, resting-state functional connectivity in the negative network could not reliably predict CAPS-IV scores (correlation between actual and predicted scores:  $r = 0.17$ ,  $P = 0.07$ ).

## Functional Anatomy

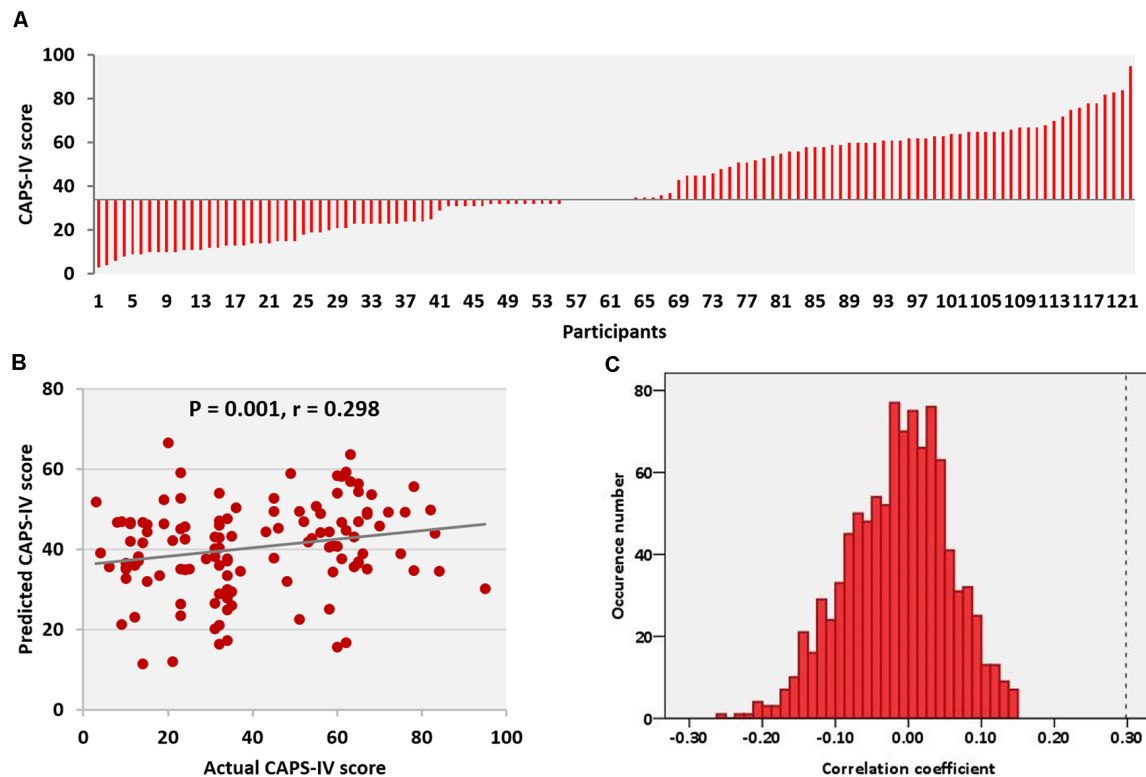
Across all folds of LOOCV, 1,006 edges (2.81% of the 35,778 total edges) in the positive prediction network appeared in every iteration of the LOOCV and were defined as the contributing network (Figure 2A). CPM analysis revealed the functional anatomy of networks in which activity was related to CAPS-IV scores. We applied the parcellation that grouped the 268 nodes into 10 macroscale brain regions, which were anatomically defined, to the positive networks to identify connections between macroscale brain regions involved in prediction. Connections between occipital lobe and cerebellum and connections of the limbic lobe with cerebellum and occipital lobe were primary predictors of CAPS-IV score (Figure 2B).

When dividing the 268 nodes into the eight canonical networks previously used in Finn et al. (2015), connectivity based on the number of connections within and between canonical networks for the positive networks is shown in Figure 2C. It was revealed that the positive network included relatively more connections of the subcortical-cerebellum network with visual I, visual II, visual association, and motor networks, and connections within the subcortical-cerebellum network were highly involved in prediction (Figure 2C).

Lastly, the top 10 nodes with the most connections were located in the bilateral visual cortex [including bilateral visual association cortex (18) and left visual cortex BA 19] and cerebellum (lobules VI–VII), indicating the critical role of these nodes in predicating the severity of PTSD-related symptoms as reflected in CAPS-IV scores (Figure 3 and Table 2). Note that single-subject levels of CAPS-IV scores were primarily represented by functional connectivity of these regions to other brain regions in addition to their intrinsic connectivity.

## Validation With Different Schemes

Using different validation schemes, the performance of prediction was re-estimated. The resultant correlation coefficients between actual and predicted CAPS-IV scores remained significant when using 5,000 times permutation test, thus validating the main findings. However, there was no significant prediction in the positive (correlation between actual and predicted scores:  $r = 0.16$ ,  $P = 0.10$ , permutation tests) or negative network model (correlation between actual and predicted scores:  $r = 0.16$ ,  $P = 0.11$ , permutation tests) when using the AAL atlas. The application of SVR to the positive networks (correlation between actual and predicted scores:



**FIGURE 1 |** Clinician Administered Post-traumatic Stress Disorder Scale (CAPS-IV) scores and performance of the prediction model. **(A)** CAPS-IV scores across all participants. **(B)** Correlation between actual and predicted CAPS-IV scores. **(C)** Permutation distribution of the correlation coefficient ( $r$ ) for the prediction analysis. CAPS, clinical-administered post-traumatic stress disorder (PTSD) score.

$r = 0.08$ ,  $P = 0.64$ , permutation tests) or negative networks (correlation between actual and predicted scores:  $r = 0.10$ ,  $P = 0.56$ , permutation tests) did not allow quantitative prediction of CAPS-IV scores with statistically significant accuracy.

### Single-Subject Classification of PTSD Patients and TENP Controls Using SVM

Using functional connectivity matrices, the mean balanced accuracy of classification of PTSD vs. TENP was 64.5%, with sensitivity 67.1% and specificity 62.0% ( $P = 0.004$ ). To identify brain regions providing greatest contribution to single-subject classification, the mean absolute value of the weights of the model across the different folds of the cross-validation was calculated. The 10 brain regions with the highest mean values are shown in **Supplementary Figure 2**. It can be seen that most of the brain regions were cerebellum and visual association regions.

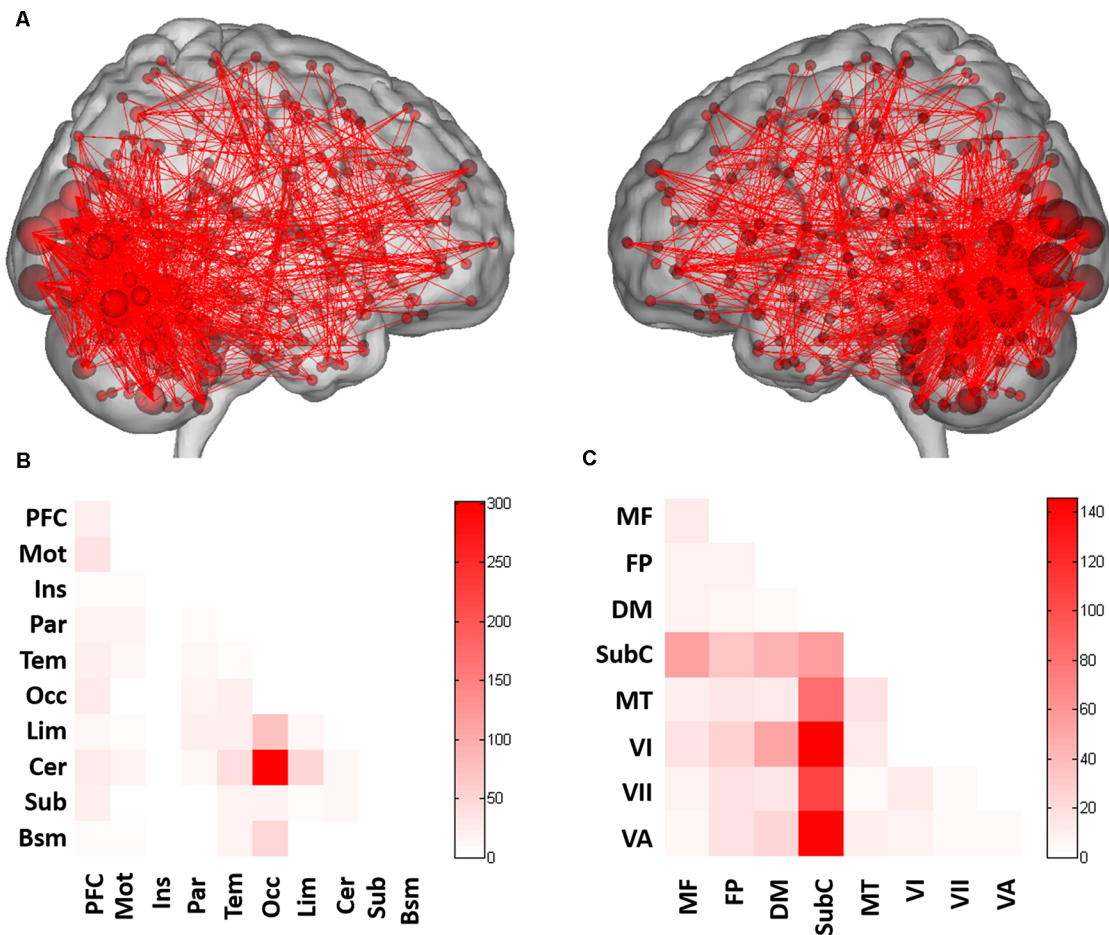
## DISCUSSION

We applied a functional brain network analysis in a recently developed machine-learning approach to use fMRI features to predict clinical severity of PTSD symptoms in a group who had experienced acute major life trauma. We have demonstrated that functional brain connectivity allowed for prediction of single-subject PTSD symptom severity

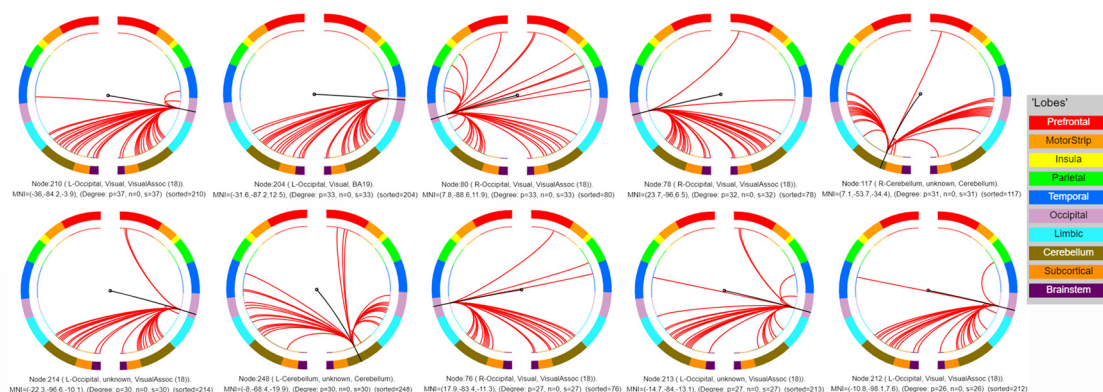
independently of confounding variables (i.e., head motion, gender, age, prior treatment with psychiatric medications, and psychiatric comorbidity). Inter-individual differences in CAPS-IV scores were mainly accounted for by the functional brain connectivity between subcortical-cerebellum, visual, limbic, and motor systems. These observations highlight the importance of brain regions outside the classic traditional fear neural circuit and the triple network model as being important in determining the severity of PTSD.

Our prior study showed that the utilization of a multivariate machine-learning approach known as SVM to structural MRI data provided for the discrimination of traumatized survivors who do and do not fulfil the criteria for PTSD (Gong et al., 2014b). However, this study focused on a binary classification between non-PTSD controls and PTSD patients and neglected the severity of PTSD symptoms as a dimensional illness feature of important clinical significance. A data-driven, whole-brain dimensional analysis centered on single-subject variations instead of binary case-non-case classification may be more helpful for obtaining features related to illness severity (Lake et al., 2019). In addition, we previously used a multivariate analytical approach known as relevance vector regression to the whole-brain fMRI data to predict the clinical scores (Gong et al., 2014a). This current research





**FIGURE 2 |** Functional connections predicting CAPS-IV scores. **(A)** Positive (red) networks selected by the prediction model. For the positive network, increased edge weights (i.e., increased functional connectivity) predict higher CAPS-IV scores. **(B)** Connections plotted as number of edges within and between each pair of macroscale regions. **(C)** Connections plotted as number of edges within and between each pair of canonical networks. Cells represent the total number of edges connecting nodes within (and between) each macroscale region or canonical network, with darker colors indicating a greater number of edges. PFC, prefrontal; Mot, motor; Ins, insula; Par, parietal; Tem, temporal; Occ, occipital; Lim, limbic; Cer, cerebellum; Sub, subcortical; Bsm, brainstem; MF, medial frontal network; FP, frontoparietal network; DM, default mode network; SubC, subcortical-cerebellum network; MT, motor network; VI, visual I network; VII, visual II network; VA, visual association network.



**FIGURE 3 |** Connectivity patterns of the top 10 nodes with the most connections. L, left; R, right.

**TABLE 2 |** Ten nodes with the most connections selected by the prediction model.

Node	MNI coordinate (mm)			Lobe	Degree
L Visual Assoc (18)	−36	−84.2	−3.9	Occipital	37
L Visual BA 19	−31.6	−87.2	12.5	Occipital	33
R Visual Assoc (18)	7.8	−88.6	11.9	Occipital	33
R Visual Assoc (18)	23.7	−96	6.5	Occipital	32
R Cerebellum	7.1	−53.7	−34.4	Cerebellum	31
L Visual Assoc (18)	−22.3	−96.6	−10.1	Occipital	30
L Cerebellum	−8	−68.4	−19.9	Cerebellum	30
R Visual Assoc (18)	17.9	−83.4	−11.3	Occipital	27
L Visual Assoc (18)	−14.7	−84	−13.1	Occipital	27
L Visual Assoc (18)	−10.8	−98.1	7.6	Occipital	26

Abbreviation: Assoc, association; L, left; R, right.

extended these earlier studies by demonstrating that the symptom severity (CAPS-IV measures) could be significantly and quantitatively predicted from a subject-level's unique resting-state functional brain connectivity by using the CPM approach. CPM has two appealing aspects compared to the multivariate machine-learning approaches (Shen et al., 2017). First, from a practicable point of view, it is simpler to perform CPM, which requires less skill in machine learning and makes it easier to the general neuropsychiatric imaging investigators for conducting replicable data-driven analyses of the relationships between individual brain imaging data and their phenotypic measures. Second, CPM provides straightforward and clearly interpretable one-to-one mapping back to the original feature space in order that the underlying brain connectivity contributing to the predictive model can be easily determined and visualized.

Our findings reveal that intrinsic functional connectivity across multiple neural systems contributes to predicting individual PTSD clinical measures. Specifically, individual CAPS-IV score was primarily accounted for by intrinsic functional connectivity between bilateral visual cortex and cerebellum. Previous studies with PTSD patients have shown hyperactive function of visual cortex compared with controls, which was positively related to PTSD symptom severity (Zhu et al., 2014, 2015; Neumeister et al., 2017). Hyperactivity of visual cortex may be related to disrupted visual imagery in PTSD and underlie the visual re-experiencing of trauma events (Zhu et al., 2014). The cerebellum, another region that integrates sensory information for sensorimotor control, is recognized increasingly to be implicated in cognitive and emotional processing (Schmahmann and Caplan, 2006). Animal studies have established a role for the cerebellum in fear-conditioning consolidation (Sacchetti et al., 2002). Following more and more neuroimaging research, interest in the cerebellum has increased in PTSD. Hyperactivity of the cerebellum in PTSD was observed, including increased resting-state activity (Bing et al., 2013; Ke et al., 2016), increased blood flow during rest (Bonne et al., 2003), and in response to threat-related stimuli in PTSD (Osuch et al., 2001; Pantazatos et al., 2012). During earthquake imagery, the PTSD group demonstrated activation in the bilateral visual cortex and cerebellum while the control group did not (Yang et al., 2004). Similarly, positive correlations were found between resting-state cerebral perfusion in the cerebellum and visual

association cortices and PTSD symptom severity in trauma survivors, in keeping with the between-group analysis (Bonne et al., 2003). In addition, a recent study showed that resting-state functional connectivity of the visual association cortices with cerebellum was increased and correlated positively with PTSD symptomatology (Rabellino et al., 2018). Altogether, the alterations in visual cortex and cerebellum might play a critical role in ongoing visual re-experiencing of trauma events and abnormal emotional processing in PTSD.

We further demonstrated that connections of the limbic lobe with cerebellum and occipital lobe were primary predictors of individual CAPS-IV score. The traditional view of PTSD has been that it is a disorder specific to the fronto-limbic fear circuit. Different from this traditional view, regions outside the fronto-limbic circuit were primarily predictive for the severity of PTSD symptoms in the current study. Our findings were consistent with the subset of studies that found functional and structural alterations between limbic and occipital/cerebellum regions (Chen et al., 2012; Leutgeb et al., 2016; McGlade et al., 2020). For instance, Leutgeb et al. (2016) found altered functional connectivity between the limbic system and cerebellum in violent offenders, suggesting that this circuit may contribute to behavioral perturbations linked to PTSD. Similarly, using voxel-based morphometry method, Chen et al. (2012) found that the gray matter volume in the limbic and occipital lobe of trauma survivors were correlated with their CAPS scores. These studies provided evidence for comparable dysfunction in the corticolimbic circuitry, specifically limbic and occipital and cerebellum connectivity in PTSD. Our analytic approach focusing on current symptom severity indicates that systems outside the fronto-limbic fear circuit are crucial to predict the current symptomatology following exposure to serious life trauma.

Prior studies have suggested that symptomatology of PTSD is related to dysfunction of a triple network model that includes the central executive, default mode, and salience network (Patel et al., 2012; Lei et al., 2015; Kennis et al., 2016; Niu et al., 2018). We therefore hypothesized that alterations in this network model would be related to PTSD symptom severity. Contrary to this hypothesis, using the CPM approach, we found that brain regions outside the triple network (e.g., visual cortex and cerebellum) primarily contributed to an accurate prediction of symptom severity. Additionally, connections between the subcortical-cerebellum and motor network and within subcortical-cerebellum were also revealed as key contributions in the prediction of CAPS-IV scores. With respect to subcortical-cerebellum and motor network connectivity, a diffusion tensor imaging study has reported direct connections between the subcortical (e.g., amygdala) and motor cortices (Grèzes et al., 2014), with a resting-state fMRI study providing evidence of a distinct amygdala-sensorimotor functional network (Thome et al., 2017), which might be related to emotional modulation of subjective sensory experiences as they are used in action planning. Disrupted resting-state functional connectivity between subcortical and motor regions in PTSD might reflect maladaptive somatosensory processing (Thome et al., 2017; Belleau et al., 2020). While

large-scale, spatially distributed triple network alterations are relatively well established in patients diagnosed with PTSD, our findings extend these studies by adding to a growing evidence base implicating visual, cerebellar, subcortical, and motor involvement in pathophysiological processes that are associated with symptom severity in PTSD. In particular, the cerebellum has, until recently, been underemphasized in PTSD research and in studies of other psychiatric disorders (Baldaçara et al., 2008). It is noteworthy that with the CPM approach, which is based on correlational associations of MRI features and clinical symptoms, we cannot draw a conclusion that PTSD symptoms were “caused” by one or a few networks. As with other studies (Lake et al., 2019), investigating illness-related biology as a continuous spectrum rather than in terms of categorical definition based on meeting and not meeting criteria for diagnosis can add an important approach for studying brain-behavior associations related to current symptom severity vs. those associated with presence of illness.

Notably, when using functional connectivity to discriminate PTSD patients and TENP controls, the accuracy of classification was 64.5%. Our recent study of PTSD found that large-scale brain networks allowed single-subject classification of patients and healthy controls with higher accuracy as might be expected (average: 89%; Zhu et al., 2020). Furthermore, most of the top 10 brain regions providing the greatest contribution to the classification of PTSD and TENP participants overlapped with the key regions in the prediction of CAPS-IV symptom severity scores: among them were the abovementioned visual and cerebellar regions. Therefore, the current study provides an important step toward data-driven diagnostic assessment in PTSD. Although machine learning is not yet available in day-to-day clinical practice, in light of the urgent clinical need for objective biomarkers in the early stage of the disease, it has the potential to inform the development of diagnostic imaging-based markers.

Finally, using a different parcellation strategy (AAL atlas) and predictive model (SVR), we did not detect a pattern of regional connectivity that showed a significant association with clinical scores. Several issues might contribute to the discrepancy. First, the 268-node Shen functional atlas comprises nodes with more coherent time series and specific functional specificity than those defined by the AAL atlas, which might account for the superior performance of the 268-node parcellation because anatomical boundaries do not always match functional ones (Shen et al., 2013). Additionally, when the number of *a priori* selected regions is very small, the risk of no edges or very few edges being selected within some iterations of cross-validation grows remarkably higher. This could lead to unstable models with poor predictive ability. Second, in the CPM model, all positive/negative features were averaged to create summary statistics, which reduced the variance of the summary statistics compared to the original set of features used in the SVR model (Yip et al., 2019). An alternative possibility is that there is a complex relationship between clinical scores and functional connectivity beyond a simple linear correlation in the SVR model. This might be addressed in future studies with larger sample sizes.

Several limitations of this study need to be acknowledged. First, although there is growing evidence that brain functional connectivity may act as a reliable and objective imaging marker of individuals’ phenotypic measures, CPM has not yet been widely used in clinical research. Also, the extent to which brain functional connectivity reflects transient states vs. stable traits is still unknown. To address this issue and determine the observed pattern as a stable feature of symptom severity, future longitudinal studies will be required. Second, participants included in the current study were following a single type of trauma, which increased the homogeneity of the study sample. Since previous studies have suggested that different types of trauma may have different cerebral deficits (Meng et al., 2014), this leaves open the question of whether the findings observed in our study can be generalized to PTSD caused by other types of trauma. Third, since brain connectivity can be acquired from different MRI modalities (i.e., T1-weighted and diffusion tensor imaging), future work might examine structural change in relation to functional patterns. Fourth, the lack of data from an independent sample precludes us from conducting an external validation analysis, and the generalization of the current findings requires further validation using an independent sample. Fifth, some confounding factors, e.g., childhood/early stress, cannot be excluded in the analysis. Future studies may address these issues.

In summary, this study used a recently developed data-driven method to provide evidence that the resting-state brain functional connectivity can reliably and effectively predict individual PTSD clinical scores of trauma-exposed survivors. The significant contribution of visual cortex, cerebellum, limbic, and motor region connectivity to individual PTSD symptom severity indicates that more brain features beyond the triple network model of PTSD need to be considered to comprehensively understand the illness, and the traditional view that PTSD is a psychiatric disorder specific to the fronto-limbic fear circuit may require reconsideration. The current data-driven approach provides a novel tool to characterize the neural underpinning of PTSD severity and might have potential applications to inform the evaluation of subjects in a clinical setting.

## DATA AVAILABILITY STATEMENT

The datasets generated for this study are available on request to the corresponding author.

## ETHICS STATEMENT

The studies involving human participants were reviewed and approved by West China Hospital of Sichuan University. The patients/participants provided their written informed consent to participate in this study.

## AUTHOR CONTRIBUTIONS

QG contributed to conception and design of the study. XS, DL and LL organized the database. XS, DL, WL and JY performed the data preprocessing and statistical analysis.



XS wrote the manuscript. DL, WL, JS and QG edited the manuscript. All authors contributed to the article and approved the submitted version.

## FUNDING

This study was supported by the National Natural Science Foundation of China (Grant Nos. 81621003, 81820108018, and

82001800) and the China Postdoctoral Science Foundation (Grant No. 2020M683317).

## SUPPLEMENTARY MATERIAL

The Supplementary Material for this article can be found online at: <https://www.frontiersin.org/articles/10.3389/fnbeh.2020.563152/full#supplementary-material>.

## REFERENCES

- Akiki, T. J., Averill, C. L., Wrocklage, K. M., Scott, J. C., Averill, L. A., Schweinsburg, B., et al. (2018). Default mode network abnormalities in posttraumatic stress disorder: a novel network-restricted topology approach. *NeuroImage* 176, 489–498. doi: 10.1016/j.neuroimage.2018.05.005
- American Psychiatric Association. (2013). *Diagnostic and Statistical Manual of Mental Disorders*. Arlington, TX: American Psychiatric Publishing.
- Baldaçara, L., Borgio, J. G., Lacerda, A. L., and Jackowski, A. P. (2008). Cerebellum and psychiatric disorders. *Braz. J. Psychiatry* 30, 281–289. doi: 10.1590/s1516-44462008000300016
- Beaty, R. E., Kenett, Y. N., Christensen, A. P., Rosenberg, M. D., Benedek, M., Chen, Q., et al. (2018). Robust prediction of individual creative ability from brain functional connectivity. *Proc. Natl. Acad. Sci. U S A* 115, 1087–1092. doi: 10.1073/pnas.1713532115
- Belleau, E. L., Ehret, L. E., Hanson, J. L., Brasel, K. J., Larson, C. L., and deRoon-Cassini, T. A. (2020). Amygdala functional connectivity in the acute aftermath of trauma prospectively predicts severity of posttraumatic stress symptoms. *Neurobiol. Stress* 12:100217. doi: 10.1016/j.ynstr.2020.100217
- Bing, X., Ming-Guo, Q., Ye, Z., Jing-Na, Z., Min, L., Han, C., et al. (2013). Alterations in the cortical thickness and the amplitude of low-frequency fluctuation in patients with post-traumatic stress disorder. *Brain Res.* 1490, 225–232. doi: 10.1016/j.brainres.2012.10.048
- Biswal, B. B., Mennes, M., Zuo, X.-N., Gohel, S., Kelly, C., Smith, S. M., et al. (2010). Toward discovery science of human brain function. *Proc. Natl. Acad. Sci. U S A* 107, 4734–4739. doi: 10.1073/pnas.0911855107
- Blake, D. D., Weathers, F. W., Nagy, L. M., Kaloupek, D. G., Gusman, F. D., Charney, D. S., et al. (1995). The development of a clinician-administered PTSD scale. *J. Trauma. Stress* 8, 75–90. doi: 10.1007/BF02105408
- Bonne, O., Gilboa, A., Louzoun, Y., Brandes, D., Yona, I., Lester, H., et al. (2003). Resting regional cerebral perfusion in recent posttraumatic stress disorder. *Biol. Psychiatry* 54, 1077–1086. doi: 10.1016/s0006-3223(03)00525-0
- Chang, C.-C., and Lin, C.-J. (2011). LIBSVM: a library for support vector machines. *ACM Transac. Intel. Syst. Technol.* 2:27. doi: 10.1145/1961189.1961199
- Chen, Y., Fu, K., Feng, C., Tang, L., Zhang, J., Huan, Y., et al. (2012). Different regional gray matter loss in recent onset PTSD and non PTSD after a single prolonged trauma exposure. *PLoS One* 7:e48298. doi: 10.1371/journal.pone.0048298
- Dubois, J., and Adolphs, R. (2016). Building a science of individual differences from fMRI. *Trends Cogn. Sci.* 20, 425–443. doi: 10.1016/j.tics.2016.03.014
- Finn, E. S., Shen, X., Scheinost, D., Rosenberg, M. D., Huang, J., Chun, M. M., et al. (2015). Functional connectome fingerprinting: identifying individuals using patterns of brain connectivity. *Nat. Neurosci.* 18, 1664–1671. doi: 10.1038/nn.4135
- Gao, S., Greene, A. S., Constable, R. T., and Scheinost, D. (2019). Combining multiple connectomes improves predictive modeling of phenotypic measures. *NeuroImage* 201:116038. doi: 10.1016/j.neuroimage.2019.116038
- Gong, Q., Li, L., Du, M., Pettersson-Yeo, W., Crossley, N., Yang, X., et al. (2014a). Quantitative prediction of individual psychopathology in trauma survivors using resting-state FMRI. *Neuropsychopharmacology* 39, 681–687. doi: 10.1038/npp.2013.251
- Gong, Q., Li, L., Tognin, S., Wu, Q., Pettersson-Yeo, W., Lui, S., et al. (2014b). Using structural neuroanatomy to identify trauma survivors with and without post-traumatic stress disorder at the individual level. *Psychol. Med.* 44, 195–203. doi: 10.1017/S0033291713000561
- Gong, Q. (2020). *Psychoradiology, Neuroimaging Clinics of North America*, Vol. 30. New York: Elsevier Inc. 1–123.
- Grèzes, J., Valabrègue, R., Gholipour, B., and Chevallier, C. (2014). A direct amygdala-motor pathway for emotional displays to influence action: a diffusion tensor imaging study. *Hum. Brain Mapp.* 35, 5974–5983. doi: 10.1002/hbm.22598
- Huang, X., Gong, Q., Sweeney, J. A., and Biswal, B. B. (2019). Progress in psychoradiology, the clinical application of psychiatric neuroimaging. *Br. J. Radiol.* 92:20181000. doi: 10.1259/bjr.20181000
- Ke, J., Zhang, L., Qi, R., Li, W., Hou, C., Zhong, Y., et al. (2016). A longitudinal fMRI investigation in acute post-traumatic stress disorder (PTSD). *Acta Radiol.* 57, 1387–1395. doi: 10.1177/0284185115585848
- Kennis, M., van Rooij, S. J., van den Heuvel, M. P., Kahn, R. S., and Geuze, E. (2016). Functional network topology associated with posttraumatic stress disorder in veterans. *Neuroimage Clin.* 10, 302–309. doi: 10.1016/j.nicl.2015.12.008
- Lake, E. M. R., Finn, E. S., Noble, S. M., Vanderwal, T., Shen, X., Rosenberg, M. D., et al. (2019). The functional brain organization of an individual allows prediction of measures of social abilities transdiagnostically in autism and attention-deficit/hyperactivity disorder. *Biol. Psychiatry* 86, 315–326. doi: 10.1016/j.biopsych.2019.02.019
- Lanius, R. A., Bluhm, R. L., Coupland, N. J., Hegadoren, K. M., Rowe, B., Theberge, J., et al. (2010). Default mode network connectivity as a predictor of post-traumatic stress disorder symptom severity in acutely traumatized subjects. *Acta Psychiatr. Scand.* 121, 33–40. doi: 10.1111/j.1600-0447.2009.01391.x
- Lei, D., Li, K., Li, L., Chen, F., Huang, X., Lui, S., et al. (2015). Disrupted functional brain connectome in patients with posttraumatic stress disorder. *Radiology* 276, 818–827. doi: 10.1148/radiol.15141700
- Lei, D., Pinaya, W. H. L., van Amelsvoort, T., Marcelis, M., Donohoe, G., Mothersill, D. O., et al. (2020). Detecting schizophrenia at the level of the individual: relative diagnostic value of whole-brain images, connectome-wide functional connectivity and graph-based metrics. *Psychol. Med.* 50, 1852–1861. doi: 10.1017/S0033291719001934
- Leutgeb, V., Wabnegger, A., Leitner, M., Zussner, T., Scharmuller, W., Klug, D., et al. (2016). Altered cerebellar-amygdala connectivity in violent offenders: a resting-state fMRI study. *Neurosci. Lett.* 610, 160–164. doi: 10.1016/j.neulet.2015.10.063
- Lin, Q., Rosenberg, M. D., Yoo, K., Hsu, T. W., O'Connell, T. P., and Chun, M. M. (2018). Resting-state functional connectivity predicts cognitive impairment related to Alzheimer's disease. *Front. Aging Neurosci.* 10:94. doi: 10.3389/fnagi.2018.00094
- McGlade, E., Rogowska, J., DiMuzio, J., Bueler, E., Sheth, C., Legarreta, M., et al. (2020). Neurobiological evidence of sexual dimorphism in limbic circuitry of US veterans. *J. Affect. Disord.* 274, 1091–1101. doi: 10.1016/j.jad.2020.05.016
- Meng, Y., Qiu, C., Zhu, H., Lama, S., Lui, S., Gong, Q., et al. (2014). Anatomical deficits in adult posttraumatic stress disorder: a meta-analysis of voxel-based morphometry studies. *Behav. Brain Res.* 270, 307–315. doi: 10.1016/j.bbr.2014.05.021
- Neumeister, P., Feldker, K., Heitmann, C. Y., Helmich, R., Gathmann, B., Becker, M. P. I., et al. (2017). Interpersonal violence in posttraumatic women: brain networks triggered by trauma-related pictures. *Soc. Cogn. Affect. Neurosci.* 12, 555–568. doi: 10.1093/scan/nsw165



- Niu, R., Lei, D., Chen, F., Chen, Y., Suo, X., Li, L., et al. (2018). Reduced local segregation of single-subject gray matter networks in adult PTSD. *Hum. Brain Mapp.* 39, 4884–4892. doi: 10.1002/hbm.24330
- Osuch, E. A., Benson, B., Geraci, M., Podell, D., Herscovitch, P., McCann, U. D., et al. (2001). Regional cerebral blood flow correlated with flashback intensity in patients with posttraumatic stress disorder. *Biol. Psychiatry* 50, 246–253. doi: 10.1016/s0006-3223(01)01107-6
- Pantazatos, S. P., Talati, A., Pavlidis, P., and Hirsch, J. (2012). Cortical functional connectivity decodes subconscious, task-irrelevant threat-related emotion processing. *NeuroImage* 61, 1355–1363. doi: 10.1016/j.neuroimage.2012.03.051
- Patel, R., Spreng, R. N., Shin, L. M., and Girard, T. A. (2012). Neurocircuitry models of posttraumatic stress disorder and beyond: a meta-analysis of functional neuroimaging studies. *Neurosci. Biobehav. Rev.* 36, 2130–2142. doi: 10.1016/j.neubiorev.2012.06.003
- Rabellino, D., Densmore, M., Theberge, J., McKinnon, M. C., and Lanius, R. A. (2018). The cerebellum after trauma: resting-state functional connectivity of the cerebellum in posttraumatic stress disorder and its dissociative subtype. *Hum. Brain Mapp.* 39, 3354–3374. doi: 10.1002/hbm.24081
- Rauch, S. L., Shin, L. M., and Phelps, E. A. (2006). Neurocircuitry models of posttraumatic stress disorder and extinction: human neuroimaging research—past, present, and future. *Biol. Psychiatry* 60, 376–382. doi: 10.1016/j.biopsych.2006.06.004
- Rosenberg, M. D., Casey, B. J., and Holmes, A. J. (2018). Prediction complements explanation in understanding the developing brain. *Nat. Commun.* 9:589. doi: 10.1038/s41467-018-02887-9
- Rosenberg, M. D., Finn, E. S., Scheinost, D., Papademetris, X., Shen, X., Constable, R. T., et al. (2016). A neuromarker of sustained attention from whole-brain functional connectivity. *Nat. Neurosci.* 19, 165–171. doi: 10.1038/nn.4179
- Sacchetti, B., Baldi, E., Lorenzini, C. A., and Bucherelli, C. (2002). Cerebellar role in fear-conditioning consolidation. *Proc. Natl. Acad. Sci. U S A* 99, 8406–8411. doi: 10.1073/pnas.112660399
- Schmahmann, J. D., and Caplan, D. (2006). Cognition, emotion and the cerebellum. *Brain* 129, 290–292. doi: 10.1093/brain/awh729
- Shen, X., Finn, E. S., Scheinost, D., Rosenberg, M. D., Chun, M. M., Papademetris, X., et al. (2017). Using connectome-based predictive modeling to predict individual behavior from brain connectivity. *Nat. Protoc.* 12, 506–518. doi: 10.1038/nprot.2016.178
- Shen, X., Tokoglu, F., Papademetris, X., and Constable, R. T. (2013). Groupwise whole-brain parcellation from resting-state fMRI data for network node identification. *NeuroImage* 82, 403–415. doi: 10.1016/j.neuroimage.2013.05.081
- Sun, H., Chen, Y., Huang, Q., Lui, S., Huang, X., Shi, Y., et al. (2018). Psychoradiologic Utility of MR imaging for diagnosis of Attention Deficit Hyperactivity Disorder: a radiomics analysis. *Radiology* 287, 620–630. doi: 10.1148/radiol.2017170226
- Thome, J., Densmore, M., Frewen, P. A., McKinnon, M. C., Theberge, J., Nicholson, A. A., et al. (2017). Desynchronization of autonomic response and central autonomic network connectivity in posttraumatic stress disorder. *Hum. Brain Mapp.* 38, 27–40. doi: 10.1002/hbm.23340
- Tursich, M., Ros, T., Frewen, P. A., Klutsch, R. C., Calhoun, V. D., and Lanius, R. A. (2015). Distinct intrinsic network connectivity patterns of post-traumatic stress disorder symptom clusters. *Acta Psychiatr. Scand.* 132, 29–38. doi: 10.1111/acps.12387
- Tzourio-Mazoyer, N., Landeau, B., Papathanassiou, D., Crivello, F., Etard, O., Delcroix, N., et al. (2002). Automated anatomical labeling of activations in SPM using a macroscopic anatomical parcellation of the MNI MRI single-subject brain. *NeuroImage* 15, 273–289. doi: 10.1006/nimg.2001.0978
- Wang, J., Wang, X., Xia, M., Liao, X., Evans, A., and He, Y. (2015). GREYNA: a graph theoretical network analysis toolbox for imaging connectomics. *Front. Hum. Neurosci.* 9:386. doi: 10.3389/fnhum.2015.00386
- Weathers, F. W., Keane, T. M., and Davidson, J. R. (2001). Clinician-administered PTSD scale: a review of the first ten years of research. *Depress. Anxiety* 13, 132–156. doi: 10.1002/da.1029
- Yang, P., Wu, M.-T., Hsu, C.-C., and Ker, J.-H. (2004). Evidence of early neurobiological alternations in adolescents with posttraumatic stress disorder: a functional MRI study. *Neurosci. Lett.* 370, 13–18. doi: 10.1016/j.neulet.2004.07.033
- Yehuda, R., and Flory, J. D. (2007). Differentiating biological correlates of risk, PTSD, and resilience following trauma exposure. *J. Trauma. Stress* 20, 435–447. doi: 10.1002/jts.20260
- Yip, S. W., Scheinost, D., Potenza, M. N., and Carroll, K. M. (2019). Connectome-based prediction of cocaine abstinence. *Am. J. Psychiatry* 176, 156–164. doi: 10.1176/appi.ajp.2018.17101147
- Zandvakili, A., Barredo, J., Swearingen, H. R., Aiken, E. M., Berlow, Y. A., Greenberg, B. D., et al. (2020). Mapping PTSD symptoms to brain networks: a machine learning study. *Transl. Psychiatry* 10:195. doi: 10.1038/s41398-020-00879-2
- Zhou, Y., Wang, Z., Qin, L. D., Wan, J. Q., Sun, Y. W., Su, S. S., et al. (2012). Early altered resting-state functional connectivity predicts the severity of post-traumatic stress disorder symptoms in acutely traumatized subjects. *PLoS One* 7:e46833. doi: 10.1371/journal.pone.0046833
- Zhu, H., Qiu, C., Meng, Y., Cui, H., Zhang, Y., Huang, X., et al. (2015). Altered spontaneous neuronal activity in chronic posttraumatic stress disorder patients before and after a 12-week paroxetine treatment. *J. Affect. Disord.* 174, 257–264. doi: 10.1016/j.jad.2014.11.053
- Zhu, H., Yuan, M., Qiu, C., Ren, Z., Li, Y., Wang, J., et al. (2020). Multivariate classification of earthquake survivors with post-traumatic stress disorder based on large-scale brain networks. *Acta Psychiatr. Scand.* 141, 285–298. doi: 10.1111/acps.13150
- Zhu, H., Zhang, J., Zhan, W., Qiu, C., Wu, R., Meng, Y., et al. (2014). Altered spontaneous neuronal activity of visual cortex and medial anterior cingulate cortex in treatment-naïve posttraumatic stress disorder. *Compr. Psychiatry* 55, 1688–1695. doi: 10.1016/j.comppsy.2014.06.009

**Conflict of Interest:** JS is a consultant for VersSci.

The remaining authors declare that the research was conducted in the absence of any commercial or financial relationships that could be construed as a potential conflict of interest.

Copyright © 2020 Suo, Lei, Li, Yang, Li, Sweeney and Gong. This is an open-access article distributed under the terms of the Creative Commons Attribution License (CC BY). The use, distribution or reproduction in other forums is permitted, provided the original author(s) and the copyright owner(s) are credited and that the original publication in this journal is cited, in accordance with accepted academic practice. No use, distribution or reproduction is permitted which does not comply with these terms.



# Placebo Effects in the Context of Religious Beliefs and Practices: A Resting-State Functional Connectivity Study

Anne Schienle\*, Andreas Gremsl and Albert Wabnegger

Department of Clinical Psychology, University of Graz, BioTechMed, Graz, Austria

## OPEN ACCESS

### Edited by:

João J. Cerqueira,  
University of Minho, Portugal

### Reviewed by:

Jeffrey C. Glennon,  
University College Dublin, Ireland  
Alessandro Grecucci,  
University of Trento, Italy

### \*Correspondence:

Anne Schienle  
anne.schienle@uni-graz.at

### Specialty section:

This article was submitted to  
Emotion Regulation and Processing,  
a section of the journal  
Frontiers in Behavioral Neuroscience

**Received:** 18 January 2021

**Accepted:** 14 April 2021

**Published:** 06 May 2021

### Citation:

Schienle A, Gremsl A and  
Wabnegger A (2021) Placebo Effects  
in the Context of Religious Beliefs  
and Practices: A Resting-State  
Functional Connectivity Study.  
Front. Behav. Neurosci. 15:653359.  
doi: 10.3389/fnbeh.2021.653359

**Background:** Placebos (inert substances or procedures) can positively influence a person's psychological and physical well-being, which is accompanied by specific changes in brain activity. There are many different types of placebos with different effects on health-related variables. This study investigated placebo effects in the context of religious beliefs and practices. The participants received an inert substance (tap water) along with the verbal suggestion that the water would come from the sanctuary in Lourdes (a major Catholic pilgrimage site with reports of miracle cures). We investigated changes in resting-state functional connectivity (rsFC) in three brain networks (default-mode, salience, cognitive control) associated with the drinking of the placebo water.

**Methods:** A total of 37 females with the belief that water from the sanctuary in Lourdes has positive effects on their spiritual, emotional, and physical well-being participated in this placebo study with two sessions. The participants drank tap water that was labeled "Lourdes water" (placebo) before a 15-min resting-state scan in one session. In the other (control) session, they received tap water labeled as tap water. The participants rated their affective state (valence, arousal) during the session and were interviewed concerning specific thoughts, feelings, and bodily sensations directly after each of the two sessions.

**Results:** The placebo reduced rsFC in the frontoparietal cognitive control network and increased rsFC in the salience network (insular-cerebellar connectivity). During the session, the participants rated their affective state as very pleasant and calm. The ratings did not differ between the two conditions. Immediately after the session, the participants reported increased intensity of pleasant bodily sensations (e.g., feelings of warmth, tingling) and feelings (e.g., gratefulness) for the "Lourdes water" condition.

**Conclusions:** The present findings provide the first evidence that placebos in the context of religious beliefs and practices can change the experience of emotional salience and cognitive control which is accompanied by connectivity changes in the associated brain networks.

**Keywords:** resting-state functional connectivity, religious belief, fronto-parietal cognitive control network, salience network, placebo

## INTRODUCTION

A placebo is defined as “a substance or procedure ... that is objectively without specific activity for the condition being treated” (Moerman and Jonas, 2002). The most common paradigm for assessing placebo effects (“placebo analgesia”) uses an inert intervention (e.g., a capsule filled with sugar, sham acupuncture, sham surgery) which is combined with the verbal suggestion of a pain-reducing treatment. Several studies have demonstrated that this approach leads to a reduction in experienced pain as well as altered brain activity in pain-sensitive regions and prefrontal cognitive control areas (for a summary see Wager and Atlas, 2015). Placebos have also been used in other areas. Placebo treatment can reduce the intensity of negative affective states (e.g., anxiety, disgust), which is accompanied by changes in brain activity in regions involved in the encoding of affective salience (e.g., insula, anterior cingulate cortex; Petrovic et al., 2005; Schienle et al., 2014). Moreover, placebos have been successfully administered to improve physical well-being and sports performance (Beedie and Foad, 2009), emotional and social well-being (e.g., interpersonal trust; Yan et al., 2018). Thus, research shows that there is not one single placebo effect, but many (Benedetti, 2014).

Another very important area of placebo application involves the treatment of illness. Placebo-induced symptom reduction has been reported for several diseases and mental disorders, such as Parkinson’s disease, depression, attention-deficit hyperactivity disorder, and binge-eating disorder (De la Fuente-Fernández and Stoessl, 2002; Weimer et al., 2015). Illness typically involves psychological aspects; patients not only sense somatic signs of illness, but they interpret these signs. Interpretations, such as cognitions of danger or loss (e.g., the threat of dying, loss of health) produce anxiety or depressed mood. A placebo counteracts these negative interpretations (Lundh, 1987). Patients who believe that a placebo is going to improve their health condition will experience reduced stress and anxiety; and these processes are accompanied by specific neurobiological processes (e.g., altered activation in cognitive control areas of the brain (Benedetti, 2014).

The present investigation focused on a specific placebo in the context of religious beliefs and practices. The participants received an inert substance (tap water), which was administered with the verbal suggestion that it is water from the sanctuary in Lourdes (a major Catholic pilgrimage site in France). Many Roman Catholics believe that Lourdes water has supernatural healing powers and the Medical Bureau of Lourdes has been recorded more than 7,000 reports of cured diseases<sup>1</sup> (December, 9th, 2020).

Geochemical analyses of the water from different springs in the Lourdes area have shown that the water contains little total dissolved solids, has a slightly alkaline pH level (7.50–7.68), and oxidizing conditions, all of which are typical characteristics of a hydrogeological system that developed in carbonate-dominated bedrock (Dobrzyński and Rossi, 2017). There are no “special”

ingredients in the water. Therefore, it does not seem to be the water in itself that has a positive effect, but the belief in it.

Placebo effects require that the treated person believes that a specific treatment or procedure will work. It has been shown that the expectancy and the desire for improvement are positively correlated with the magnitude of the placebo effect (e.g., Enck et al., 2008). Thus, what we believe we will experience from a treatment has a substantial impact on what we experience. Moreover, spirituality is associated with placebo responsiveness. Hyland et al. (2006) showed that spirituality predicted perceived improvement of individual problems, such as unexplained fears and worries, after placebo (flower essence) treatment independently of expectancy.

In the present study, we focused on resting-state functional connectivity (rsFC), which is widely used in neuroscience research to investigate intrinsic neural circuits and their functional states (for a summary see Uddin et al., 2019). The term “resting state” refers to a state in which the individual is awake (lying quietly with eyes closed) and does not perform a specific experimental task (Raichle et al., 2001). Several large-scale functional brain networks have been identified during resting states, such as the default-mode network (involved in self-referential processing, mentalizing), the salience network (involved in detecting/integrating interoceptive, autonomic, and emotional information), and the frontoparietal cognitive control network (involved in the deliberate selection of thoughts, emotions, and behaviors; for a description of the networks see Marek and Dosenbach, 2018; Uddin et al., 2019). For example, it has been shown that religiously inspired techniques, such as mindfulness meditation can increase rsFC in the default-mode network between the posterior cingulate cortex and the dorsolateral prefrontal cortex (Creswell et al., 2016).

To the best of our knowledge, this is the first study to explore the effects of (Christian) religious belief on rsFC in different functional networks (cognitive control, salience, default-mode). We focused on these networks because previous neuroimaging research has indicated that placebo responding as well as religious/spiritual experiences are linked to the structure and function of neural components of these networks (e.g., prefrontal cortex, insula, superior/posterior parietal regions; e.g., Wiech et al., 2008; Schjoedt et al., 2009; McClintock et al., 2019; Schienle et al., 2019). The mentioned brain areas are involved in emotion regulation, attention control, and self-awareness (Tang et al., 2015). For example, in the study by Wiech et al. (2008), practicing Catholics and non-religious participants received noxious stimulation while they were either presented with an image of the Virgin Mary or a portrait without religious connotation. The religious group perceived less pain while looking at the religious image, which was associated with increased activation in the ventrolateral prefrontal cortex. This area plays a central role in pain modulation *via* reappraisal.

In the present study, females who believed in the miracles of Lourdes drank tap water directly before two resting-state scans separated by approximately 1 week. The water was labeled “water from the sanctuary of Lourdes” in one condition (placebo), and “tap water” in another condition (control). It was tested, whether the placebo would change reported well-being (emotional,

<sup>1</sup><https://www.lourdes-france.org/en/miraculous-healings/retrieved>

cognitive, bodily) and rsFC in brain networks (cognitive control, salience, default-mode) compared to the control condition.

## MATERIALS AND METHODS

### Sample

A total of 37 females (mean age:  $M = 30.59$  years,  $SD = 13.8$ ) participated in this study. To reduce sex-related variance in resting-state functional connectivity (e.g., Weis et al., 2020), and religious well-being (Unterrainer et al., 2010) the sample was restricted to females. They had been selected based on their answers in an internet-based survey that contained the following questions: (a) Do you think that water from the sanctuary in Lourdes can have positive (spiritual, emotional, somatic) effects?; (b) Would you use Lourdes water if you had a serious illness?; and (c) Do you believe in miracles in a religious/spiritual sense? The questions were answered on Likert scales ranging from 0 = “no” to 6 = “definitely.” The inclusion criterion for the study was an average “Lourdes score”  $>3$  ( $M = 3.76$ ,  $SD = 1.1$ ). The Lourdes score had sufficient reliability (McDonald’s omega = 0.75).

All of the participants had a highschool diploma; 76% were University students and the remaining participants were white-collar workers. The religious affiliation of the majority of participants was Roman-Catholic (73%), while others stated to be Protestants (6%), or not religiously affiliated (21%). None of the participants reported a current serious somatic illness (e.g., cancer, neurological disease) or mental disorder.

### Stimuli and Design

The study had a repeated-measures design. The participants were scanned twice and received a glass of tap water (60 ml) labeled as water from the sanctuary in Lourdes (placebo) in one session and tap water labeled as tap water in the other session (control). The sequence of the sessions was counterbalanced.

### Procedure

We invited the participants to two functional magnetic resonance imaging (fMRI) sessions, which were scheduled 1 week apart from each other. In the placebo condition, the participants first obtained written information (one sheet) describing the religious visions of Saint Bernadette of Lourdes. In the control condition, the sheet provided basic knowledge about fMRI. The information in the two conditions was also summarized as a poster on the wall of the room, where the instruction took place. Subsequently (directly before the MRI recording), the water was served. The water was poured out of a little bottle into the glass. The label of the bottle either stated “Sanctuary of Lourdes” or “tap water.”

The fMRI session started with the resting-state measurement. The experimenter who conducted the scanning was not aware of the condition. The participants were instructed “Close your eyes and let your thoughts wander freely.” Directly after the 15-min resting-state scan, the participants rated their experience on two basic affective dimensions, valence, and arousal, on 9-point Likert scales (9 = very pleasant, aroused). Afterward, a structural scan was obtained (duration: 4.5 min). Following the MRI session, the participants were asked by the experimenter to report specific thoughts, feelings, and somatic sensations experienced

during the MRI recording. Each reported symptom was rated on a 9-point Likert scale according to experienced intensity (9 = very intense). The participants also rated the “overall effects of the water” on a 9-point scale (9 = very strong) and were invited to give open comments.

Finally, the participants completed the scale “general religiosity” of the multidimensional instrument for the measurement of religious-spiritual well-being (MI-RSWB 48 by Unterrainer et al., 2010). The scale contains eight statements (e.g., My faith gives me a feeling of security; Cronbach’s alpha = 0.94), which are answered on a 6-point Likert scale ranging from 1 = “strongly disagree” to 6 = “strongly agree.”

All participants received detailed instructions before data collection. The study protocol was approved by the ethics committee of the University (GZ: 39/19/63 ex 2018/19). Following their study involvement, all participants were fully debriefed and received written information about the aim of the study, the procedure (placebo approach), and the main findings of the experiment. We also offered the option of personal communication with the experimenter.

### MRI Recording and Analysis

The MRI session was conducted with a 3T scanner (Skyra, Siemens, Erlangen, Germany) with a 32-channel head coil. In both sessions (“Lourdes water”, Tap water) structural images were recorded using a T1-weighted MPAGE sequence with following settings: TR = 1.680 s; TE = 0.00188 s; acquisition matrix = 256; flip angle = 8°; 192 transverse slices; FoV = 224 mm; slice thickness = 0.88 mm; fat suppression: water excit. fast; acquisition time = 4.29 s). Functional images were acquired using a CMRR-multiband<sup>2</sup> with following settings: sequence type = epfid, acceleration factor = 3; TR = 1.4 s; TE = 0.0304 s; flip angle = 72 degrees; slice thickness = 3 mm; total readout time = 0.046 s; spacing between slices: 3 mm; acquisition matrix = 80; phase encoding direction: anterior-posterior; number of volumes = 650).

Resting-state analyses were carried out by using the CONN toolbox (version 18.b<sup>3</sup>, RRID:SCR\_009550; Whitfield-Gabrieli and Nieto-Castanon, 2012) and SPM12<sup>4</sup> (version 7487) implemented in Matlab (2017b). Preprocessing followed the default pipeline suggested by the CONN toolbox (realignment, slice-timing, normalization, and spatial smoothing with an 8 mm Gaussian kernel to ameliorate individual anatomical differences). The final voxel size was 3 mm isotropic. The subsequent component-based noise-reduction approach (CompCor) included 15 dimensions of white matter and cerebrospinal fluid, as well as 12 realignment parameters (including 1st-order derivatives). Scrubbing controlled for additional motion-related variance. Finally, a bandpass filter (0.0–10.1 Hz) was applied.

### Statistical Analysis

#### Self-report

We used paired *t*-tests to compare the effects of Condition (PLACEBO: “Lourdes water” vs. CONTROL: Tap water) on the

<sup>2</sup><https://www.cmrr.umn.edu/multiband/>

<sup>3</sup>[www.nitrc.org/projects/conn](http://www.nitrc.org/projects/conn)

<sup>4</sup><https://www.fil.ion.ucl.ac.uk/spm/software/spm12/>



ratings reported in the scanner (arousal, pleasure) and outside of the scanner (intensity of experienced emotions, thoughts, bodily sensations, perceived effectiveness of the treatment). Additionally, we computed Pearson correlations between questionnaire scores (general religiosity, the perceived overall effect of the “Lourdes water”). We used the Bonferroni-Holm correction for multiple comparisons (Holm, 1979).

### fMRI Data

We computed weighted GLM bivariate region of interest (ROI) correlations between 29 network ROIs provided by the CONN toolbox. The labeling of each ROI can be found in the supplementary material. The ROIs are based on the analysis of the human connectome project (HCP) dataset with 497 subjects. In the second-level analysis step, we investigated the contrast PLACEBO—CONTROL. Age was introduced as a covariate because of the substantial age range (18–58 years). Moreover, we computed exploratory correlation analyses between resting-state connectivity and difference scores of self-reports (e.g., the intensity of bodily sensations in the placebo condition minus bodily sensations in the control condition). We used false-discovery rate (FDR) seed-level correction provided by the CONN-toolbox, that corrects across multiple target areas. Results were considered statistically significant if  $p_{(FDR)} < 0.05$ .

## RESULTS

### Self-reports

#### Ratings in the Scanner

The conditions (PLACEBO: “Lourdes water” vs. CONTROL: Tap water) did not differ concerning reported valence and arousal (see **Table 1**). The participants experienced their affective state as very pleasant ( $M = 6.56$ ,  $SD = 1.36$ ) and calm ( $M = 2.63$ ,  $SD = 1.45$ ) across both conditions.

#### Ratings Outside of the Scanner

The participants rated the water as more effective in the placebo condition than in the control condition ( $p = 0.001$ ). The perceived intensity of bodily sensations and feelings was higher after the application of “Lourdes water” compared to tap water labeled as such ( $ps < 0.015$ ). The intensity of thoughts did not differ between the conditions (**Table 1**). The reported bodily sensations involved skin sensations (tingling), feeling of warmth, and “bodily relaxation” (mentioned by  $n = 25$  participants; 68%). Thoughts mainly involved other people (friends, partners),

daily duties, and past experiences (e.g., movies, parties). Specific emotions that were reported included happiness, satisfaction, gratefulness, anxiety, and nervousness. Negative emotions were predominantly reported in the control condition (CONTROL vs. PLACEBO; nervousness: 8 vs.1; anxiety: 5 vs. 0).

### Open Comments

Of the participants, 32% ( $n = 12$ ) reported a specific taste of the “Lourdes water” (e.g., “tastes like spring water”, “tastes fresher than tap water”). Twelve participants stated that they experienced a different time perception in the “Lourdes water” condition compared to the tap water condition (“Time went by faster”). One participant reported a considerable symptom reduction concerning her chronic obstructive pulmonary disease after the “Lourdes water” condition (reduced breathing problems). Nine participants (24%) reported a religious experience during the “Lourdes water” condition, such as mental images of Jesus at the cross, the grotto of Lourdes, or Saint Bernadette.

### Exploratory Correlation Analyses

The mean score on the general religiosity scale (MI-RSWB 48 by Unterrainer et al., 2010) was  $M = 3.65$  ( $SD = 1.40$ ). This score was positively correlated with the “overall effect” of the “Lourdes water” ( $r = 0.524$ ,  $p = 0.001$ ). Additionally, the “Lourdes score” (belief in the healing power of Lourdes water) was positively correlated with “general religiosity” ( $r = 0.496$ ,  $p = 0.002$ ), the intensity of reported feelings in the “Lourdes water” condition ( $r = 0.425$ ,  $p = 0.009$ ), and with the estimated “overall effect” of the “Lourdes water” ( $r = 0.354$ ,  $p = 0.031$ ).

### Resting-State Functional Connectivity

The findings of the rsFC analysis are displayed in **Table 2** and **Figure 1**. The placebo condition (compared to the control condition) was associated with reduced rsFC between the posterior parietal cortex (PPC) and the lateral prefrontal cortex (LPFC) as well as the inferior frontal gyrus (IFG). Moreover, reduced rsFC was observed between the cerebellum and the LPFC.

Increased rsFC during the “Lourdes water” condition (compared to control) characterized the anterior insula and the cerebellum.

### Exploratory Analyses

To follow up on the finding that “Lourdes water” increased the intensity of pleasant bodily sensations and feelings, we

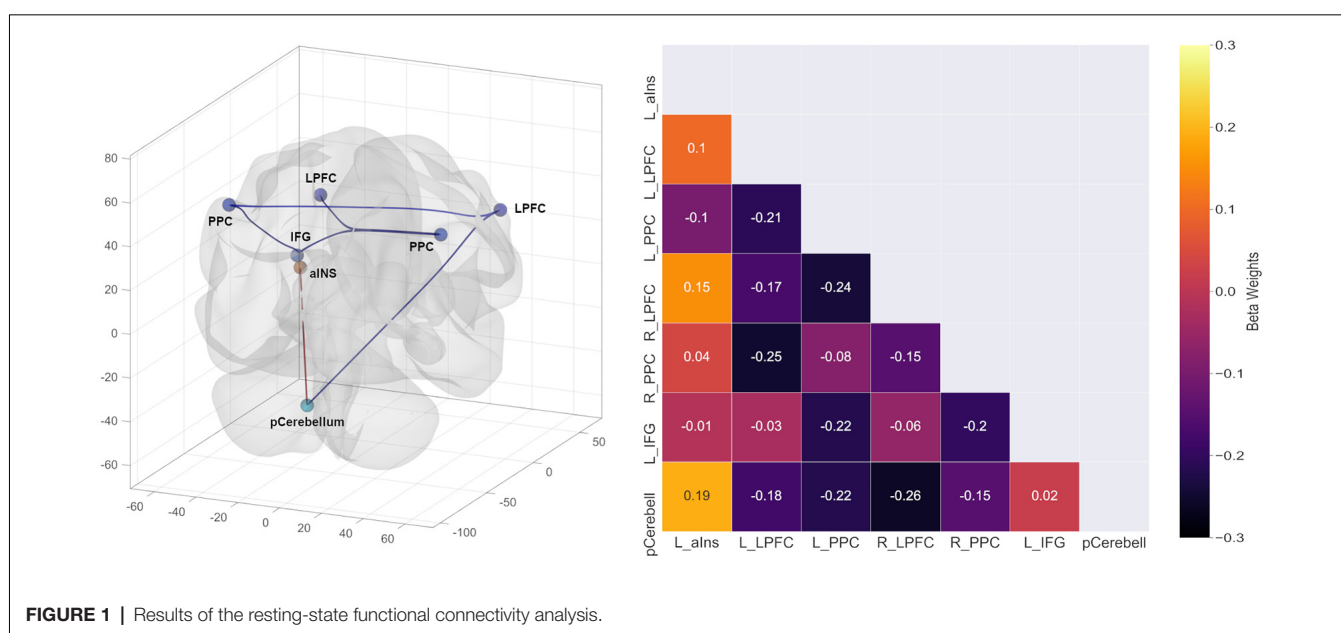
**TABLE 1 |** Self-reports for the conditions with “Lourdes water” suggestion vs. “tap water” suggestion.

	PLACEBO: “Lourdes water” M (SD) [95% BCa CI]	CONTROL: “tap water” M (SD) [95% BCa CI]	T <sub>36</sub> (p)	Cohen's d
<b>Inside-scanner ratings (1..9)</b>				
Pleasantness	6.81 (1.57) [6.24–7.32]	6.31 (1.86) [5.62–6.96]	1.42 (0.165)	0.23
Arousal	2.54 (1.71) [2.06–3.11]	2.72 (1.87) [2.19–3.28]	0.51 (0.617)	0.08
<b>Outside-scanner ratings (intensity 1..9)</b>				
Thoughts	5.09 (2.11) [4.29–5.76]	4.89 (1.97) [4.26–5.57]	0.53 (0.599)	0.09
Feelings	6.15 (1.96) [5.28–6.76]	4.99 (2.16) [4.17–5.92]	2.90 (0.006)	0.48
Bodily sensations	4.47 (2.19) [3.59–5.27]	3.30 (1.58) [2.37–3.84]	2.58 (0.014)	0.42
Estimated overall effect of the water	4.35 (2.38) [3.62–5.09]	1.89 (1.33) [1.46–2.44]	6.60 (0.001)	1.09

**TABLE 2** | Results of the resting-state functional connectivity analysis.

ROI (seed)	ROI	<i>t</i>	<i>p</i> (FDR)
<b>CONTROL (“Tap water”)–PLACEBO (“Lourdes water”)</b>			
Posterior parietal cortex (l)	Inferior frontal gyrus (l)	−4.28	0.004
Posterior parietal cortex (l)	Lateral prefrontal cortex (r)	−3.50	0.018
Posterior parietal cortex (r)	Inferior frontal gyrus (l)	−3.27	0.049
Posterior parietal cortex (r)	Lateral prefrontal cortex (l)	−3.13	0.049
Lateral prefrontal cortex (r)	Posterior parietal cortex (l)	−3.50	0.037
Lateral prefrontal cortex (r)	Posterior cerebellum	−3.24	0.037
Inferior frontal gyrus (l)	Posterior parietal cortex (l)	−4.28	0.004
Inferior frontal gyrus (l)	Posterior parietal cortex (r)	−3.27	0.034
Posterior cerebellum (r)	Lateral prefrontal cortex (r)	−3.24	0.044
<b>PLACEBO (“Lourdes water”)–CONTROL (“Tap water”)</b>			
Posterior cerebellum (r)	Anterior insula (l)	3.17	0.044

ROI, region of interest; l/r: left/right; FDR, false discovery rate.

**FIGURE 1** | Results of the resting-state functional connectivity analysis.

correlated rsFC with the difference scores for the ratings in the two conditions (PLACEBO minus CONTROL). Changes in bodily sensations were positively correlated with rsFC between occipital and inferior frontal regions, and negatively with rsFC between inferior frontal regions and temporal/parietal regions (Table 3). Changes in the intensity of feelings were not correlated with rsFC.

Additionally, we compared participants with Roman-Catholic affiliation ( $n = 27$ ) and other affiliations ( $n = 10$ ) with each other concerning resting-state connectivity and questionnaire/rating data. Roman-Catholics reported greater general religiosity on the MI-RSWB 48 (Unterrainer et al., 2010;  $M = 3.94$ ,  $SD = 1.32$ ) compared to participants who were not Roman-Catholic ( $M = 2.88$ ,  $SD = 1.40$ ;  $t_{(35)} = 2.15$ ,  $p = 0.039$ ). All other variables (ratings and resting-state) did not reveal statistically significant group differences ( $p > 0.05$ ).

## DISCUSSION

This resting-state functional connectivity (rsFC) study examined a specific placebo. The participants received an inert substance (tap water) along with the verbal suggestion that they would drink water from the sanctuary in Lourdes. Compared to drinking tap water labeled as such, “Lourdes water” changed the strength of temporal correlations between specific brain sites, including both increased as well as decreased connectivity.

The placebo increased the connectivity between the anterior insula and the posterior cerebellum. Both regions are part of the salience network (e.g., Habas et al., 2009; Uddin, 2015). The salience network is involved in detecting, integrating, and filtering interoceptive, autonomic, and emotional information. The label “salience” is applied to this network for its broad role in identifying

**TABLE 3** | Association between resting-state functional connectivity and experienced bodily changes (“PLACEBO: Lourdes water”–“CONTROL: Tap water”).

ROI (seed)	ROI	<i>t</i>	<i>p</i> (FDR)
Occipital cortex (l)	Inferior frontal gyrus (l)	3.79	0.017
Inferior frontal gyrus (l)	Occipital cortex (l)	3.79	0.015
Superior temporal gyrus (r)	Inferior frontal gyrus (r)	−3.77	0.015
Superior temporal gyrus (r)	Inferior frontal gyrus (l)	−3.59	0.015
Superior temporal gyrus (l)	Supramarginal gyrus (r)	−3.48	0.039
Supramarginal gyrus (r)	Superior temporal gyrus posterior (l)	−3.48	0.039
Inferior frontal gyrus (r)	Inferior frontal gyrus (l)	−3.59	0.015
Inferior frontal gyrus (r)	Superior temporal gyrus posterior (r)	−3.77	0.017
Inferior frontal gyrus (l)	Superior temporal gyrus posterior (r)	−3.59	0.015

Note: experienced bodily changes: intensity of bodily sensation in the Lourdes water condition minus intensity of bodily sensation in the Tap water condition; ROI, region of interest; l/r, (left, right); negative/positive *t*-score indicates the direction of correlation; FDR, false discovery rate.

(subjectively) important, or salient, information. It has been shown that the salience network with the insula as a central hub mediates placebo effects in different areas (e.g., placebo analgesia, reduction of negative affect; Schienle et al., 2014; Wager and Atlas, 2015). The insular cortex can integrate and transform information about salience into perceptual decisions. This brain region links emotional/motivational/decision processes, which is central for placebo responding (Wager and Atlas, 2015). Moreover, the role of the insula in spiritual experience has been identified before (Hölzel et al., 2008; Haase et al., 2016). An fMRI study by Haase et al. (2016) showed that religiously inspired training (20-h mindfulness training) altered insula activation to a stressor (loaded breathing).

In line with the observed changes in rsFC within the salience network (insula-cerebellum connectivity), the “Lourdes water” application increased the intensity of experienced positive feelings (e.g., gratefulness) and bodily sensations. Many participants experienced tingling and warming, which they interpreted as signs of “bodily relaxation.” On the one hand, it is well-known that tingling and warming are associated with autonomic relaxation (i.e., an increase in parasympathetic activity and a decrease in sympathetic activity). These sensations are typically experienced by individuals who practice relaxation training. On the other hand, focusing one’s attention on a body part can give rise to various “spontaneous sensations” without external stimulation. These attention-related sensations strongly depend on expectations and prior information (Tihanyi et al., 2018). In the present study, the “Lourdes water” suggestion implied possible somatic changes since water from the sanctuary has been linked with the healing of somatic illness.

It is noteworthy, that the placebo-induced change in the bodily state was correlated with frontoparietal rsFC. The connectivity within this network was generally reduced through the placebo. More specifically, the coupling of the IFG and the lateral prefrontal cortex (LPFC) with the PPC was lowered. The mentioned regions are part of a frontoparietal cognitive control network (e.g., Dosenbach et al., 2008; Dixon et al., 2018; Marek and Dosenbach, 2018). Cognitive control refers to the deliberate selection of thoughts, emotions, and behaviors based on current task demands and social context,

as well as inhibition of inappropriate actions (Miller and Cohen, 2001). An influential model suggests that the lateral prefrontal cortex (LPFC) represents rules or instructions in working memory. This information guides perceptual and motor processing in parietal regions, thus resulting in action selection or inhibition (Miller and Cohen, 2001). The LPFC represents relationships between contexts, task rules, and anticipated outcomes (Dixon et al., 2018). The mentioned functions are central for placebo responding, which typically involves the LPFC (e.g., Wager et al., 2004; Petrovic et al., 2010). Placebos only work if the recipients believe in the effectiveness of the treatment. The belief is associated with anticipation and positive outcome expectations, which are represented in the LPFC.

Functional brain imaging studies with a localization approach have detected associations between neural activation in lateral prefrontal regions (Wiech et al., 2008), the IFG (Kapogiannis et al., 2009), superior/posterior parietal regions (Kapogiannis et al., 2009), and religious/spiritual experiences. In the study by Kapogiannis et al. (2009), the participants indicated whether they agreed to religious statements (e.g., addressing God’s involvement in the world) or not. In a reanalysis of the data set, the authors (Kapogiannis et al., 2014) focused on effective connectivity (causal binding) between specific brain regions. They identified a pathway from the IFG to the superior medial frontal gyrus, and the precuneus when the participants were thinking about God’s level of involvement. Thus, the placebo intervention of the present investigation affected the connectivity of those brain areas involved in both, placebo responding and spiritual experience.

This study has several limitations that merit consideration. First, we only studied females. Therefore, the results cannot be generalized to males. Second, the time for recording rsFC was relatively short. The reliability of resting-state correlations can be increased with longer periods of data acquisition (~45 min) (Marek and Dosenbach, 2018). Third, we investigated a sample of healthy individuals. The placebo effects on rsFC can be possibly enhanced by studying a sample with a greater need for positive effects of “Lourdes water” (e.g., patients with various illnesses). However, this approach has ethical issues.

The present study differs from previous placebo research regarding the use of verbal suggestions. Typical instructions

in placebo studies involve a clear statement of the expected effect (e.g., “this pill will reduce your pain”). In contrast, in the present investigation, each participant had to create her own “instruction” based on her concept about Lourdes water effects. Some authors have pointed out that when individuals report their experience through concepts and beliefs, they significantly distort their direct experience (Pashko, 2013). They report opinions instead of direct experience. This might also explain, why rating differences between the placebo and control conditions were more pronounced when interpreting the experience after the session instead of during the session.

In summary, the findings of the present study allow us to draw preliminary conclusions about the placebo effect in the context of religious beliefs and practices. We found that this type of placebo can enhance emotional-somatic well-being, and can lead to changes in rsFC in cognitive control/emotional salience networks of the brain. Future research is warranted to replicate the results. Moreover, future research should investigate whether the observed effects generalize across different religious affiliations. The idea of “holy water” (or blessed water) is common in several religions, from Christianity, Islam, Buddhism to Sikhism.

## REFERENCES

- Beedie, J., and Foad, A. J. (2009). The placebo effect in sports performance. A brief review. *Sports Med.* 39, 313–329. doi: 10.2165/00007256-200939040-00004
- Benedetti, F. (2014). Placebo effects: from the neurobiological paradigm to translational implications. *Neuron* 84, 623–637. doi: 10.1016/j.neuron.2014.10.023
- Creswell, J. D., Taren, A. A., Lindsay, E. K., Greco, C. M., Gianaros, P. J., Fairgrieve, A., et al. (2016). Alterations in resting-state functional connectivity link mindfulness meditation with reduced interleukin-6: a randomized controlled trial. *Biol. Psychiatry* 80, 53–61. doi: 10.1016/j.biopsych.2016.01.008
- De la Fuente-Fernández, R., and Stoessl, A. J. (2002). The placebo effect in Parkinson's disease. *Trends Neurosci.* 25, 302–306. doi: 10.1016/s0166-2236(02)02181-1
- Dixon, M. L., De La Vega, A., Mills, C., Andrews-Hanna, J., Spreng, R. N., Cole, M. W., et al. (2018). Heterogeneity within the frontoparietal control network and its relationship to the default and dorsal attention networks. *Proc. Natl. Acad. Sci. U S A* 115, E1598–E1607. doi: 10.1073/pnas.1715766115
- Dobrzyński, D., and Rossi, D. (2017). Geochemistry of trace elements in spring waters of the Lourdes area (France). *Annales Societatis Geologorum Poloniae* 87, 199–212. doi: 10.14241/asgp.2017.010
- Dosenbach, N. U., Fair, D. A., Cohen, A. L., Schlaggar, B. L., and Petersen, S. E. (2008). A dual-networks architecture of top-down control. *Trends Cogn. Sci.* 12, 99–105. doi: 10.1016/j.tics.2008.01.001
- Enck, P., Benedetti, F., and Schedlowski, M. (2008). New insights into the placebo and nocebo responses. *Neuron* 59, 195–206. doi: 10.1016/j.neuron.2008.06.030
- Haase, L., Thom, N. J., Shukla, A., Davenport, P. W., Simmons, E. N., Stanley, E. A., et al. (2016). Mindfulness-based training attenuates insula response to an aversive interoceptive challenge. *Soc. Cogn. Affect. Neurosci.* 11, 182–190. doi: 10.1093/scan/nsu042
- Habas, C., Kamdar, N., Nguyen, D., Prater, K., Beckmann, C. F., Menon, V., et al. (2009). Cerebellar contributions to intrinsic connectivity networks. *J. Neurosci.* 29, 8586–8594. doi: 10.1523/JNEUROSCI.1868-09.2009
- Holm, S. (1979). A simple sequential rejective multiple test procedure. *Scand. J. Stat.* 6, 65–70. doi: 10.2307/4615733

## DATA AVAILABILITY STATEMENT

The datasets generated during and/or analyzed during the current study are available from the corresponding author on reasonable request.

## ETHICS STATEMENT

The studies involving human participants were reviewed and approved by ethics committee of the University (GZ: 39/19/63 ex 2018/19). The patients/participants provided their written informed consent to participate in this study.

## AUTHOR CONTRIBUTIONS

All authors were involved in the conception of this study, data analysis and writing of the manuscript. All authors contributed to the article and approved the submitted version.

## FUNDING

This research has been supported by a grant from the BIAL foundation (Fundação Bial) 02/1. The publication has been supported by the University of Graz.

- Hölzel, B. K., Ott, U., Gard, T., Hempel, H., Weygandt, M., Morgen, K., et al. (2008). Investigation of mindfulness meditation practitioners with voxel-based morphometry. *Soc. Cogn. Affect. Neurosci.* 3, 55–61. doi: 10.1093/scan/nsm038
- Hyland, M. E., Geraghty, A., Joy, O., and Turner, S. (2006). Spirituality predicts outcome independently of expectancy following flower essence self-treatment. *J. Psychosom. Res.* 60, 53–58. doi: 10.1016/j.jpsychores.2005.06.073
- Kapogiannis, D., Barbey, A. K., Su, M., Zamboni, G., Krueger, F., Grafman, J., et al. (2009). Cognitive and neural foundations of religious belief. *Proc. Natl. Acad. Sci. U S A* 106, 4876–4881. doi: 10.1073/pnas.0811717106
- Kapogiannis, D., Deshpande, G., Krueger, F., Thornburg, M. P., and Grafman, J. H. (2014). Brain networks shaping religious belief. *Brain Connectivity* 4, 70–79. doi: 10.1089/brain.2013.0172
- Lundh, S. G. (1987). Placebo, belief and health. A cognitive-emotion model. *Scand. J. Psychol.* 28, 128–143. doi: 10.1111/j.1467-9450.1987.tb00747.x
- Marek, S., and Dosenbach, N. U. (2018). The frontoparietal network: function, electrophysiology and importance of individual precision mapping. *Dialogues Clin. Neurosci.* 20, 133–140. doi: 10.31887/DCNS.2018.20.2/smarek
- McClintock, C. H., Worhunsky, P. D., Xu, J., Balodis, I. M., Sinha, R., Miller, L., et al. (2019). Spiritual experiences are related to engagement of a ventral frontotemporal functional brain network: implications for prevention and treatment of behavioral and substance addictions. *J. Behav. Addict.* 8, 678–691. doi: 10.1556/2006.8.2019.71
- Miller, E. K., and Cohen, J. D. (2001). An integrative theory of prefrontal cortex function. *Annu. Rev. Neurosci.* 24, 167–202. doi: 10.1146/annurev.neuro.24.1.167
- Moerman, D. E., and Jonas, W. B. (2002). Deconstructing the placebo effect and finding the meaning response. *Anna. Intern. Med.* 136, 471–476. doi: 10.7326/0003-4819-136-6-200203190-00011
- Pashko, W. (2013). Shifting between our two self-identities can cause the placebo effect and response shift. *J. Transpersonal Psychol.* 45, 8–23. doi: 10.1177/002216787701700308
- Petrovic, P., Dietrich, T., Fransson, P., Andersson, J., Carlsson, K., Ingvar, M., et al. (2005). Placebo in emotional processing—induced expectations of anxiety relief activate a generalized modulatory network. *Neuron* 46, 957–969. doi: 10.1016/j.neuron.2005.05.023
- Petrovic, P., Kalso, E., Petersson, K. M., Andersson, J., Fransson, P., Ingvar, M., et al. (2010). A prefrontal non-opioid mechanism in placebo analgesia. *Pain* 150, 59–65. doi: 10.1016/j.pain.2010.03.011



- Raichle, M. E., MacLeod, A. M., Snyder, A. Z., Powers, W. J., Gusnard, D. A., Shulman, G. L., et al. (2001). A default mode of brain function. *Proc. Natl. Acad. Sci. U S A* 98, 676–682. doi: 10.1073/pnas.98.2.676
- Schienle, A., Höfler, C., and Wabnegger, A. (2019). Belief in the miracles of Lourdes: A voxel-based morphometry study. *Brain Behav.* 10:e01481. doi: 10.1002/brb3.1481
- Schienle, A., Übel, S., Schöngaßner, F., Ille, R., and Scharmüller, W. (2014). Disgust regulation via placebo: an fMRI study. *Soc. Cogn. Affect. Neurosci.* 9, 985–990. doi: 10.1093/scan/nst072
- Schjoedt, U., Stødkilde-Jørgensen, H., Geertz, A. W., and Roepstorff, A. (2009). Highly religious participants recruit areas of social cognition in personal prayer. *Soc. Cogn. Affect. Neurosci.* 4, 199–207. doi: 10.1093/scan/nsn050
- Tang, Y. Y., Holzel, B. K., and Posner, M. I. (2015). The neuroscience of mindfulness meditation. *Nat. Rev. Neurosci.* 16, 213–225. doi: 10.1038/nrn3916
- Tihanyi, B. T., Ferentzi, E., Beissner, F., and Köteles, F. (2018). The neuropsychophysiology of tingling. *Conscious. Cogn.* 58, 97–110. doi: 10.1016/j.concog.2017.10.015
- Uddin, L. Q. (2015). Salience processing and insular cortical function and dysfunction. *Nat. Rev. Neurosci.* 16, 55–61. doi: 10.1038/nrn3857
- Uddin, L. Q., Yeo, B. T., and Spreng, R. N. (2019). Towards a universal taxonomy of macro-scale functional human brain networks. *Brain Topogr.* 32, 926–942. doi: 10.1007/s10548-019-00744-6
- Unterrainer, H. F., Huber, H. P., Ladenhauf, K. H., Wallner-Liebmann, S. J., and Liebmann, P. M. (2010). MI-RSB 48 Die entwicklung eines multidimensionalen inventars zum religiös-spirituellen befinden. *Diagnostica* 2, 82–93. doi: 10.1026/0012-1924/a000001
- Wager, T. D., and Atlas, L. Y. (2015). The neuroscience of placebo effects: Connecting context, learning and health. *Nat. Rev. Neurosci.* 16, 403–418. doi: 10.1038/nrn3976
- Wager, T. D., Rilling, J. K., Smith, E. E., Sokolik, A., Casey, K. L., Davidson, R. J., et al. (2004). Cohen Placebo-induced changes in fMRI in the anticipation and experience of pain. *Science* 303, 1162–1167. doi: 10.1126/science.1093065
- Weimer, K., Colloca, L., and Enck, P. (2015). Placebo effects in psychiatry: mediators and moderators. *The Lancet Psychiatry* 2, 246–257. doi: 10.1016/S2215-0366(14)00092-3
- Weis, S., Patil, K. R., Hoffstaedter, F., Nostro, A., Yeo, B. T., Eickhoff, S. B., et al. (2020). Sex classification by resting-state brain connectivity. *Cereb. Cortex* 30, 824–835. doi: 10.1093/cercor/bhz129
- Whitfield-Gabrieli, S., and Nieto-Castanon, A. (2012). Conn: A functional connectivity toolbox for correlated and anticorrelated brain networks. *Brain Connectivity* 2, 125–141. doi: 10.1089/brain.2012.0073
- Wiech, K., Farias, M., Kahane, G., Shackel, N., Tiede, W., Tracey, I., et al. (2008). An fMRI study measuring analgesia enhanced by religion as a belief system. *Pain* 139, 467–476. doi: 10.1016/j.pain.2008.07.030
- Yan, X., Yong, X., Huang, W., and Ma, Y. (2018). Placebo treatment facilitates social trust and approach behavior. *Proc. Natl. Acad. Sci. U S A* 115, 5732–5737. doi: 10.1073/pnas.1800779115

**Conflict of Interest:** The authors declare that the research was conducted in the absence of any commercial or financial relationships that could be construed as a potential conflict of interest.

Copyright © 2021 Schienle, Gremsl and Wabnegger. This is an open-access article distributed under the terms of the Creative Commons Attribution License (CC BY). The use, distribution or reproduction in other forums is permitted, provided the original author(s) and the copyright owner(s) are credited and that the original publication in this journal is cited, in accordance with accepted academic practice. No use, distribution or reproduction is permitted which does not comply with these terms.



## OPEN ACCESS

## EDITED BY

João J. Cerqueira,  
University of Minho, Portugal

## REVIEWED BY

Szu-Han Wang,  
University of Edinburgh,  
United Kingdom  
David F. Werner,  
Binghamton University, United States

## \*CORRESPONDENCE

Jonathan R. Epp  
Jonathan.epp1@ucalgary.ca

## SPECIALTY SECTION

This article was submitted to  
Emotion Regulation and Processing,  
a section of the journal  
Frontiers in Behavioral Neuroscience

RECEIVED 30 March 2022

ACCEPTED 23 August 2022

PUBLISHED 09 September 2022

## CITATION

Terstege DJ, Durante IM and Epp JR  
(2022) Brain-wide neuronal activation  
and functional connectivity are  
modulated by prior exposure  
to repetitive learning episodes.  
*Front. Behav. Neurosci.* 16:907707.  
doi: 10.3389/fnbeh.2022.907707

## COPYRIGHT

© 2022 Terstege, Durante and Epp.  
This is an open-access article  
distributed under the terms of the  
[Creative Commons Attribution License](#)  
(CC BY). The use, distribution or  
reproduction in other forums is  
permitted, provided the original  
author(s) and the copyright owner(s)  
are credited and that the original  
publication in this journal is cited, in  
accordance with accepted academic  
practice. No use, distribution or  
reproduction is permitted which does  
not comply with these terms.

# Brain-wide neuronal activation and functional connectivity are modulated by prior exposure to repetitive learning episodes

Dylan J. Terstege, Isabella M. Durante and Jonathan R. Epp\*

Department of Cell Biology and Anatomy, Hotchkiss Brain Institute, Cumming School of Medicine, University of Calgary, Calgary, AB, Canada

Memory storage and retrieval are shaped by past experiences. Prior learning and memory episodes have numerous impacts on brain structure from micro to macroscale. Previous experience with specific forms of learning increases the efficiency of future learning. It is less clear whether such practice effects on one type of memory might also have transferable effects to other forms of memory. Different forms of learning and memory rely on different brain-wide networks but there are many points of overlap in these networks. Enhanced structural or functional connectivity caused by one type of learning may be transferable to another type of learning due to overlap in underlying memory networks. Here, we investigated the impact of prior chronic spatial training on the task-specific functional connectivity related to subsequent contextual fear memory recall in mice. Our results show that mice exposed to prior spatial training exhibited decreased brain-wide activation compared to control mice during the retrieval of a context fear memory. With respect to functional connectivity, we observed changes in several network measures, notably an increase in global efficiency. Interestingly, we also observed an increase in network resilience based on simulated targeted node deletion. Overall, this study suggests that chronic learning has transferable effects on the functional connectivity networks of other types of learning and memory. The generalized enhancements in network efficiency and resilience suggest that learning itself may protect brain networks against deterioration.

## KEYWORDS

cognitive stimulation, functional connectivity, context memory, immediate early genes, mouse model

## Introduction

It has been well established that prior learning experiences alter the canvas against which new learning occurs. Learning results in numerous structural changes in the brain ranging from cellular and synaptic changes (Lendvai et al., 2000; Nyberg et al., 2003; Holtmaat et al., 2005; De Paola et al., 2006; Epp et al., 2013) to altered macroscale

measurements of regional size and shape (Maguire et al., 2003; Draganski et al., 2004; Bermudez et al., 2008; Hyde et al., 2009; Scholz et al., 2009). A classic example of learning-induced structural changes is the change in hippocampal volume that occurs as a result of intense practice with spatial navigation in London taxi drivers (Maguire et al., 2000). Similar increases in hippocampal volume have also been observed in mice that were trained on a spatial learning task (Lerch et al., 2011).

To the extent that there are relationships between brain function and underlying structure, it should be predicted that learning-induced structural changes should also induce functional changes. Training-induced increases in hippocampal volume for example are also associated with enhanced memory performance (Bohbot et al., 2007).

In addition to structural changes, learning has been shown in some studies to change the organization of memories in the brain. In rats, previous studies have indicated that prior training with a memory task can prevent lesion-induced deficits in both similar and slightly distinct memory tasks (Clark and Delay, 1991; Ocampo et al., 2018). This suggested that prior learning experiences fundamentally change how and where future memories are encoded (Owen et al., 2010; Nouchi et al., 2012; West et al., 2017). Experiments such as these suggest some form of reorganization but do not give a complete picture as to how this reorganization has occurred.

Functional imaging experiments in humans have provided evidence that cognitive stimulation, or memory training, alters brain functional connectivity (Martínez et al., 2013; Dresler et al., 2017; Bagarinao et al., 2019; Miró-Padilla et al., 2019; Finc et al., 2020). These findings are of significant importance because reorganization of functional networks could increase the efficiency of learning and memory and could even increase the resilience of cognitive processes to damage or deterioration. However, investigating the influence of prior learning on altered functional connectivity in humans is complicated by the diverse cognitive, genetic and lifestyle differences in different individuals.

In the present study, to further elucidate the impact of prior learning on memory related functional connectivity, we have developed a mouse model in which mice are trained in a repeated acquisition spatial learning and memory task for several months. Using mice, we are able to control for environmental and genetic factors, and we can also control for prior learning experiences. Our aim was to investigate whether learning a spatial memory task would increase the efficiency of the functional networks underlying a different form of memory (contextual fear memory). Although spatial and contextual memories are independent of each other, the circuits involved in both of these forms of memory likely overlap in numerous places including, most notably, the hippocampus and connected structures. The repeated activation of regions that are mutually involved in circuits across multiple forms of learning and memory is likely a key factor in determining the

breadth of tasks that would be influenced by prior learning. To examine the extent to which spatial memory training influences contextual memory circuits, we adopted a brain-wide functional connectivity approach using immediate early gene imaging that has been recently described (Wheeler et al., 2013; Vetere et al., 2017; Scott et al., 2020).

In this study, we show that chronic cognitive stimulation, in the form of spatial learning is sufficient to induce generalized changes in the organization of functional connectivity networks underlying a test of contextual fear memory.

## Materials and methods

### Mice

8-week-old male C57BL/6J mice purchased from The Jackson Laboratory (Bar Harbor, ME, United States) were used for all experiments. Upon arrival, mice were group housed, 3-4 mice per cage, under a 12-h light/12-h dark cycle with *ad libitum* access to food and water. Testing and handling was performed during the light phase of the cycle. Behavioral tests and network analyses were conducted using groups of  $n = 10$ . Mice from the Morris Water Maze training group and the cage control group were co-housed, and all mice received equal handling throughout the study. All procedures were conducted in accordance with protocols approved by the University of Calgary, Health Sciences Animal Care Committee, following the guidelines of the Canadian Council for Animal Care.

### Morris water maze training

In order to provide mice with chronic cognitive stimulation, we trained half of the mice on a repeated acquisition and performance testing variant of the Morris Water Maze (MWM; see Figure 1A for an outline of the testing schedule and Figure 1B for the maze itself) (Spanswick et al., 2007). This task was chosen because it provides considerable flexibility in design, whereby a hidden platform can be moved to many different locations within the maze to encourage continuous learning. Furthermore, the spatial learning which occurs during MWM training is supported by many of the same neuroanatomical regions as contextual conditioning (Jo et al., 2007; Miller et al., 2014; Giustino and Maren, 2015; Kwapis et al., 2015; Milczarek et al., 2018). In this version of the task, the hidden escape platform is moved every second day which requires mice to repeatedly acquire new spatial memories throughout a 10-week training period. We used 10 different platform locations, with each platform location occurring on 2 separate occasions. Mice were trained 4 days per week (2 platform locations). During each daily session, mice were given four trials. Each trial lasted a maximum of 60 s and was initiated by placing the mouse

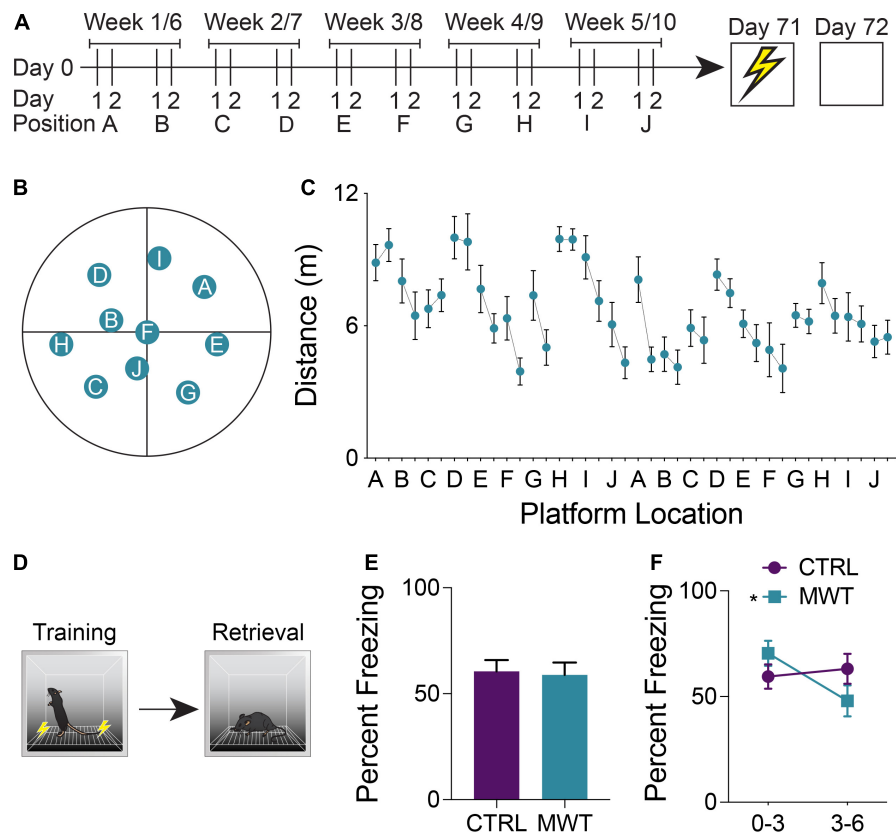


FIGURE 1

(A) Mice were trained on a repeated acquisition and performance testing variation of the MWM ( $n = 10$ ) or kept in conventional housing conditions ( $n = 10$ ) for 10 weeks. Afterward all mice underwent contextual fear conditioning and a retention test 24 h later. (B) During water maze training, the escape platform was moved every second day between 10 locations. After the 10<sup>th</sup> position, the platform was returned to the 1st position and the cycle was restarted. (C) Mean distance traveled in the water maze across each of the 20 locations. (D) During contextual fear memory retrieval, (E) there was no overall difference in freezing rates between the control group and the group which had underwent Morris Water Maze training (Paired two-tailed  $t$  test;  $P > 0.05$ ). (F) Mice who had underwent Morris Water Maze training froze significantly more during the first half (minutes 0-3) of the test than they did during the second half of the test (minutes 3-6; Two-Way Repeated Measures ANOVA; Time  $\times$  Treatment interaction:  $F_{1,18} = 7.763$ ,  $p = 0.0122$ ; MWM 0-3 – 3-6:  $p < 0.0066$ ), while control mice showed no difference in task performance across these two halves of the test. Data shown are mean  $\pm$  SEM when applicable.

gently into the pool, facing the wall. The start location was from a different cardinal compass position around the pool for each trial and the order of start locations was randomized each day. Trials were terminated once the mouse located the hidden platform. If the platform was not found after 60 s, mice were gently guided to the platform by the experimenter. Once on the platform, mice were given 15 s to remain on the platform before being returned to their cage. Trials were interleaved, whereby each mouse performed their first trial before the first mouse performed its second of four daily trials. This resulted in an intertrial interval of approximately 10 min. The circular pool had a diameter of 150 cm and a depth of 50 cm. The pool was filled so that the water level was 2 cm above the surface of a circular escape platform that had a diameter of 11 cm. The water was made opaque using white non-toxic tempera paint. The water was kept at a constant temperature of 22°C and stirred and cleaned of debris before each trial. Automated tracking software

(ANY-Maze, Stoelting, Wood Dale, IL, United States) was used to record and analyze swim behaviors in the pool, primarily the distance traveled prior to locating the hidden platform. When analyzing these results, linear regression was applied to the mean distance traveled by each mouse across each training session to assess the influence of the memory of previous platform locations on the ability to learn new platform locations. The extent to which mice learned platform position within blocks of consistent locations was assessed by examining the mean slope of the regression lines between distance traveled at all first-day trials and between all second day trials.

## Contextual fear conditioning

After the conclusion of the Morris Water Maze training protocol, all mice were trained in contextual fear conditioning.



Training was conducted in sound-attenuated chambers with grated floors through which shocks (0.5 mA; 2 s) were delivered (Ugo Basile, Gemonio, Italy). Mice were first allowed to acclimate to the chamber for 2 min prior to the presentation of a series of 3 shocks, each separated by an interval of 90 s. 24 h after the training session, mice were returned to the conditioning chambers for a 6-min retention test. During this test, no shocks were administered, and behavior was monitored via an overhead infrared camera in conjunction with an automated tracking software (ANY-Maze, Stoelting, Wood Dale, IL, United States). The chamber was cleaned using 70% ethanol and allowed to dry before and after each trial. When analyzing these results, freezing criteria was defined as bouts of a minimum of two seconds without ambulation. The percentage of the trial spent exhibiting freezing behavior was compared between groups.

## Perfusions and histology

Mice were transcardially perfused with 0.1 M phosphate buffered saline (PBS) followed by 4% formaldehyde 90 min after retention testing. Brains were then extracted and post-fixed in 4% formaldehyde for 24 h. Fixed brains were cryoprotected in 30% W/V sucrose solution at 4°C until no longer buoyant. From cryoprotected brains, serial coronal sections with a thickness of 40  $\mu\text{m}$  were cut on a cryostat (Leica Biosystems, Concord, ON, Canada) and stored in 12 series at  $-20^{\circ}\text{C}$  in antifreeze solution.

## Immunohistochemistry

When conducting labeling for c-Fos expression, all tissue was processed concurrently. Tissue sections were washed 3 times (10 min per wash) in 0.1M PBS before being incubated in a primary antibody solution of 1:2000 rabbit anti-c-Fos primary antibody (226 003, Synaptic Systems, Göttingen, Germany), 3% normal donkey serum, and 0.03% Triton-X100 for 48 h at room temperature on a tissue shaker. Tissue sections were washed  $3 \times 10$  min in 0.1M PBS before secondary antibody incubation. The secondary antibody solution was composed of 1:500 donkey anti-rabbit Alexa Fluor 488 (111-545-003, Cedar Lane Labs, Burlington, ON, Canada) in PBS for 24 h at room temperature. Sections were then transferred to 1:2000 DAPI solution for 15 min before being washed  $3 \times 10$  minutes in 0.1M PBS. Labeled sections were mounted to glass slides and coverslipped with PVA-DABCO mounting medium.

## Brain-wide c-Fos quantification

Quantification of fluorescent c-Fos labeled cells was conducted using a custom semi-automated segmentation and

registration pipeline (**Figure 2A**). All slides were imaged as a single batch using an Olympus VS120-L100-W slide scanning microscope (Richmond Hill, ON, Canada). Images were collected using a 10x objective with a numerical aperture of 0.40 and a Hamamatsu ORCA-Flash4.0 camera. Labeled c-Fos was imaged using a FITC filter cube and a 9.00 V lamp at an intensity of 100% and an exposure time of 140 ms. DAPI staining was imaged under the same conditions, but with a DAPI filter cube and an exposure time of 65 ms. Cells expressing a c-Fos label were segmented using the machine learning-based pixel and object classification program, *Ilastik* (Berg et al., 2019). To further prepare *Ilastik* output images and DAPI channel photomicrographs for regional registration, a custom plug-in was written for *ImageJ*. The pixel intensity threshold of the *Ilastik* outputs was adjusted so as to only contain objects which the program determined to be within the correct range of pixel intensities and shapes. To compensate for inadequate regional area measurements at an image-by-image level in the atlas registration software, a mask of evenly spaced binary points was generated from the DAPI channel image. The pixel intensity thresholds of these images were adjusted to create a binary mask in the shape of the tissue section. Grid lines were then overlaid to create a mask of binary points arranged in a square grid in the shape of the tissue section. Adjacent binary points were spaced by 22  $\mu\text{m}$ , therefore, each point in the mask accounted for an area of 484  $\mu\text{m}^2$ .

Next, tissue sections were registered to plates of the *Allen Mouse Brain Atlas* using the R-based *Whole Brain* software (Fürth et al., 2018). Using this software, DAPI channel images were used as references to which the atlas plates were aligned. The number of segmented c-Fos labeled cells per neuroanatomical region was quantified in *Whole Brain*. Similarly, the binary point masks were processed to count the number of points in each region. Regional areas were then approximated using a Cavalieri-based point counting approach, whereby the number of mask points in each region was multiplied by the area accounted for by each point. This allowed for the c-Fos labeled cells to be normalized by area and presented as regional cell densities.

## Validation of c-Fos quantification and regional area approximation

A separate cohort of mice was used for the validation of c-Fos labeled cell segmentation and regional area approximation. c-Fos immunostaining and imaging was identical to the methods described previously. To generate ground truth cell counts as a gold standard for our automated counting procedure, ten 500  $\mu\text{m}$  x 500  $\mu\text{m}$  regions of interest (ROI) were randomly generated from each of several regions including the basolateral amygdala, CA1, dentate gyrus, paraventricular nucleus, and the retrosplenial

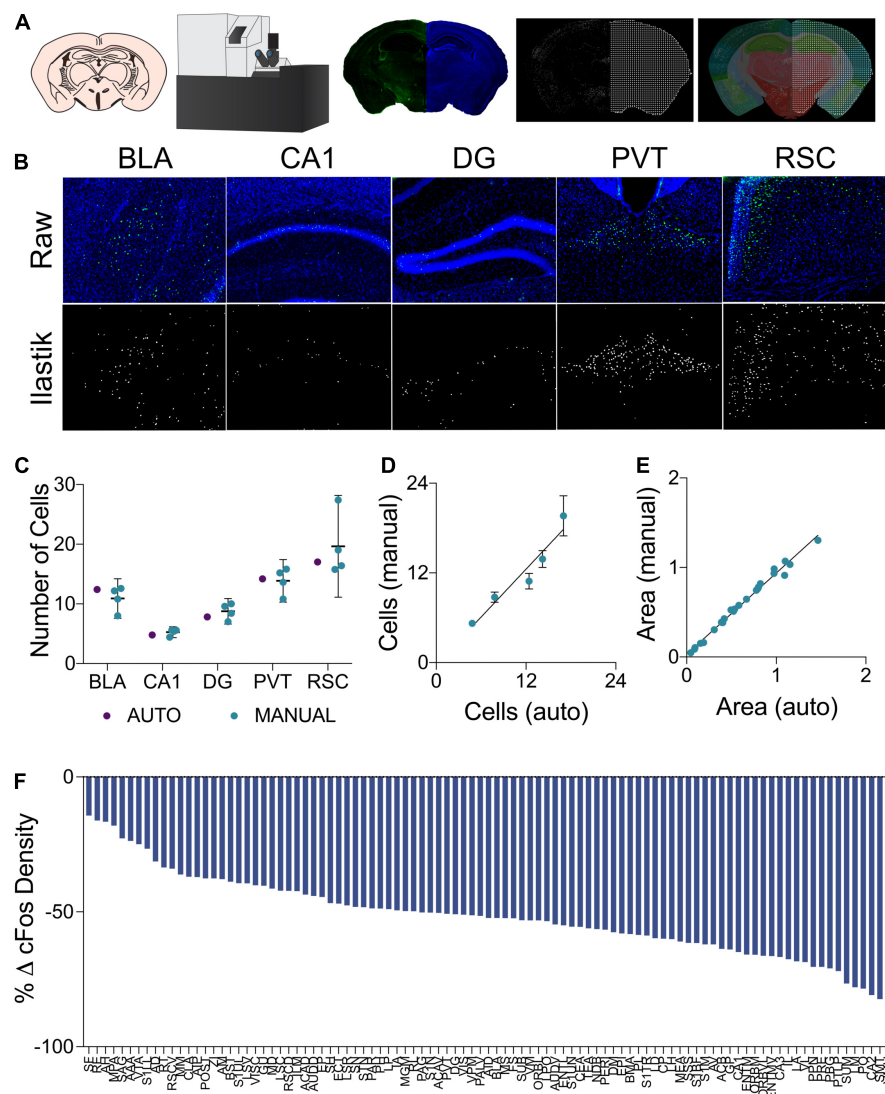


FIGURE 2

(A) In the cell segmentation and tissue registration pipeline, tissue was sectioned, immuno-labeled, and mounted on slides prior to being imaged on a fluorescent slide scanning microscope. Images of labeled c-Fos and DAPI staining were then processed using *Ilastik* and *ImageJ* to generate binary c-Fos labels and a mask of evenly spaced grid points in the shape of the tissue sections. These binary images were then applied to plates from the *Allen Mouse Brain Atlas* which had been morphed to align with the tissue sections using *Whole Brain*, yielding regional c-Fos densities. (B) Examples of raw c-Fos<sup>+</sup> cells in the BLA, CA1, DG, PVT, and RSC (top, L-R) and cells segmented using *Ilastik* (bottom). (C) A set of ROIs was quantified for validation. Automated *Ilastik* segmentation yielded cell counts within the 95% confidence intervals of counts acquired from trained independent experimenters in each of the aforementioned regions (Two-Way ANOVA; segmentation method factor:  $F_{1,15} = 0.09515$ ,  $p = 0.7620$ ). Data presented as mean  $95\% \pm$  confidence interval. (D) Cell counts collected using automated *Ilastik* processing were found to correlate highly with mean counts gathered through manual counting ( $Pearson\ r = 0.9610$ ,  $p < 0.01$ ). Data presented as mean  $95\% \pm$  confidence interval. (E) Area approximations generated using the pipeline were correlated with areas acquired by tracing regions manually in *ImageJ* ( $Pearson\ r = 0.9941$ ,  $p < 0.0001$ ). (F) c-Fos quantification across the 97 brain regions of interest. Relative to the control group, c-Fos expression in the mice that had previously received Morris Water Maze training was decreased to a variable extent in all brain regions.

cortex. These ROIs were processed through our *Ilastik* label segmentation pipeline (representative raw and processed images in Figure 2B). In addition, the same ROIs were hand counted independently by 4 experimenters blind to the automated cell count results. The total numbers of cells counted across all counting boxes were then compared to assess whether or not

*Ilastik* could segment fluorescent c-Fos labels within natural and acceptable inter-rater variability.

To assess the accuracy of regional area approximations, areas generated using the Cavalieri-based point counting approach were compared to the areas of these same regions which were manually traced in *ImageJ*. During this analysis,

five photomicrographs of each of the following regions were examined: basolateral amygdala, CA1, dentate gyrus, paraventricular nucleus, and the retrosplenial cortex.

## Functional connectivity network generation

We focused on a selection of 97 regions based on our ability to discriminate these regions using a DAPI stained image as reference (see [Supplementary Table 1](#) for list of regions and abbreviations). From this list of regions, c-Fos label densities were cross correlated within each group to generate pairwise correlation matrices. Correlations were filtered by statistical significance and a false discovery rate of 5% ([Benjamini and Hochberg, 1995](#); [Bassett et al., 2009](#)). For network analyses, correlation matrices were binarized to adjacency matrices based on Pearson's correlation coefficient and statistical significance ( $r > 0.9$ ;  $\alpha = 0.005$ ). This threshold allowed for sufficient network density to study global brain dynamics, while still limiting the analyses to only the strongest and most biologically plausible connections ([Schneidman et al., 2006](#)). To ensure that the thresholding parameters did not bias network analyses, additional adjacency matrices were generated using either more ( $r > 0.95$ ;  $\alpha = 0.0005$ ) or less ( $r > 0.8$ ;  $\alpha = 0.05$ ) conservative thresholds. To analyze adjacency matrices as network graphs, the 97 neuroanatomical regions were plotted as nodes. Connections were drawn between nodes whereby correlations surpassed correlation matrix thresholding parameters.

## Functional connectivity network analysis

Graph theoretical analyses were applied to network graphs to examine global and local properties of the network. These analyses were guided by the use of the *Brain Connectivity Toolkit* ([Rubinov and Sporns, 2010](#)), the *SBEToolbox* ([Konganti et al., 2013](#)), and other custom analyses. Network properties examined include *node degree*, *network density*, *global efficiency*, *betweenness centrality*, *Katz centrality*, and *network resiliency*. In the following definitions,  $N$  is the array of nodes in the network represented by adjacency matrix  $A$ . The number of nodes in the network is represented by  $n$  and the number of connections between nodes is  $l$ . The variable  $a_{ij}$  is the index into the adjacency matrix which indicates the connection status of nodes  $i$  and  $j$ . The presence of a connection is represented by  $a_{ij} \neq 0$  ([Rubinov and Sporns, 2010](#)). *Node degree* is the number of connections that link a node to the rest of the network ([Rubinov and Sporns, 2010](#)).

$$k_i = \sum_{j \in N} a_{ij} \quad (1)$$

*Network density* is a metric of network dispersion. It is expressed as a proportion of the number of connections in a given network over the number of connections which would be required to saturate a network of the same size ([Rubinov and Sporns, 2010](#)).

$$k_{den} = \frac{2l}{n^2 - n} \quad (2)$$

*Global efficiency* is defined as the inverse of the average shortest path of connections between all possible pairs of nodes ([Latora and Marchiori, 2001](#); [Achard and Bullmore, 2007](#); [Rubinov and Sporns, 2010](#)).

$$E = \frac{1}{n} \sum_{i \in N} \frac{\sum_{j, h \in N, j \neq i} d_{ij}^{-1}}{n - 1} \quad (3)$$

*Betweenness centrality* and *Katz centrality* are measures which can be used to assess the importance of a node in the effective communication of a network. *Betweenness centrality* quantifies the number of shortest paths between nodes that pass through a given node ([Freeman, 1978](#); [Brandes, 2001](#); [Rubinov and Sporns, 2010](#)).

$$b_i = \frac{1}{(n-1)(n-2)} \sum_{\substack{h, j \in N \\ h \neq j, h \neq i, j \neq i}} \frac{\rho_{hj}(i)}{\rho_{hj}} \quad (4)$$

*Katz centrality* applies an eigenvector approach to this metric by weighting the connections involving more highly connected nodes more heavily than those from lesser connected nodes when considering the makeup of the shortest paths which pass through a given node ([Katz, 1953](#); [Hubbell, 1965](#)). The attenuation factor,  $\alpha$ , used for this analysis was 0.1 ([Zhan et al., 2017](#)).

$$C_{Katz, i} = \sum_{k=1}^{\infty} \sum_{j=1}^n \alpha^k (A^k)_{ij} \quad (5)$$

*Network resiliency* was assessed through targeted node deletion and an assessment of the size of the largest community of connected nodes and global network efficiency with each deletion. Nodes were targeted for deletion in decreasing order, from nodes with the highest degree to those with the lowest. Degree was recalculated after each deletion and the list was reordered accordingly.

Network metrics were both compared across conditions as well as used to assess small world-like network properties compared to random control network topology. Small world network distribution can be described as being efficient at both local and global scales ([Watts and Strogatz, 1998](#)). Random null control networks were generated for both the cognitive training and control groups and were matched for network size, overall degree, and degree distribution. Local efficiency was assessed by comparing mean clustering coefficients, while global efficiency was assessed by comparing bootstrapped global efficiency values with one hundred replacements. Networks were considered to

display small world-like properties if they had displayed both the high global efficiency characteristic of a random network and increased local efficiency relative to random networks (Wheeler et al., 2013).

## Statistical analyses

Behavioral data from all tasks was recorded and analyzed using ANY-Maze (Stoelting, Wood Dale, IL, United States). All *t*-tests and Two-Way ANOVA for comparing behavioral data, regional c-Fos expression, segmentation and regional area approximation validation, and functional connectivity networks were conducted using GraphPad Prism (GraphPad Software, San Diego, CA, United States). GraphPad Prism was also used to conduct the linear regression used to assess inter-position memory and repeated new learning in the Morris Water Task. The analysis of functional connectivity networks was conducted using MATLAB. Figures were generated using MATLAB, Cytoscape, and GraphPad Prism.

## Results

### Morris water maze training alters memory performance in unrelated tasks

A repeated acquisition and performance testing variant of the Morris Water Maze was used to provide chronic cognitive stimulation (Figures 1A–C). Simple linear regression was applied to assess inter-position memory and the presence of repeated new learning. The slope of the best fit line of the linear regression applied to the mean distance traveled by each mouse across each training session was  $-0.067$ . When examining the mean distances traveled across all first days at a given platform position, the line of best fit had a slope of  $-0.068$ . Across all second days at a given platform position, this slope was determined to be  $-0.069$ . Within each platform location, the line of best fit of the linear regression yielded a mean slope of  $-0.97$  which differed significantly from zero and was indicative of improved performance over time within the same platform location (one sample *t* test;  $p = 0.0010$ ).

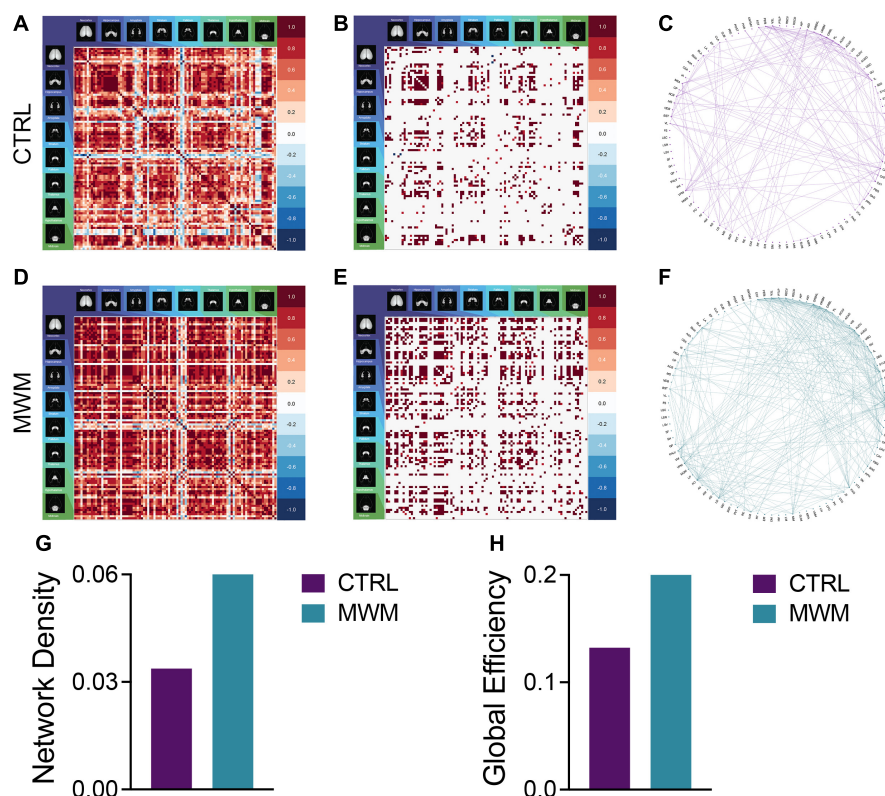


FIGURE 3

Pairwise correlation matrices (A,D), binarized adjacency matrices (B,E) and circle plots (C,F) showing significant correlations between regions for control (A–C) and Morris Water Maze trained (D–F) groups. See [Supplementary Table 1](#) for full list of regions. MWM training increased (G) network density and (H) global network efficiency.



To assess the generalization of improved cognitive performance following long-term spatial learning, mice were trained and tested in a contextual fear conditioning paradigm (Figure 1D). The percentage of time that mice exhibited freezing behavior was compared between groups and across the training and retention test sessions. Across both sessions, there were no significant differences in freezing behavior (Figure 1E). However, when the retention was divided into a first half and a second half, mice who had received cognitive training displayed increased freezing behavior during the first half of the test and then decreased freezing during the second half of the test (Figure 1F).

## Validation of c-Fos segmentation and neuroanatomical atlas registration

To assess the reliability of the semi-automated c-Fos segmentation and mouse brain atlas registration pipeline used in this study (Figure 2A), we compared c-Fos counts obtained using this pipeline to those gathered manually (see representative images Figure 2B). We found that the number of c-Fos labeled cells quantified using *Ilastik* processing fell within the range of values counted manually by four different experimenters across a subset of regions with varying levels of background autofluorescence (Figure 2C). The inter-rater

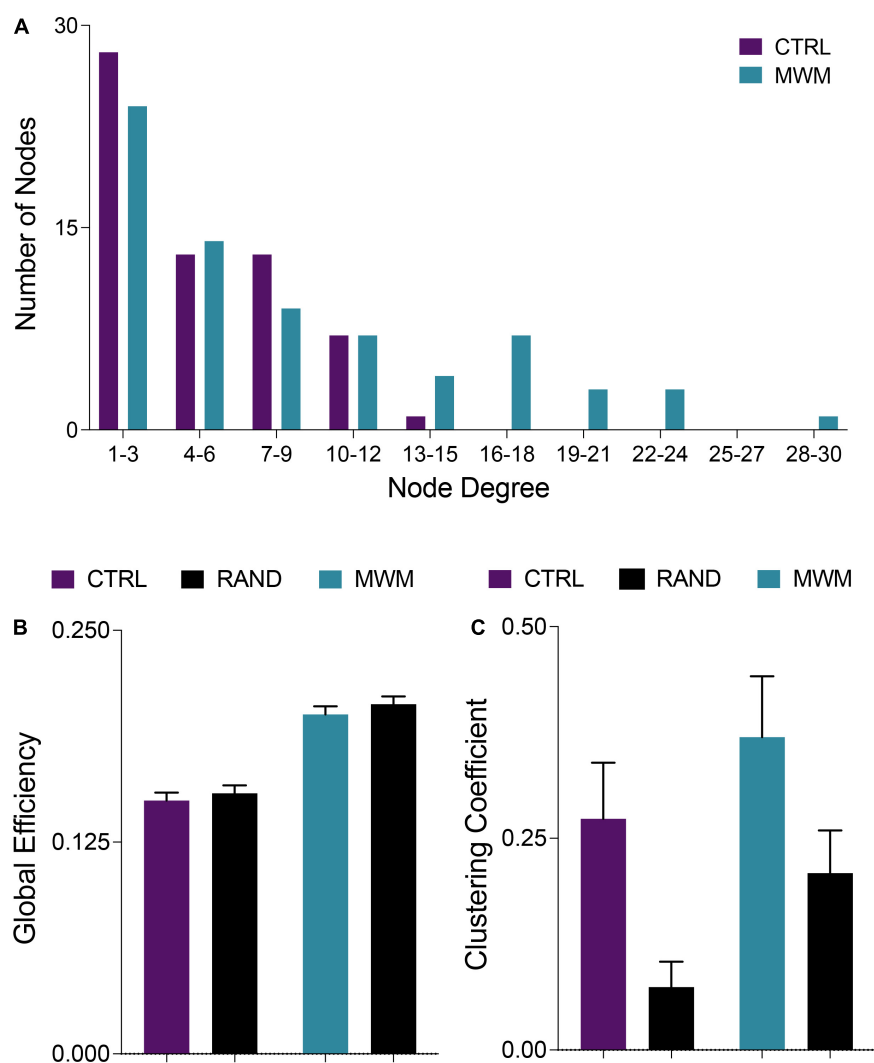


FIGURE 4

(A) Consistent with definitions of small world organization, in both control and MWM trained networks the majority of nodes were of a low degree. However, water maze training shifted the degree distribution and increased the number of highly connected nodes. (B) Also consistent with small world organization, both control and MWM trained networks showed equivalent global efficiency to random networks matched for degree distribution. (C) A third requirement for the classification of a small world organization is a higher clustering coefficient than a random network. Compared to random networks matched for degree distribution, both control and MWM trained networks showed heightened clustering. Data shown are mean  $\pm$  95% confidence intervals.

reliability was determined to be 15% across the datasets as a whole and the semi-automated cell counts were within 3.75% of the average of the manual cell counts. Manual and automated cell counts were highly correlated across the sampled brain regions (**Figure 2D**). *WholeBrain* region registration also produced regional area approximations that correlated highly with hand-traced regional area values (**Figure 2E**).

## Prior spatial learning alters c-Fos expression associated with context memory recall

Changes in regional c-Fos expression density are depicted in **Figure 2F** as the percent change from the regional c-Fos expression density from the control condition to the group which had undergone long-term spatial learning. We observed decreased c-Fos expression density in all brain regions that were analyzed in mice that had received prior spatial training. With respect to brain-wide activity, prior spatial training resulted in an overall significant decrease in c-Fos expression (**Supplementary Figure S1**. Unpaired t test;  $p = 0.0003$ ).

## Morris water maze training alters functional connectivity network topology

Analyses of cross-correlated regional c-Fos expression density revealed differences in global functional connectivity network topology. On a global scale, we observed a reorganization of connections throughout the brain (**Figures 3A–F**). Relative to control conditions, mice that underwent prior cognitive training exhibited an increase in the overall density of functional connections during subsequent contextual fear memory retrieval (**Figure 3G**). Furthermore, the organization of these networks after prior cognitive training resulted in increased global efficiency relative to the control condition (**Figure 3H**). These increases were also present in the networks constructed with both more or less conservative thresholds, indicating that this effect was not an artifact of the thresholding level (**Supplementary Figure S2**).

## Control and morris water maze training networks exhibit small-world qualities

Networks from both control and spatial learning groups exhibited heavy-tailed degree distribution characteristic of a small-world network, with the majority of nodes making very few connections and a lesser number of nodes carrying

disproportionate importance to the overall connectivity of the network (**Figure 4A**) (Bassett et al., 2006; Bullmore and Sporns, 2009). Comparisons to random null networks also highlighted that both the control and spatial learning networks maintained the high global efficiency characteristic of random networks (**Figure 4B**) while displaying increased clustering (**Figure 4C**). Together, these analyses indicate that the functional connectivity networks engaged during memory recall in both the control and spatial learning conditions exhibit properties that are consistent with small-world topology.

## Morris water maze training alters cluster organization and connectivity

Changes in network topology were also observed at the local level. The organization of local communities within global networks changes with long-term spatial learning. While the size of the giant component (GC) (**Figures 5A–C**) underwent very little change with MWM training, differences arose in the connectivity patterns within this component. Within the GC, MWM training increases the mean number of connections per node (**Figure 5D**). The changes in connectivity coincided with changes in network resiliency. When faced targeted deletion of nodes, with deletions occurring in the order of decreasing degree, long-term spatial learning increased the ability of the network to preserve its giant component size (**Figure 5E**) and global efficiency (**Figure 5F**).

Coinciding with these changes in network resiliency were changes in Katz centrality. Katz centrality is a measure of centrality which differentially weighs connections based on the degrees of the nodes involved (Katz, 1953). This measure has previously been shown to correlate highly with neuronal activity compared to other measures of centrality (Fletcher and Wennekers, 2018). While most nodes in the control network had similar Katz centrality vectors (**Figure 5G**), MWM training increased the centrality of a subset of regions (**Figure 5H**). There was considerable overlap between these regions with increased Katz centrality and the regions in the most densely connected region of the GC. This was further corroborated by analysis of regional degree distribution (**Supplementary Figure S3**) and change in Katz centrality (**Supplementary Figure S4**) which further highlighted an increase in connectivity and of importance of numerous amygdala subregions following spatial learning.

## Discussion

In the current study we employed a brain-wide activity mapping approach to examine the impact of a prolonged period of repeated spatial learning on brain-wide patterns of activation and functional connectivity. We posited that repeated activation

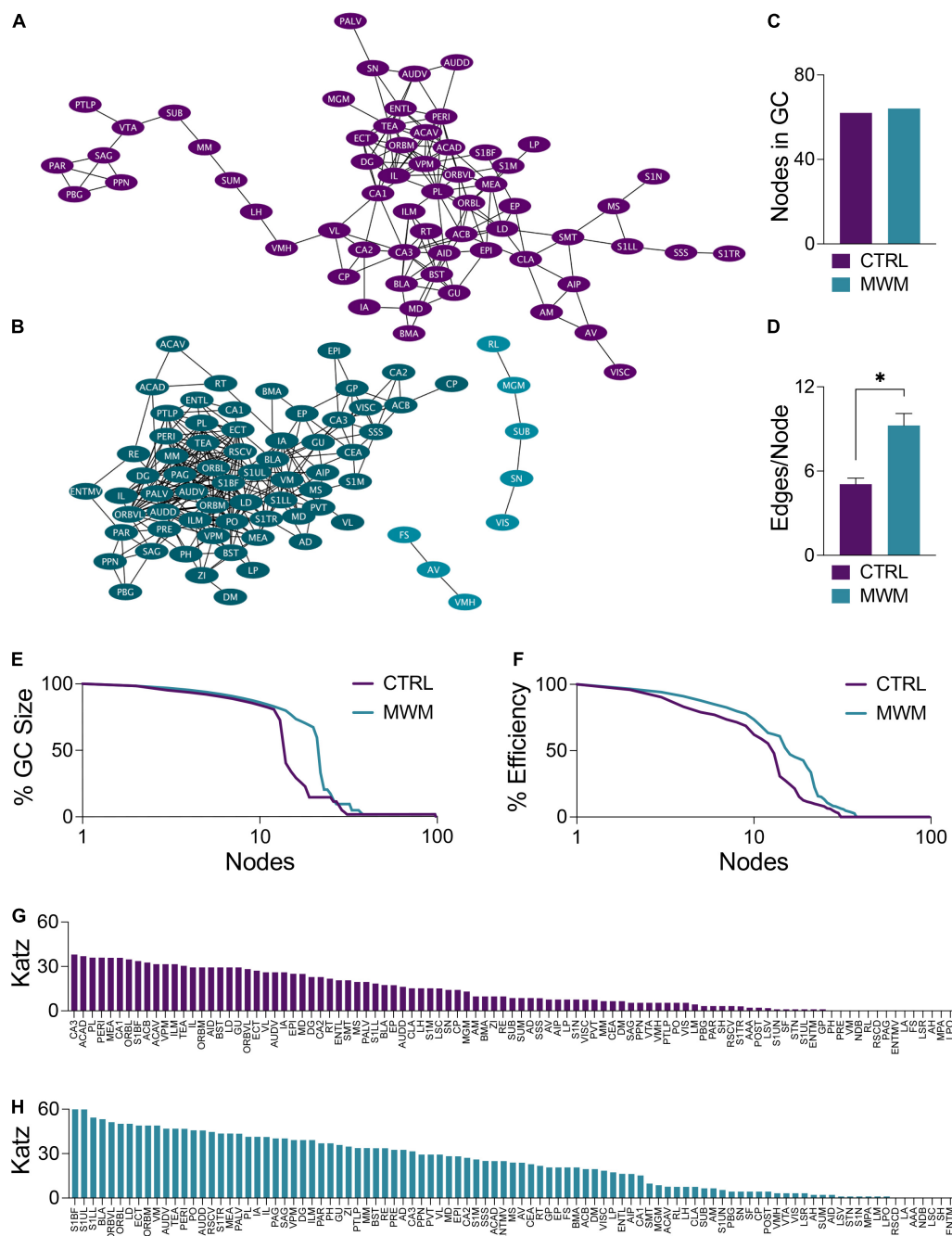


FIGURE 5

Network plots of (A) control and (B) MWM trained networks with the giant component (GC) highlighted in each in the darker shade. (C) In these networks, there is very little difference in the size of the GC. (D) Within the GC, there was an increase in the mean number of edges per node with MWM training (Two-tailed *t* test,  $p < 0.0001$ ). MWM training also made the (E) integrity of the GC and the (F) global efficiency of the network more resilient to targeted node deletion. Relative to the control condition (G), MWM training (H) also increased Katz centrality of a subset of regions within the network. Data shown are mean  $\pm$  SEM when applicable.

of the circuits underlying spatial learning and memory might alter the networks that represent other forms of hippocampus dependent memory in the future. During the spatial learning manipulation, we saw that in changing the hidden platform location in the Morris Water Maze every second day, mice were

encouraged to continuously learn. This continuous learning was evident by improved performance within platform positions between the first and second days, supported by a significantly negative slope in the regression analysis performed on the mean distances travelled between these days. Furthermore, there

was minimal change in performance across all trials with new platform locations, as was evident by the minimal slope of the regression line when analyzing mean swimming distance across all trials, all first days only, and all second days only. These findings suggest that mice were continuously learning new platform positions and that this new learning was only minimally altered by prior learning of conflicting platform locations. Our results also clearly indicate that this prior spatial learning manipulation caused significant changes to the task-related functional connectivity associated with retrieval of a contextual memory. In the current study, prior exposure to repeated spatial learning episodes had minimal effects on the overall retrieval of a subsequently acquired contextual fear memory. Interestingly, when subdividing the retrieval period, we noticed that the nature of the memory was different in mice that had prior spatial training. Specifically, the retention was stronger in the first half of the test and decreased in the second half, whereas control mice showed stable retention throughout the test. This could be indicative of an increase in behavioral flexibility and/or increased rate of extinction in the absence of additional foot shocks. That we did not observe major differences in memory retrieval was not surprising given that the subjects were normal mice without memory deficits, the memory in control mice was already very strong and the retention interval was short (24 h). This similarity in behavioral performance between conditions allowed us to assess patterns of neuronal activation without the confound of differential memory ability. When we examined neuronal activation and network organization underlying the memory in these two groups, we observed a number of differences that could enhance retention/retrieval in the face of cognitive decline.

We were most interested in investigating whether such a manipulation, which might be viewed as memory practice or training, would enhance measures of efficiency when examining the storage and retrieval of future memories. The efficiency of brain activity underlying cognitive function is vulnerable to aging and disease. Decreased efficiency of cognitive processing has been reported in several neurological conditions, including major depressive disorder (Zhang et al., 2020), schizophrenia (Sheffield et al., 2016), and Alzheimer's disease (Srivishagan et al., 2020). Even in healthy adults, patterns of brain activation become less efficient with age (Ajilore et al., 2014; Chong et al., 2019). These decreases in efficiency also coincide with decreased cognitive performance, thereby indicating that an intervention which can improve the efficiency of the functional connectome may preserve cognitive function in these conditions (van den Heuvel et al., 2009). We show here that the efficiency of brain-wide activation, as measured by c-Fos expression, is greatly increased in the mice that had prior spatial training. Efficiency can be defined as equal or greater memory performance with the expenditure of fewer resources (i.e., a decrease in activation) (McQuail et al., 2020). Our results show that contextual memory retrieval following spatial learning was associated with

a decrease in the total c-Fos expressing cells throughout the brain compared to mice that had not previously experienced any spatial training. Previously, it has been reported that c-Fos expression density is increased in several neuroanatomical regions following water maze training (Guzowski et al., 2001; Teather et al., 2005). When interpreting the results of the current study, it is imperative that we highlight the differences in experimental designs which could underlie this difference. In these studies, c-Fos expression was tagged directly to water maze performance, while in the present study this expression was tagged to the recall of a contextually conditioned memory. Furthermore, the duration of the spatial learning period in these previous studies was much shorter than that used in the current design. Therefore, our results showing that all brain regions exhibited reduced activity are not contradictory with existing literature. Taken together, this pattern of activity perhaps indicates that the behavioral expression of the memory retrieval is more efficient on the level of neuronal activation.

At a network level, global efficiency can be estimated as the inverse of the average shortest path lengths between all network nodes. This measure represents the relative ease or difficulty of integrating information between nodes in a network. Using this measure, we found that mice which had received prior spatial training exhibited enhanced global efficiency and higher clustering compared to controls during subsequent contextual memory retrieval. Both of these findings are consistent with the effects of memory training observed using human functional neuroimaging (Langer et al., 2013). This analysis corroborates the interpretations of increased efficiency based on overall brain activation. Further corroborating these interpretations are changes in the Katz centrality within these networks. Centrality measures can be used as proxies of the relative importance of a node in the maintenance of effective communication across a network and as indicators of the functional segregation of the network as a whole. Spatial training increased the centrality of a subset of nodes. This pattern of distribution suggests a higher degree of network segregation and that this subset of regions is relatively more important to the behavioral expression of the context memory. Comparatively, based on the variability of regional Katz centrality, all regions in the network generated from untrained mice are of similar importance in the expression of this same behavior. These findings coincide with increased centrality in resting state memory networks following working memory training in human neuroimaging studies (Takeuchi et al., 2017). Together these metrics illustrate that the redistribution of neuronal activation induced by prior spatial learning is not only more efficient from the perspective of energetic resources, but also proves to be more efficient with respect to global flow of information throughout the brain.

Functional connectivity networks in the brain are considered to be complex networks. Many complex networks exhibit small world organization. Small-world networks balance global efficiency with local clustering by having a



small proportion of nodes to contribute disproportionately to the overall connectivity of the network (Watts and Strogatz, 1998; Bassett et al., 2006; Sporns and Honey, 2006). This type of organization facilitates specialized processing in dense, local clusters while maintaining efficient information transfer between clusters. Regardless of prior spatial training exposure, the networks engaged by contextual memory retrieval displayed characteristic small-world properties. Compared to random networks, we observed that the memory networks had a small number of highly connected regions, an increase in clustering coefficient, and equivalent global efficiency. Small world organization facilitates specialized processing in densely connected local communities while also allowing for efficient transfer of information between local communities. We used Markov chain clustering to detect the structure of these communities within the networks. In both networks there was a large interconnected central component, referred to as the giant component, which did not change in size as a result of prior spatial training. However, there was a significant increase in the density of connections within the GC of the group of mice who had received prior spatial learning. The densely connected giant component at the core of the network underlying context memory expression in mice with prior spatial training contained many redundant connections. Therefore, we hypothesized that more successive deletions would be required to break apart communities in a way which would be consequential to the effective communication of the network. This hypothesis was supported by the results of targeted node deletion. By sequentially deleting nodes in the descending order of their degree, we noted that mice which had prior spatial training were able to retain a higher percentage of their basal global efficiency and giant component size. In being more resistant to targeted attack, this network can be said to be more resilient than the network obtained from control mice (Achard et al., 2006).

Increased resiliency to targeted node deletion presents interesting possibilities from the perspective of neurodegenerative disease. The pathology of many neurodegenerative conditions does not arise uniformly throughout the brain and rather targets the most highly involved regions of a network reviewed in Crossley et al. (2014). In addition to suffering from targeted attacks, the functional connectomes characteristic of many neurodegenerative conditions networks also display decreased redundancy in their connectivity patterns, rendering networks more vulnerable to these attack (Langella et al., 2021). An efficient network which is more resilient to attack has the potential to delay or reduce cognitive decline during early neurodegenerative disease progression (Rittman et al., 2019). The present study found that cognitive stimulation through repetitive learning experiences was able to increase network efficiency and resilience. Therefore, the potential exists for prior exposure to repetitive learning experiences to increase resiliency to deterioration. Future studies of this phenomenon might build upon this by

examining whether prolonged cognitive stimulation and the resulting alterations in functional connectivity are sufficient for reducing cognitive deficits observed in early stages of neurodegeneration. From the current results it is not known whether the observed change in functional connectivity and activity would be observed in tasks other than contextual fear conditioning and as such this should also be investigated in future studies.

In the present study, networks were generated based on correlated expression of c-Fos across the brain. While this method has been demonstrated at various levels of regional organization in previous publications (Wheeler et al., 2013; Vetere et al., 2017; Silva et al., 2019; Scott et al., 2020), it is worth acknowledging the limitations of this approach. While exhibiting excellent spatial resolution at the single cell level, c-Fos expression is limited in its temporal resolution. It is important to consider the delay that occurs between cellular activity and c-Fos expression. A delay of 90 minutes between cellular activity and peak c-Fos expression allows us to use c-Fos to examine brain-wide activity tagged to behavioral paradigms which are incompatible with head-fixed neuroimaging techniques. However, it is impossible under the current design to establish patterns of c-Fos expression during distinct bouts of freezing or movement during conditioned context reintroduction. In an experiment such as this in which freezing behaviors were consistent between groups, it is possible that this limitation has less of an impact on the ability to interpret the results than in an experiment in which the behaviors corresponding with the tagged neuronal activity vary greatly between groups. In such scenarios, follow-up experiments using an *in vivo* measure of regional activation would be advised to assess the specificity functional connections to distinct behavioral outputs.

When analyzing networks based on brain-wide correlated c-Fos expression density the entire group is treated as a single network. This limits the inferential statistics that can be applied when comparing network metrics between groups. However, it can be easy to overlook that underlying each cell in a correlation matrix is a *p* value. In thresholding these correlation matrices to generate the binary adjacency matrices that form the bases of the presented network analyses, the statistical significance of each correlation is heavily weighted. The thresholds examined in the present study ( $\alpha = 0.05$ ,  $\alpha = 0.005$ , and  $\alpha = 0.0005$ ) were implemented so as to only consider the most statistically significant correlations in the network analysis, thereby ensuring that any descriptive comparisons between networks were based on the organization of highly significant patterns of co-activation.

Additionally, while we attribute the changes in network topology to spatial learning, there are other possible factors present during these episodes which may also contribute to network reorganization. These heavily intertwined factors include, exercise, motor activity, sensory exposure, and repeated

acute stress. Among these factors, there is considerable debate surrounding stress in the Morris water maze (Sandi et al., 1997; Engelmann et al., 2006; Harrison et al., 2009). Repeated exposure to this mild stressor could result in changes in the HPA axis, which could then impact behavior and the organization of functional connectivity networks underlying a contextually conditioned fear memory (Sandi et al., 2003; Rodríguez Manzanares et al., 2005). Mice given pool exposure matched to the duration of the water maze training group without an escape platform location to learn, commonly referred to as a yoked control group, may superficially control for exposure to the water maze. However, other issues arise with yoked control group as there may be differences between escapable and inescapable stressors. These points considered, it was decided that measures controlling for exercise, such as the use of a yoked control group might induce further variability. However, the important conclusion of the current study is that repeated learning and memory episodes induce widescale changes in brain activity and functional connectivity during encoding and/or retrieval of subsequent unrelated memory tasks. Future studies will be required to assess the relative influence of specific factors occurring during task exposure.

## Data availability statement

The datasets presented in this study can be found in online repositories. The names of the repository/repositories and accession number(s) can be found below: <https://github.com/dterstege/PublicationRepo/tree/main/Terstege2022A>.

## Ethics statement

The animal study was reviewed and approved by University of Calgary Health Sciences Animal Care Committee in accordance with the guidelines of the Canadian Council on Animal Care.

## Author contributions

DJT and JRE conceived and designed the experiment and conducted the analyses and wrote the manuscript. DJT and

IMD conducted the experiments. All authors contributed to the article and approved the submitted version.

## Funding

Funding for this study was provided by The Brain Canada Foundation/The Azrieli Foundation Early Career Capacity Building Grant (4709) and an NSERC Discovery Grant (RGPIN-2018-05135) to JRE.

## Acknowledgments

We acknowledge the Hotchkiss Brain Institute Advanced Microscopy Platform and the Cumming School of Medicine for support and use of the Olympus VS120-L100-W slide scanning microscope.

## Conflict of interest

The authors declare that the research was conducted in the absence of any commercial or financial relationships that could be construed as a potential conflict of interest.

## Publisher's note

All claims expressed in this article are solely those of the authors and do not necessarily represent those of their affiliated organizations, or those of the publisher, the editors and the reviewers. Any product that may be evaluated in this article, or claim that may be made by its manufacturer, is not guaranteed or endorsed by the publisher.

## Supplementary material

The Supplementary Material for this article can be found online at: <https://www.frontiersin.org/articles/10.3389/fnbeh.2022.907707/full#supplementary-material>

## References

- Achard, S., and Bullmore, E. (2007). Efficiency and cost of economical brain functional networks. *PLoS Comput. Biol.* 3:e17. doi: 10.1371/journal.pcbi.0030017
- Achard, S., Salvador, R., Whitcher, B., Suckling, J., and Bullmore, E. (2006). A resilient, low-frequency, small-world human brain functional network with highly connected association cortical hubs. *J. Neurosci.* 26, 63–72. doi: 10.1523/JNEUROSCI.3874-05.2006
- Ajilore, O., Lamar, M., and Kumar, A. (2014). Association of brain network efficiency with aging, depression, and cognition. *Am. J. Geriatr. Psychiatry* 22, 102–110. doi: 10.1016/j.jagp.2013.10.004
- Bagarinao, E., Watanabe, H., Maesawa, S., Mori, D., Hara, K., Kawabata, K., et al. (2019). Reorganization of brain networks and its association with general cognitive performance over the adult lifespan. *Sci. Rep.* 9:11352. doi: 10.1038/s41598-019-47922-x

- Bassett, D. S., Bullmore, E. T., Meyer-Lindenberg, A., Apud, J. A., Weinberger, D. R., and Coppola, R. (2009). Cognitive fitness of cost-efficient brain functional networks. *Proc. Natl. Acad. Sci. U.S.A.* 106, 11747–11752. doi: 10.1073/pnas.0903641106
- Bassett, D. S., Meyer-Lindenberg, A., Achard, S., Duke, T., and Bullmore, E. (2006). Adaptive reconfiguration of fractal small-world human brain functional networks. *Proc. Natl. Acad. Sci. U.S.A.* 103, 19518–19523. doi: 10.1073/pnas.0606005103
- Benjamini, Y., and Hochberg, Y. (1995). Controlling the false discovery rate: A practical and powerful approach to multiple testing. *J. R. Stat. Soc.* 57, 289–300. doi: 10.1111/j.2517-6161.1995.tb02031.x
- Berg, S., Kutra, D., Kroeger, T., Straehle, C. N., Kausler, B. X., Haubold, C., et al. (2019). ilastik: Interactive machine learning for (bio)image analysis. *Nat. Methods* 16, 1226–1232. doi: 10.1038/s41592-019-0582-9
- Bermudez, P., Lerch, J. P., Evans, A. C., and Zatorre, R. J. (2008). Neuroanatomical Correlates of Musicianship as Revealed by Cortical Thickness and Voxel-Based Morphometry. *Cereb. Cortex* 19, 1583–1596. doi: 10.1093/cercor/bhn196
- Bohbot, V. D., Lerch, J., Thorndyraft, B., Iaria, G., and Zijdenbos, A. P. (2007). Gray matter differences correlate with spontaneous strategies in a human virtual navigation task. *J. Neurosci.* 27, 10078–10083. doi: 10.1523/JNEUROSCI.1763-07.2007
- Brandes, U. (2001). A faster algorithm for betweenness centrality. *J. Math. Soc.* 25, 163–177. doi: 10.1080/0022250X.2001.9990249
- Bullmore, E., and Sporns, O. (2009). Complex brain networks: Graph theoretical analysis of structural and functional systems. *Nat. Rev. Neurosci.* 10, 186–198. doi: 10.1038/nrn2575
- Chong, J. S. X., Ng, K. K., Tandil, J., Wang, C., Poh, J.-H., Lo, J. C., et al. (2019). Longitudinal Changes in the Cerebral Cortex Functional Organization of Healthy Elderly. *J. Neurosci.* 39, 5534–5550. doi: 10.1523/JNEUROSCI.1451-18.2019
- Clark, R. E., and Delay, E. R. (1991). Reduction of lesion-induced deficits in visual reversal learning following cross-modal training. *Restor. Neurol. Neurosci.* 3, 247–255. doi: 10.3233/RNN-1991-3503
- Crossley, N. A., Mechelli, A., Scott, J., Carletti, F., Fox, P. T., McGuire, P., et al. (2014). The hubs of the human connectome are generally implicated in the anatomy of brain disorders. *Brain* 137, 2382–2395. doi: 10.1093/brain/awu132
- De Paola, V., Holtmaat, A., Knott, G., Song, S., Wilbrecht, L., Caroni, P., et al. (2006). Cell type-specific structural plasticity of axonal branches and boutons in the adult neocortex. *Neuron* 49, 861–875. doi: 10.1016/j.neuron.2006.02.017
- Draganski, B., Gaser, C., Busch, V., Schuier, G., Bogdahn, U., and May, A. (2004). Changes in grey matter induced by training. *Nature* 427, 311–312. doi: 10.1038/427311a
- Dresler, M., Shirer, W. R., Konrad, B. N., Müller, N. C. J., Wagner, I. C., Fernández, G., et al. (2017). Mnemonic Training Reshapes Brain Networks to Support Superior Memory. *Neuron* 93, 1227–1235.e6. doi: 10.1016/j.neuron.2017.02.003
- Engelmann, M., Ebner, K., Landgraf, R., and Wotjak, C. T. (2006). Effects of Morris water maze testing on the neuroendocrine stress response and intrahypothalamic release of vasopressin and oxytocin in the rat. *Horm. Behav.* 50, 496–501. doi: 10.1016/j.yhbeh.2006.04.009
- Epp, J. R., Chow, C., and Galea, L. A. M. (2013). Hippocampus-dependent learning influences hippocampal neurogenesis. *Front. Neurosci.* 7:57. doi: 10.3389/fnins.2013.00057
- Finc, K., Bonna, K., He, X., Lydon-Staley, D. M., Kühn, S., Duch, W., et al. (2020). Dynamic reconfiguration of functional brain networks during working memory training. *Nat. Commun.* 11:2435. doi: 10.1038/s41467-020-15631-z
- Fletcher, J. M., and Wennekers, T. (2018). From Structure to Activity: Using Centrality Measures to Predict Neuronal Activity. *Int. J. Neural. Syst.* 28:1750013. doi: 10.1142/S0129065717500137
- Freeman, L. C. (1978). Centrality in social networks conceptual clarification. *Soc. Netw.* 1, 215–239. doi: 10.1016/0378-8733(78)90021-7
- Fürth, D., Vaissière, T., Tzortzi, O., Xuan, Y., Martin, A., Lazaridis, I., et al. (2018). An interactive framework for whole-brain maps at cellular resolution. *Nat. Neurosci.* 21, 139–149. doi: 10.1038/s41593-017-0027-7
- Giustino, T. F., and Maren, S. (2015). The role of the medial prefrontal cortex in the conditioning and extinction of fear. *Front. Behav. Neurosci.* 9:298. doi: 10.3389/fnbeh.2015.00298
- Guzowski, J. F., Setlow, B., Wagner, E. K., and McGaugh, J. L. (2001). Experience-dependent gene expression in the rat hippocampus after spatial learning: A comparison of the immediate-early genes Arc, c-fos, and zif268. *J. Neurosci.* 21, 5089–5098. doi: 10.1523/JNEUROSCI.21-14-05089.2001
- Harrison, F. E., Hosseini, A. H., and McDonald, M. P. (2009). Endogenous anxiety and stress responses in water maze and Barnes maze spatial memory tasks. *Behav. Brain Res.* 198, 247–251. doi: 10.1016/j.bbr.2008.10.015
- Holtmaat, A. J. G. D., Trachtenberg, J. T., Wilbrecht, L., Shepherd, G. M., Zhang, X., Knott, G. W., et al. (2005). Transient and persistent dendritic spines in the neocortex in vivo. *Neuron* 45, 279–291. doi: 10.1016/j.neuron.2005.01.003
- Hubbell, C. H. (1965). An Input-Output Approach to Clique Identification. *Sociometry* 28, 377–399. doi: 10.2307/2785990
- Hyde, K. L., Lerch, J., Norton, A., Forgeard, M., Winner, E., Evans, A. C., et al. (2009). Musical training shapes structural brain development. *J. Neurosci.* 29, 3019–3025. doi: 10.1523/JNEUROSCI.5118-08.2009
- Jo, Y. S., Park, E. H., Kim, I. H., Park, S. K., Kim, H., Kim, H. T., et al. (2007). The medial prefrontal cortex is involved in spatial memory retrieval under partial-cue conditions. *J. Neurosci.* 27, 13567–13578. doi: 10.1523/JNEUROSCI.3589-07.2007
- Katz, L. (1953). A New Status Index Derived From Sociometric Analysis. *Psychometrika* 18, 39–43. doi: 10.1007/BF02289026
- Konganti, K., Wang, G., Yang, E., and Cai, J. J. (2013). SBEToolbox: A Matlab toolbox for biological network analysis. *Evol. Bioinform. Online* 9, 355–362. doi: 10.4137/EBO.S12012
- Kwapit, J. L., Jarome, T. J., Lee, J. L., and Helmstetter, F. J. (2015). The retrosplenial cortex is involved in the formation of memory for context and trace fear conditioning. *Neurobiol. Learn. Mem.* 123, 110–116. doi: 10.1016/j.nlm.2015.06.007
- Langella, S., Sadiq, M. U., Mucha, P. J., Giovanello, K. S., Dayan, E., Alzheimer's Disease, et al. (2021). Lower functional hippocampal redundancy in mild cognitive impairment. *Transl. Psychiatry* 11:61. doi: 10.1038/s41398-020-01166-w
- Langer, N., von Bastian, C. C., Wirz, H., Oberauer, K., and Jäncke, L. (2013). The effects of working memory training on functional brain network efficiency. *Cortex* 49, 2424–2438. doi: 10.1016/j.cortex.2013.01.008
- Latora, V., and Marchiori, M. (2001). Efficient behavior of small-world networks. *Phys. Rev. Lett.* 87:198701. doi: 10.1103/PhysRevLett.87.198701
- Lendvai, B., Stern, E. A., Chen, B., and Svoboda, K. (2000). Experience-dependent plasticity of dendritic spines in the developing rat barrel cortex in vivo. *Nature* 241404, 876–881. doi: 10.1038/35009107
- Lerch, J. P., Yiu, A. P., Martinez-Canabal, A., Pekar, T., Bohbot, V. D., Frankland, P. W., et al. (2011). Maze training in mice induces MRI-detectable brain shape changes specific to the type of learning. *Neuroimage* 54, 2086–2095. doi: 10.1016/j.neuroimage.2010.09.086
- Maguire, E. A., Gadian, D. G., Johnsrude, I. S., Good, C. D., Ashburner, J., Frackowiak, R. S., et al. (2000). Navigation-related structural change in the hippocampi of taxi drivers. *Proc. Natl. Acad. Sci. U.S.A.* 97, 4398–4403. doi: 10.1073/pnas.070039597
- Maguire, E. A., Spiers, H. J., Good, C. D., Hartley, T., Frackowiak, R. S. J., and Burgess, N. (2003). Navigation expertise and the human hippocampus: A structural brain imaging analysis. *Hippocampus* 13, 250–259. doi: 10.1002/hipo.10087
- Martínez, K., Solana, A. B., Burgaleta, M., Hernández-Tamames, J. A., Alvarez-Linera, J., Román, F. J., et al. (2013). Changes in resting-state functionally connected parietofrontal networks after videogame practice: Videogame Practice and Functional Connectivity. *Hum. Brain Mapp.* 34, 3143–3157. doi: 10.1002/hbm.22129
- McQuail, J. A., Dunn, A. R., Stern, Y., Barnes, C. A., Kempermann, G., Rapp, P. R., et al. (2020). Cognitive Reserve in Model Systems for Mechanistic Discovery: The Importance of Longitudinal Studies. *Front. Aging Neurosci.* 12:607685. doi: 10.3389/fnagi.2020.607685
- Milczarek, M. M., Vann, S. D., and Sengpiel, F. (2018). Spatial memory engram in the mouse retrosplenial cortex. *Curr. Biol.* 28, 1975–1980.e6. doi: 10.1016/j.cub.2018.05.002
- Miller, A. M. P., Vedder, L. C., Law, L. M., and Smith, D. M. (2014). Cues, context, and long-term memory: The role of the retrosplenial cortex in spatial cognition. *Front. Hum. Neurosci.* 8:586. doi: 10.3389/fnhum.2014.00586
- Miró-Padilla, A., Bueichekú, E., Ventura-Campos, N., Flores-Compañ, M.-J., Parcet, M. A., and Ávila, C. (2019). Long-term brain effects of N-back training: An fMRI study. *Brain Imaging Behav.* 13, 1115–1127. doi: 10.1007/s11682-018-9925-x
- Nouchi, R., Taki, Y., Takeuchi, H., Hashizume, H., Akitsuki, Y., Shigemune, Y., et al. (2012). Brain training game improves executive functions and processing

- speed in the elderly: A randomized controlled trial. *PLoS One* 7:e29676. doi: 10.1371/journal.pone.0029676
- Nyberg, L., Sandblom, J., Jones, S., Neely, A. S., Petersson, K. M., Ingvar, M., et al. (2003). Neural correlates of training-related memory improvement in adulthood and aging. *Proc. Natl. Acad. Sci. U.S.A.* 100, 13728–13733. doi: 10.1073/pnas.1735487100
- Ocampo, A. C., Squire, L. R., and Clark, R. E. (2018). The beneficial effect of prior experience on the acquisition of spatial memory in rats with CA1, but not large hippocampal lesions: A possible role for schema formation. *Learn. Mem.* 25, 115–121. doi: 10.1101/lm.046482.117
- Owen, A. M., Hampshire, A., Grahn, J. A., Stenton, R., Dajani, S., Burns, A. S., et al. (2010). Putting brain training to the test. *Nature* 465, 775–778. doi: 10.1038/nature09042
- Rittman, T., Borchert, R., Jones, S., van Swieten, J., Borroni, B., Galimberti, D., et al. (2019). Functional network resilience to pathology in presymptomatic genetic frontotemporal dementia. *Neurobiol. Aging* 77, 169–177. doi: 10.1016/j.neurobiolaging.2018.12.009
- Rodríguez Manzanares, P. A., Isoardi, N. A., Carrer, H. F., and Molina, V. A. (2005). Previous stress facilitates fear memory, attenuates GABAergic inhibition, and increases synaptic plasticity in the rat basolateral amygdala. *J. Neurosci.* 25, 8725–8734. doi: 10.1523/JNEUROSCI.2260-05.2005
- Rubinov, M., and Sporns, O. (2010). Complex network measures of brain connectivity: Uses and interpretations. *Neuroimage* 52, 1059–1069. doi: 10.1016/j.neuroimage.2009.10.003
- Sandi, C., Davies, H. A., Cordero, M. I., Rodríguez, J. J., Popov, V. I., and Stewart, M. G. (2003). Rapid reversal of stress induced loss of synapses in CA3 of rat hippocampus following water maze training. *Eur. J. Neurosci.* 17, 2447–2456. doi: 10.1046/j.1460-9568.2003.02675.x
- Sandi, C., Loscertales, M., and Guaza, C. (1997). Experience-dependent facilitating effect of corticosterone on spatial memory formation in the water maze. *Eur. J. Neurosci.* 9, 637–642. doi: 10.1111/j.1460-9568.1997.tb01412.x
- Schneidman, E., Berry, M. J. II, Segev, R., and Bialek, W. (2006). Weak pairwise correlations imply strongly correlated network states in a neural population. *Nature* 440, 1007–1012. doi: 10.1038/nature04701
- Scholz, J., Klein, M. C., Behrens, T. E. J., and Johansen-Berg, H. (2009). Training induces changes in white-matter architecture. *Nat. Neurosci.* 12, 1370–1371. doi: 10.1038/nn.2412
- Scott, G. A., Terstege, D. J., Vu, A. P., Law, S., Evans, A., and Epp, J. R. (2020). Disrupted Neurogenesis in Germ-Free Mice: Effects of Age and Sex. *Front. Cell Dev. Biol.* 8:407. doi: 10.3389/fcell.2020.00407
- Sheffield, J. M., Repovs, G., Harms, M. P., Carter, C. S., Gold, J. M., MacDonald, A. W. III, et al. (2016). Evidence for Accelerated Decline of Functional Brain Network Efficiency in Schizophrenia. *Schizophr. Bull.* 42, 753–761. doi: 10.1093/schbul/sbv148
- Silva, B. A., Burns, A. M., and Gräff, J. (2019). A cFos activation map of remote fear memory attenuation. *Psychopharmacology* 236, 369–381. doi: 10.1007/s00213-018-5000-y
- Spaniswick, S. C., Epp, J. R., Keith, J. R., and Sutherland, R. J. (2007). Adrenalectomy-induced granule cell degeneration in the hippocampus causes spatial memory deficits that are not reversed by chronic treatment with corticosterone or fluoxetine. *Hippocampus* 17, 137–146. doi: 10.1002/hipo.20252
- Sporns, O., and Honey, C. J. (2006). Small worlds inside big brains. *Proc. Natl. Acad. Sci. U.S.A.* 103, 19219–19220. doi: 10.1073/pnas.0609523103
- Srivishagan, S., Perera, A. A. I., Hojjat, A., and Ratnarajah, N. (2020). Brain Network Measures for Groups of Nodes: Application to Normal Aging and Alzheimer's Disease. *Brain Connect* 10, 316–327. doi: 10.1089/brain.2020.0747
- Takeuchi, H., Taki, Y., Nouchi, R., Sekiguchi, A., Kotozaki, Y., Nakagawa, S., et al. (2017). Neural plasticity in amplitude of low frequency fluctuation, cortical hub construction, regional homogeneity resulting from working memory training. *Sci. Rep.* 7:1470. doi: 10.1038/s41598-017-01460-6
- Teather, L. A., Packard, M. G., Smith, D. E., Ellis-Behnke, R. G., and Bazan, N. G. (2005). Differential induction of c-Jun and Fos-like proteins in rat hippocampus and dorsal striatum after training in two water maze tasks. *Neurobiol. Learn. Mem.* 84, 75–84. doi: 10.1016/j.nlm.2005.03.006
- van den Heuvel, M. P., Stam, C. J., Kahn, R. S., and Hulshoff Pol, H. E. (2009). Efficiency of functional brain networks and intellectual performance. *J. Neurosci.* 29, 7619–7624. doi: 10.1523/JNEUROSCI.1443-09.2009
- Vetere, G., Kenney, J. W., Tran, L. M., Xia, F., Steadman, P. E., Parkinson, J., et al. (2017). Chemogenetic Interrogation of a Brain-wide Fear Memory Network in Mice. *Neuron* 94, 363–374.e4. doi: 10.1016/j.neuron.2017.03.037
- Watts, D. J., and Strogatz, S. H. (1998). Collective dynamics of “small-world” networks. *Nature* 393, 440–442. doi: 10.1038/30918
- West, G. L., Zendel, B. R., Konishi, K., Benady-Chorney, J., Bohbot, V. D., Peretz, I., et al. (2017). Playing Super Mario 64 increases hippocampal grey matter in older adults. *PLoS One* 12:e0187779. doi: 10.1371/journal.pone.0187779
- Wheeler, A. L., Teixeira, C. M., Wang, A. H., Xiong, X., Kovacevic, N., Lerch, J. P., et al. (2013). Identification of a functional connectome for long-term fear memory in mice. *PLoS Comput. Biol.* 9:e1002853. doi: 10.1371/journal.pcbi.1002853
- Zhan, J., Gurung, S., and Parsa, S. P. K. (2017). Identification of top-K nodes in large networks using Katz centrality. *J. Big Data* 4:16. doi: 10.1186/s40537-017-0076-5
- Zhang, R., Kranz, G. S., Zou, W., Deng, Y., Huang, X., Lin, K., et al. (2020). Rumination network dysfunction in major depression: A brain connectome study. *Prog. Neuropsychopharmacol. Biol. Psychiatry* 98:109819. doi: 10.1016/j.pnpbp.2019.109819





## OPEN ACCESS

## EDITED BY

Lars Michels,  
University of Zurich, Switzerland

## REVIEWED BY

Mikaela A. Laine,  
Northeastern University, United States  
Raimo Kalevi Rikhard Salokangas,  
University of Turku, Finland

## \*CORRESPONDENCE

Bin Xu  
✉ tjkdxbu@tust.edu.cn

## SPECIALTY SECTION

This article was submitted to  
Emotion Regulation and Processing,  
a section of the journal  
Frontiers in Behavioral Neuroscience

RECEIVED 24 April 2022

ACCEPTED 01 February 2023

PUBLISHED 22 February 2023

## CITATION

Xu B, Wei S, Yin X, Jin X, Yan S and Jia L (2023)  
The relationship between childhood emotional  
neglect experience and depressive symptoms  
and prefrontal resting functional connections in  
college students: The mediating role of  
reappraisal strategy.  
*Front. Behav. Neurosci.* 17:927389.  
doi: 10.3389/fnbeh.2023.927389

## COPYRIGHT

© 2023 Xu, Wei, Yin, Jin, Yan and Jia. This is an  
open-access article distributed under the terms  
of the [Creative Commons Attribution License](https://creativecommons.org/licenses/by/4.0/)  
(CC BY). The use, distribution or reproduction  
in other forums is permitted, provided the  
original author(s) and the copyright owner(s)  
are credited and that the original publication in  
this journal is cited, in accordance with  
accepted academic practice. No use,  
distribution or reproduction is permitted which  
does not comply with these terms.

# The relationship between childhood emotional neglect experience and depressive symptoms and prefrontal resting functional connections in college students: The mediating role of reappraisal strategy

Bin Xu\*, Shilin Wei, Xiaojuan Yin, Xiaokang Jin, Shizhen Yan and  
Lina Jia

Faculty of Psychology, Tianjin Normal University, Tianjin, China

Childhood emotional neglect (CEN) has a relatively high incidence rate and substantially adverse effects. Many studies have found that CEN is closely related to emotion regulation and depression symptoms. Besides, the functional activity of the prefrontal lobe may also be related to them. However, the relationships between the above variables have not been thoroughly studied. This study recruited two groups of college students, namely, those with primary CEN (neglect group) and those without childhood trauma (control group), to explore the relationships among CEN, adulthood emotion regulation, depressive symptoms, and prefrontal resting functional connections. The methods used in this study included the Childhood Trauma Questionnaire (CTQ), Emotion Regulation Questionnaire (ERQ), Beck Depression Inventory-II (BDI-II) and resting-state functional magnetic resonance imaging (rs-fMRI). The results showed that compared with the control group, the neglect group utilized the reappraisal strategy less frequently and displayed more depressive symptoms. The prefrontal functional connections with other brain regions in the neglect group were more robust than those in the control group using less stringent multiple correction standards. Across the two groups, the functional connection strength between the right orbitofrontal gyrus and the right middle frontal gyrus significantly negatively correlated with the ERQ reappraisal score and positively correlated with the BDI-II total score; the ERQ reappraisal score wholly mediated the relationship between the functional connection strength and the BDI-II total score. It suggests that primary CEN may closely correlate with more depressive symptoms in adulthood. Furthermore, the more robust spontaneous activity of the prefrontal lobe may also be closely associated with more depressive symptoms by utilizing a reappraisal strategy less frequently.

## KEYWORDS

childhood emotional neglect, reappraisal strategy, depressive symptoms, resting-state functional magnetic resonance, college student

## 1. Introduction

Childhood emotional neglect (CEN) refers to the failure to meet children's basic emotional needs, the lack of emotional response to children's pain, the inability to take into account children's social needs, and the expectation that they will deal with situations beyond their maturity or insecurity (Teicher and Samson, 2013). Several studies have identified CEN

as a relatively common subtype of childhood trauma with a relatively high incidence rate and substantially adverse effects (Finkelhor et al., 2013; Dias et al., 2015; Shen et al., 2015; Maguire and Naughton, 2016; Taillieu et al., 2016).

Many studies have indicated that CEN is closely related to emotion regulation and depression symptoms. For instance, Huh et al. (2017) demonstrated that adaptive emotion regulation strategies significantly mediated the relationship between CEN and depressive symptoms. According to a study by O'Mahen et al. (2015), there was a strong correlation between the CEN score and the avoidance strategy score. This strategy significantly mediated the relationship between CEN and depressive symptoms. In addition, Wang et al. (2017) also demonstrated a significant negative correlation between CEN and reappraisal strategies in patients with depression. These studies suggest that CEN may change the tendency to utilize emotion regulation strategies in adulthood, which may be an essential reason that CEN leads to depression. Early adulthood, especially the college stage when one first leaves home life, is an important period for individuals to develop their emotion regulation ability. Exploring the relationship between CEN and college students' emotion regulation and depressive symptoms will help prevent and intervene in college students' depressive symptoms.

In addition, some studies have suggested that the CEN experience of individuals may alter not only the behaviors related to adulthood emotion regulation but also the functional activity of the brain associated with emotion regulation. Resting-state functional magnetic resonance imaging (rs-fMRI) does not require experimental tasks. Therefore, the observed individual differences in spontaneous BOLD signal fluctuations are not disturbed by experimental manipulation differences when using rs-fMRI, which reflects the inherent characteristics of a particular brain activity. In conclusion, it can be purer to explore the state-dependent brain functional differences between individuals (Tavor et al., 2016). Using rs-fMRI, Wang et al. (2014) discovered significant negative correlations between CEN and the functional connections of the bilateral thalamus and also the dorsolateral and medial prefrontal gyrus in adults with major depression. Fadel et al. (2021) found that CEN experience was correlated with decreased functional connections within the salience network and increased functional connections between the salience network and the default mode network in adults with major depression. Based on the region of interest analysis, Souza-Queiroz et al. (2016) found that CEN significantly negatively correlated with the abnormal functional connections between the left ventromedial prefrontal lobe and amygdala in adults with bipolar disorder. These studies found a close relationship between CEN and prefrontal functional connections in adults with severe depressive symptoms. The prefrontal cortex has been consistently implicated in perceiving and understanding emotional information and cognitive and attentional control (Li et al., 2020a,b). Abnormal prefrontal cortex functional activities have been reported in a large number of studies to closely correlate with difficulties in emotion regulation and emotional disorders (Wager et al., 2008; Kanske et al., 2011; Rabinak et al., 2014; Koch et al., 2016; Yang et al., 2020). In addition, because the region of interest analysis can avoid the possibility of false-negative results caused by numerous multiple comparison

corrections (the brain is divided into more than 6,000 voxels) in whole-brain analyses, it may better detect small but meaningful differences (Poldrack, 2007; Price et al., 2021).

Finally, we conclude that CEN may be closely linked to the tendency to utilize emotion regulation strategies, depressive symptoms, and changes in prefrontal functional connections in adults. However, the limitations of existing literature in the screening of subjects restrict the validity of the results. As can be seen, the adults with childhood trauma in the aforementioned literature were mostly accompanied by severe physical or psychological disorders (Wang et al., 2014; Souza-Queiroz et al., 2016; Fadel et al., 2021). Moreover, even healthy control adults experienced some childhood trauma (including CEN) (Wang et al., 2014; Souza-Queiroz et al., 2016). Furthermore, some studies suggested that the relationship between CEN and emotion regulation, depressive symptoms, and brain functional activity might be specific to other childhood trauma subtypes. For example, Huh et al. (2017) demonstrated that only CEN, but not other childhood trauma subtypes, could lead to more depressive symptoms causing less frequent utilization of adaptive emotion regulation strategies. Similarly, O'Mahen et al. (2015) found that only CEN could exacerbate depressive symptoms through avoidance strategies. Dannlowski et al. (2013) discovered that just CEN, rather than other childhood trauma subtypes, was the most critical predictor of abnormal brain activity when individuals watched sad faces. The latter has been linked to many negative emotional symptoms. Thus, further research is needed to investigate whether there is a strong relationship between primary CEN experience and emotion regulation strategies, depressive symptoms, and resting state prefrontal functional connectivity abnormalities in healthy college students without psychological disorders, with interference from other traumatic experiences excluded whenever possible.

Accordingly, the present study aims to explore the relationships among primary CEN, the tendency to utilize emotion regulation strategies, depressive symptoms, and resting state prefrontal functional connections by combining Childhood Trauma Questionnaire (CTQ), Emotion Regulation Questionnaire (ERQ), Baker Depression Inventory-II (BDI-II), and rs-fMRI. First, two groups of healthy college students with primary CEN (neglect group) and no childhood trauma (control group) were screened by evaluating CTQ and clinical interviews by psychiatrists. Second, between the two groups, ERQ and BDI-II were used to investigate the differences in the tendency to utilize emotion regulation strategies and depressive symptoms, and rs-fMRI was used to investigate the differences in prefrontal functional connections. Finally, combined with the questionnaire and imaging data, the potential mediating role of emotion regulation strategies in the relationship between prefrontal functional connections and depressive symptoms was explored.

This study's hypotheses are as follows: (1) The neglect group may utilize the adaptive strategy (reappraisal) less frequently and have more depressive symptoms; (2) There may be significant differences in prefrontal functional connections with other brain regions between the two groups; and (3) The prefrontal functional connections with other brain regions may be significantly correlated with the scores of emotion regulation strategies and

depressive symptoms, and emotion regulation strategies may mediate the relationship between the above functional connections and depressive symptoms.

## 2. Methods

### 2.1. Participants

Potential participants were screened by the online survey from March to June 2020. A total of 5,010 college students from four universities in Tianjin, China, participated in the survey. The content included Childhood Trauma Questionnaire (CTQ) and relevant demographic information (age, gender, student origin distribution, and whether only child). There were 4,566 questionnaires with complete details that were carefully answered, with an effective completion rate of 91.14%. After a minimum of 1 month, video interviews were conducted with potential participants identified in the initial investigation, including the retesting of CTQ, screening for mental illness, and significant physical hazards [completed jointly by two attending psychiatrists according to the DSM-IV-TR Axis I Clinical Examination Patient Edition for Disorders (SCID-I/P)].

The cutoff scores of CTQ subscales recommended by relevant studies were used as the basis for screening the two groups of participants for a formal experiment (Sáez-Francàs et al., 2015; Lu et al., 2016; Frodl et al., 2017; Kim et al., 2018; Peters et al., 2018; Wu et al., 2021). The inclusion criteria for the neglect group were as follows: emotional neglect  $\geq 15$ , emotional abuse  $< 12$ , physical abuse  $< 9$ , sexual abuse  $< 7$ , and physical neglect  $< 9$ ; for the control group: emotional neglect, emotional abuse, physical abuse, sexual abuse, and physical neglect all scored a minimum of 5. All the above results were consistent across two CTQ assessments for each group. Exclusion criteria for both groups were (1) any mental disorder that met the diagnostic criteria for the DSM-IV-TR axis I; (2) severe physical diseases, such as hypertension, diabetes, heart disease, thyroid disease, and basic metabolic diseases; (3) head injury with coma lasting for more than 5 min; (4) epilepsy or febrile seizures; (5) receiving or having received electroconvulsive, acupuncture, and other physical therapy; (6) being pregnant or planning to be pregnant; and (7) contraindications for MRI.

The final number of participants was 21 in the neglect group (10 male participants,  $19.19 \pm 0.68$  years old) and 26 in the control group (13 male participants,  $19.04 \pm 0.87$  years old). All the participants signed the informed consent and received specific remuneration after the study. The ethics committee of Tianjin Normal University approved the experimental scheme.

## 2.2. Questionnaire

### 2.2.1. Childhood trauma

The childhood trauma of college students was assessed using the Chinese version of the Childhood Trauma Questionnaire-Short Form (CTQ-SF, Bernstein et al., 2003), translated and revised by Zhao et al. (2005). It is a retrospective self-assessment questionnaire with 28 items, assessing five factors, namely, emotional abuse, physical abuse, sexual abuse, emotional neglect, and physical

neglect. Each factor contains five items; each is rated on a five-point Likert scale from 1 (never) to 5 (always). The higher the subscale scores and total score are, the more serious the individual's childhood trauma is. The Chinese version was tested on 819 high school students, and the reliability and validity were good (Zhao et al., 2005). In this study, Cronbach's  $\alpha$  coefficient of the total scale was 0.80.

### 2.2.2. Emotion regulation strategies

The emotion regulation strategies of college students were assessed using the Chinese version of the Emotion Regulation Questionnaire (ERQ, Gross and John, 2003), translated and revised by Wang et al. (2007). It is a retrospective self-assessment questionnaire with 10 items, assessing two factors: reappraisal and suppression. The reappraisal factor contains six items and the suppression factor contains four items; each is rated on a seven-point Likert scale from 1 (strongly disagree) to 7 (strongly agree). The higher each subscale score is, the more likely the individual will utilize this strategy. The Chinese version was tested on 1,163 college students, and the reliability and validity were good (Wang et al., 2007). In this study, Cronbach's  $\alpha$  coefficient of the reappraisal was 0.86 and the suppression was 0.71.

### 2.2.3. Depressive symptoms

The depressive symptoms of college students were assessed using the Chinese version of the Beck Depression Inventory-II (BDI-II, Beck et al., 1996), translated and revised by Yang et al. (2014). It is a retrospective self-assessment questionnaire with 21 items, assessing two factors, namely, cognitive-affective and somatic. The cognitive-affective factor contains 16 items, and the somatic factor contains five items; each is rated on a four-point Likert scale from 0 (no symptoms) to 4 (pronounced symptoms). The higher the subscales scores and total score are, the more serious the individual's depressive symptoms are. The Chinese version was tested on 2,797 college students, and the reliability and validity were good (Wang et al., 2018). In this study, Cronbach's  $\alpha$  coefficient of the total scale was 0.90.

### 2.2.4. Socioeconomic status in childhood

Previous studies have found that childhood socioeconomic status represented by family economic status, education level, and work status of the father and mother may be associated with changes in adulthood brain functional activities (Ly et al., 2011; Neville et al., 2013; Muscatell, 2018). Therefore, parent's education level and work status and also the subjective perceived family economic status during childhood were additionally collected as covariates in the following analysis of brain function to exclude the interference of the differences between groups in childhood socioeconomic status on the results. According to the study of Luo and Waite (2005), parents' education level was divided into six dimensions: 1 = none, 2 = primary school, 3 = junior middle school, 4 = high school or technical secondary school, 5 = university or junior college, and 6 = master's degree or above. Parents' work status was divided into seven dimensions: 1 = none, 2 = education system, 3 = health system, 4 = state-owned enterprises, 5 = government departments, 6 = private enterprises,

and 7 = others. The subjective perceived family economic status was divided into three dimensions: 1 = poor, 2 = medium, and 3 = rich.

## 2.3. Resting-state fMRI data collection and preprocessing

### 2.3.1. Data collection

All the rs-fMRI data were collected at Tianjin Normal University. ERQ and BDI-II were completed before fMRI scanning using the Siemens MAGNETOM Prisma 3.0T Scanner and 64-channel head coil. The participants were supine and we placed a sponge pad inside the coil to fix their heads. They were asked to keep their heads and bodies still and their eyes focused on the cross on the screen without systematic thinking. For the resting state functional imaging, AB11\_bold\_rest sequence and sagittal scanning were used, TR = 2,000 ms, TE = 30 ms, FA = 90°, FOV = 224 × 224 mm, matrix = 112 × 112, voxel size = 2 × 2 × 2 mm, slices = 75, slice thickness = 2 mm, no interval, time points = 240, and acceleration factor = 3. The acquisition time was 495 s. For the whole brain structural imaging, AB11\_t1iso\_mprage sequence and sagittal scanning were used; TR = 2,530 ms, TE = 2.98 ms, FA = 7°, FOV = 256 × 256 mm, matrix = 256 × 256, voxel size = 1 × 1 × 1 mm, slices = 192, slice thickness = 1 mm, no interval. The acquisition time was 363 s.

### 2.3.2. Data preprocessing

DPABI V4.3 (<http://rfmri.org/dpabi>) was used for data preprocessing. The steps included are as follows: (1) The images were retained in the NIFTI format; (2) The first 10 time points were deleted; (3) Slice-time correction, considering that rs-fMRI adopted the sequence with acceleration factor = 3, MATLAB R2015b (MathWorks, <http://www.mathworks.com/>) was used to find the reference time point of each participant, then SPM12 (<http://www.fil.ion.ucl.ac.uk/spm>) was used to conduct slice-time correction according to the reference time point; (4) Motion correction, the data that translation exceeds 1.5 mm and rotation exceeds 1.5° were deleted (two in the neglect group and one in the control group, see Appendix 1 for details); (5) Normalization, DARTEL was used to normalize functional images into Montreal Neurological Institute (MNI) space: the structural images of each participant were registered into the average functional images, and then the structural images were divided into gray matter, white matter, and cerebrospinal fluid, so a matrix was generated; finally, the functional images were normalized to the MNI standard space by using the matrix generated when the structural images were segmented with resampling voxel size = 2 × 2 × 2 mm; and (6) spatial smoothing (FWHM = 6 × 6 × 6 mm).

## 3. Statistical analysis

### 3.1. Demographic and questionnaire data analysis

SPSS 25.0 (IBM Corporation, Armonk, NY, USA) was used to conduct an independent sample *T*-test for the age of the two groups

( $p < 0.05$ ) and a chi-square test for other demographic variables ( $p < 0.05$ ). An independent sample *t*-test was conducted for the CTQ subscales scores, BDI-II total score, and ERQ reappraisal and suppression scores ( $p < 0.05$ ).

### 3.2. Functional connection analysis of the prefrontal lobe and its correlation and mediation analysis with questionnaire data

#### 3.2.1. Extracting PFC subregions as ROI

According to the Brainnetome Atlas (BN Atlas) developed by the Brainnetome Center, Institute of Automation, Chinese Academy of Sciences (<http://atlas.brainnetome.org>, see Appendix 2 for details), we marked all the 68 subregions of PFC (BN1-68). After that, REST V1.8 (<http://www.restfmri.net/forum>) was used to extract binary masks for these subregions of ROI.

#### 3.2.2. Voxel-wise functional connection analysis

(1) After smoothing, the data were used to extract and remove covariates (including linear drift trend, Friston 24 head parameters, cerebrospinal fluid, and white matter), and then band-pass was filtered (0.01~0.1 Hz). ROIs were the aforementioned 68 subregions of PFC extracted from the BN Atlas. The average time series of all the ROIs of the two groups were extracted, their linear correlation coefficients with the voxels of the whole brain were calculated, and then Fisher-*z* transformation to obtain the zFC statistical map was conducted. (2) A total of 10 items of FD Jenkinson head movement parameters, age, gender, whether only child, student origin distribution, education level, work status of parents, and subjective perceived family economic status in childhood were taken as covariates (the same below), and two-sample *t*-test was conducted on the zFC statistical map of each ROI of the two groups using SPM12. Two methods, “family wise error rate” (FWE,  $p < 0.05$ ) and “false discovery rate” (FDR,  $p < 0.05$ ), were used for multiple corrections as the first and second options. If the results cannot pass the above multiple corrections, according to previous studies (Petersen et al., 2017; Lin et al., 2020; Schneider et al., 2021), the method “a threshold of  $p < 0.001$  (uncorrected at the voxel level) followed by an empirically determined threshold of  $p < 0.05$  (FWE at the extent level)” was used as the third option. All the clusters with significant differences between the two groups were labeled according to the BN Atlas and compared with AAL (Anatomical Automatic Labeling) using xjView. (3) Taking the central coordinate of the above clusters with significant differences between the two groups as the center of the circle and 3 mm as the radius, DPABI V4.3 was used to extract the zFC values of the clusters. The correlation analysis was conducted with the questionnaire data (the ERQ reappraisal and suppression scores, and the BDI-II total score), controlling all covariates (Bonferroni correction). (4) If some zFC values were significantly correlated with the ERQ reappraisal or suppression score and BDI-II total score simultaneously, the BDI-II total score was taken as the dependent variable and the zFC values and ERQ reappraisal or suppression scores were taken as the independent and mediating variables, respectively; in turn, a mediation analysis was conducted controlling all covariates.



TABLE 1 Differences in questionnaire data between the two groups ( $n = 47$ ).

Variables	Neglect group ( $n = 21$ )		Control group ( $n = 26$ )		Cohen's $d$	$t$	$p$
	$n$	$M \pm SD$	$n$	$M \pm SD$			
CTQ:CEN	21	$16.00 \pm 1.22$	26	$5.00 \pm 0.00$	12.751	45.918	<0.001
CTQ:emotional abuse		$8.10 \pm 2.43$		$5.00 \pm 0.00$	1.804	6.520	<0.001
CTQ:physical abuse		$6.05 \pm 1.40$		$5.00 \pm 0.00$	1.061	3.838	<0.001
CTQ:sexual abuse		$5.52 \pm 0.81$		$5.00 \pm 0.00$	0.908	3.292	0.002
CTQ:physical neglect		$7.76 \pm 1.34$		$5.00 \pm 0.00$	2.913	10.553	<0.001
ERQ:reappraisal		$27.29 \pm 5.02$		$34.08 \pm 5.47$	-1.293	-4.388	<0.001
ERQ:suppression		$15.57 \pm 4.65$		$13.85 \pm 4.75$	0.366	1.250	0.218
BDI-II:total		$16.38 \pm 7.43$		$4.19 \pm 4.32$	2.001	7.031	<0.001

## 4. Results

### 4.1. Differences in demographic and questionnaire data between the two groups

#### 4.1.1. Differences in demographic data between the two groups

There was no significant difference between the two groups regarding age, gender, whether only child, student origin distribution, parents' education level, and work status in childhood ( $p > 0.05$ ). However, there were significant differences in subjective perceived family economic status in childhood ( $p = 0.005$ ) (see [Appendix 3](#) for details).

#### 4.1.2. Differences in questionnaire data between the two groups

As shown in [Table 1](#), all CTQ subscales scores and the BDI-II total score in the neglect group were significantly higher than those in the control group ( $p < 0.001$ ), and the ERQ reappraisal score was significantly lower than that in the control group ( $p < 0.001$ ). There was no significant difference in the ERQ suppression score between the two groups ( $p > 0.05$ ).

#### 4.1.3. Correlation and linear regression analysis of questionnaire data

Controlling all covariates, partial correlation analysis showed that only the ERQ reappraisal score was significantly negatively correlated with the BDI-II total score ( $r = -0.597$ ,  $p_{\text{correction}} < 0.001$ ). In contrast, the ERQ suppression score was not significantly correlated with the BDI-II total score ( $r = -0.032$ ,  $p_{\text{correction}} > 0.05$ ).

Controlling all covariates, linear regression analysis further proved that the ERQ reappraisal score was significantly negatively correlated with the BDI-II total score [ $\text{Beta} = -0.698$ ,  $t = -5.401$ ,  $p < 0.001$ , 95.0% confidence interval ( $-1.310$ ,  $-0.586$ )].

### 4.2. Differences in the functional connections of PFC subregions between the two groups and the correlation with questionnaire data

#### 4.2.1. Differences in the functional connections of PFC subregions between the two groups

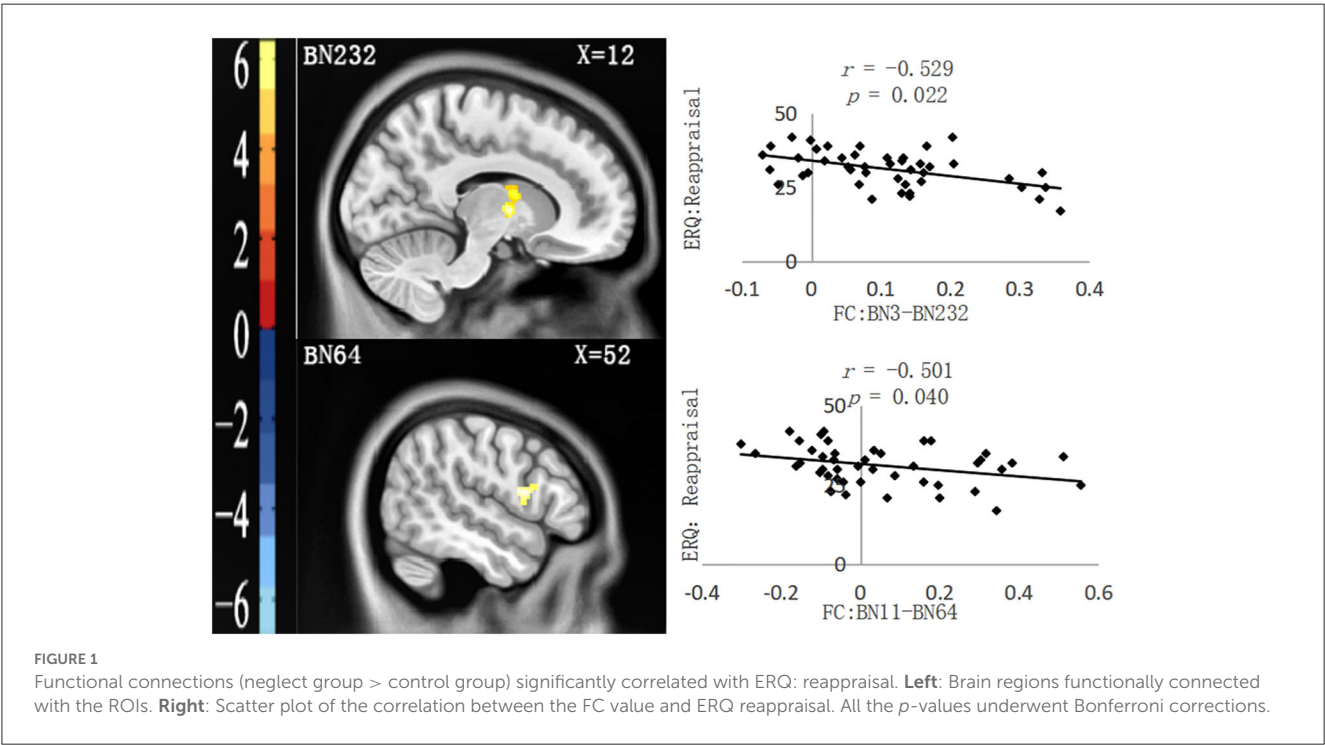
There was no significant difference between the two groups that could pass the multiple corrections of FWE and FDR. However, some clusters with significant differences between the two groups could pass the multiple corrections of the third method [ $p < 0.001$  (uncorrected at the voxel level) followed by  $p < 0.05$  (FWE at the extent level)]. In addition, the results indicated that BN7 (with BN179 and BN122), BN40 (with BN12 and BN51), BN46 (with BN22 and BN166), BN3 (with BN232), BN8 (with BN3), BN11 (with BN64), BN12 (with BN64), BN16 (with BN3), BN20 (with BN46), BN36 (with BN204), BN38 (with BN3), BN39 (with BN62), BN42 (with BN23), BN44 (with BN64), BN47 (with BN221), and BN52 (with BN204) showed more robust functional connections in the neglected group than those in the control group (see [Appendix 4](#) for details).

#### 4.2.2. Correlation between the functional connections of PFC subregions and questionnaire data

As shown in [Table 2](#), four functional connection values between PFC subregions and other brain regions significantly correlated with questionnaire data. After controlling for all covariates, partial correlation analysis showed that two functional connection values were only significantly negatively correlated with the ERQ reappraisal score, namely, FC: BN3–BN232 (the right thalamus in the AAL Atlas) and FC: BN11–BN64 (the right Rolandic oper in the AAL Atlas), as shown in [Figure 1](#). Moreover, two functional connection values were significantly negatively correlated with the ERQ reappraisal score and significantly positively correlated with the BDI-II total score, namely, FC: BN12–BN64 (right Rolandic Oper in AAL Atlas) and FC: BN46–BN22 (right Frontal Mid in AAL Atlas), as shown in [Figure 2](#). Functional

TABLE 2 Functional connections (neglect group > control group) significantly correlated with the questionnaire data (n = 45).

ROI	Brain regions functionally connected with the ROI		Voxels	t	MNI coordinates (x, y, z)
	Label ID	Gyrus			
BN3 (Left superior frontal gyrus)	232	Right thalamus	208	5.92	12, -2, 4
BN11 (Left superior frontal gyrus)	64	Right precentral gyrus	126	4.61	52, 8, 14
BN12 (Right superior frontal gyrus)	64	Right precentral gyrus	232	6.30	52, 8, 14
BN46 (Right orbital gyrus)	22	Right middle frontal gyrus	236	5.69	44, 56, 6



connection values were not significantly correlated with the ERQ suppression score.

According to the results of partial correlation analysis, taking the ERQ reappraisal score and the BDI-II total score as dependent variables, the functional connection values significantly correlated with the two scores and all the covariates as common independent variables, and a linear regression analysis was conducted. It was found that only FC: BN46–BN22 was significantly negatively correlated with the ERQ reappraisal score [ $\text{Beta} = -0.603$ ,  $t = -3.312$ ,  $p = 0.004$ , 95.0% confidence interval ( $-31.037$ ,  $-7.001$ )] and significantly positively correlated with the BDI-II total score [ $\text{Beta} = 0.477$ ,  $t = 2.750$ ,  $p = 0.012$ , 95.0% confidence interval ( $5.013$ ,  $36.131$ )].

The results of linear regression analysis indicated that by taking FC: BN46–BN22 as the independent variable, the BDI-II total score as the dependent variable, and the ERQ reappraisal score as the mediating variable, a mediation analysis was conducted, controlling all covariates. The indirect and total effects were significant, suggesting that the ERQ

reappraisal score wholly mediated the relationship between FC: BN46–BN22 and the BDI-II total score, as seen in Figure 3.

Logically speaking, the functional connections of PFC may also mediate the relationship between the ERQ reappraisal score and the BDI-II total score, so the following steps were attempted. By taking the ERQ reappraisal score as the independent variable, the BDI-II total score as the dependent variable, and FC: BN46–BN22 as the mediating variable, a mediation analysis was conducted, controlling all covariates. The results showed that FC: BN46–BN22 could not mediate the relationship between the ERQ reappraisal score and the BDI-II total score, as shown in Appendix 5.

## 5. Discussion

This study investigated the relationships between the tendency to utilize emotion regulation strategies, depressive symptoms, and the functional connections of the PFC in college students with

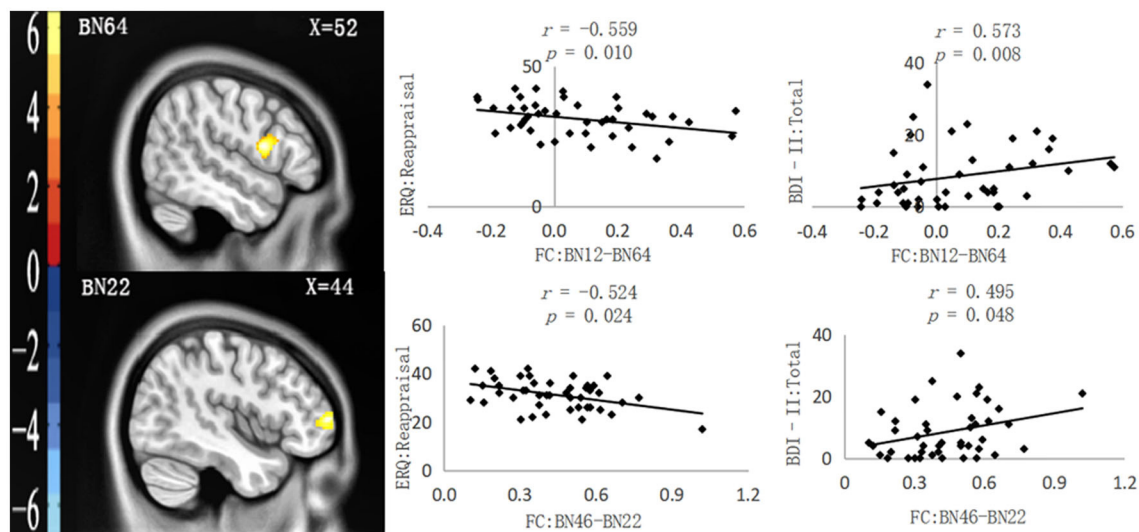


FIGURE 2

Functional connections (neglect group > control group) significantly correlated with ERQ: Reappraisal and BDI-II: Total. **Left:** Brain regions functionally connected with the ROIs. **Right:** Scatter plot of the correlation between the FC value and ERQ reappraisal and BDI-II: Total. All the  $p$ -values underwent Bonferroni corrections.

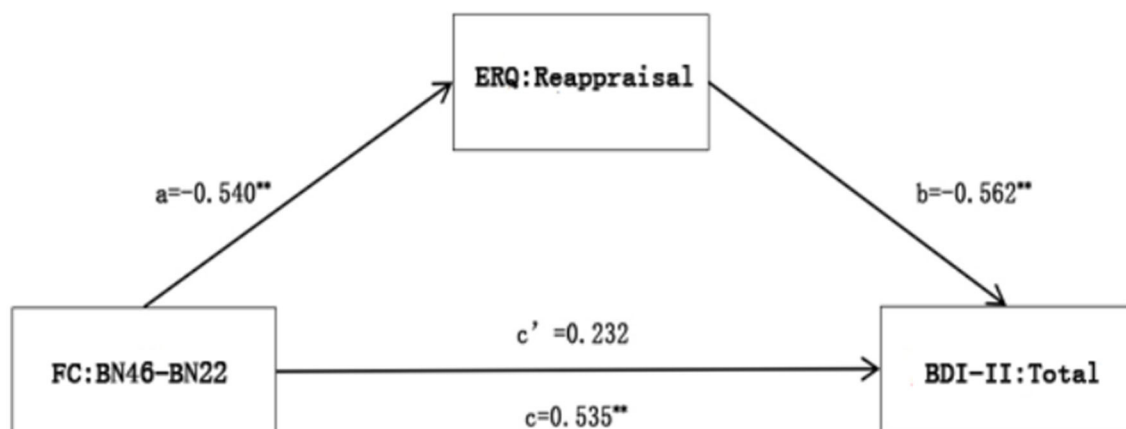


FIGURE 3

A mediation analysis of FC: BN46-BN22 with ERQ reappraisal and BDI-II total.  $**p < 0.01$ .

primary CEN, based on a questionnaire survey and the rs-fMRI technique. The questionnaire survey results showed that the BDI-II total score in the neglect group was significantly higher than that in the control group, and the ERQ reappraisal score in the neglect group was considerably lower than that in the control group. However, the two groups had no significant difference in the ERQ suppression score. Brain-behavior correlation analysis revealed that the functional connection value of BN46 with BN22 was significantly negatively correlated with the ERQ reappraisal score and significantly positively correlated with the BDI-II total score; the ERQ reappraisal score was significantly negatively correlated with the BDI-II total score. The ERQ reappraisal score wholly mediated the relationship between the functional connection of BN46 with BN22 and the BDI-II total score.

## 5.1. Relationships among primary CEN, emotion regulation, and depressive symptoms

Shipman et al. (2005) found that children who experienced chronic emotional neglect tended to develop psychological disorders in adulthood due to the less utilization of adaptive emotion regulation skills such as reappraisal. Wang et al. (2017) also found that adults with depression had experienced CEN, and this experience was correlated with the tendency to utilize adaptive emotion regulation strategies less frequently. These results provide a reliable basis for the view that relationships may exist between CEN, the tendency to utilize emotion regulation strategies, and depressive symptoms in adulthood. In the present study, taking

healthy college students with primary CEN, the BDI-II total score in the neglect group was significantly higher than that in the control group, and the ERQ reappraisal score was considerably lower than that in the control group. Moreover, the ERQ reappraisal score was significantly negatively correlated with the BDI-II total score, further verifying the above views.

According to Gross's emotion regulation process model, reappraisal may be more adaptive and protective than suppression. Reappraisal is one of the antecedent-focused emotion regulation strategies because it focuses on helping individuals reinterpret and understand the nature and significance of the situation or stimulus that triggers their emotions and makes them take action at the early stage of the emotion generation process (Gross, 2002). The aforementioned characteristics of reappraisal make it possible to effectively control improper emotional expression, improve the bad subjective emotional experience, and simultaneously reduce an excessive emotional physiological response (Gross, 1998; Ochsner et al., 2002; Ray et al., 2010; Kim and Hamann, 2012). Individuals who often use the reappraisal strategy have better emotional and mental health (Gross and John, 2003). Compared with reappraisal, suppression may only forcibly reduce the impulse of negative emotional expression. For individuals who often use the suppression strategy, their negative experience and corresponding physiological response may not be effectively improved (Gross and Levenson, 1997; Harris, 2001).

The results suggest that although primary CEN may not necessarily induce depression that meets the clinical diagnostic criteria, it may be more prone to related depression symptoms. Because these individuals may choose the reappraisal strategy less frequently to deal with significant emotional events, it is also necessary for college educators to pay attention to the daily emotional state of these individuals to avoid the occurrence of psychological crises.

## 5.2. The mediating role of the reappraisal strategy in the relationship between the functional connections of PFC and depressive symptoms

Previous studies found that depression patients with CEN had abnormal brain functional connections related to emotion regulation, particularly the PFC (Wang et al., 2014; Souza-Queiroz et al., 2016; Duque-Alarcón et al., 2019). Based on the result from questionnaire data in this study, we further explored the relationships among brain functional connections in the resting state, emotion regulation strategies, and the depressive symptoms of individuals with primary CEN. The results showed that compared with the control group, the neglect group had a more robust functional connection between BN46 (right orbital gyrus) and BN22 (right middle frontal gyrus). The value of the functional connection was significantly negatively correlated with the ERQ reappraisal score and significantly positively correlated with the BDI-II total score. Furthermore, mediation analysis further found that the ERQ reappraisal score wholly mediated the relationship between the functional connection and the BDI-II total score. These findings are the first to fully reveal the relationships among

CEN, emotion regulation strategies, depressive symptoms, and resting-state brain function in adulthood.

It has been suggested that the orbitofrontal cortex (OFC) plays an essential role in receiving and processing emotional information and expressing and controlling dynamic behavior by suppressing unwanted or uncomfortable feelings and related neural activities (Shimamura, 2000). However, some studies revealed that OFC had a top-down suppressing effect on the amygdala affecting negative emotional symptoms (Price, 2007; Salzman and Fusi, 2010). For example, Zhang et al. (2014) found that the functional connections of OFC with the amygdala in patients with MDD were significantly decreased compared with those of the control group. There is growing evidence that the middle frontal gyrus (MFG) could regulate the function of OFC. MFG is a part of the dorsal attention network (DAN), which participates in goal-oriented top-down processing and plays a crucial role in emotion regulation tasks involving high-order cognition (such as utilizing the reappraisal strategy) (Corbetta and Shulman, 2002). The changes in the activity in MFG may affect the evaluation and feedback process of the emotional stimulus of OFC, leading to possible emotional disorders (Ochsner et al., 2004; Eippert et al., 2007). For example, Xu et al. (2017) found that compared with healthy people, people with schizophrenia exhibited a series of cognitive and emotional disorders, and the functional connections of the bilateral orbitofrontal gyrus with right MFG significantly decreased.

Interestingly, this study found the prefrontal functional connection to be significantly positively correlated with the score of depressive symptoms, which was inconsistent with some previous study results. For example, Wang et al. (2014) found that the prefrontal functional connections of patients with MDD significantly got reduced compared with that of healthy people. One possible explanation for these differences is that the subjects in those studies were patients diagnosed with depression or other psychological diseases. In addition, even among patients with depression, the prefrontal lobe activity or the strength of functional connections may not be reduced. Xu et al. (2019) found that compared with healthy people, the ALLF of the left inferior frontal gyrus orbital in patients with MDD significantly increased. It is speculated that the neglect group in this study had more robust prefrontal functional connections and more depressive symptoms, which may be a compensatory mechanism developed by them to offset the increase of depressive symptoms related to CEN.

## 5.3. Limitations

There are some limitations in this study. (1) It is difficult to obtain the dynamic changes of the process of the emotion regulation ability, depressive symptoms, and neural activities during the period of experiencing CEN and later the longer life cycle, especially the relationship between the time factor and the above variables. (2) To manipulate the variable of CEN better, the inclusion criteria of the control group adopted the strict standard of no childhood traumatic experience, but this also blocked the possibility of taking CEN as a continuous variable to investigate its relationship with emotion regulation strategies and depressive symptoms. (3) The data analysis method of rs-fMRI is not comprehensive. For example, the relationships among



brain local functional activities (ALFF and ReHo), the topological attributes of the brain network and emotion regulation strategies, and depressive symptoms have not been investigated. (4) The multiple correction standard used for brain imaging analysis was not stringent enough. In the future, it is necessary to expand the age range of subjects, make more effective screening by the extensive use of multiple tools, and use more comprehensive data analysis methods to explore the relationships among primary CEN and emotion regulation, depressive symptoms, as well as the functional brain activity.

## 6. Conclusion

For the first time, this study investigated the relationships among primary CEN, adulthood emotion regulation strategies, depression symptoms, and prefrontal functional connections. The results showed that college students with primary CEN utilized the reappraisal less frequently and had more depressive symptoms and more robust prefrontal functional connections. Moreover, the tendency to utilize the reappraisal strategy mediated the relationship between prefrontal functional connections and depression symptoms. The results suggest that primary CEN may closely correlate with more depressive symptoms in adulthood. Moreover, the more robust spontaneous activity of the prefrontal lobe may also be closely associated with more depressive symptoms by utilizing the reappraisal strategy less frequently.

## Data availability statement

The raw data supporting the conclusions of this article will be made available by the authors, without undue reservation.

## Ethics statement

The studies involving human participants were reviewed and approved by the Ethics Committee of Tianjin Normal University. The patients/participants provided their written informed consent

to participate in this study. Written informed consent was obtained from the individual(s) for the publication of any potentially identifiable images or data included in this article.

## Author contributions

All authors were involved in the statistical analyses and data collection of the study. All authors contributed and have approved the final manuscript.

## Funding

This research has been extracted from a research project supported by School Mental Health Education Project in Tianjin in 2018 (Grant number: XLZX-G201804).

## Conflict of interest

The authors declare that the research was conducted in the absence of any commercial or financial relationships that could be construed as a potential conflict of interest.

## Publisher's note

All claims expressed in this article are solely those of the authors and do not necessarily represent those of their affiliated organizations, or those of the publisher, the editors and the reviewers. Any product that may be evaluated in this article, or claim that may be made by its manufacturer, is not guaranteed or endorsed by the publisher.

## Supplementary material

The Supplementary Material for this article can be found online at: <https://www.frontiersin.org/articles/10.3389/fnbeh.2023.927389/full#supplementary-material>

## References

- Beck, A. T., Steer, R. A., and Brown, G. K. (1996). *Manual for the Beck Depression Inventory*. San Antonio, TX: Psychological Corporation. doi: 10.1037/t00742-000
- Bernstein, D. P., Stein, J. A., Newcomb, M. D., Walker, E., Pogge, D., Ahluvalia, T., et al. (2003). Development and validation of a brief screening version of the Childhood Trauma Questionnaire. *Child Abuse Neglect*. 27, 169–190. doi: 10.1016/S0145-2134(02)00541-0
- Corbetta, M., and Shulman, G. L. (2002). Control of goal-directed and stimulus-driven attention in the brain. *Nat. Rev. Neurosci.* 3, 201–215. doi: 10.1038/nrn755
- Dannlowski, U., Kugel, H., Huber, F., Stuhrmann, A., Redlich, R., Grotegerd, D., et al. (2013). Childhood maltreatment is associated with an automatic negative emotion processing bias in the amygdala. *Human Brain Map.* 34, 2899–2909. doi: 10.1002/hbm.22112
- Dias, A., Sales, L., Hessen, D. J., and Kleber, R. J. (2015). Child maltreatment and psychological symptoms in a Portuguese adult community sample: the harmful effects of emotional abuse. *Eur Child Adolescent Psychiatry* 24, 767–778. doi: 10.1007/s00787-014-0621-0
- Duque-Alarcón, X., Alcalá-Lozano, R., González-Olvera, J. J., Garza-Villarreal, E. A., and Pellicer, F. (2019). Effects of childhood maltreatment on social cognition and brain functional connectivity in borderline personality disorder patients. *Front. Psychiatry* 10, 156. doi: 10.3389/fpsy.2019.00156
- Eippert, F., Veit, R., Weiskopf, N., Erb, M., Birbaumer, N., Anders, S., et al. (2007). Regulation of emotional responses elicited by threat-related stimuli. *Human Brain Map.* 28, 409–423. doi: 10.1002/hbm.20291
- Fadel, E., Boeker, H., Gaertner, M., Richter, A., Kleim, B., Seifritz, E., et al. (2021). Differential alterations in resting state functional connectivity associated with depressive symptoms and early life adversity. *Brain Sci.* 11, 591. doi: 10.3390/brainsci11050591
- Finkelhor, D., Turner, H. A., Shattuck, A., and Hamby, S. L. (2013). Violence, crime, and abuse exposure in a national sample of children and youth: an update. *JAMA Pediatr.* 167, 614–621. doi: 10.1001/jamapediatrics.2013.42
- Frodl, T., Janowitz, D., Schmaal, L., Tozzi, L., Dobrowolny, H., Stein, D. J., et al. (2017). Childhood adversity impacts on brain subcortical structures relevant to depression. *J. Psychiatric Res.* 86, 58–65. doi: 10.1016/j.jpsychires.2016.11.010

- Gross, J. J. (1998). Antecedent- and response-focused emotion regulation: divergent consequences for experience, expression, and physiology. *J. Personal. Social Psychol.* 74, 224–237. doi: 10.1037/0022-3514.74.1.224
- Gross, J. J. (2002). Emotion regulation: affective, cognitive, and social consequences. *Psychophysiology* 39, 281–291. doi: 10.1017/S0048577201393198
- Gross, J. J., and John, O. P. (2003). Individual differences in two emotion regulation processes: implications for affect, relationships, and wellbeing. *J. Personal. Social Psychol.* 85, 348–362. doi: 10.1037/0022-3514.85.2.348
- Gross, J. J., and Levenson, R. W. (1997). Hiding feelings: the acute effects of inhibiting negative and positive emotion. *J. Abnormal Psychol.* 106, 95–103. doi: 10.1037/0021-843X.106.1.95
- Harris, C. R. (2001). Cardiovascular responses of embarrassment and effects of emotional suppression in a social setting. *J. Personal. Social Psychol.* 81, 886–897. doi: 10.1037/0022-3514.81.5.886
- Huh, H. J., Kim, K. H., Lee, H.-K., and Chae, J.-H. (2017). The relationship between childhood trauma and the severity of adulthood depression and anxiety symptoms in a clinical sample: the mediating role of cognitive emotion regulation strategies. *J. Affect. Disorders* 213, 44–50. doi: 10.1016/j.jad.2017.02.009
- Kanske, P., Heissler, J., Schönfelder, S., Bongers, A., and Wessa, M. (2011). How to regulate emotion? Neural networks for reappraisal and distraction. *Cerebral Cortex* 21, 1379–1388. doi: 10.1093/cercor/bhq216
- Kim, S., Kim, J. S., Jin, M. J., Im, C.-H., and Lee, S.-H. (2018). Dysfunctional frontal lobe activity during inhibitory tasks in individuals with childhood trauma: an event-related potential study. *NeuroImage Clin.* 17, 935–942. doi: 10.1016/j.nicl.2017.12.034
- Kim, S. H., and Hamann, S. (2012). The effect of cognitive reappraisal on physiological reactivity and emotional memory. *Int. J. Psychophysiol.* 83, 348–35. doi: 10.1016/j.ijpsycho.2011.12.001
- Koch, S. B. J., Zuiden, M. V., Nawijn, L., Frijling, J. L., Veltman, D. J., Olff, M., et al. (2016). Intranasal oxytocin normalizes amygdala functional connectivity in posttraumatic stress disorder. *Neuropsychopharmacology*, 41, 2041–2051. doi: 10.1038/npp.2016.1
- Li, J., Biswal, B. B., Meng, Y., Yang, S., Duan, X., Cui, Q., et al. (2020a). A neuromarker of individual general fluid intelligence from the white-matter functional connectome. *Translat. Psychiatry* 10, s41398-020-0829-3 doi: 10.1038/s41398-020-0829-3
- Li, Y., He, L., Zhuang, K., Wu, X., Sun, J., Wei, D., et al. (2020b). Linking personality types to depressive symptoms: a prospective typology based on neuroticism, extraversion and conscientiousness. *Neuropsychologia* 136, 107289. doi: 10.1016/j.neuropsychologia.2019.107289
- Lin, X., Zhou, R., Huang, J., Su, Y., Mao, R., Niu, Z., et al. (2020). Altered resting-state fMRI signals and network topological properties of bipolar depression patients with anxiety symptoms. *J. Affect. Disord.* 277, 358–367. doi: 10.1016/j.jad.2020.08.007
- Lu, S., Gao, W., Wei, Z., Wang, D., Hu, S., Huang, M., et al. (2016). Intrinsic brain abnormalities in young healthy adults with childhood trauma: a resting-state functional magnetic resonance imaging study of regional homogeneity and functional connectivity. *Aust. New Zealand J. Psychiatry* 51, 614–623. doi: 10.1177/0004867416671415
- Luo, Y., and Waite, L. J. (2005). The impact of childhood and adult SES on physical, mental, and cognitive well-being in later life. *J. Gerontol. B Psychol. Sci. Soc. Sci.* 60, S93–S101. doi: 10.1093/geronb/60.2.S93
- Ly, M., Haynes, M. R., Barter, J. W., Weinberger, D. R., and Zink, C. F. (2011). Subjective socioeconomic status predicts human ventral striatal responses to social status information. *Current Biol.* 21, 794–797. doi: 10.1016/j.cub.2011.03.050
- Maguire, S., and Naughton, A. (2016). Neglect: widespread, damaging and difficult to identify. *Paediatr. Child Health* 26, 485–487. doi: 10.1016/j.paed.2016.06.010
- Muscattell, K. A. (2018). Socioeconomic influences on brain function: implications for health. *Ann. N. Y. Acad. Sci.* 1428, 14–32. doi: 10.1111/nyas.13862
- Neville, H. J., Stevens, C., Pakulak, E., Bell, T. A., Fanning, J., Klein, S., et al. (2013). Family-based training program improves brain function, cognition, and behavior in lower socioeconomic status preschoolers. *Proc. Nat. Acad. Sci.* 110, 12138–12143. doi: 10.1073/pnas.1304437110
- Ochsner, K. N., Bunge, S. A., Gross, J. J., and Gabrieli, J. D. (2002). Rethinking feelings: an fMRI study of the cognitive regulation of emotion. *J. Cogn. Neurosci.* 14, 1215–1229. doi: 10.1162/089892902760807212
- Ochsner, K. N., Ray, R. D., Cooper, J. C., Robertson, E. R., Chopra, S., Gabrieli, J. D. E., et al. (2004). For better or for worse: neural systems supporting the cognitive down- and up-regulation of negative emotion. *Neuroimage* 23, 483–99. doi: 10.1016/j.neuroimage.2004.06.030
- O'Mahen, H. A., Karl, A., Moberly, N., and Fedock, G. (2015). The association between childhood maltreatment and emotion regulation: two different mechanisms contributing to depression? *J. Affect. Disord.* 174, 287–295. doi: 10.1016/j.jad.2014.11.028
- Peters, A. T., Burkhouse, K. L., Kinney, K. L., and Phan, K. L. (2018). The roles of early-life adversity and rumination in neural response to emotional faces amongst anxious and depressed adults. *Psychol. Med.* 49, 2267–2278. doi: 10.1017/S0033291718003203
- Petersen, N., Ghahremani, D. G., Rapkin, A. J., Berman, S. M., Liang, L., London, E. D., et al. (2017). Brain activation during emotion regulation in women with premenstrual dysphoric disorder. *Psychol. Med.* 48, 1795–1802. doi: 10.1017/S0033291717003270
- Poldrack, R. A. (2007). Region of interest analysis for fMRI. *Soc. Cogn. Affect. Neurosci.* 2, 67–70. doi: 10.1093/scan/nsm006
- Price, J. L. (2007). Definition of the orbital cortex in relation to specific connections with limbic and visceral structures and other cortical regions. *Ann. N. Y. Acad. Sci.* 1121, 54–71. doi: 10.1196/annals.1401.008
- Price, R. B., and Tervo-Clemmens, B. C. Panny, B., Degutis, M., Griffo, A., Woody, M. (2021). Biobehavioral correlates of an fMRI index of striatal tissue iron in depressed patients. *Translat. Psychiatry* 11, 448. s41398-021-01553-x doi: 10.1038/s41398-021-01553-x
- Rabinak, C. A., MacNamara, A., Kennedy, A. E., Angstadt, M., Stein, M. B., Liberzon, I., et al. (2014). Focal and aberrant prefrontal engagement during emotion regulation in veterans with posttraumatic stress disorder. *Depress. Anxiety* 31, 851–861. doi: 10.1002/da.22243
- Ray, R. D., McRae, K., Ochsner, K. N., and Gross, J. J. (2010). Cognitive reappraisal of negative affect: converging evidence from EMG and self-report. *Emotion* 10, 587–592. doi: 10.1037/a0019015
- Sáez-Francás, N., Calvo, N., Alegre, J., Castro-Marrero, J., Ramírez, N., Hernández-Vara, J., et al. (2015). Childhood trauma in chronic fatigue syndrome: focus on personality disorders and psychopathology. *Compr. Psychiatry*, 62, 13–19. doi: 10.1016/j.comppsy.2015.06.010
- Salzman, C. D., and Fusi, S. (2010). Emotion, cognition, and mental state representation in amygdala and prefrontal cortex. *Ann. Rev. Neurosci.* 33, 173–202. doi: 10.1146/annurev.neuro.051508.135256
- Schneider, I., Neukel, C., Bertsch, K., Fuchs, A., Möhler, E., Zietlow, A., et al. (2021). Early life maltreatment affects intrinsic neural function in mothers. *J. Psychiatr. Res.* 143, 176–182. doi: 10.1016/j.jpsychires.2021.09.004
- Shen, L., Zhang, Y., Liang, W., and Zhang, Y. (2015). Investigation of child maltreatment: survey among junior school pupils in Henan province of China. *Asia Pacific Psychiatry* 7, 85–90. doi: 10.1111/appy.12105
- Shimamura, A. P. (2000). The role of the prefrontal cortex in dynamic filtering. *Psychobiology* 28, 207–218. doi: 10.3758/BF03331979
- Shipman, K., Schneider, R., and Sims, C. (2005). Emotion socialization in maltreating and non-maltreating mother-child dyads: implications for children's adjustment. *J. Clin. Child Adolescent Psychol.* 34, 590–596. doi: 10.1207/s15374424jccp3403\_14
- Souza-Queiroz, J., Boisgontier, J., Etain, B., Poupon, C., Duclap, D., d'Albis, M.-A., et al. (2016). Childhood trauma and the limbic network: a multimodal MRI study in patients with bipolar disorder and controls. *J. Affect. Disord.* 200, 159–164. doi: 10.1016/j.jad.2016.04.038
- Taillieu, T. L., Brownridge, D. A., Sareen, J., and Afifi, T. O. (2016). Childhood emotional maltreatment and mental disorders: results from a nationally representative adult sample from the United States. *Child Abuse Neglect* 59, 1–12. doi: 10.1016/j.chiabu.2016.07.005
- Tavor, I., Jones, O. P., Mars, R. B., Smith, S. M., Behrens, T. E., Jbabdi, S., et al. (2016). Task-free MRI predicts individual differences in brain activity during task performance. *Science* 352, 216–220. doi: 10.1126/science.1248127
- Teicher, M. H., and Samson, J. A. (2013). Childhood maltreatment and psychopathology: a case for ecophenotypic variants as clinically and neurobiologically distinct subtypes. *Am. J. Psychiatry* 170, 1114–1133. doi: 10.1176/appi.ajp.2013.12070957
- Wager, T. D., Davidson, M. L., Hughes, B. L., Lindquist, M. A., and Ochsner, K. N. (2008). Prefrontal-subcortical pathways mediating successful emotion regulation. *Neuron* 59, 1037–1050. doi: 10.1016/j.neuron.2008.09.006
- Wang, J. Y., Cao, W. J., Guan, Z. J., Wu, T., Wang, R. J., Liu, X. D., et al. (2018). Evaluation and application of reliability and validity of the beck depression inventory among medical students. *Chin. J. Health Stat.* 35, 1369–1381.
- Wang, L., Dai, Z., Peng, H., Tan, L., Ding, Y., He, Z., et al. (2014). Overlapping and segregated resting-state functional connectivity in patients with major depressive disorder with and without childhood neglect. *Hum. Brain Mapp.* 35, 1154–1166. doi: 10.1002/hbm.22241
- Wang, L., Liu, H. C., Li, Z. Q., and Du, W. (2007). Reliability and validity of emotional regulation questionnaire Chinese revised version. *China J. Health Psychol.* 15, 503–505. doi: 10.13342/j.cnki.cjhp.2007.06.012
- Wang, X., Zhang, L., Wang, K., and Cai, Z. (2017). Study on childhood psychological trauma impact on the emotion regulation and alexithymia of patients with depression. *Acta Universitatis Medicinalis Anhui* 52, 1550–1553. doi: 10.19405/j.cnki.issn1000-1492.2017.10.030

- Wu, Z. Y., Luo, Q. Y., Wu, H. W., Wu, Z. Y., Zheng, Y. J., Yang, Y. L., et al. (2021). Amplitude of low-frequency oscillations in major depressive disorder with childhood trauma. *Front Psychiatry* 11, 596337. doi: 10.3389/fpsy.2020.596337
- Xu, Y., Qin, W., Zhuo, C., Xu, L., Zhu, J., Liu, X., et al. (2017). Selective functional disconnection of the orbitofrontal subregions in schizophrenia. *Psychol. Med.* 47, 1637–1646. doi: 10.1017/S0033291717000101
- Xu, Z., Zhang, J., Wang, D., Wang, T., Zhang, S., Ren, X., et al. (2019). Altered brain function in Drug-Naïve major depressive disorder patients with early-life maltreatment: a resting-state fMRI study. *Front. Psychiatry* 10, 255. doi: 10.3389/fpsy.2019.00255
- Yang, J. Y., Mao, Y., Niu, Y. S., Wei, D. T., Wang, X. Q., Qiu, J., et al. (2020). Individual differences in neuroticism personality trait in emotion regulation. *J. Affect. Disord.* 265, 468–474. doi: 10.1016/j.jad.2020.01.086
- Yang, W. H., Liu, S. L., Zhou, T., Peng, F., Liu, X. M., Yi, L. L., et al. J. Y. (2014). Reliability and validity of Chinese version of the beck depression inventory-II in Chinese adolescents. *Chin. J. Clin. Psychol.* 22, 240–245. doi: 10.16128/j.cnki.1005-3611.2014.02.018
- Zhang, X. C., Zhu, X. L., Wang, X., Zhu, X. Z., Zhong, M. T., Yi, J. Y., et al. (2014). First-episode medication-naïve major depressive disorder is associated with altered resting brain function in the affective network. *PLoS ONE* 9, e85241. doi: 10.1371/journal.pone.0085241
- Zhao, X. F., Zhang, Y. L., Li, L. F., Zhou, Y. F., Li, H. Z., Yang, S. C., et al. (2005). Reliability and validity of the Chinese version of childhood abuse questionnaire. *Chinese J. Clin. Rehabilitat.* 9, 105–107. doi: 10.3321/j.issn:1673-8225.2005.20.052

# Frontiers in Behavioral Neuroscience

Explores the neural mechanisms underlying animal and human behavior

Part of the world's most cited neuroscience journal series, this journal highlights research in all species that advances our understanding of the neural mechanisms underlying behavioral outcomes.

## Discover the latest Research Topics

[See more →](#)

### Frontiers

Avenue du Tribunal-Fédéral 34  
1005 Lausanne, Switzerland  
[frontiersin.org](https://frontiersin.org)

### Contact us

+41 (0)21 510 17 00  
[frontiersin.org/about/contact](https://frontiersin.org/about/contact)

